The foundaTions of coordination chemistry

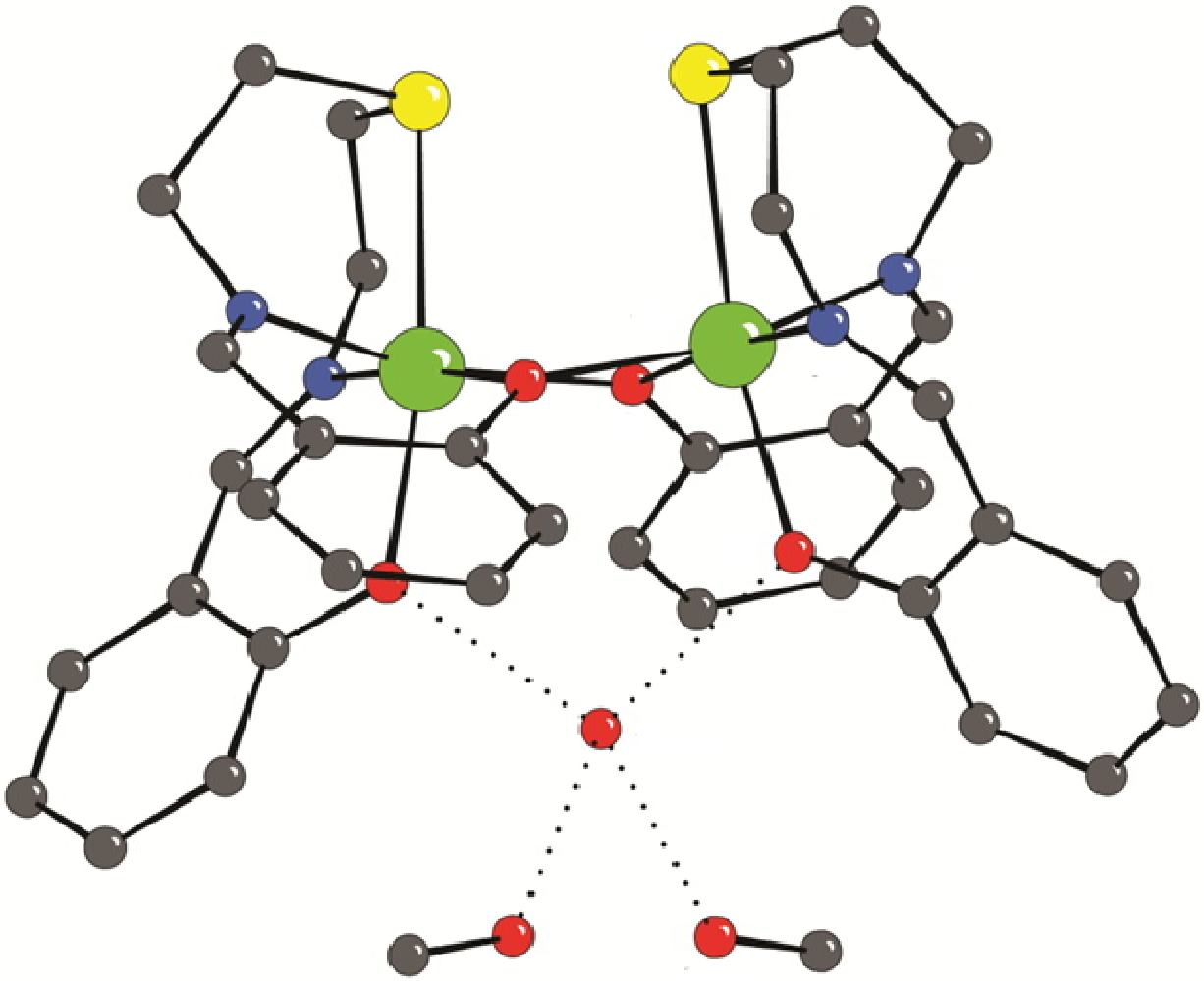

Chapter 1

CHEMICAL BONDS

I) Historical

The atom as an entity to "build" matter was born since antiquity. Thus in 1812 the model of the ionic bond was born with the hypothesis of Swedish chemist J**öns Jacob BERZELIUS**. At the same time, French chemist **Jean Baptiste DUMAS** who worked on organic compounds imagined another model of bonding that of the covalent bond. In 1897, with the discovery of electrons due to Nobel Laureate **Joseph John THOMSON**, chemists knew that the latter, by their valence shell, were responsible for the bonds between atoms. In 1916 **Walther Ludwig Julius Kossel** German physicist developed the theory of the ionic bond by noting that ions generally have a rare gas structure, peripheral shell saturated by gain or loss of electron (s). **Gilbert Newton LEWIS**, American physical chemist the same year, proposed a model of the so-called covalent bond of molecules by postulating that each atom tends to have the structure of the closest rare gas in the periodic table. Thus the notion of chemical bond was born from the conception of the notion of valence of an element which is equal to the number of bonds that the latter can form [1]. This concept which is a technical means of understanding the way in which atoms associate with each other is itself linked to the electrons of the valence shell also called the peripheral shell.

Examples : $_{8}O: \quad 1s^2 2s^2 2p^4$

$_{16}S: \quad 1s^2 2s^2 2p^6 3s^2 3p^4$

Oxygen and sulfur have the same number of valence electrons. However :

- Oxygen cannot use d-type Atomic Orbitals (AOs) and therefore has only one valence state with 2 unpaired electrons.
- On the other hand, sulfur can mobilize 3d OAs and present 3 valence states with 2, 4, 6 single electrons as follows :

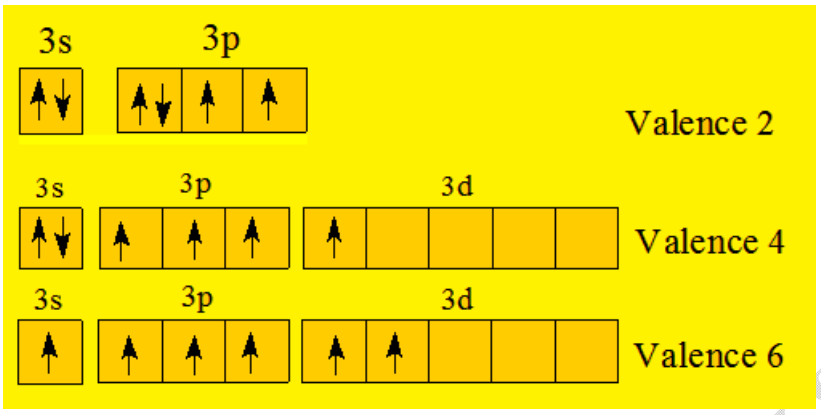

Figure 1 : some electronic configurations

- Neutral atoms can assemble by sharing electrons: in this case, the electron density will be significant between the atoms (covalent bond, metallic bond).
- Charged ions or atoms can assemble by electrostatic interaction between atoms carrying charges of opposite signs (ionic bond, so-called low-energy bonds).

It is however important to note that very often, the cases are not perfectly clear-cut, and we will then speak of more or less significant ionic or metallic character.

II) Covalent bond

1°) Classical theory

1-1 While ionic bonding easily accounts for the combinations occurring between elements of very different electronegativity, it is, on the other hand, totally powerless to explain the formation of bonds between elements of the same electronegativity. It was Lewis and Kossel who, in 1916, put forward the hypothesis of covalent bonding.

1-2 Definitions

- The **valence** of an atom in a molecule or in a polyatomic ion is the number of bonds around this atom. For the elements of the second period of the periodic table of elements (Li, Be, B, C) the valence is equal to the number of electrons on the peripheral shell; it is equal to **8 - n** for the elements beyond carbon (N, O, F), **n** being the number of electrons on the peripheral shell [2].
- A **covalent bond** is said to exist when there is a sharing of electrons between two atoms.

1-2 Lewis Representations and Rules *(Gilbert Newton Lewis 1875-1945)*

Lewis's representation draws on three essential notions :

- Only the last electron layer of atoms participates in the formation of bonds ;

- **The octet rule:** any atom engaged in one or more bonds tends to surround itself with 8 electrons (2 around hydrogen) in order to acquire the electronic structure of the closest rare gas in the periodic table.
- There are two types of bonds :

1-2-1 Pure covalent bond : it is the sharing of two electrons; each atom contributing an electron; the electronic doublet between the two atoms being symbolized by a connecting line.

Example

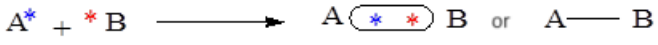

1-2-2 Coordinating bond or dative bond : An atom with an electron pair can share it with another atom or ion that does not yet have 8 electrons. The connecting line between the 2 atoms is symbolized by an arrow.

Example

To write **Lewis** diagrams of molecules :

- We first start by identifying the ***central atom*** : This is usually the one with the highest valence. The other atoms directly linked to the central atom are peripheral atoms or **ligands**. Multivalent atoms such as Cl, Br, I, S, etc., can be peripheral or central atoms. Strictly monovalent atoms such as H and F can only be peripheral atoms ;
- The external electronic configuration of each atom is determined by indicating the electronic pairs, the single electrons and any electronic vacancies ;
- Covalent bonds are then established between the central atom and the ligands.

1-3 The shortcomings of the octet rule

The octet rule is sometimes violated by :

- So-called Lewis acids like BF_3, $AlCl_3$, etc.
- Some elements of the 3rd period (Si, P, S, Cl) or subsequent periods, which can use more than four orbitals for bond formation: Examples PCl_5, SF_6, IF_5, BF_3, etc.

To obtain the Lewis diagrams of such structures, it is necessary to unpair the electronic pairs of the external layer of the central atom: we then pass to its excited state.

Examples

- $PC\ell_5$

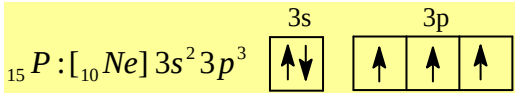

Phosphorus fundamentally can form only three covalent bonds. However, there are 5 P–Cl covalent bonds in the PCl_5 molecule.

To explain this pentavalence, the intervention of a 3d orbital by passage to the excited state is necessary, let P^* be the activated form of P :

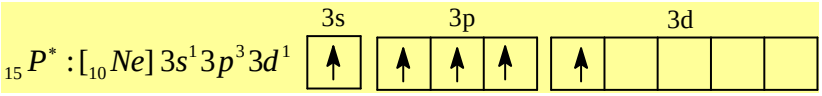

This external electronic configuration allows the formation of 5 P – Cl covalent bonds, hence the following Lewis formula, which clearly shows that the octet rule is not satisfied.

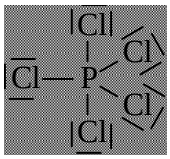

Sheme 1 : Lewis formula of PCl_5

- BrF_3

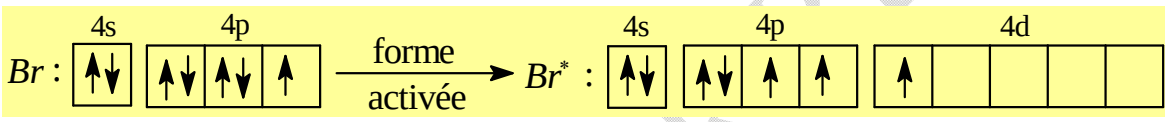

Hence the Lewis formula is as follows :

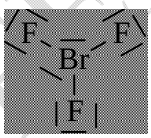

Sheme 2 : Lewis formula of BrF_3

1-4 The rule of sixteen or eighteen (18) electrons or Sidgwick's rule

Atoms or ions of the transition series belonging to the 4th, 5th and 6th periods and having nine subshells: one n "***s***", three n "***p***" and five (***n-1***)"***d***" incompletely filled, form with ligands complexes of high stability when the total number of electrons contributed by the central ion and by the ligands is equal to 18. This total number of electrons is also called the **effective atomic number** (EAN). The central atom or ion thus acquires the external electronic structure of the nearest rare gas in the periodic table. Exceptions are molecules whose central metal is surrounded by 16 electrons. These complexes are sometimes as stable, if not more stable, than those where the same metal is surrounded by 18 electrons (d^8 or d^{10} metals). These complexes are either square planar or trigonal [3].

Application exercise

Give the Lewis representations of the following molecules :

N_2O, N_2O_4, ClO_2F, HNO_3, NO, NO^+, NO_2^-, CO_3^{2-}, NO_3^-, NH_4^+.

Correction

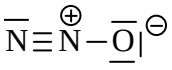

N_2O

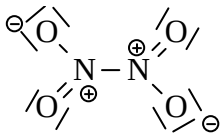

N_2O_4

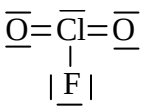

ClO_2F

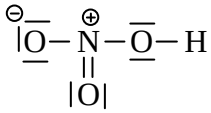

HNO_3

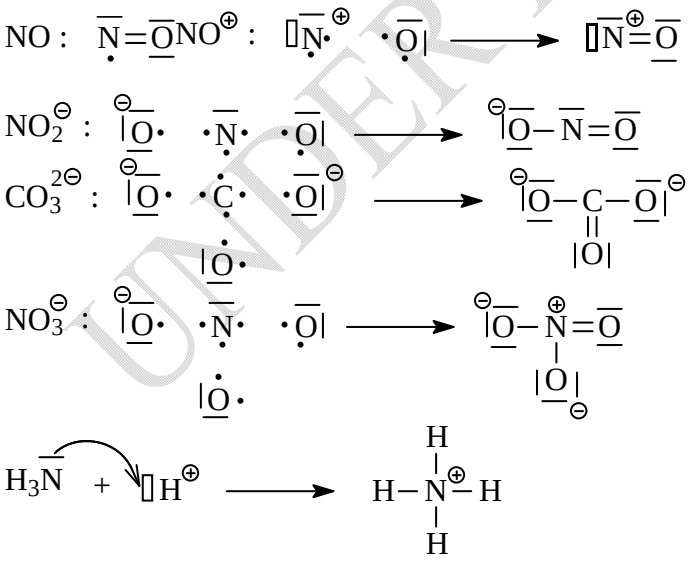

2°) Partial ionic character of covalent bonds: the iono-covalent bond

2-1 Highlighting

At the level of hydrogen chloride HCl, we observe in the bond the existence of an electric dipole since the asymmetry of the distribution does not allow the barycenters of the positive and negative charges to coincide, the bond is therefore polarized, which can be schematized in the following manner :

$$+\delta \quad -\delta$$

$$H - Cl$$

+δ and –δ indicate that everything happens as if each end of the dipole were affected by the charge δ, positive on the hydrogen atom side and negative on the chlorine atom side. This formed dipole has a dipole moment μ represented by a vector having the direction of the bond and a modulus equal to the product of the charge by the distance separating the two charges (here the length of the bond); chemists direct it from the negative charge to the positive charge. This dipole moment can only be determined experimentally.

If the asymmetry of charge distribution were such that the chlorine atom appropriates the electron brought by the hydrogen atom, then the charge δ would be equal to the charge of the electron and we would be in the presence of ions. The moment μ of the dipole would therefore be :

$\mu = 1.6.10^{-19}.1.28.10^{-10} = 20.48.10^{-30}$C.m either 6.139D, where 1D (debye) = $3.336.10^{-30}$C.m (Coulomb.meter).

The real bond can then be characterized by the ratio between the dipole moment of the bond and its extreme value for a hypothetical bond between ions; this ratio will be expressed as a percentage :

Dipole moment measured experimentally $\mu_{exp} = 3.48.10^{-30}$C.m = 1.043D

$\mu_{exp}/\mu . 100 = 17\%$. The covalent bond studied will be said to have a partial ionic character of 17%. A bond is therefore strictly covalent only in the case of molecules formed of identical atoms. In fact, a more appropriate term to designate this type of bond is the iono-covalent bond [2].

Generally, when a heteronuclear A–B bond is formed, the electron cloud is deformed, i.e. the more electronegative atom attracts the electron pair of the bond more towards itself, which leads to the appearance of partial charges on each atom :

$+\delta$ on the least electronegative atom ;

$-\delta$ on the most electronegative atom ;

The bond is said to be polarized. This polarization is due to the existence of a permanent dipole moment $\vec{\mu}$: $\vec{\mu}_{AB} = q \cdot \overrightarrow{AB}$

Either in module :

$$\left\|\vec{\mu}_{AB}\right\| = q \cdot \left\|\overrightarrow{AB}\right\| = q \cdot d_{AB}$$

d_{AB} (*metre*)

q (*Coulomb*)

$\vec{\mu}_{AB}$ (Cm) or : *Debye* (D) : $1D \approx \frac{1}{3} \cdot 10^{-29}\ Cm$

The partial ionic character of the polar bond or percentage of ionic character is defined as follows :

$$\%\,(ionicité) = \frac{\mu_{\exp}}{\mu_{ion}} \cdot 100$$

$\mu_{\exp}$ is the dipole moment of the bond formed, $\mu_{\exp} = \delta_{AB} \cdot d_{AB}$

μ_{ion} is the (fictitious) dipole moment of the bond assumed to be totally ionic, $\mu_{ion} = e \cdot d_{AB}$

δ_{AB} is the partial charge on each atom

hence the percentage of ionic character will be :

$$\%\,(ionicité) = \frac{\delta_{AB}}{e} \cdot 100$$

The value of this ratio is between 0 (purely covalent bond, $\mu_{\exp} = 0$) and 1 (purely ionic bond, $\mu_{\exp} = \mu_{ion}$).

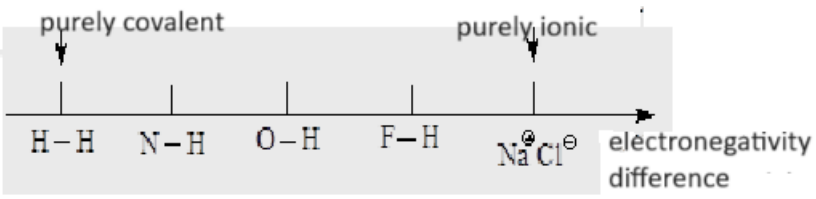

Figure 2 : electronegativity difference

Table 1 : some examples of ionicity percentage

Liaison	d_{A-B} (Å)	μ (D)	Δχ	% I_{AB}
H-I	1.61	0.38	0.4	5
H-Br	1.41	0.79	0.7	12
H-N	1.01	1.31	0.9	27
H-Cl	1.27	1.07	0.9	17
H-O	0.96	1.57	1.4	33
H-F	0.92	1.82	1.9	41

Δχ = difference in electronegativity between the two atoms A and B.

d_{A-B} = distance separating the two atoms A and B.

- Bond dipole moments are vector quantities and add like vectors.

2-2 Consequence of bond polarization

When a molecule is made up of more than two atoms, we must take into account all the effects of the possible dipoles formed by the bonds. To do this, we can find the resulting dipole moment by summing the vectors representing each dipole moment. If this sum is not zero, the molecule is said to be polar; otherwise, it is called apolar.

2-3 Diamagnetism and paramagnetism

Magnetism is due to the spin magnetic moment of electrons.

- If the electrons are paired in doublets (opposite spins) then : **μ = 0 : diamagnetism**

Example : He, Mg, Na^+…

- If there are single electrons then : **μ ≠ 0 : paramagnetism**

Example dioxygen O_2.

The measurement of paramagnetism provides information on the electronic structure: existence, number, location of single electrons. $\mu = \left[n(n+2) \right]^{\frac{1}{2}}$

The magnetic moment μ is expressed in **Bohr magneton**; n = number of single electrons.

III) Bond with ionic and metallic characteristics

The covalent bond model mainly concerns molecular or organic compounds. However, there are unlimited assemblies of atoms that occur at room temperature generally in a condensed state and are such that the infinite number of atoms in a sample has no influence on the properties of the substance and its structure. The behavior of these chemical compounds is very different from that of molecular compounds [1].

1°) Ionic bond

1-1 Properties

Ionic bonding is an electrostatic interaction between ions of opposite signs, for example Na+ and Cl- within an ionic crystal. The most spectacular property of ionic compounds is that they are electrical insulators in the solid state and become conductors in the molten state or in solution, which gives them the name electrolytes. They also have a total lack of plasticity. These compounds are made up of elements of the periodic table with a peripheral layer close to that of a rare gas. They generally contain, associated with them, an element with an atomic number close to that of a rare gas but lower, and an element with an atomic number close to that of a rare gas (which may be different from the previous one) but higher. Examples: KCl, NaCl, CaO.

Transition series elements can give ionic compounds without having an atomic number close to that of a rare gas.

The stability of the crystal lattice depends on the electrostatic interactions between the different ions. The evolution of the ionic character of the bond depends on the ionic radius and the charge of the ion. A bond is all the more ionic as :

- the cation is “large” and weakly charged (weak polarizing power) ;
- the anion is “small” and weakly charged (low polarizability).

Otherwise, i.e. a “small” and highly charged cation with a “large” and highly charged anion, the bond will have a certain tendency towards covalence.

1-2 Model

The properties of electrolytes have made it possible to consider the presence of ions in these ionic compounds. The proximity of a rare gas with a stable electronic structure makes it possible to interpret the ionization of atoms to achieve this stability; they only have a few electrons to gain or lose to stabilize. The chosen model can be summarized :

- Ionic solids are made up of cations and anions arranged alternately so as to respect, even at the scale of a few particles, electrical neutrality, hence we speak of a statistical formula ;

- in solids, electrons remain localized under the influence of each nucleus ;
- he cohesion of the whole is ensured by electrostatic attractions and repulsions.

1-3 The energy of cohesion

The ionic bond found in solid ionic compounds can be destroyed by an input of energy. In this case, not a single bond is broken, but the cohesion of all the ions is cancelled. We then define a bond or cohesion energy of the network which is also called lattice energy. The lattice energy of a crystallized ionic solid AB is the enthalpy variation used to move the A+ and B- ions in the gaseous state apart to infinity (zero interaction), from one mole of solid AB.

$$AB_{(solid)} \rightarrow A^{+}_{(gas)} + B^{-}_{(gas)}$$

This enthalpy variation can be calculated by applying the principle of the initial state and the final state. We then construct a hypothetical cycle called the **Born-Haber** cycle, named after the chemists who worked on these lattice energies. The stability of a crystal is characterized by its **lattice energy** E_r. The larger E_r, the more stable the solid. For the example of solid sodium chloride, the different steps required to transform metallic sodium (Na) and gaseous chlorine (Cl_2) into a sodium chloride crystal are described below. Its lattice energy Er is calculated from the following data :

- Solid sodium is transformed into gaseous sodium, the energy required for this transformation corresponds to its **enthalpy of sublimation** : $Na_{(s)} \rightarrow Na_{(g)}$ et $\Delta H_s = 109$ kJ/mol.
- Atomic sodium gas is ionized into Na+ ion, the energy required is the **ionization potential** (IP) or **ionization energy**: $Na_{(g)} \rightarrow Na^{+}_{(g)} + e^{-}$, $\Delta H_i = 496$ kJ/mol.
- Chlorine gas is homolytically dissociated into two chlorine gas atoms, the **energy required** is the bond or **dissociation ener**gy Cl – Cl : $Cl_{2(g)} \rightarrow 2\ Cl_{(g)}$, $\Delta H_l = \Delta H_{dis} = 240$ kJ/mol.
- Atomic chlorine gas receives an electron and becomes Cl^{-}, the energy required is the **electron affinity** of the chlorine element: $Cl_{(g)} + e^{-} \rightarrow Cl^{-}_{(g)}$, $\Delta H_{ae} = AE = -359$ kJ/mol.
- The **energy of formation** represents the energy received or absorbed during the formation of sodium chloride from the elements in the native state (i.e. metallic sodium and gaseous chlorine). The **enthalpy of formation** of solid sodium chloride:
  $Na_{(s)} + ½\ Cl_{2(g)} \rightarrow NaCl_{(s)}$ et $\Delta H_f = -411$ kJ/mol.

We can finally write the balance sheet as follows :

$$E_r = -\Delta H_f + \Delta H_s + ½\ \Delta H_l + \Delta H_i + \Delta H_e$$

By choosing two thermodynamically different paths from solid sodium chloride to isolated gaseous sodium and chloride ions, we obtain the following hypothetical cycle :

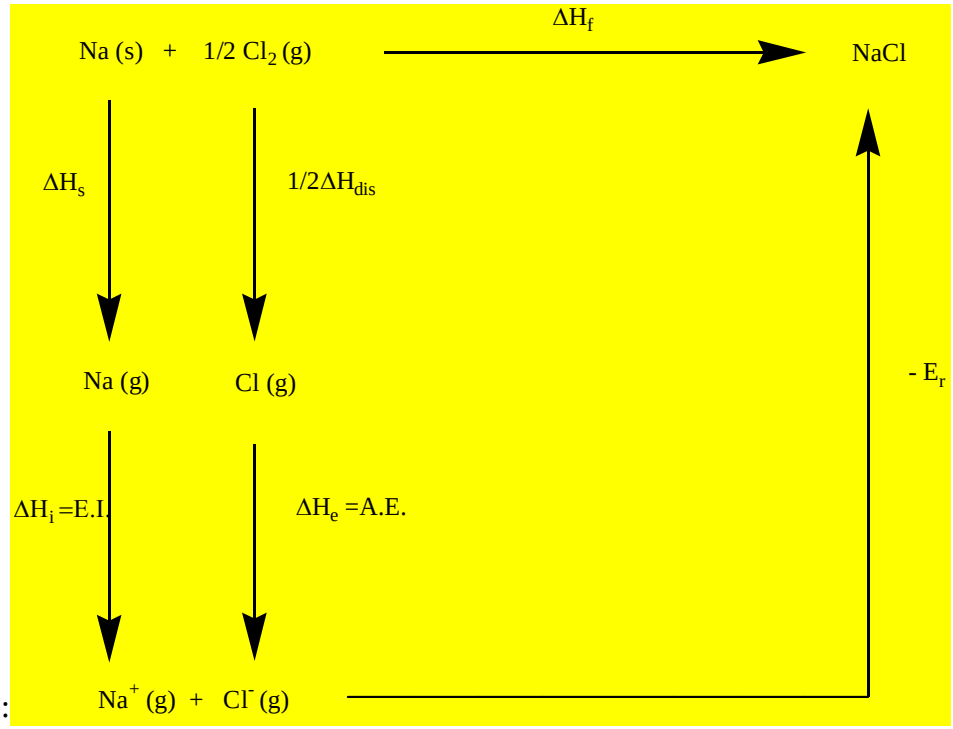

Figure 3 : Born-Haber cycle of NaCl formation

These two paths involve the same variation in enthalpy, which translates mathematically to : $E_r = -\Delta H_f + \Delta H_s + ½\ \Delta H_{dis} + \Delta H_i + \Delta H_e = 411 + 109 + ½\ 240 + 496 – 359 = 777$ kJ/mol.

This energy is particularly high, which explains why the cohesion of the solid can only be destroyed, for example, by a strong rise in temperature. Indeed, the melting temperatures of ionic solids are quite high (801°C for NaCl, 870°C for LiF and 790°C for KCl).

2°) Metal bond

2-1 Properties

The simplest model considers that the metal is not made up of metal atoms M, but of metal cations M^+ each having one electron in common. The sharing with a delocalization over the entire crystal accounts for the stability of the crystal. A metal is characterized by its metallic luster, its high electrical and thermal conductivities; its plasticity (malleability and ductility) and its property to form alloys are sometimes used. In addition, what characterizes the electronic configuration of metal atoms is an external layer containing only one, two, and sometimes three electrons [1].

Metals are located on the left side of the periodic table :

- ***s*** block : alkaline and alkaline-earth,
- ***d*** and ***f*** block : transition elements, lanthanides and actinides,
- ***p*** block : certain elements of groups 13 (Al, Ga) and 14 (Sn, Pb).

In total, more than 75% of the elements are metals. Metals are characterized by :

- good electrical and thermal conductivity,
- high reflective power (metallic shine),
- special mechanical properties: they are malleable (by hammering, thin sheets are formed) and ductile (they can be stretched into wires),
- easy loss of electrons,
- low electronegativity.

2-2 Model

This model must involve all identical atoms since metals are simple bodies. The model of pooling electrons in the outer shell does not allow us to conceive of localized electrons since the electronic structure of the rare gas that follows in the periodic table cannot be achieved; these external electrons would not be numerous enough. It therefore remains to assume that these external electrons are pooled, not on two, but on an unlimited number of atoms. This is a phenomenon of delocalization of these electrons throughout the sample. We can therefore describe the model of the metallic bond using the following points :

- metal atoms lose, in establishing the bond, the influence on their external electrons; they therefore become cations whose positions are fixed relative to each other (if the metal is in solid form) ;
- the outer electrons are delocalized and behave as if they were free, while remaining confined inside the sample.

Metals (except mercury) are solid at room temperature. The description of the structures of metals is very easy because all the atoms in the sample are identical. The crystal of a pure metal can be represented by a stack of spheres tangent to each other.

2-3 The energy of cohesion

When we destroy a metal structure, we are led, not to break a bond, but to cancel the cohesion of all the metal atoms. We will therefore not define a bond energy, but a cohesion energy of the metal. This cohesion energy can take various values, which is found in the large differences between the temperatures of change of state of various metals. It is defined as the variation in

enthalpy used to move the metal atoms in the gaseous state apart to infinity (zero interaction) from one mole of solid metal.

$M_{(s)} \rightarrow M_{(g)}$; which also represents the enthalpy variation during the sublimation of the metal. For sodium the energy is of the order of 109 kJ/mol; and for chromium of the order of 390 kJ/mol.

IV) Weak interactions

1°) Van Der Waals bond

1-1 Model

The Van Der Waals bond is a weak interaction between atoms, molecules or a molecule and a crystal. It is due to the interactions between the electric dipole moments of the two atoms involved. No electrons are shared between the two atoms. The model is built on the hypothesis that Van Der Waals made when he noticed that gases subjected to high pressures do not obey the same laws as under low pressures. Each electron, associated with the positive charge of the nucleus, forms a dipole. Therefore, outside the atom there is an instantaneous electric field. The latter, produced by an atom, can deform another atom as long as it is close enough. This will then be an attraction between instantaneous dipoles. We can summarize the characteristics of this interaction model: these are electrostatic type interactions, only occurring at short distances of the order of a few 10-10 m, and requiring a low energy input to break them, of the order of 0.1 to 10 kJ/mol (the energy of a covalent bond is a hundred times greater). These interactions are present in all molecular solids and in particular in organic crystals. These solids have very low melting temperatures and thermal agitation quickly destroys the crystal by compensating for the Van Der Waals interactions. We can distinguish three types of Van Der Waals interactions.

1-2 Van Der Waals interactions between polar molecules

A polar molecule AB is obtained when the two atoms A and B have different electronegativities [2].

Si $\chi_A \succ \chi_B$: $A^{-\delta} - B^{+\delta}$, the barycenters of the negative and positive charges are different: the molecule is characterized by a permanent dipole moment $\vec{\mu}$ such as : $\mu = \delta . d_{AB}$

δ : Partial charge appearing on each atom in coulomb, d_{AB} internuclear distance in meters ;

μ_1 and μ_2 two electrostatic dipoles interacting attractively and tending to orient each other in such a way that their interaction energy is minimal. This energy is expressed as :

$$E_1(r) = -2\left(\frac{\mu_1 \mu_2}{4\pi\varepsilon_O}\right)^2 . \frac{1}{r^6} . \frac{1}{3kT}$$

μ_1 and μ_2 are the values of the dipole moments of the molecules, r their shortest approach distance, k is the Boltzmann constant (k = R/N) and T the temperature expressed in Kelvin.

If we express the dipole moments in debye, the distances in nm, we obtain at 300K

$$E_1(r)/kJmol^{-1} = -\frac{(\mu_1\mu_2)^2}{1000r^6}$$

Digital application : $\mu_1 = \mu_2 = 1.5D$; r = 0.3 nm ; E_1 = - 3kJ/mol.

It should be noted that the energy is in r^{-6}, therefore the force of attraction is in r^{-7}, therefore only noticeable at very short distances.

1-3 Van Der Waals interactions between polar and nonpolar molecules

The permanent dipole of a polar molecule $\vec{\mu}_1$ can induce an electric field in its vicinity and create an asymmetry of charge distribution in a neighboring apolar molecule. The latter then has an induced dipole moment $\vec{\mu}_i$ and the two dipoles can attract each other. The term $\vec{\mu}_i$ is proportional to the field $\vec{E}$ created by $\vec{\mu}_1$. $\vec{\mu}_i = \alpha\vec{E}$

The term α corresponds to the polarizability of the apolar molecule: quantity proportional to its volume and which reflects the ease with which the electronic cloud of a molecule can deform under the action of a local field $\vec{E}$ (α is in m^{-3}). The attractive energy between μ_1 and μ_2 is given by :

$$E_2(r) = -\frac{\alpha\mu_1^2}{(4\pi\varepsilon_0)^2}\cdot\frac{1}{r^6}$$

1-4 Van Der Waals interactions between nonpolar molecules

These are, for example, rare gases, halogens, etc.

Even if the dipole moment is zero overall, at a given time t, we can define an instantaneous dipole moment $\vec{\mu}_1(t)$ for a molecule 1. $\vec{\mu}_1(t)$ is due to fluctuations of electrons in the electron cloud. $\vec{\mu}_1(t)$ induces in a neighboring molecule 2 an instantaneous moment induced $\vec{\mu}_2(t)$. $\vec{\mu}_1(t)$ and $\vec{\mu}_2(t)$ interact in an attractive way.

Formula of **London** : $E_3(r) = -\frac{3}{2}\frac{1}{(4\pi\varepsilon_0)^2}\frac{\alpha_1\alpha_2}{r^6}\frac{EI_1EI_2}{EI_1+EI_2}$

α_1 and α_2 : Polarizability of molecules 1 and 2 at distance r. EI_1 and EI_2 are the first ionization energies of molecules 1 and 2.

2°) Hydrogen bond

The hydrogen bond or hydrogen bridge is a weak bond that connects molecules. It can also be within the same molecule. It involves a hydrogen atom and a more electronegative atom (such as

oxygen). First of all, note that this behavior, which appears as an anomaly, only occurs for molecules with a hydrogen atom bonded to an atom of an electronegative element. Experience shows that it is sensitive for groups of atoms such as O - H, N - H, F - H, etc.

2-1 Experimental demonstration

The physical constants of some hydrogen compounds such as NH_3, H_2O, HF (melting temperature, boiling point, heat of vaporization) are abnormally high. These significant anomalies for the boiling temperatures of solutions containing the latter can be interpreted by the fact that they are linked by new types of bonds called hydrogen bonds.

2-2 Nature of hydrogen bonding

This is a relatively energetic electrostatic interaction (a few tens of kJ/mol) that is established between two groups of the same molecule (intramolecular bond) or two neighboring molecules (intermolecular bond). These are electrostatic or Van Der Waals type bonds. Some molecules are polar ; they are made up of polarized bonds. For example, if we consider the water molecule, H_2O: it is made up of an oxygen atom that is more electronegative than the hydrogen atoms. Consequently, although it is electrically neutral as a whole, the molecule has one end that is positively charged and another that is negatively charged, so that it is a polar molecule. Polar molecules attract each other and this attraction is called a dipole-dipole attraction.

V) Molecular orbital theory

1°) The model of hybridization of atomic orbitals

The theory of hybridization was developed in the 1930s, notably by the American chemist **Linus PAULING**. It allows to account for the geometry of compounds having no lone pairs on the central element and to interpret the formation of the bonds present by the overlap of orbitals. It is a descriptive theory of chemical bonding which is still very successful in organic chemistry, because it accounts quite well for experimental facts, which were absolutely incomprehensible by Lewis theory, such as the existence of σ and π bonds.

A **σ** bond is obtained by **axial** overlap of two orbitals and a **π** bond is obtained by **lateral** overlap of two orbitals. The modification of the state of the external electrons of the atoms concerned by the bond, compared to the state of the isolated atoms, is such that we will speak of electron sharing. We recall the electronic configuration of each isolated atom where the electron is not localized in the point sense of the term but we can describe regions of space where it has a high probability of being there: this is the **atomic orbital**. The single electron is described by an atomic

orbital ***1s***. Stabilization shows that when two atoms come together, we can imagine a partial overlap of these two atomic orbitals. This overlap is necessary to ensure the greatest stability corresponding to a maximum overlap, it will only occur along well-defined privileged directions. This makes it possible to interpret the fact that the covalent bond has a very strongly directed character which imposes on the molecules very characteristic geometries which are identified by measuring the angles between the bonds. For example, the water molecule is bent, presenting an angle of 104.5° between the two O – H bonds. To determine the geometry of a chemical entity, by this theory, we will seek to determine the state of hybridization of the central element. To do this :

- We first begin by determining the Lewis structure of this chemical entity.
- We then count the number of **σ** bonds around the central element (we do not count the ***π*** bonds).
- We then consider the part of the electronic structure of the central element corresponding to the valence electrons. Starting from thisfundamental thus determined (given directly by the periodic table), we move to the excited state of this central element by "breaking" all the doublets of thefundamental by electronic promotions of the electrons towards the orbitals with **higher energies** so that there is **only one** electron per orbital in this excited state.
- We then "sum" as many orbitals in the excited state as there are σ bonds around the central element, starting with the lowest energy orbital (this is always an s orbital in non-transitional elements). These n "summed" orbitals will give rise to n equivalent **hybrid orbitals** each containing an electron. These hybrid orbitals, by axial type overlap with the ***s*** or ***p*** orbitals of the elements linked to the central element, form the **σ** bonds. A lateral type overlap between two parallel orbitals gives a ***π*** bond.

L'état d'hybridation est donné par les orbitales "sommées". Il est de la forme $\boldsymbol{sp^n d^m}$ (n = 1, 2, 3 ; m = 0, 1, 2, 3). Dans ce cas une orbitale ***ns***, n orbitales ***p*** et m orbitales ***d*** ont été "sommées". Pour chaque état d'hybridation, il y a une géométrie correspondante ; elle est la géométrie la plus stable. Cette dernière correspond à la distribution spatiale la plus stable des orbitales hybrides.

The hybridization state is given by the "summed" orbitals. It is of the form $\boldsymbol{sp^n d^m}$ (n = 1, 2, 3; m = 0, 1, 2, 3). In this case one ***ns*** orbital, n orbitals ***p*** and m orbitals ***d*** have been "summed". For each

hybridization state, there is a corresponding geometry; it is the most stable geometry. The latter corresponds to the most stable spatial distribution of hybrid orbitals.

Noticed : to make hybrid orbitals in the same energy level we first start with the ***ns*** and ***np*** orbitals before the ***nd*** orbitals.

The following figures show cross-sections of the electron cloud (**electron density diagram**) where the denser the points, the higher the probability of finding that electron.

- The ***s*** orbital is spherical ($l = 0$).

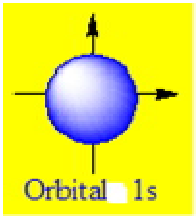

Scheme 3 : representation of the s orbital

- The ***p*** orbital (l = 1) is formed by 2 symmetrical lobes of opposite signs on a common axis. There are 3 ***p*** orbitals (m = -1, 0, +1), p_x along the x axis, p_y along the y axis and p_z along the z axis.

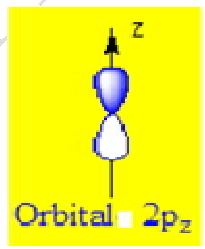

Scheme 4 : representation of the p orbital

The shape of the ***d*** orbitals (l = 2) is more complicated and there are 5 ***d*** orbitals (m = -2, -1, 0, 1, 2):

- Three ***d*** orbitals have 4 lobes that develop in the planes bisecting the axes: (d_{xy}, d_{xz}, d_{yz}). These are mixed ***d*** orbitals.

- The other two ***d*** orbitals are centered on the axes: they are square ***d*** orbitals.

  - $\boldsymbol{d_{x^2-y^2}}$ along the x and y axes,

- d_{z^2} a has two lobes centered on the z axis and has a small volume in the xOy plane.

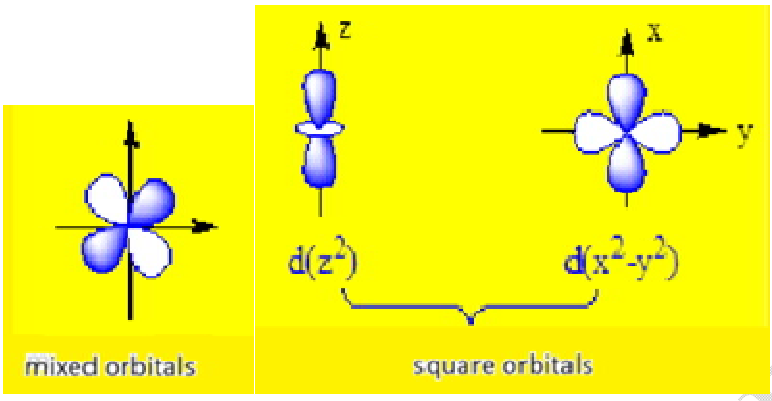

Scheme 5 : representation of orbitals d

In light of the wave model of matter, it has been shown that each atom has atomic orbitals. Molecules also have orbitals, called molecular orbitals.

1-1 Origin

Consider a molecule formed of three atoms: $BeCl_2$. To know the atomic orbitals involved in the formation of the two bonds between the beryllium atom and the two chlorine atoms, we write the electronic structures of these two atoms.$_4Be : 1s^2 2s^2$

The two bonds carried by the Be atom can only be considered for a so-called “excited” structure of this atom, i.e.:

$_4Be^* : 1s^2 2s^1 2p^1$; and by materializing the valence layer with the quantum boxes:

$_4Be^* : 2s^1 2p^1$ 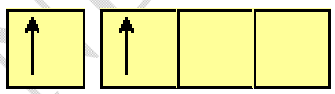

The chlorine atom has the electronic structure: $_{17}Cl : 1s^2 2s^2 2p^6 3s^2 3p^5$

For the valence layer:

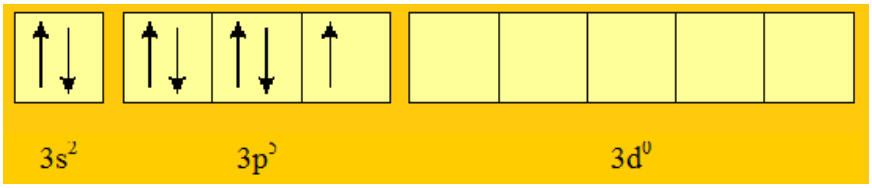

A first covalent bond σ can be formed between the ***2p*** atomic orbital of the beryllium atom and the ***3p*** orbital of the first chlorine atom. Such a bond leads to the formation of a localized molecular orbital between these two atoms as well as to a strong overlap.

To form the second Be—Cl bond, we again have a ***3p*** atomic orbital provided by the second chlorine atom. The beryllium atom now only has a ***2s*** orbital with spherical symmetry. The bond constructed from these s and p atomic orbitals cannot have a preferred direction. This bond also has a lower energy than the previous bond because the ***2s***, ***3p*** overlap is lower than the ***2p***, ***3p*** overlap. However, these results are in disagreement with the experiment which says that the two Be—Cl bonds are of the same nature and characterized by the same energy, the $BeCl_2$ molecule is a linear molecule. In conclusion this result shows that the formation of bonds from the atomic orbitals of atoms can only be used for diatomic molecules. For the $BeCl_2$ molecule (3 atoms) we do not find the experimental data (bond energy - geometry of the molecule). If we want to account for reality as well as possible it is necessary to introduce an additional operation called the **hybridization of orbitals.**

1-2 Principle of hybridization

Atomic orbitals are mathematical functions. We know that these functions are the solutions of the differential equation (Schrödinger equation) that describes the movement of electrons. These functions form a vector space of functions because they have the characteristic properties of vectors in a vector space: **additivity**, **multiplication** by a **scalar**. It is therefore possible to construct from the two atomic orbitals ***2s*** and ***2p*** of the beryllium atom two new orbitals h_1 and h_2 from the linear combinations:

$$h_1 = a\,(2s) + b\,(2p)$$
$$h_2 = a\,(2s) - b\,(2p)$$

These new atomic orbitals are called **hybrid** orbitals. The terms a and b are arbitrary (scalar) coefficients.

1-2-1 Single bonds and multiple bonds

There are single bonds, called **σ** bonds, and we briefly mentioned the existence of multiple bonds, especially in the case of carbon, these additional bonds to **σ**, are **π** bonds. **σ** bonds are stronger bonds than **π** bonds.

1-2-2 The case of the hydrogen molecule (H_2)

The configuration of the hydrogen atom is the simplest: $1s^1$, the orbital of a hydrogen atom is spherical (s). Let two hydrogen atoms: Knowing that orbitals are wave functions, during the bond, by assembling these two volumes, we obtain the molecular orbital of H_2. The hydrogen molecule has an electron cloud composed of the addition of the two volumes.

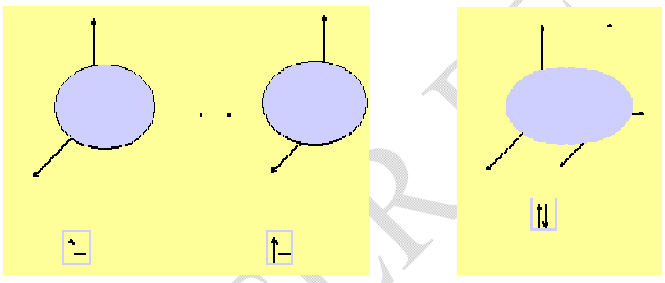

Scheme 6 : orbital overlap s

1-2-3 σ (p + s) bond: the HCl molecule

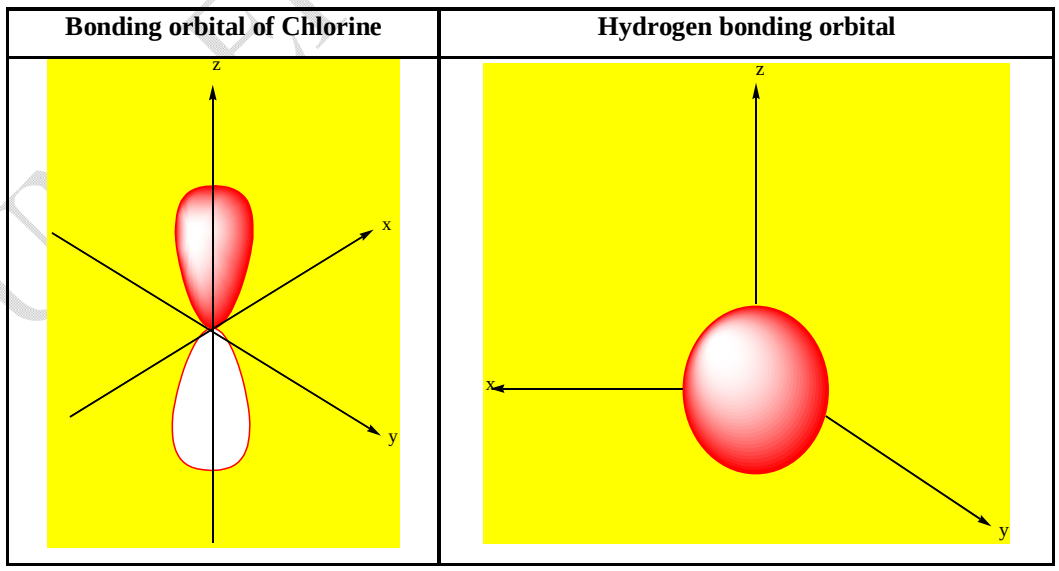

Scheme 7 : representation of s and p orbitals

We define, by convention, the axis on which the connection is made as being the **z'z** axis:

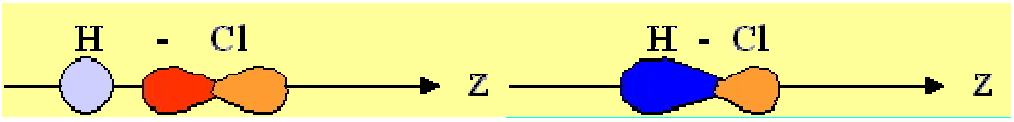

Scheme 8 : overlap of s and p orbitals

This is indeed a **σ** bond, which is formed by **overlap on the z axis**. **π** bonds are weaker bonds than **σ** bonds. This is because the overlap of the orbitals is not completely complete. For π bond orbitals, this is a lateral overlap, less complete and less effective than an overlap on the corresponding axis:

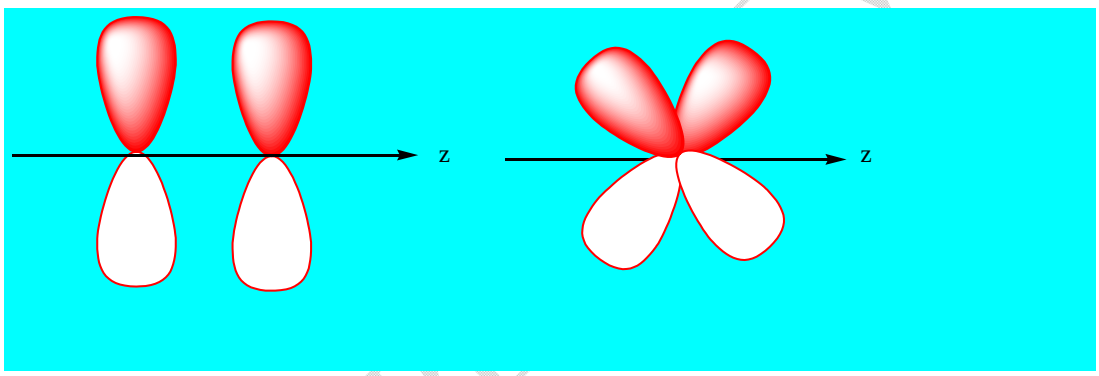

Scheme 9 : lateral overlap of π orbitals

1-3 Sp hybridization

Linear combinations being of the form:

$$h_1 = a\,(2s) + b\,(2p)$$
$$h_2 = a\,(2s) - b\,(2p)$$

They lead to two new hybrid orbitals h_1 and h_2. Among the infinite number of possible combinations, there is a combination that concentrates the greater part of the hybrid in the direction of the molecular orbital that we want to construct. In the case of $BeCl_2$, the more the hybrid orbital carried by beryllium is concentrated in the direction of chlorine, the greater the overlap with the ***3p*** atomic orbital of the chlorine atom. The combinations shown below comply with this condition.

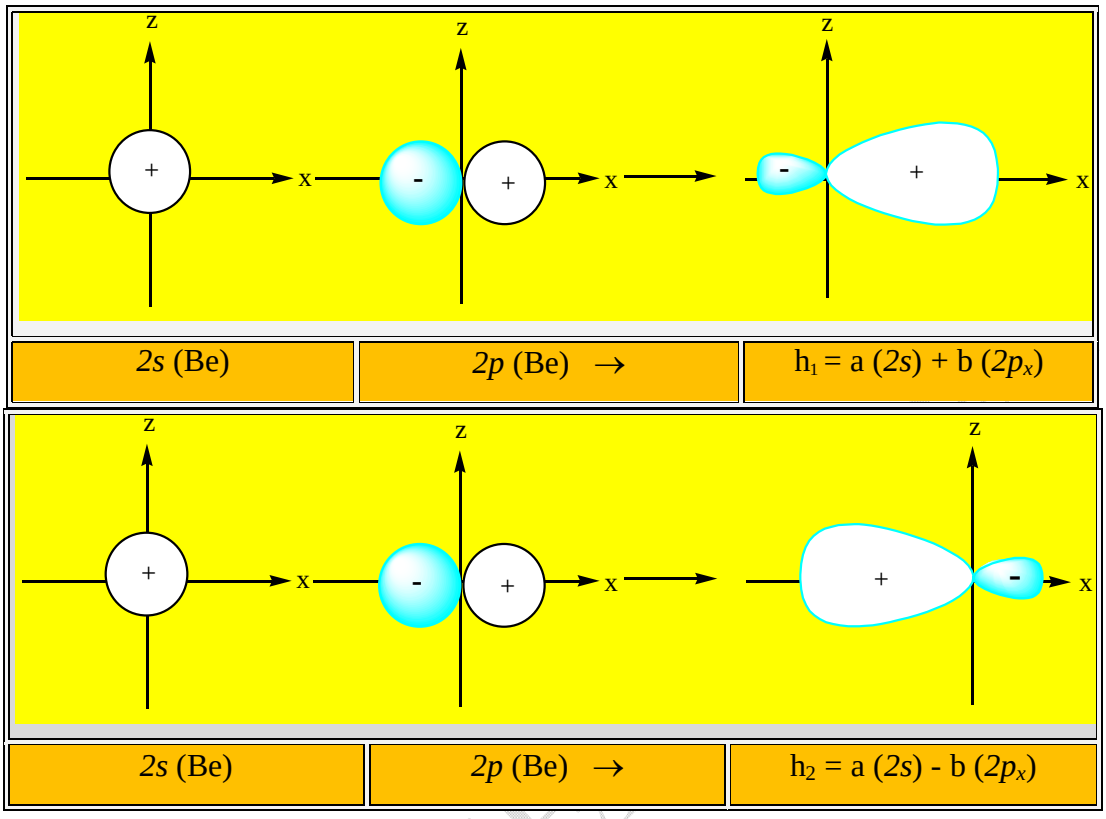

Scheme 10 : hybrid overlap of s and p orbitals

The two linear combinations lead to two identical hybrid orbitals but directed in two opposite directions. They are in accordance with the geometric arrangement which allows to construct with each chlorine atom two **identical** covalent **σ** bonds. These two bonds are obtained by the overlap of each hybrid atomic orbital of the beryllium atom with a ***3p*** atomic orbital of each chlorine atom. These two bonds have the same energy since the overlaps are the same and they form an angle of 180° between them. The molecule obtained is therefore linear in accordance with the experiment. It is said that in the BeCl2 molecule the Beryllium atom is in the ***sp*** **hybridization state or** ***sp*** **hybridized.**

Construction of orbitals of BeH_2 and $BeCl_2$ (ground state GS, excited state ES)

σ σ

H – Be – H

Be : $1s^2 2s^2$: F.S.

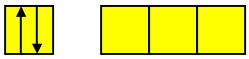

E.S.

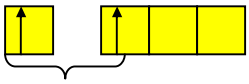

sp

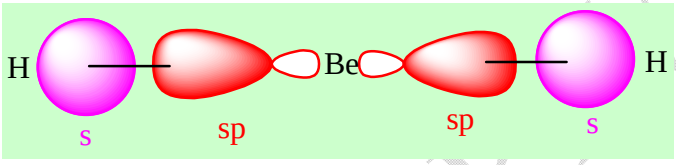

Scheme 11 : sp hybrid orbital formation

$BeCl_2$: Cl ; F.S.

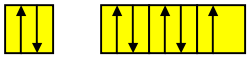

P_z

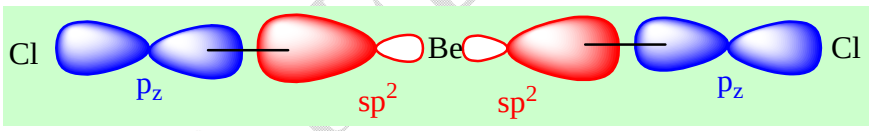

Scheme 12 : overlap between the p orbital and the sp^2 hybrid orbital

1-4 sp^2 hybridization

This molecule is planar, and the three equivalent BF bonds form angles of 120° between them (**Gillespie**'s rule).

The electronic structure of the boron atom in its "excited" state is written:

$_5B^*$: $1s^2 2s^1 2p_x^1 2p_y^1$ 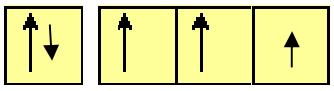

To construct the three covalent B-F bonds, it will therefore be necessary to use three equivalent, coplanar, 120° hybrid orbitals. These three hybrids can be constructed from the ***2s*** orbital and the ***2p$_x$*** and ***2p$_y$*** orbitals of the boron atom.

Example : BH_3

However, it does not exist in a monomeric state; it exists in a dimer and its formula is B2H6. There are 3 bonds **σ**.

B : $1s^2 2s^2 2p^1$ F.S. 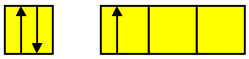

E.S. 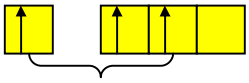

sp^2

We have a triangular distribution.

H : $1s^1$: F.S. 

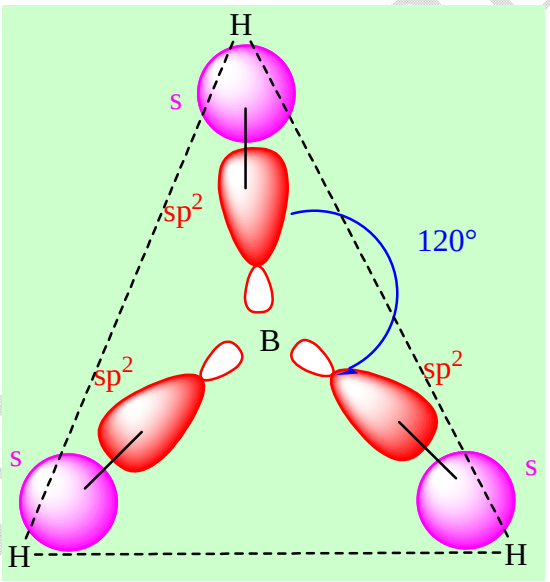

Scheme 13 : overlap between the s orbital and the sp^2 hybrid orbital

1-5 sp^3 hybridization

The methane molecule CH_4 has a tetrahedral geometric structure (tetrahedron angle: 109°28'). The four C-H bonds of this molecule are equivalent: length, energy. To obtain such a structure, it is necessary to hybridize the ***2s*** orbital and the three ***2p*** orbitals of the carbon atom.

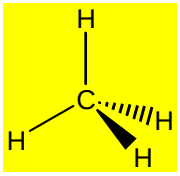

Scheme 14: methane representation

Each C-H bond will be a **σ** covalent bond resulting from the overlap between an ***sp^3*** hybrid orbital of the carbon atom and the ***1s*** orbital of a hydrogen atom. These four bonds are equivalent (same energy) and directed according to the four vertices of the tetrahedron.

Example : CCl_4 : there are 4 **σ** bonds.

C : $1s^2 2s^2 2p^2$: F.S.

E.S.

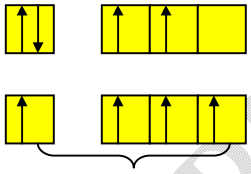

sp^3

It is a tetrahedral distribution.

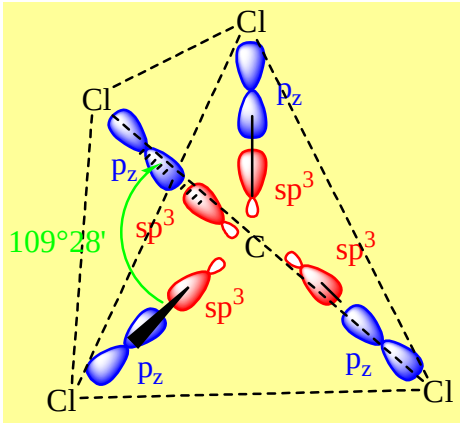

Scheme 15 : overlap between sp^3 and p orbitals

1-6 sp^3d hybridization

1-6-1 Case of a trigonal bipyramid

Example du PF_5. There are 5 σ bonds around P.

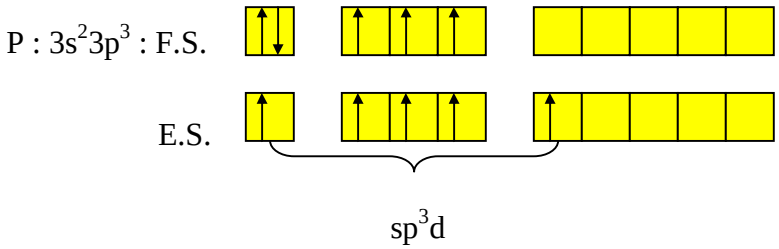

The five hybrid orbitals will be distributed in a trigonal bipyramid. An axial overlap between the p_z orbitals of fluorines and the sp^3d hybrid orbitals of P allows to account for the **σ** bonds.

In a trigonal bipyramid there are 3 equivalent equatorial positions that correspond to the vertices of the triangle. The two positions that are located on either side of the triangle are called axial positions; they are also equivalent. We have:

$$F_{eq}\hat{P}F_{eq} = 120°$$

If the bonding atoms are not identical then they are distributed in such a way as to have the minimum repulsion. Thus the largest and most electronegative atoms always occupy the equatorial positions and the more electropositive ones the axial positions.

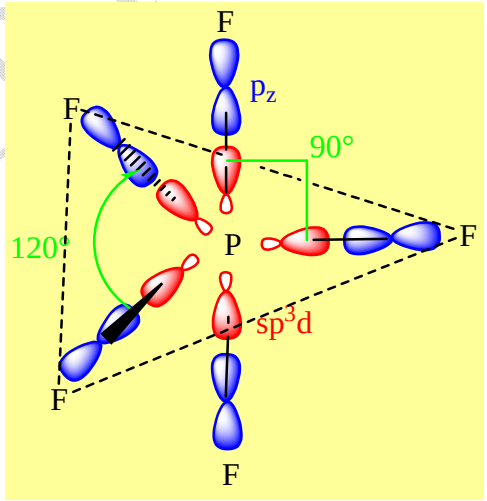

Scheme 16 : overlap between sp^3d and p orbitals in a trigonal bipyramid

Noticed : For transitional elements the trigonal bipyramid is generally the **most stable** geometry except for antimony Sb.

1-6-2 Case of a square-based pyramid

Les angles valent 90°. Antimony Sb and phosphorus have the same number of electrons on the peripheral layer. We will have the same type of Lewis structure for SbF_5 and PF_5. We will also have the same hybridization state for the central element, i.e. $\boldsymbol{sp^3d}$. But in this case the hybrid orbitals are distributed according to a square-based pyramid, this is the most stable spatial distribution of hybrid orbitals. We will make an axial type overlap between the hybrid orbitals and the $\boldsymbol{p_z}$ of fluorines to account for the formation of Sb–F bonds. The angles are 90°.

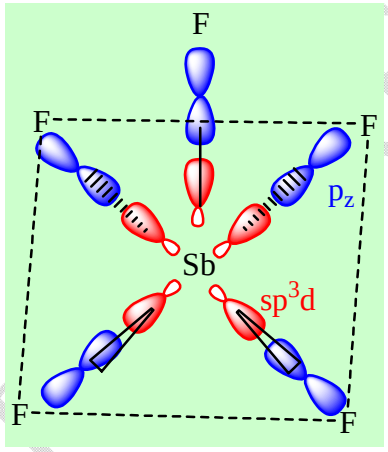

Scheme 17 : overlap between sp^3d and p orbitals in a square-based pyramid

1-7 sp^3d^2 hybridization

Example : SF_6. There are 6 **σ** bonds around S.

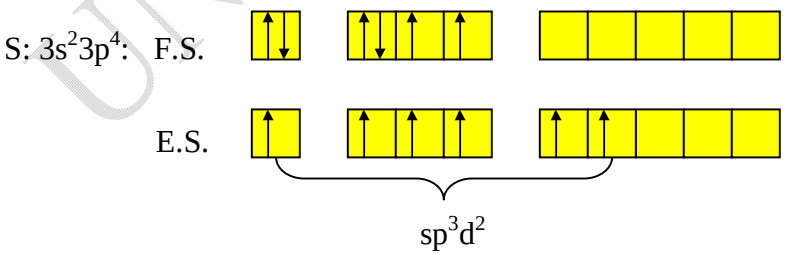

There are six σ bonds so the hybridization is $\boldsymbol{sp^3d^2}$. The most stable spatial distribution is the octahedral distribution. All angles are 90°. An axial overlap is made between the $\boldsymbol{p_z}$ atomic orbitals

of fluorines and the sp^3d^2 hybrid orbitals of sulfur to form the σ bonds. The largest and most electronegative atoms will be in the trans position.

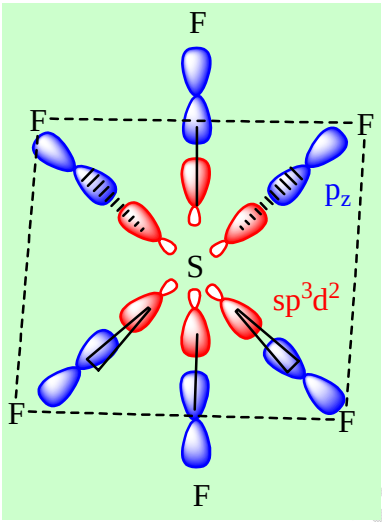

Scheme 18 : overlap between sp^3d and p orbitals in an octahedron

1-8 sp^3d^3 hybridization

Example : IF_7. There are 7 σ bonds around I.

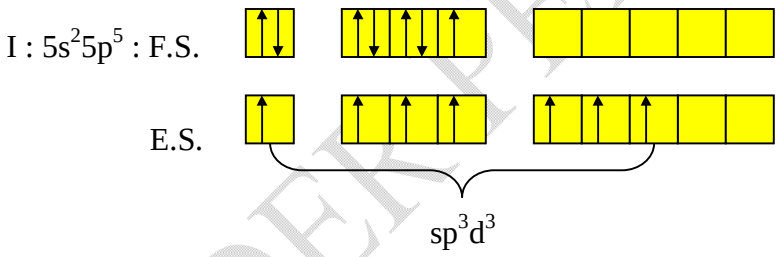

Seven σ bonds; the hybridization will be sp^3d^3. The most stable spatial distribution is the pentagonal bipyramid. For the **σ** bonds there will be an axial type overlap between the hybrid orbitals and the p_z of the fluorines. Unlike a trigonal bipyramid in the case of a pentagonal bipyramid the largest or most electronegative bonding atoms are placed in an axial position with $F_{eq}\hat{I}F_{eq} = 72°$ and $F_{ax}\hat{I}F_{eq} = 90°$.

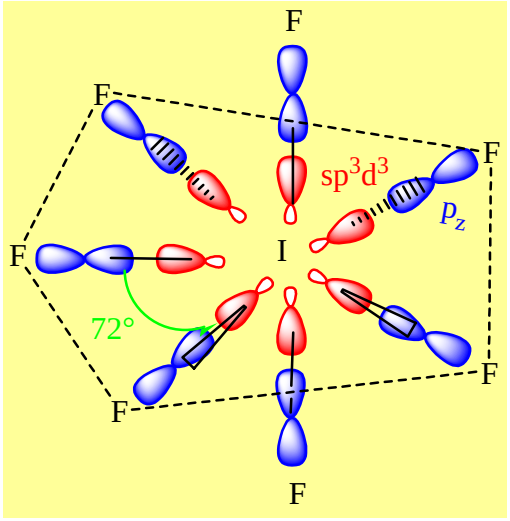

Scheme 19 : overlap between sp^3d and p orbitals in a pentagonal bipyramid

1-9 Hybridization-geometry relationship

Table 2 : some geometries in relation to hybridization types

Bond number σ	Types of Added Orbitals	Result	Geometry
2	*1s + 1 p*	2 orbitals *sp*	linear
3	*1s + 2 p*	3 orbitals sp^2	plane triangle
4	*1 s + 3 p*	4 orbitals sp^3	tetrahedron
5	*1s + 3p + 1d*	5 orbitals dsp^3	trigonal bipyramid

1-9-1 sp^2 hybridization with π bond

A ***π*** bond is obtained by lateral overlap of two parallel orbitals. We can have two parallel ***p*** orbitals or one ***p*** orbital and one ***d*** orbital.

Example : ethylene

C : $2s^2 2p^2$: F.S. 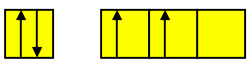

E.S. 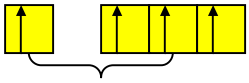

sp^2 p_z

There are 3 hybrid orbitals for each carbon.

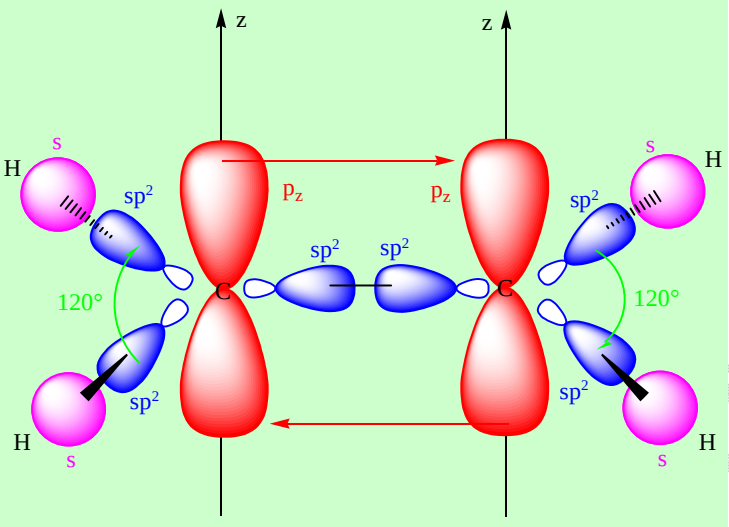

Scheme 20 : lateral overlap between two p orbitals of ethylene

The hybridization of the carbons is sp^2. An axial type overlap between two hybrid orbitals of each carbon with the ***s*** orbitals of the hydrogens on the one hand; between the two remaining orbitals on the other hand makes it possible to account for the **σ** skeleton of ethylene, that is to say all the bonds present in this molecule. After the sp^2 hybridization; there remains on each carbon a p_z orbital. The two p_z orbitals are parallel and give a lateral type overlap with a **π** bond. The angles are 120°. The **π** bond causes the molecule to be globally planar.

1-9-2 sp hybridization with π bond

Example : acetylene

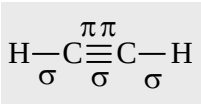

C : E.S. 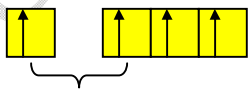

sp p_y p_z

We have two σ bonds.

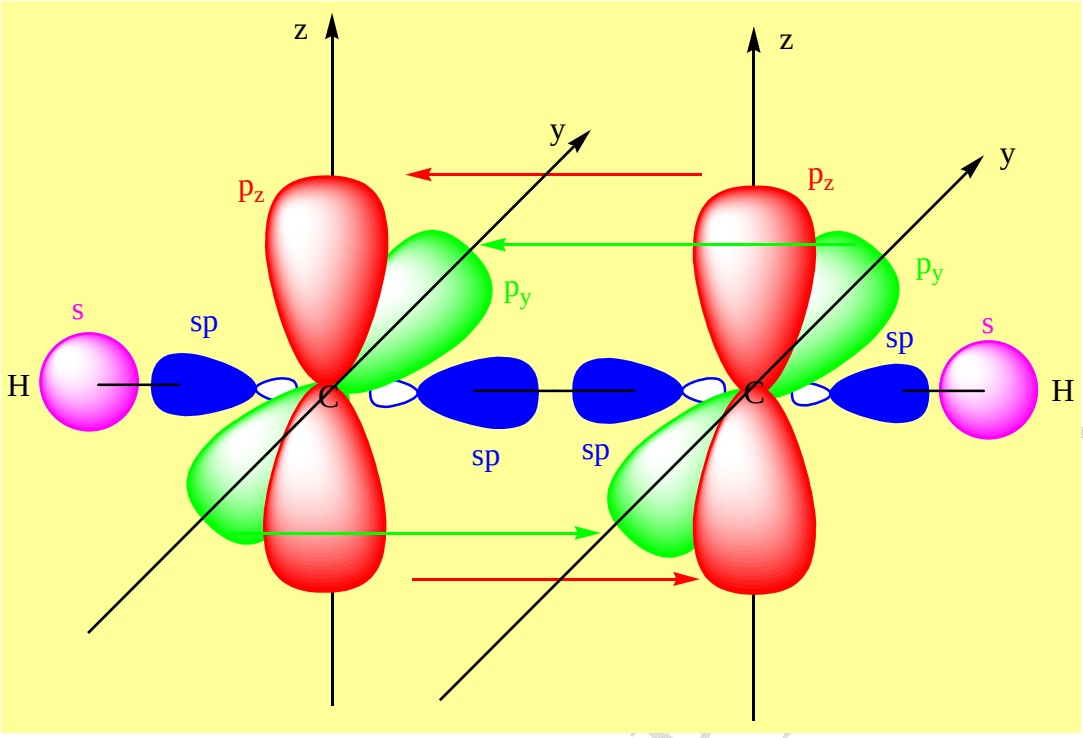

Scheme 21 : lateral overlaps between p orbitals of acetylene

p_y and p_z of one of the carbon atoms are respectively parallel to the orbitals of the same name of the other carbon atom and give by lateral type overlap the π bonds. Example of carbon dioxide.

$$O \overset{\sigma}{\underset{\pi}{=}} C \overset{\sigma}{\underset{\pi}{=}} O$$

C : E.S.

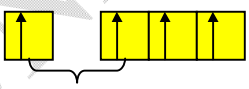

sp

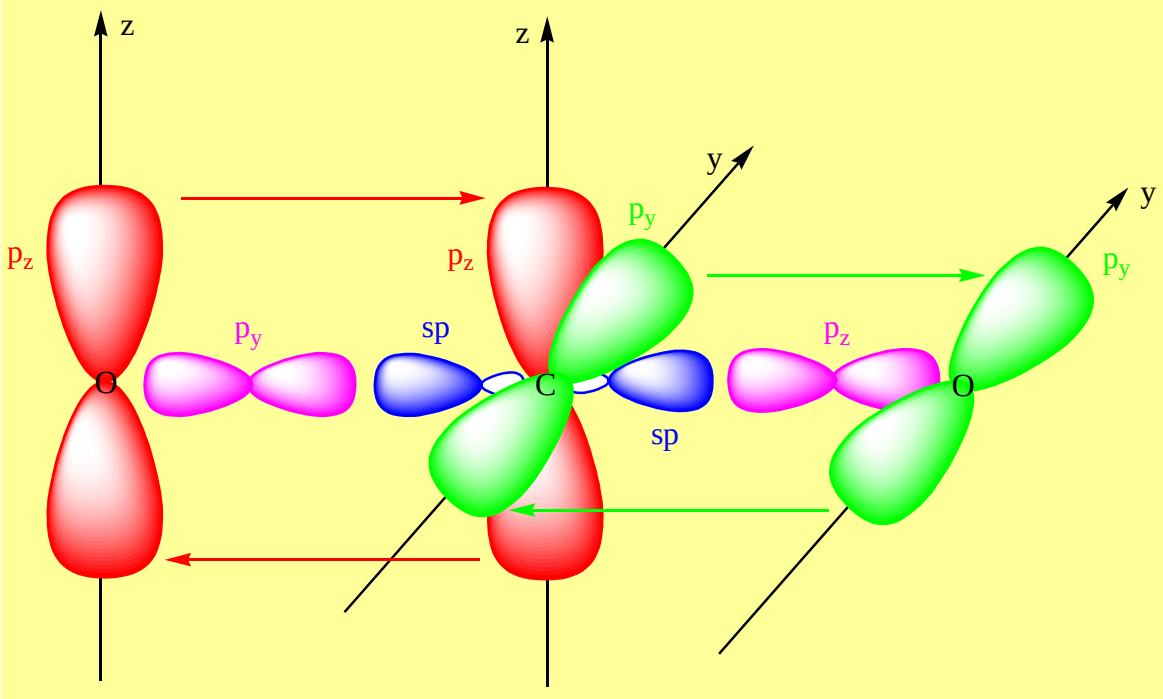

Scheme 22 : lateral overlaps between p orbitals of carbon monoxide

The hybridization state of carbon is ***sp***; we can use the p_y or p_z orbitals of oxygen. After the hybridization of carbon, there remains a p_y orbital and a p_z orbital; it would therefore be necessary for the orbitals that remain on the two oxygens after the **σ** bond has been accounted for to be a p_y orbital and a p_z orbital so that they are respectively parallel to p_y and p_z of carbon. We realize this by taking orbitals of the same name for the **π** bonds on the oxygens; they cannot be parallel to orbitals of different names on carbon. By lateral type overlap these orbitals will give **π** bonds.

1-9-3 sp^3 hybridization with *pπdπ* bond: Resonance phenomenon

Example : sulfate ion

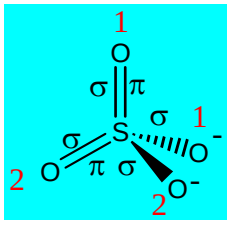

Scheme 23 : representation of the sulfate ion

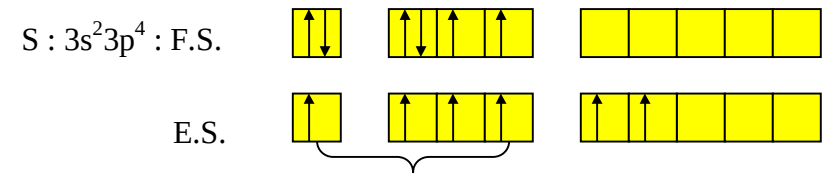

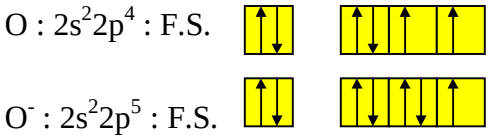

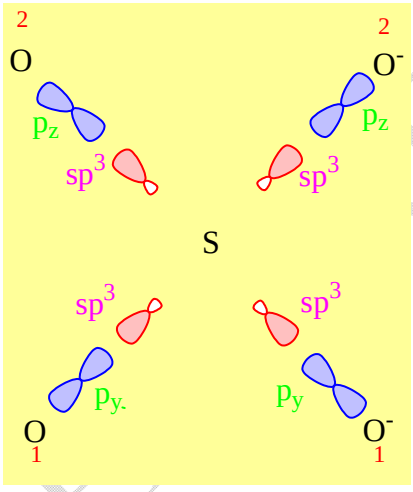

Scheme 24 : overlap between sp3 and p orbitals of sulfate ion

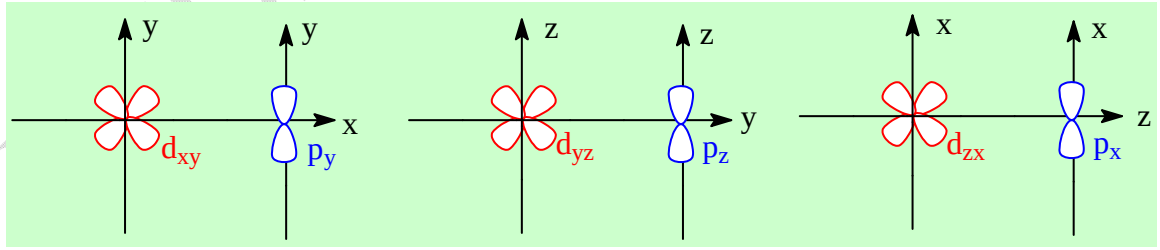

Scheme 25 : overlap between mixed d and p orbitals

Since sulfur is ***sp*^{3}** hybridized, 2 electrons will remain on the ***d*** orbitals. These are the orbitals that will be used for ***π*** bonds as in the case of C_2H_4; C_2H_2 and CO_2.

Remember that only 3 of the 5 ***d*** orbitals can give ***π*** bonds; they are called mixed orbitals: d_{xy}, d_{yz} and d_{zx}.

d_{xy} is parallel to p_y, d_{yz} is parallel to p_z, and d_{zx} is parallel to p_x.

For the axial type overlap; we will use for the uncharged oxygens 2 orbitals of different names (p_y and p_z) so that the remaining orbitals (p_z and p_y) are respectively parallel to d_{yz} and d_{xy} which receive the electrons coming from the double electronic promotion. A lateral type overlap between these ***d*** orbitals on the one hand and ***p*** on the other makes it possible to account for the ***π*** bonds in SO_4^{2-}. These bonds are thus called ***pπdπ*** bonds; the name coming from the fact that one of the orbitals of the π bond is a ***d*** orbital and the other a ***p*** orbital.

The 4 oxygens of the sulfate are normally all equivalent. We can number them 1; 2; 3; 4 and make them carry the charge and the double bond in turn; we will have 4 **limit resonant** structures which are:

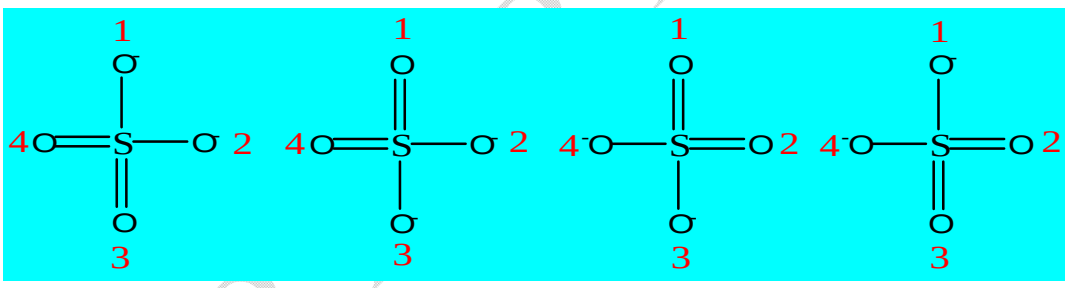

Scheme 26 : Limiting resonant structures of the sulfate ion

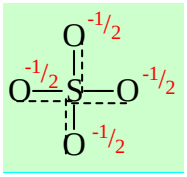

Scheme 27 : average structure of sulfate ion

The structure of diagram 27 is the true structure which will be an average structure that will take into account the 4 limit structures. Everything happens as if the π bonds were shared between the 4 oxygens and the 2 charges as well. The bond order would therefore be 1.5 for each S-O since next to the **σ** bond there is a half ***π*** bond and a charge – ½ on each oxygen which gives the sulfate ion a rigorously **tetrahedral** structure. We say that the oxygens are equivalent by **resonance**

phenomenon; this is applicable to all **oxoanions**. We always have this phenomenon in an oxoanion. The bond order between the central atom and the oxygens will be given by:

$$B.O. = \frac{\text{number bonds } \sigma + \text{number bonds } \pi}{\text{number of oxygens}}$$

And the charge carried by each oxygen will be:

$$\text{charge} = \frac{\text{total charge}}{\text{number of oxygens}}$$

2°) Molecular orbital theory

This theory was developed during the 1930s, following in particular the work of Erwin **SCHRÖDINGER**. Nobel Prize–winning Austrian It appeared necessary because neither the theory of LEWIS nor the theory of hybridization (or of the valence bond) allowed to adequately describe the behavior of molecules, sometimes simple, such as dioxygen O_2. We will start with the hydrogen atom, the simplest of the chemical elements, and we will study the formation of the dihydrogen molecule H_2.

The SCHRÖDINGER equation gave as a solution describing the behavior of the single electron of the hydrogen atom, in itsfundamental, the wave function Ψ_{1s}. The mathematical form of this wave function is as follows:

Radial part R(r)	Angular part Θ(θ).Φ(ϕ)
$2\left[\frac{Z}{a_0}\right]^{\frac{3}{2}} \exp\left(\frac{-Zr}{a_0}\right)$	$\frac{1}{2\sqrt{\pi}}$

In the case of hydrogen, Z is 1 and a_0 denotes the radius of the first BOHR orbit, namely 0.53 angstroms. Note that it is independent of θ and ϕ. Similarly, the sign of Ψ is given by that of the radial part R(r). It is obviously positive since the exponential is always positive.

Thus, we will construct the dihydrogen molecule H_2 using a linear combination (purely mathematical operation) of the Ψ_{1s} orbitals of the hydrogen atom "number 1" and the hydrogen atom "number 2" of the future molecule. The **linear combination of atomic orbitals** will lead to a "molecular orbital".

This theory is called in French abbreviated form "C.L.O.A"; that is to say "linear combination of atomic orbitals" and, in English "L.C.A.O.", that is to say "linear combination of atomic orbitals". There will in fact be two ways of combining these atomic orbitals: a "constructive" way, which we will call "bonding" and a "destructive" way, which we will call "antibonding":

- **"Bonding" way** of combining the Ψ_{1s} atomic orbitals of two hydrogen atoms:

Ψ^+ bonding molecular orbital = $A\Psi_{1s}$ (atom 1) + $B\Psi_{1s}$ (atom 2) denoted **σ**.

A and B are two normalization constants of the molecular binding function Ψ, so that molecular binding Ψ^2 is, when integrated over the whole space, equal to unity, that is to say, having a 100% chance of finding the binding electrons in the whole space. A and B are positive. We add in the binding way the two wave functions Ψ_{1s} which are both positive.

- **"Antibonding" way** of combining the Ψ_{1s} atomic orbitals of two hydrogen atoms:

Ψ^- antibonding molecular orbital = $A\Psi_{1s}$ (atom 1) - $B\Psi_{1s}$ (atom 2) denoted σ*.

A and B are the same normalization constants as before, during the "binding" linear combination, but we will notice the minus sign between the two terms. The wave function Ψ_{1s} being positive, we note here that we remove a negative part, in this case B. Ψ_{1s} (atom 2) from a positive part, in this case A. Ψ_{1s} (atom 1).

The development of these overlap integrals reveals for the binding OM an overlap zone between the 2 nuclei; which corresponds to the creation of a chemical bond between the 2 protons. The antibonding OM also shows a probability of zero presence of the 2 electrons at an equal distance from these 2 nuclei.

The basic idea for a new representation is to keep the notion of particle, but abandon the classical idea of the localization of the particle on a trajectory. A quantum particle is associated with a function $\Psi(\vec{r},t)$ called wave function, which characterizes the state of the particle. The space and time variables can be separated as follows:

$$\Psi(\vec{r},t)=\Psi(x,y,z,t)=\Psi(x,y,z)\cdot e^{-i\omega t}$$

- $\Psi(\vec{r},t)$ is a real or complex mathematical function that has no physical meaning of its own. It does not allow the trajectory of the particle to be determined since this notion no longer has any meaning [2].
- However, the square of the modulus $|\Psi(\vec{r},t)|^2$ or $(\Psi^*\cdot\Psi)$ the product if $\Psi(\vec{r},t)$ is complex has a physical meaning, since it represents the **probability density of the presence** of the particle at time t. In other words, the probability of finding the particle in an element of volume $dV = dx\cdot dy\cdot dz$, centered around the point $M(x,y,z)$, is given by the relation:

$$dP=\Psi^2(x,y,z)\cdot dV.$$

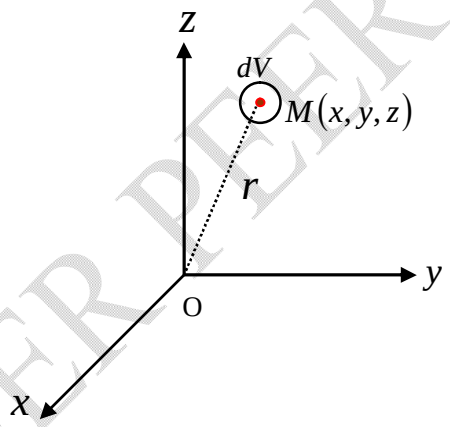

Figure 4 : representation of the particle in space

Some properties of Ψ

- Ψ is the amplitude of the wave function associated with the moving electron.
- Ψ must be stationary, that is, periodically return to the same value at each point.
- Ψ must be normalized: the probability of finding the electron in all the space around the nucleus must be equal to 1, that is to say certain.

$$P=\int dP=\iiint_{espace}\Psi^2 dV=1$$

- Ψ must be continuous, finite, univocal, differentiable (twice), and cancel at the places where the particle cannot be found ($\Psi \to 0$ when the electron is at an infinite distance from the nucleus).

The overlap of two functions Ψ_i and Ψ_j is called the integral calculated over the entire space of the product of Ψ_i by Ψ_j. To simplify the writing, we will use **Paul Dirac**'s notation:

$\langle \Psi_i | \Psi_j \rangle$, of «*bra* «$\langle \Psi_i |$ and «*ket* «$| \Psi_j \rangle$.

$$S = \langle \Psi_i | \Psi_j \rangle = \int_{espace} \Psi_i^* \Psi_j \, dV$$

With Ψ_i^*: is the complex conjugate function of Ψ_i; dV s an infinitesimal volume element.

- The overlap between two solution functions Ψ_i and Ψ_j is zero. Functions are said to be orthogonal : $\langle \Psi_i | \Psi_j \rangle = 0 \quad si \quad i \neq j$ if

- The overlap of a function Ψ_i with itself, $\langle \Psi_i | \Psi_i \rangle$ is equal to 1, if it is normalized: $\langle \Psi_i | \Psi_i \rangle = 1$. In our case $S_{AB} = \prec \Psi_A | \Psi_B \succ$ is called the overlap integral. Each orbital is normalized:

$$\int_{espace} \left\| \Psi^+ \right\|^2 dV = \int_{espace} \left\| \Psi^- \right\|^2 dV = 1$$

Thus, we will establish an energy **diagram of the molecular orbitals** of the dihydrogen molecule. The filling of the OM is carried out taking into account:

- from the stability principle: we start by occupying the lowest energy OMs;
- of the **Pauli** exclusion principle: at most two electrons in an OM;
- from **Hund**'s rule: we occupy the maximum of OM of the same energy; the electrons having parallel spins.

↑ Growing sense of energies	O.A. Atomic orbitals of hydrogen atom number 1	O.M. Molecular orbitals of the dihydrogen molecule, H_2	O.A. Atomic orbitals of hydrogen atom number 2
	.	—— Antibonding molecular orbital	.
	_↑_	.	_↑_
	.	_↑↓_ Bonding molecular orbital	.

Figure 5 : Diagram of the molecular orbital of the dihydrogen molecule

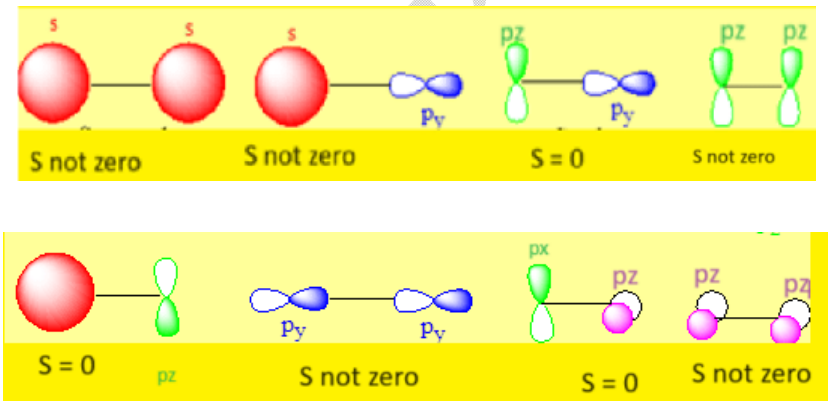

Scheme 28 : Zero and non-zero overlaps of some pairs of s and p orbitals

3°) Molecular orbital diagram (MOD)

3-1 Diatomic molecules A_2

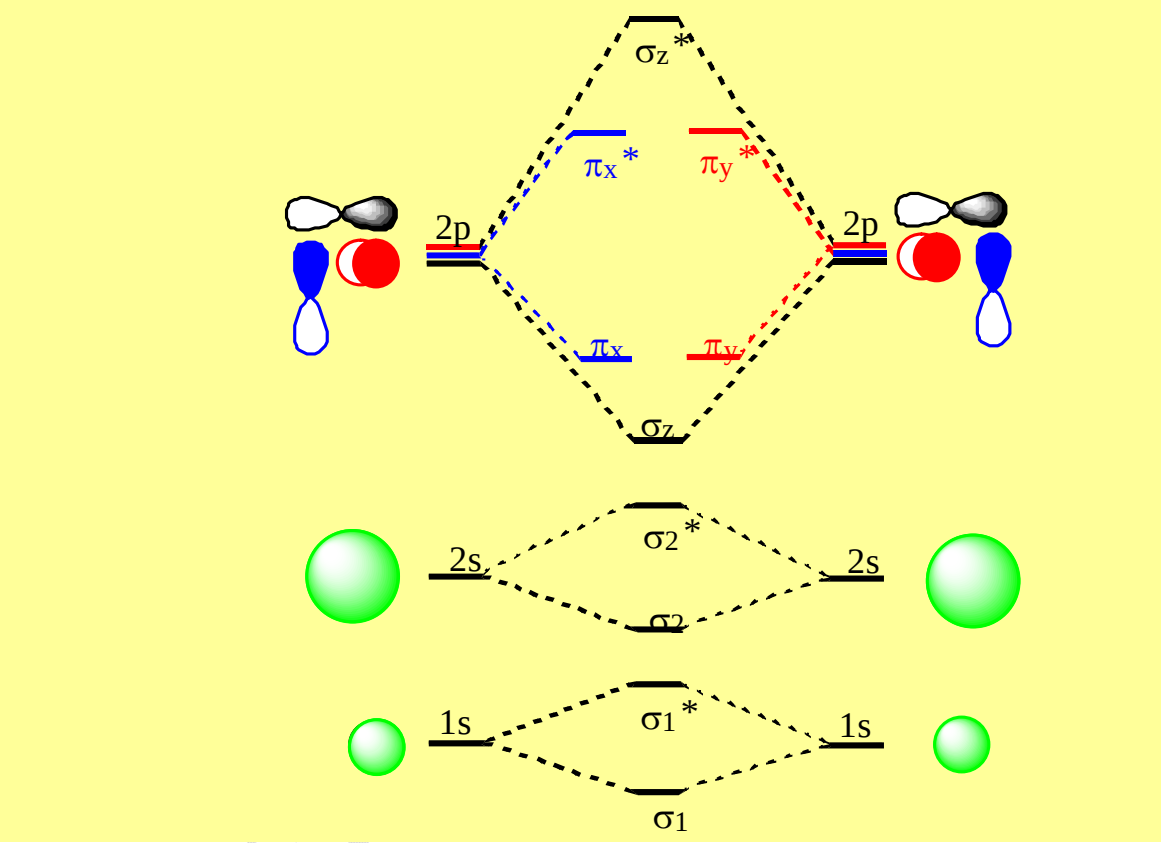

Figure 6 : Diagram of the molecular orbital of a diatomic molecule

To characterize the number of bonds formed in a molecule, we use the concept of bond index **b.i.** = ½ (number of e^- contained in the bonding MOs – number of e^- in the antibonding MOs)

Examples

For hydrogen: H_2 $1s^2$

The MOD of dihydrogen is represented. A molecular orbital cannot contain more than two electrons. The energy of the system is the sum of the energies of each electron. The 2 electrons are placed in the bonding orbital **σ**.

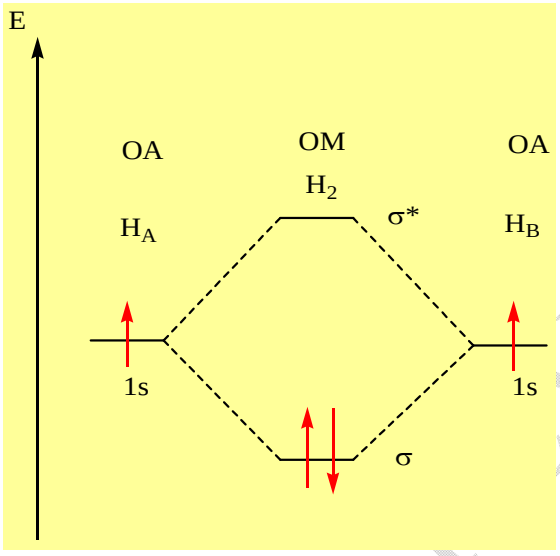

Figure 7 : MOD of the dihydrogen molecule

For nitrogen : N : $1s^2 2s^2 2p^3$

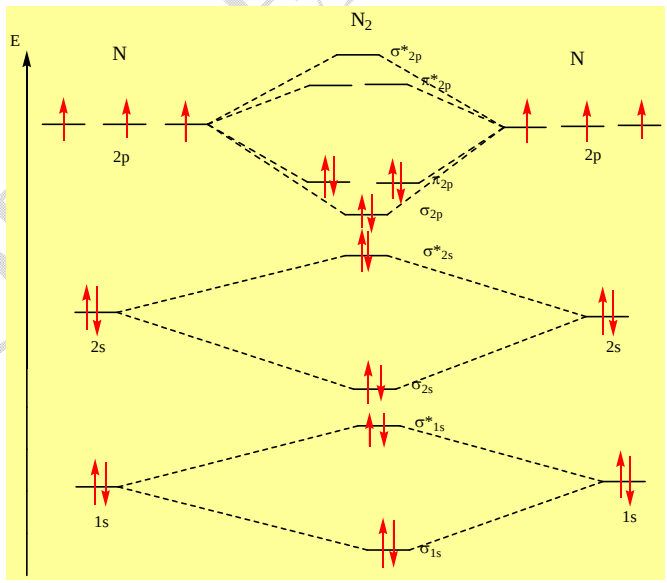

Figure 8 : MOD of the dinitrogen molecule

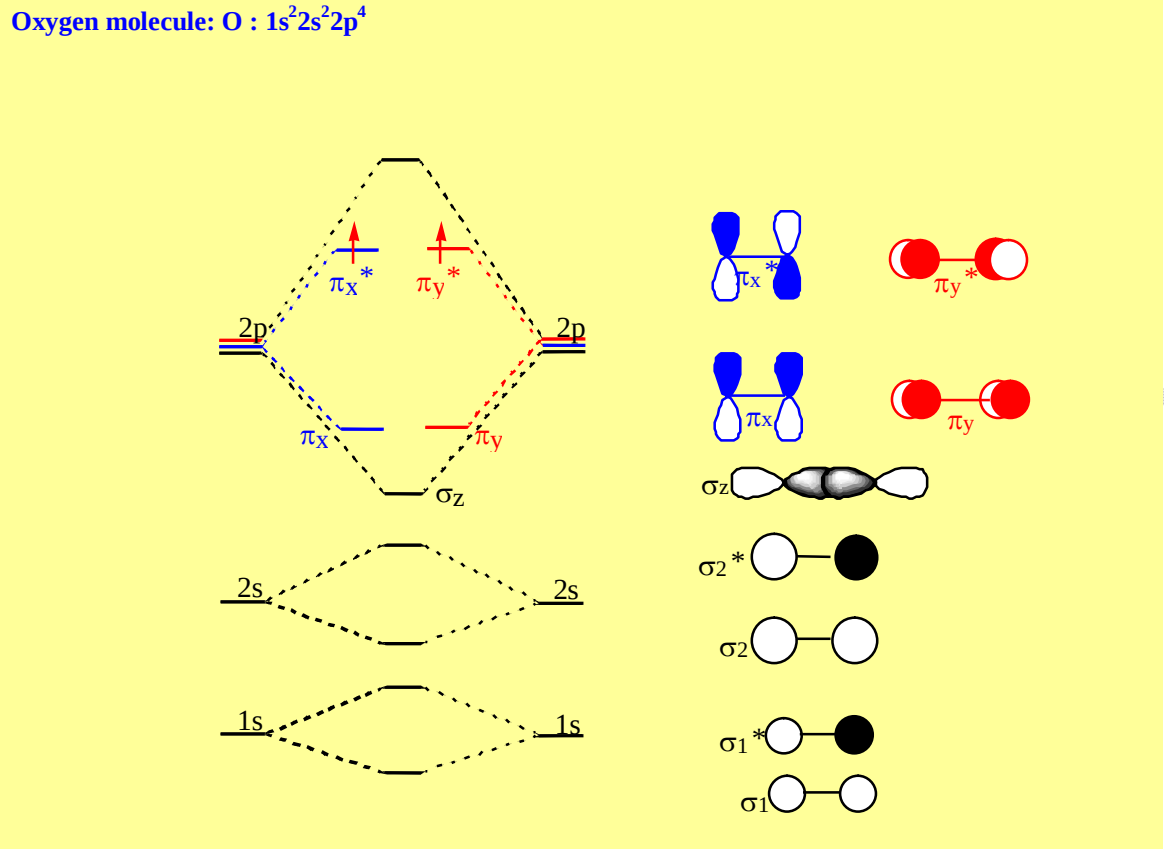

Figure 9 : MOD of the dioxygen molecule

3-2 Organometallic complex of transition metals

These complexes are those for which the metal has as ligands CO, amines, N donor ligands, O donors, X- halides. The donor orbital has a lower energy than that of the acceptor orbital.

Example : $[Cr(NH_3)_6]^{3+}$, Cr^{3+} et NH_3 ; Cr^{3+} : $3d^3 4s^0 4p^0$.

$\sigma_s = 4s + (h_1 + h_2 + h_3 + h_4 + h_5 + h_6)$; $\sigma_s^* = 4s - (h_1 + h_2 + h_3 + h_4 + h_5 + h_6)$

$\sigma_1 (p) = p_y + (h_2 - h_4)$; $\sigma_1^*(p) = p_y - (h_2 - h_4)$; $\sigma_2 (p) = p_x + (h_3 - h_1)$ et $\sigma_2^*(p) = p_x - (h_3 - h_1)$;

$\sigma_3 (p) = p_Z + (h_5 - h_6)$ et $\sigma_3^*(p) = p_Z - (h_5 - h_6)$; $\sigma_1 (d) = d (z^2) + (h_5 + h_6 - h_1 - h_2 - h_3 - h_4)$;

$\sigma_1^*(d) = d (z^2) - (h_5 + h_6 - h_1 - h_2 - h_3 - h_4)$; $\sigma_2 (d) = d (x^2 - y^2) + (h_1 + h_3 - h_2 - h_4)$;

$\sigma_2^*(d) = d (x^2 - y^2) - (h_1 + h_3 - h_2 - h_4)$. Les h_i are hybridized sp^3.

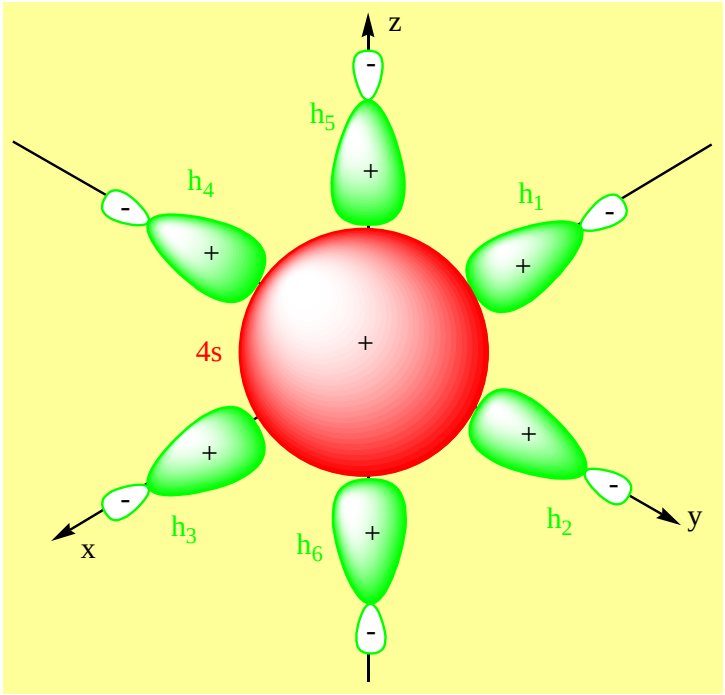

Scheme 29 : overlap between Cr^{3+} s orbitals and NH_3 hybrids

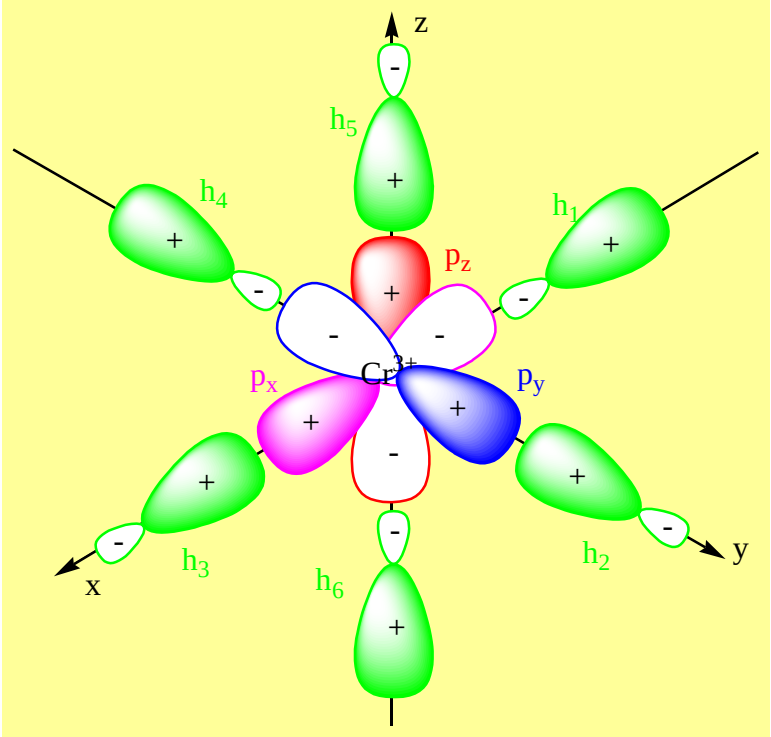

Scheme 30 : overlap between Cr^{3+} p orbitals and NH_3 hybrids

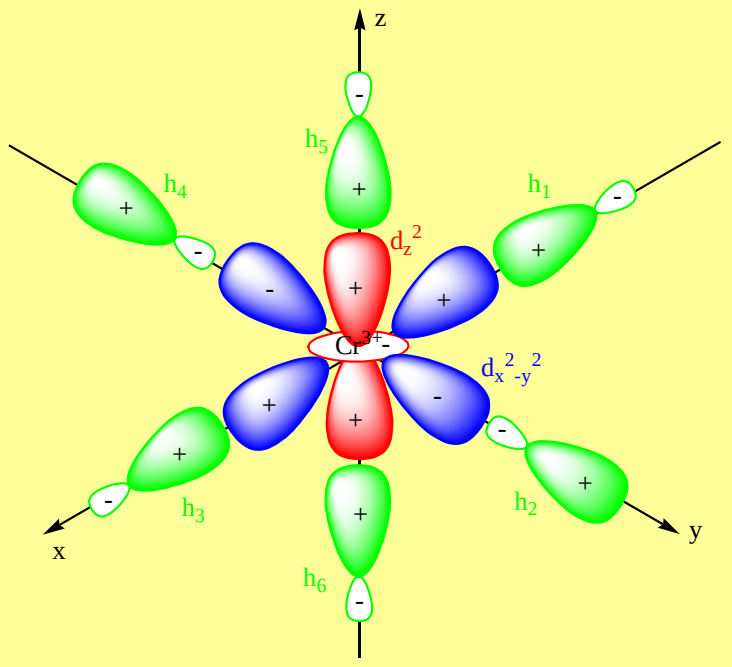

Scheme 31 : overlap between Cr^{3+} d orbitals and NH_3 hybrids

The d_{xy}, d_{yz} and d_{zx} orbitals are between the axes so will not be on the directions from which there is no perturbation when approaching the ligand. These are the d_{z^2} + σ (NH_3) and $d_{x^2-y^2}$ + σ (NH_3) orbitals which interact. The ωd are degenerate (of the same energy) so have parallel spins because of **Hund**'s rule. The ωd has three electrons so is not saturated hence $Cr(NH_3)_6^{3+}$ is **unstable**; it can therefore accept other electrons. On the other hand for $Cr(CO)_6$; Cr is a d^4 hence we have 6 electrons in σ_p; 2 electrons in σs; 4 electrons in σ_d; 6 electrons in ω_d or in all 18 electrons around the Chromium. $Cr(CO)_6$ is therefore more **stable** than $Cr(NH3)_6^{3+}$.

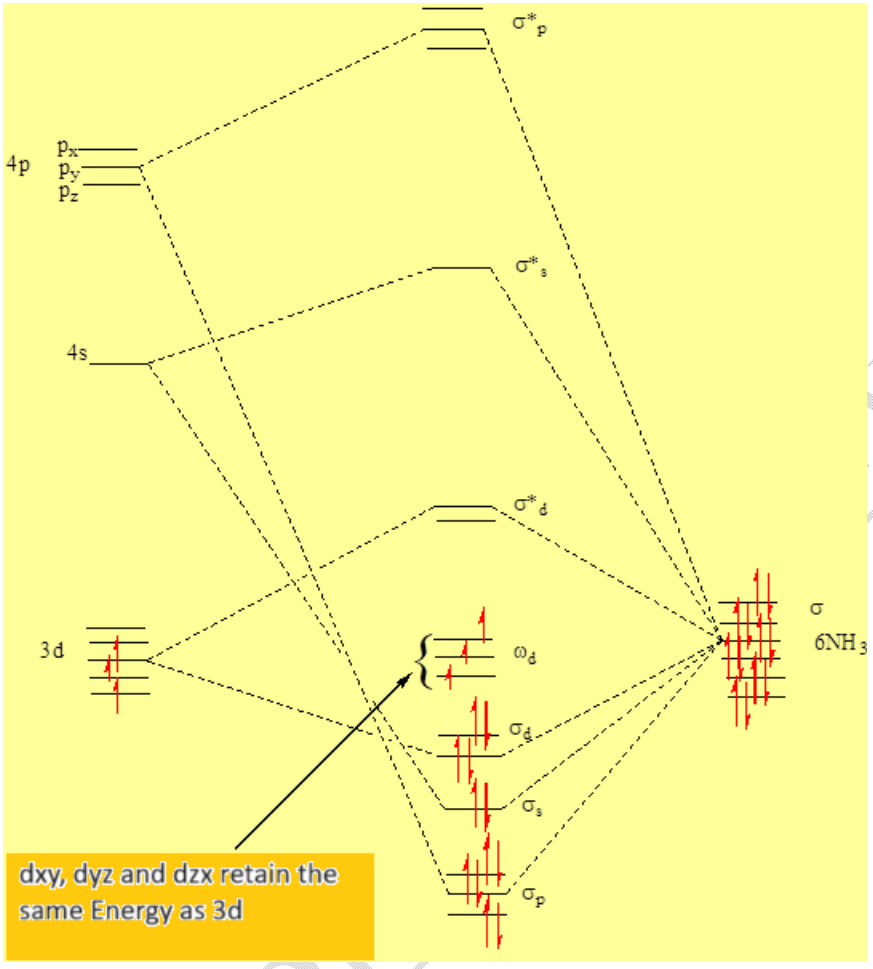

Figure 10 : MOD of the complex $[Cr(NH_3)_6]^{3+}$

Chapter 2

Geometry of compounds

I- The charge repulsion model or Gillespie model (VSEPR)

This model, very simple, does not require the use of quantum theory; it therefore does not involve the constructions of atomic orbitals. It is satisfied, as a starting point, with the **Lewis** notation for atoms. The central element has or does not have free pairs.

1°) Origin

In 1957, the Canadian chemist **R. J. Gillespie**, taking up an idea put forward by the British **N. Sigdwick** and **H. Powell** in 1940, developed the theory of **VSEPR** (Valence Shell Electron Pair Repulsion). The VSEPR method can be considered as an extension in the stereochemical field of the description of chemical bonding by electronic pairing by **G. N. Lewis** (1916). It allows the geometry of all simple molecules to be predicted [4].

The electrons in the valence shell of most molecules and stable ions are even in number (there are molecules with an odd number of electrons such as NO_2 but this remains quite rare). **Pauli**'s principle (1920) states that only electrons with opposite spin quantum numbers evolve in the same region of space because they are described by the same orbital. These electrons can be grouped in pairs or doublets.

In the **Lewis** model, the bond between two atoms is described by the sharing of a pair of electrons: this is called a bonding pair. The pairs of electrons not used to describe the bonds constitute the non-bonding pairs denoted E.

Doublets	Binders	Non-binding
Number	n	p

2°) Basic Principles

The initial approximation of the theory consists in assimilating the pairs of electrons to point electric charges. As a first approximation, they are subject to moving on a sphere whose center is occupied by the central atom. The geometric arrangement that they adopt on this sphere is the consequence of their mutual repulsion.

Although this is not strictly speaking an electrostatic interaction between point charges, because the behavior of electrons is governed by the laws of quantum mechanics, a correct result is obtained by looking for the arrangement that maximizes the distances between pairs of electrons.

At this first level of approximation, there is no distinction to be made between a bonding doublet and a non-bonding doublet.

Under these conditions, the arrangement that minimizes the repulsion of the doublets depends only on their number**: n + p**. This corresponds to the following geometric figures, limiting itself to coordination seven. If $p = 0$ the environment is equal to the geometry; if $p \neq 0$ the environment is different from the geometry.

Table 3 : Arrangement in relation to the environment

n + p	Arrangement
2	Straight line segment
3	Triangle
4	Tetrahedron
5	Trigonal bipyramid
6	Octahedron
7	Pentagonal bipyramid

These six types of arrangements correspond to more distributions of electron pairs that we will review. In the following, **X** denotes a bonding pair and **E** a non-bonding doublet.

As a first approximation, multiple bonds are treated as if they involved only a single doublet.

Principle : Bonding and lone electron pairs repel each other. Therefore, they are distributed in space in such a way as to minimize their repulsion.

This model explains the geometry of electronic pairs around a central atom. Several shapes of molecules can correspond to the same geometry.

3°) Rules and notations VSEPR

To determine the geometry of a molecule by theory VSEPR :

- We start by determining the Lewis structure of the molecule;
- We count the number of free pairs and bonding pairs;
- The molecule is written in the form AX_nE_p where **A** is the central atom of the molecule, **X** represents the bonding pairs, **E** the free pairs, **n** and **p** represent the number of pairs of each type;
- The total number of **n + p** pairs gives the most stable spatial distribution. This arrangement indicates the environment of the central element.

Ruler n°1 : The repulsion between the electron pairs (free and bonding) must be minimized. These are distributed in the available space. Therefore the n electron pairs are distributed in space in such a way as to ensure maximum distribution.

Ruler n°2 : Lone pairs occupy more space than bonding pairs because they are only subject to the attraction of a single nucleus, unlike the bonding pair which is compressed by the attraction of two nuclei. In addition, if the different positions are not equivalent, the lone pairs will preferentially place themselves where there is more space.

Case of molecules with 2 electronic pairs

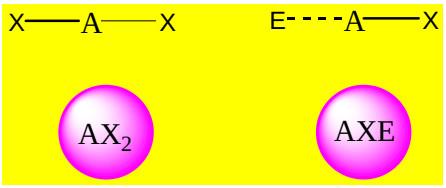

Scheme 32 : representation of molecules with 2 electronic pairs

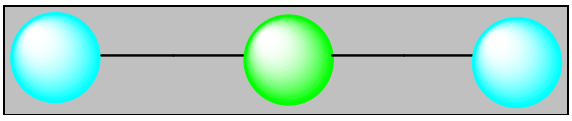

Scheme 33 : Example $BeCl_2$

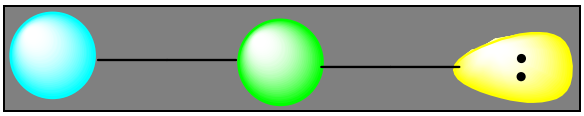

Scheme 34 : Example CO

If we have two pairs, they will be opposite; the molecule will be linear and the angle between the two pairs is a flat angle (180°). The arrangement and geometry of these types of molecules are linear. These are the AX_2 type molecules. Beryllium, an element in the second column of the periodic table with electronic configuration $\boldsymbol{1s^2 2s^2}$, is linked by 2 single bonds to two chlorine atoms in the $BeCl_2$ molecule.

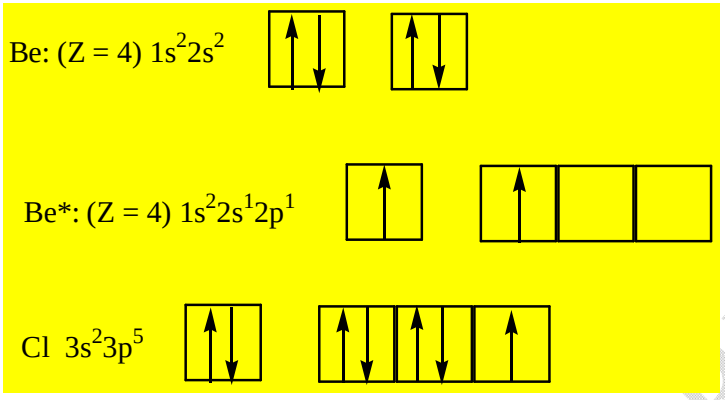

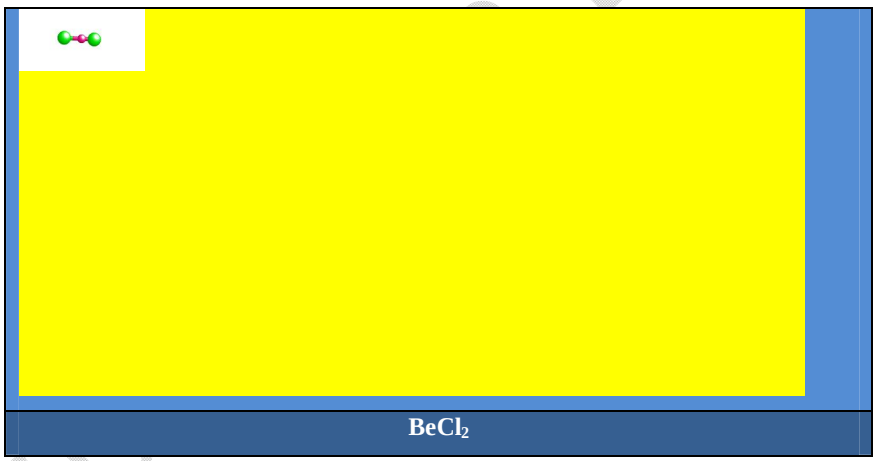

Figure 11 : molécule of $BeCl_2$

Molecules with multiple bonds

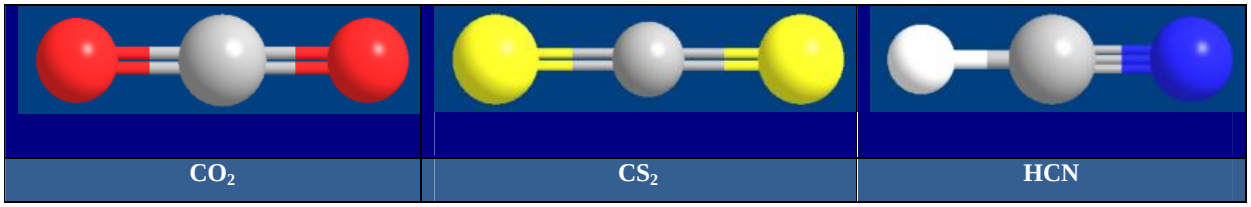

Figure 12 : Some molecules

- ***Case of molecules with 3 electronic pairs***

There are two families. The molecules can be of type AX_3 and AX_2E.

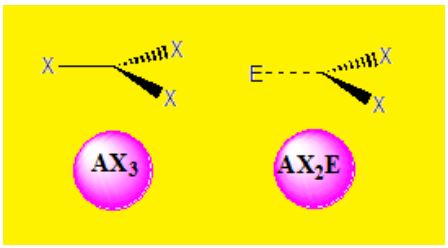

Scheme 35 : representation of molecules with 3 electronic pairs

For a compound of type AX_3, we will have three pairs located in the same plane and at equal distance from each other: 120° (***sp²***), The molecule has the shape of an equilateral triangle. The molecule is triangular (example BF_3).

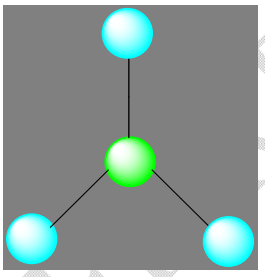

Scheme 36 : representation of the AX_3 molecule

A molecule of type AX_2E is angular but the arrangement remains triangular. The angle is close to 120° (example $SnCl_2$).

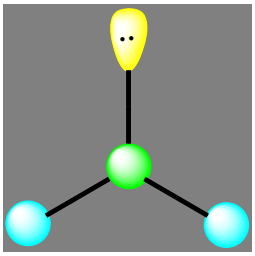

Scheme 37 : representation of the molecule of AX_2E

Molecules with single bonds:

B: [He] $2s^2 2p^1$

Sn: [Kr] $4d^{10} 5s^2 5p^2$

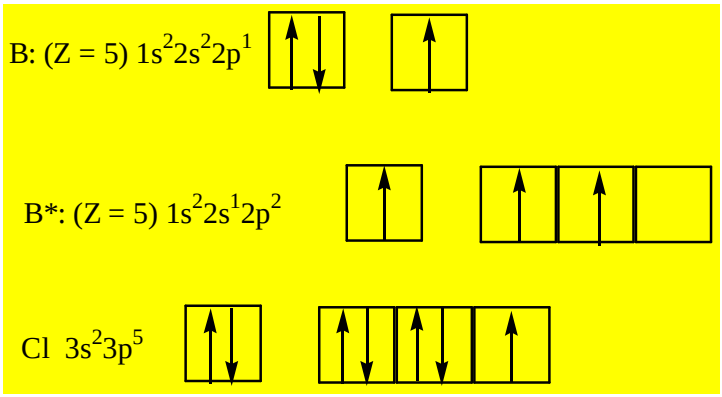

Figure 13 : representation of the electronic structures of boron and chlorine

The decrease in angle from 120° to 109° is due to the presence of the free pair which tends to occupy much more space.

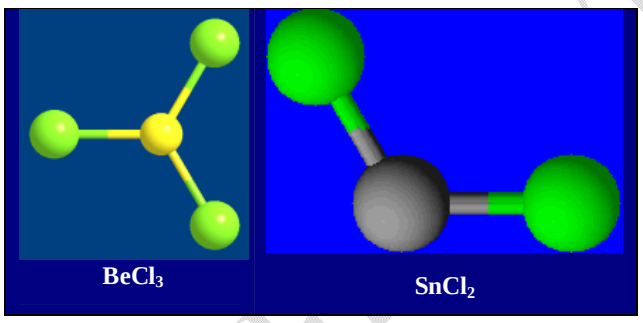

Figure 14 : representation of $BeCl_3$ and $SnCl_2$

Molecules with multiple bonds: S: [Ne] $3s^2 3p^4$; O : [He] $2s^2 2p^4$ et N : [He] $2s^2 2p^3$

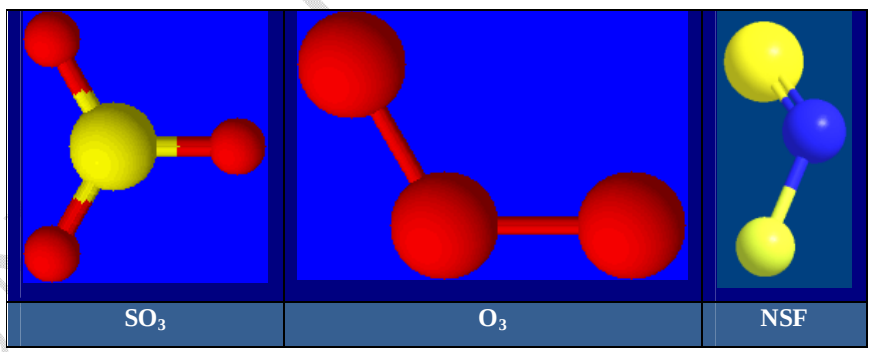

Figure 15 : reprexentation of SO_3, O_3 and NSF

Case of molecules with 4 electronic pairs

There are three families: AX_4 ; AX_3E et AX_2E_2

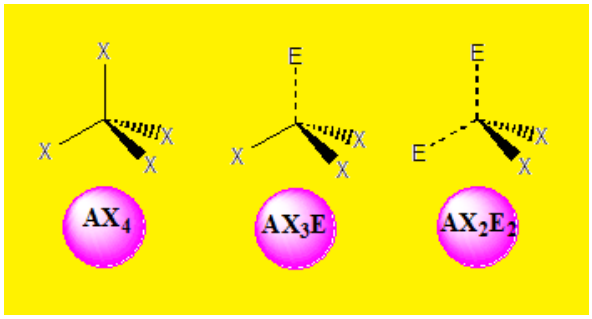

Scheme 38 : representation of molecules with 4 electronic pairs

For AX_4 the molecule is tetrahedral. Four bonding pairs directed towards the vertex of a regular tetrahedron and located at 109°5 from each other. The molecule is tetrahedral in shape. An example is methane CH_4.

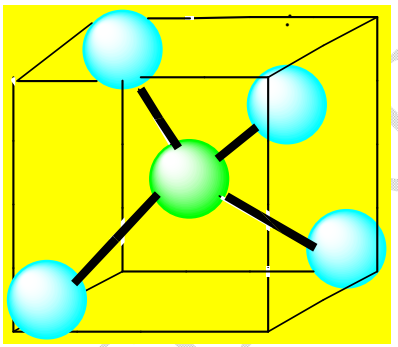

Scheme 39 : representation of AX_4

For AX_3E we have a tetrahedral distribution the angle is 107°3 in the case of ammonia NH_3; the geometry is pyramidal.

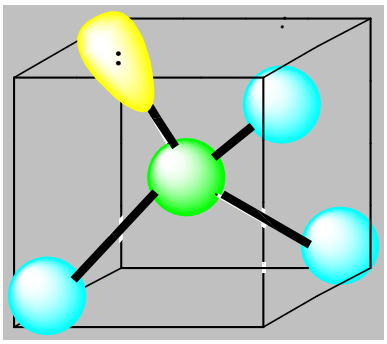

Scheme 40 : representation of AX_3E

For AX_2E_2 the environment is tetrahedral the geometry is “V” or angular or angled. For H_2O the angle is 104.5°.

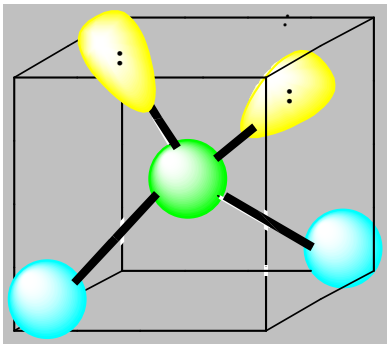

Scheme 41 : representation of AX_2E_2

Molecules with single bonds.

Si : [Ne] $3s^2 3p^2$; P : [Ne] $3s^2 3p^3$ et O : [He] $2s^2 2p^4$

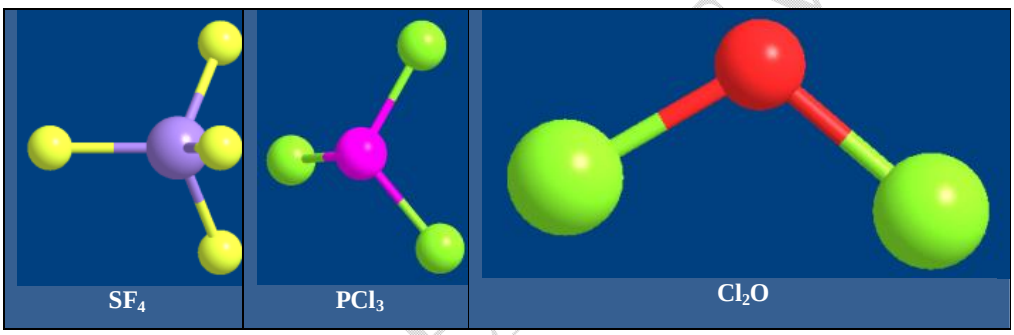

Figure 16 : representation of molecules SF_4, PCl_3 and Cl_2O

The angles decrease when moving from AX_4 to AX_2E_2 because the number of free pairs increases around the central element.

Molecules and ions with multiple bonds

S : [Ne] $3s^2 3p^4$

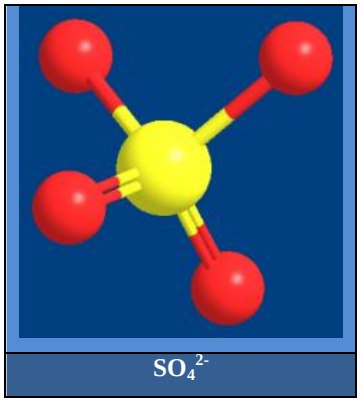

Figure 17 : representation of the sulfate ion

Case of molecules with 5 electronic pairs

The most widespread and **stable** geometric figure corresponding to this arrangement is the trigonal bipyramid. A complication arises here due to the non-equivalence of the positions at the vertices of the bipyramid. They can be classified into two categories: axial (a) and equatorial (e):

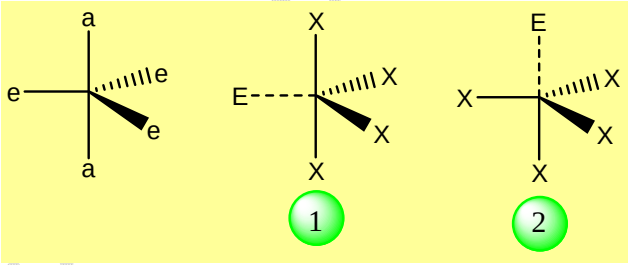

Scheme 42 : representation of the spatial distribution of the 5 pairs

The average volume in which the electrons of a non-bonding doublet evolve is greater than that available to the electrons of a bonding doublet. These simple considerations allow us to establish the following hierarchy in the repulsion between the pairs

Non-Binder-Non-Binder stronger than Binder-Binder

A convenient parameter to evaluate the order of magnitude of the repulsion between the doublets is the central angle α formed by the directions between them and the central atom. Using this parameter, we can compare the stabilities of the two arrangements (1) and (2) by counting the interactions on the basis of the previous inequalities, taking into account only the interactions for which $\alpha \leq 90°$, the others being assumed to be negligible.

For arrangement (**1**) the E doublet interacts with 2 X atoms ;

For arrangement (2) the E doublet interacts with 3 X atoms.

The first arrangement is therefore more **stable** than the second. This arrangement corresponds to a category of molecules that we can call with **Gillespie**: deformed tetrahedral molecules and to which SF_4 belongs. Experimentally, no stereoisomer of this molecule is known.

A study of the same type carried out for the other a priori possible arrangements in pentagonal geometry, shows that the non-bonding electronic pairs and the multiple bonds (double or triple) and the large substituents must preferentially occupy the **equatorial positions** where they take up the most space.

There are four families: AX_5 ; AX_4E ; AX_3E_2 and AX_2E_3. In a trigonal bipyramid the lone pairs are always placed in the equatorial position where they occupy the most space.

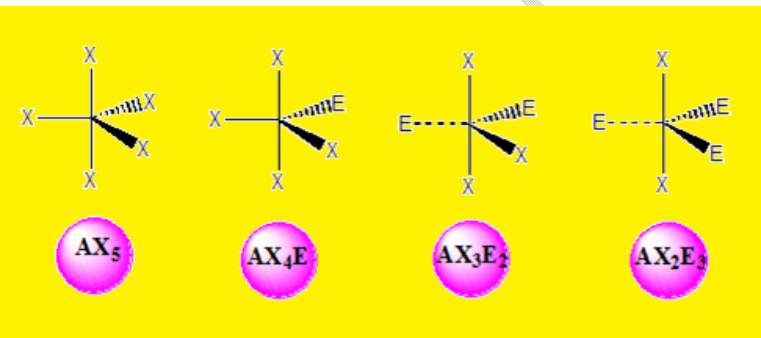

Scheme 43 : representation of molecules with 5 pairs

For AX_5, there are five bonding pairs. The pairs form an angle of 120° between them. The geometry of PCl_5 is trigonal bipyramidal.

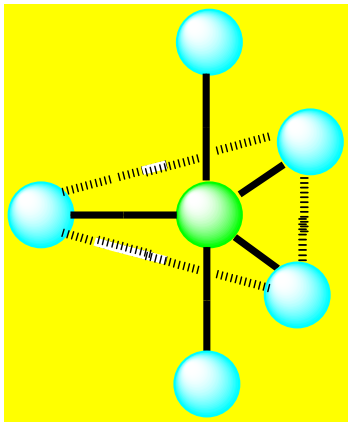

Scheme 44 : representation of AX_5

For AX_4E geometry is a deformed tetrahedron. Example SF_4.

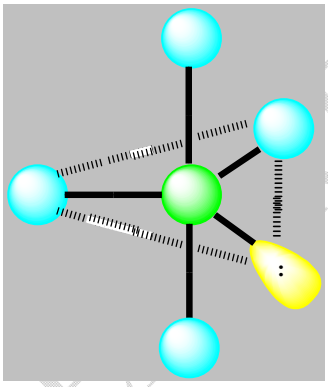

Scheme 42 : representation of AX_4E

For AX_3E_2 the geometry is peaked or “T” shaped. Example ClF_3.

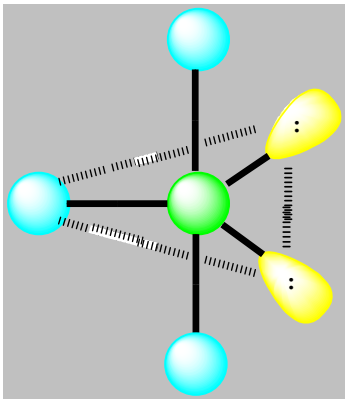

Scheme 45 : representation of AX_3E_2

For AX_2E_3 geometry is linear. This is the example of XeF_2.

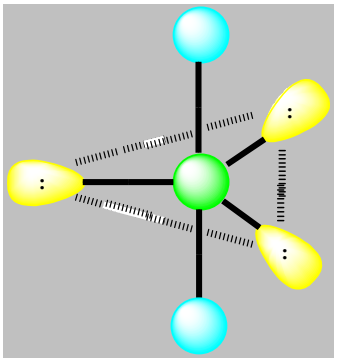

Scheme 46 : representation of AX_2E_3

Molecules and ions with single bonds

P	S	Cl	I
[Ne] $3s^2 3p^3$	[Ne] $3s^2 3p^4$	[Ne] $3s^2 3p^5$	[Kr] $4d^{10} 5s^2 5p^5$

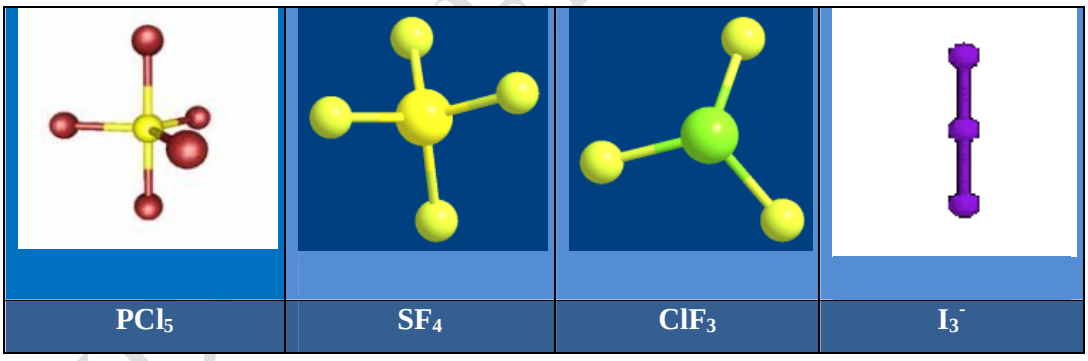

Figure 18 : representation of PCl_5, SF_4, ClF_3 and I_3^-

Molecules and ions with multiple bonds

S : [Ne] $3s^2 3p^4$ et I : [Kr] $4d^{10} 5s^2 5p^5$

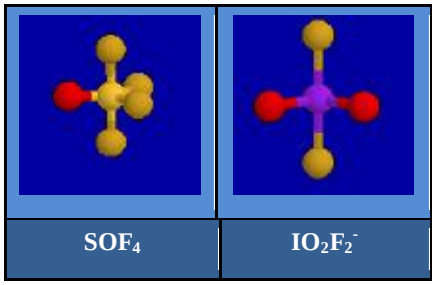

Figure 19 : represrntation of SOF_4 and $IO_2F_2^-$

NB : Antimony Sb tends to have a square-based pyramidal environment (example SbF_5).

- ***Case of molecules with 6 electronic pairs***

We distinguish the following three families: AX_6 ; AX_5E and AX_4E_2.

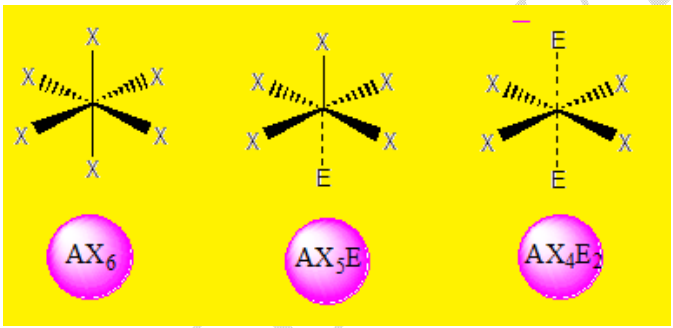

Scheme 47 : representation of molecules with 6 electronic pairs

For AX_6 we have six bonding pairs. The pairs in the equatorial plane form 90° angles with each other. The axial bonds form an angle of 120° with the others. The free pairs that occupy different but geometrically equivalent positions in the octahedron in the equatorial plane must be placed as far as possible from each other. Thus in AX_4E_2 we say that these free pairs are in the trans position and the bonding pairs in the cis position.

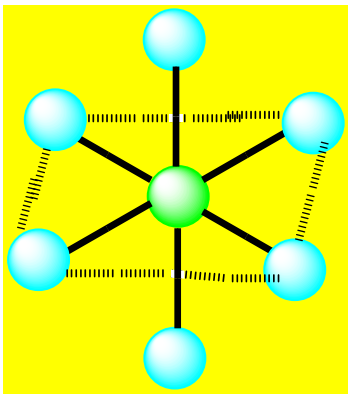

Scheme 48 : representation of AX_6

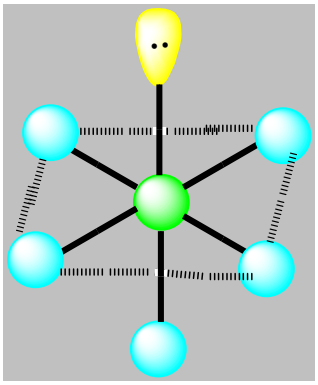

Scheme 49 : representation of AX_5E

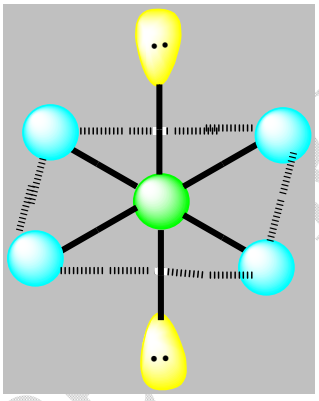

Scheme 50 : representation of AX_4E_2

Molecules with single bonds: S : [Ne] $3s^2 3p^4$; Br : [Kr] $3d^{10} 4s^2 4p^5$ et I : [Kr] $4d^{10} 5s^2 5p^5$

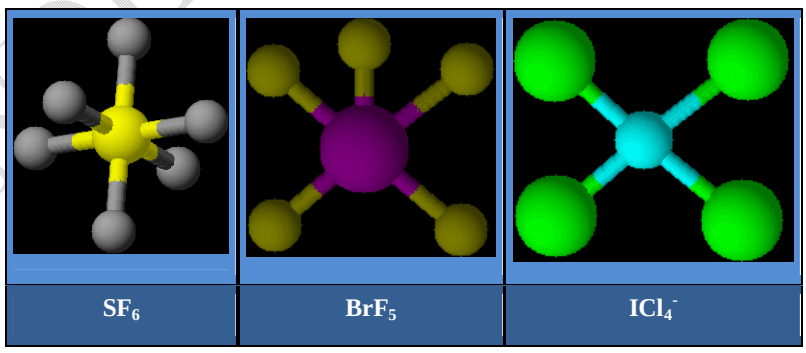

Figure 20 : representation of SF_6, BrF_5 and ICl_4^-

Molecules with multiple bonds: In a molecule when we have a multiple bond; we treat it as the lone pair because a multiple pair is larger than a single bonding pair.

I : [Kr] $4d^{10}5s^25p^5$ et Xe : [Kr] $4d^{10}5s^25p^6$

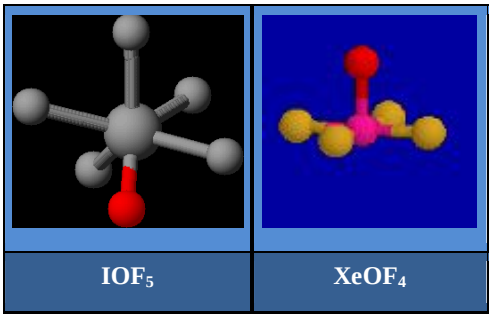

Figure 21 : representation of IOF_5 and $XeOF_4$

4°) Case of molecules with multiple bonds

- For trigonal bipyramids, multiple bonds and lone pairs always place themselves in equatorial positions to minimize repulsions because they occupy more space. Similarly, the largest and most electropositive atoms occupy the equatorial positions.
- For square-based pyramids, multiple bonds and lone pairs always place themselves in axial positions. Similarly, more electronegative atoms occupy these positions.

5°) Case of ions

- In the case of ions we follow the same rules as in that of neutral molecules.
- To determine the structure of anions, negative charges are assigned to the most electronegative atoms except in the case of oxoanions where the charges are carried by the oxygen atoms.

6°) Second order effects

- **Influence of lone pairs on standard bond angles**

At a second level of approximation, it is logical to admit that the non-bonding doublets, less confined in the internuclear space than the bonding doublets, occupy a higher average volume. This is how we interpret the progressive decrease in the angle between the bonds when going from CH_4 to NH_3 then H_2O. The free pair occupies more space; the bonding pairs will come **closer** to make room for it, which explains the **closing** of the solid angle of nitrogen (107°3) instead of 109°5 in the regular tetrahedron.

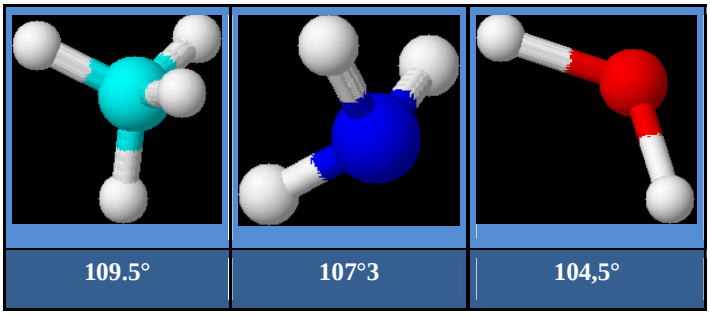

Figure 22 : representation of CH_4, NH_3 and H_2O

A similar trend is observed for ionic derivatives of ammonia.

Table 4 : Angles of ionic deviations of ammonia

NH_4^+	NH_3	NH_2^-
109.5°	107°3	104°

Triangular arrangement:

In the molecules of HCHO and $COCl_2$ shown below, the angle between the single bonds is less than 120°.

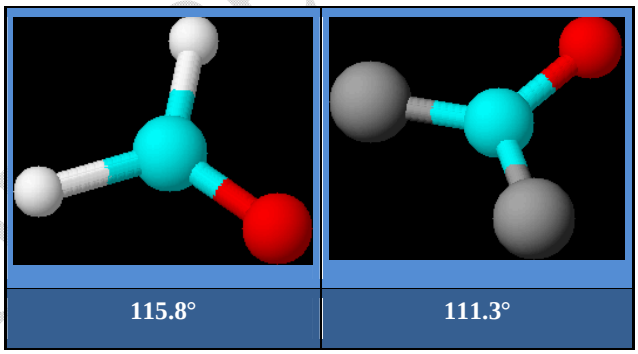

Figure 23 : representation of HCHO and $COCl_2$

Tetrahedral arrangement: The angle between single bonds closes as the bond order increases in the series: SiF_4, POF_3, NSF_3.

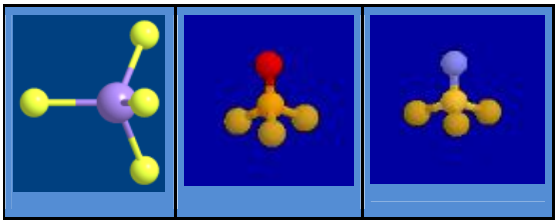

109.5°	102°	98°

Figure 24 : representation of SiF_4, POF_3, NSF_3

Pentagonal arrangement: The FSF angle is less than 120° in SOF_4.

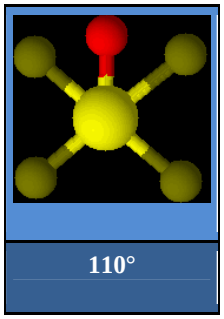

Figure 25 : representation of SOF_4

If we take the case of ClF_3; the environment is a trigonal bipyramid, the geometry is peaked due to the 2 pairs in equatorial position; the angle $F_{ax}ClF_{eq}$ = 87° instead of 90° because of the 2 free pairs.

Octahedral arrangement: If we take the case of BrF_5 ; the angle $F_{ax}BrF_{eq}$ = 85° instead of 90°.

- **Influence of multiple bond volume**

The overall geometric shape depends only on the □ bonds. We can therefore classify molecules with multiple bonds in the same groups as those with single bonds. On the other hand, the volume occupied by the electrons in space increases with the bond order. We therefore see a closing of the angle opposite the multiple bond.

- **Influence of electronegativity**

The volume occupied by the bonding doublets decreases when the difference in electronegativity of the bonded atoms increases. Drained towards the most electronegative atom, the bonding electrons more confined in the internuclear space repel each other less. For the same central atom, we observe a decrease in the angle between the bonds with the increase in the electronegativity of the peripheral atom. The evolution of the angles in the series: PI_3, PBr_3, PCl_3 and PF_3 testifies to this.

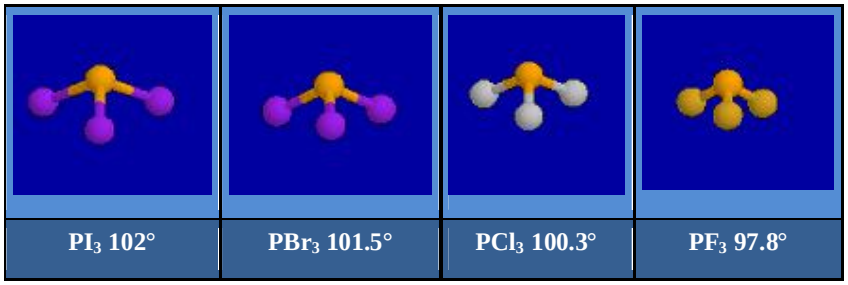

Figure 26 : representation of PI_3, PBr_3, PCl_3 and PF_3

Molecules NH_3, PH_3 and AsH_3 each have three hydrogen atoms and central atoms that are less and less electronegative.

Table 5 : Electronegativity of some elements

Element	N	P	As
χ (Pauling)	3.04	2.19	2.17

Moving from NH_3 to PH_3 and then AsH_3, the sharing of bond electrons is increasingly important and the bond doublets occupy less and less space in space. A decrease in the angle at the top of the pyramid is observed.

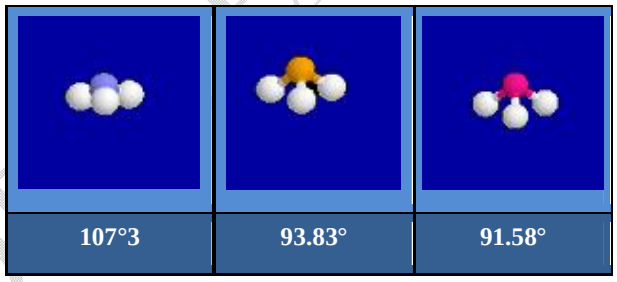

Figure 27 : representation of NH_3, PH_3 and AsH_3

Combination of volume and electronegativity effects

The effects described above can naturally add to or partially compensate for each other. In molecules C_2H_4 et $C_2F_2H_2$, the angles opposite the double bond are less than 120°. This is interpreted as follows: the volume occupied by the electrons of the double bond is greater than that occupied by the electrons of a single bond. In $C_2F_2H_2$ this angle is smaller than that observed in C_2H_4 because the highly polarized C-F bonds occupy less space than the C-H bonds.

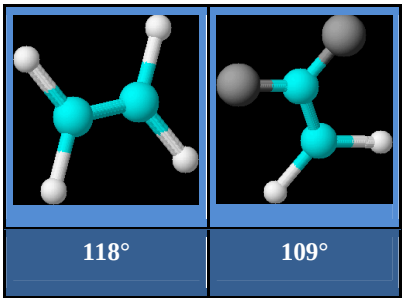

Figure 28 : representation of C_2H_4 and $C_2F_2H_2$

- **Non-equivalence of axial and equatorial positions in pentagonal geometry**

  It is known that the axial and equatorial positions are not equivalent in molecules such as PF_5 or PCl_5. The interaction involving lone pairs in the equatorial position is less than in the axial position. This results in a decrease in the length of the equatorial bonds and an elongation of the axial bonds.

  - Table 6 : bond length in axial and equatorial positions P-Cl

Bond	$P\text{-}Cl_{éq}$	$P\text{-}Cl_{ax}$
d (nm)	0.202	0.214

The non-equivalence between axial and equatorial position is also manifested for the bonding doublets. In the molecule PF_3Cl_2, Cl is less electronegative than F. The doublet ensuring the bond between P and Cl occupies a larger place than that between P and F. This explains why the isomer in which these atoms are in the equatorial position is the most stable.

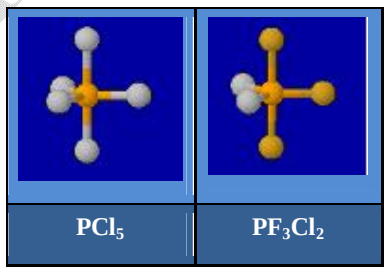

Figure 29 : representation of PCl_5 and PF_3Cl_2

For AX_5E type molecules like BrF_5, we observe a slight decrease in the angle between the bonds (85° instead of 90°) and an equatorial bond longer than the axial bond.

Table 7 : bond length in axial and equatorial positions Br-F

Bond	$Br\text{-}F_{éq}$	$Br\text{-}F_{ax}$
d (nm)	0.177	0.168

7°) Limitations of the method VSEPR

VSEPR theory is a method that allows predicting the geometries of all molecules whose central element is non-transitional or if it is transitional its internal layer is nd^5 or nd^{10}. This method most of the time allows the correct prediction of the local arrangement of electron pairs around an atom when it can be chosen unambiguously as the central atom. On the other hand, its application is much more problematic when it comes to predicting the global geometry of complex molecules. Thus it is not possible to predict the planarity of the ethylene molecule nor to explain why in allenes; the substituents are located in perpendicular planes. Furthermore, molecules are not static objects. This is particularly clear in molecules involving pyramidal atoms such as NH_3, PH_3. There are also more complex phenomena such as the exchange of axial and equatorial positions in pentagonal geometry.

II- Lewis Acid-Base Theory

According to Lewis an acid is an electron acceptor and a base an electron donor. A Lewis acid is a chemical entity with an electron vacancy which means that it can receive an electron pair.

Example : BF_3

In BF_3 boron is surrounded by six electrons on its outer shell and given the octet rule; it can have another doublet to surround itself with eight electrons. BF_3 therefore has an electronic vacancy hence it is acidic compared to boron. A Lewis base is a chemical entity having one or more free doublets on one of its atoms. Example NH_3 is a Lewis base compared to nitrogen.

A Lewis acid receives a pair of electrons from a Lewis base through its electron vacancy by **dative** bonding. A Lewis acid reacts with a Lewis base to form a coordination complex.

To write the formula of the complexes, we first write the metal then the ligands which we put in parentheses if they contain more than one atom, all between brackets and outside of these in superscript and on the right the charge of the complex, example $[Ni(CN)_4]^{2-}$.

Transitional and non-transitional metals are Lewis acids in most of their oxidation states. They can receive a doublet from each of the ligands surrounding them to give a coordination complex.

Example : $Zn^{2+} + 4\ Cl^- \rightarrow [ZnCl_4]^{2-}$

1°) Steric effects

When reacting an acid and a base one must always keep in mind the distortion that each molecule undergoes in its configuration within the compound formed. The presence of large substituents can affect the stability of the compound formed. This stability is reduced by the fact that the acid and base cannot come close enough to each other for the orbital overlap to be maximal.

Consider the complex formed between triethylamine and trimethylborane: $Et_3N: \rightarrow BMe_3$

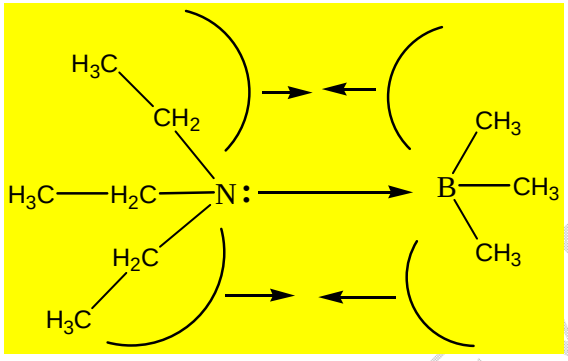

Scheme 51 : interaction between triethylamine and trimethylborane

This frontal hindrance phenomenon is called F-strain and it can have a considerable influence on the stability of the compounds formed since the cones of revolution of the large substituents can have a very wide base. If we compare this complex with $NH_3 - BF_3$; the distance between nitrogen and boron is smaller than that of the previous complex. The approach of nitrogen in this latter complex is hindered by the free rotation of the large substituents around the σ bonds which describe cones of revolution. There comes a time when these cones interfere and it will no longer be possible for the acceptor and donor atoms to get closer to each other [5].

2°) Back-strain or B-strain :

If we consider trimethylamine $N(CH_3)_3$ and trisilylamine $N(SiH_3)_3$ these two molecules according to the V.S.E.P.R. theory should have pyramidal geometries; we see that the first is pyramidal while the second is **planar**. This anomaly is explained by considering that in $N(SiH_3)_3$ we should have a pyramid but given the **size** of the silyl substituents there are **strong repulsions** between them and the molecule is not stable in this configuration. To stabilize itself, the molecule begins a process that allows it to move the substituents away from each other and for this it collapses on itself following the normal to the plane of the three silicon atoms passing through the nitrogen atom. When this process of collapsing on itself is complete, the molecule is flat but we cannot explain the flat geometry of this molecule without there being a **back-bonding** N – Si (lateral type overlap to give a π bond). We consider as excited state of nitrogen:

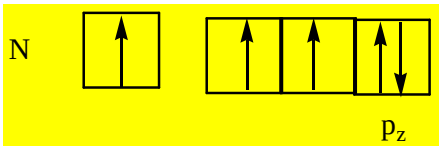

The p_z orbital of nitrogen is parallel to the d_{yz} orbital of silicon and we will have a lateral type overlap; which gives a back-bonding $p\pi d\pi$. There is a resonance phenomenon for the symmetry of the molecule. In this example we start from an sp^3 hybridization and we arrive at an sp^2 hybridization and the angles are standard. The B-strain process is not necessarily a process that makes a molecule go from a standard angle to another standard angle. The molecule seeks to move the substituents away from each other to have good stability. If by arriving at an angle between 109 and 120°, it minimized these repulsions; it would not need to extend the B-strain process to an angle of 120° and it would simply have stopped at this angle. All intermediate states between 109° and 120° corresponding to a value α are a possible equilibrium state. This B-strain process is always accompanied by a back-bonding. Le back-bonding is complete when the B-strain moves from one standard angle to another standard angle. The presence of one or more lone pairs on the central atom and one or more empty orbitals on the Lewis acid are necessary but not sufficient conditions for having a B-strain. It may happen that some molecules have a lone pair on the central element and empty orbitals on the Lewis acid and not undergo a B-strain.

The role of the central element is very important in the B-strain. If we consider the trisilylphosphine molecule $P(SiH_3)_3$; it is much more basic than the trisilylamine $N(SiH_3)_3$ which means that the phosphorus doublet is completely freed from back-bonding type interactions, in other words despite the presence of a lone pair and empty d orbitals; there is no B-strain. In fact, phosphorus is larger than nitrogen, so the SiH_3 are further apart in trisilylphosphine than in trisilylamine. Since the repulsions are weak in trisilylphosphine, the molecule does not need to impose a B-strain and it remains pyramidal and retains its lone pair, whereas trisilylamine engages in a B-strain process to stabilize itself, and this phenomenon is accompanied by back-bonding using the lone pair of nitrogen. Hence its basicity decreases.

III- Geometries of complexes containing bridged bonds

In some complexes, atoms are observed that have empty orbitals. These atoms behave as Lewis acids and receive doublets from the ligands of the complex. These ligands thus form single or multiple bridges between these atoms.

1°) Single bridge

These are compounds in which two atoms share a ligand. We can have two octahedra or tetrahedra joined by a vertex.

Let the ion $Al_2Cl_7^-$. To determine the geometry of the latter, we dissociate this anion into Cl^- and two $AlCl_3$. $AlCl_3$ is a triangular planar molecule and is a Lewis acid with respect to Al. Cl^- is a Lewis base so will be shared between two $AlCl_3$. The aluminum environment changes from a triangular environment to a tetrahedral environment. The geometry is therefore made up of two tetrahedra joined by a vertex. The angle of the bridge is close to 109° since there are in all four pairs around chloride.

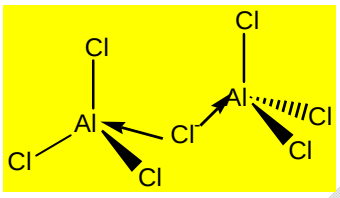

Scheme 52 : representation of ion $Al_2Cl_7^-$

2°) Double bridge

These compounds are formed by two molecules that behave as Lewis acids with respect to their central atom and as Lewis bases with respect to the bonding atoms. We can have two tetrahedra or two octahedra joined by one side ($As_2F_8O_2^{2-}$). Aluminum trichloride in the vapor state is dimeric and its formula is Al_2Cl_6. To account for its geometry, we consider that the two aluminum halides associate by dative bond. We have two tetrahedra joined by one side.

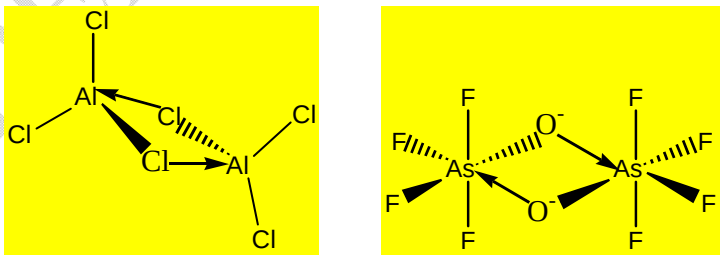

Scheme 53 : representation of Al_2Cl_6 and $As_2F_8O_2^{2-}$

3°) Triple bridge

In these compounds there are two molecules that share an atom on the one hand and on the other hand each of them behaves as a Lewis acid with respect to the central atom and as a Lewis base with respect to the bonding atoms. We can have two square-based pyramids

joined by one side and one vertex (or one face). We can also have two octahedra joined by one side and one vertex (face). We can also encounter complexes that have infinite chain or layer structures.

Consider nonachlorodithallate $Tl_2Cl_9^{3-}$ that we dissociate into 3 Cl^- and 2 $TlCl_3$ which are Lewis acids. We can have two possibilities:

Each $TlCl_3$ receives a Cl^- and the two $TlCl_3$ share a Cl^-;

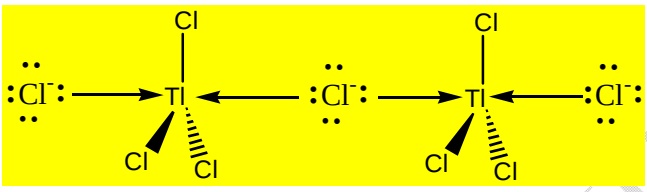

Scheme 54 : representation of $Tl_2Cl_9^{3-}$

- The two $TlCl_3$ share $3Cl^-$ following the same principle as the single bridge.

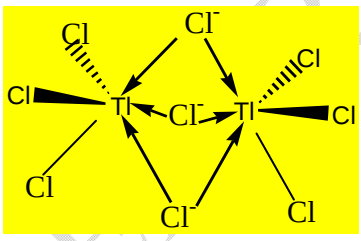

Scheme 55 : autre representation of $Tl_2Cl_9^{3-}$

This last geometry is the only one that is stable; the other, although theoretically possible, has never been isolated.

IV- Multi-centered bonds

A multicentered bond is a bond in which several atoms share a single electron pair. These types of bonds are mainly found in molecules with electron deficiency such as boranes, carboranes, etc. These bonds are only used when the compounds are electron deficient. An example is three-center, two-electron bonds (3c-2e). Reduction of boron halides can lead to boranes BH_3 : $BCl_3 + 3\ NaH \rightarrow BH_3 + 3\ NaCl$.

The BH_3 monomer has never been isolated and all syntheses lead to diborane B_2H_6. Another example of an electron-deficient compound is digallane Ga_2H_6. This type of bond contains an electron pair delocalized on three atoms, thus creating a low density in the valence shell of each of these atoms compared to a normal bond. B_2H_6 is composed of two BH_3 molecules

connected by hydrogen bridges. To account for the bonds in the molecule, each boron is considered to be sp^3 hybridized.

- The single bonds between boron and hydrogen arise from an axial-type overlap between a ***1s*** orbital of hydrogen and a sp^3 orbital of boron;
- The bridge bonds between boron and hydrogen arise from an axial-type overlap between a ***1s*** orbital of hydrogen and two sp^3 orbitals of boron in which one contains a single electron and the other is empty. The electron pair of the bridge is delocalized on the three atoms (B – H – B); two electrons connecting 3 cores; the pair occupies the center of gravity of the three vertices of the triangle formed by the three atoms.

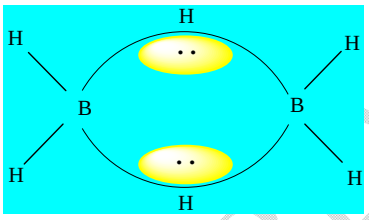

Scheme 56 : representation of B_2H_6

Replacing a boron atom in a borane with a carbon atom gives a carborane. The compound $C_2B_{10}H_{12}$ is isoelectronic to $B_{12}H_{12}^{2-}$.

When a pair connects 4 cores; the latter are at the top of a tetrahedron. This is the example of B_4Cl_4. This results in a closed tricenter bond at the bridge. With this type of bond, several boron compounds can be constructed, the simplest of which is tetrahydroborate or boron hydride BH_4^-.

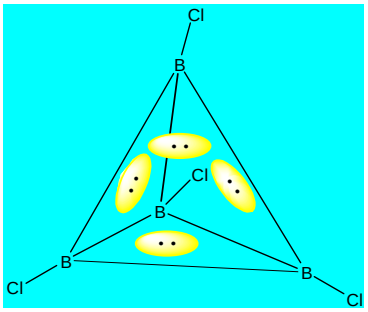

Scheme 57 : representation of B_4Cl_4

This type of geometry is also observed in the form of trimethylaluminium $Al_2(CH_3)_6$ where carbon atoms form Al-C-Al bridges between the two centers. This is also the case for $B_2(CH_3)_6$. These compounds are made from boranes or carboranes with substitution of hydrogen by an alkyl group; we generally obtain compounds having 5-legged carbon atoms and its formal valence is five.

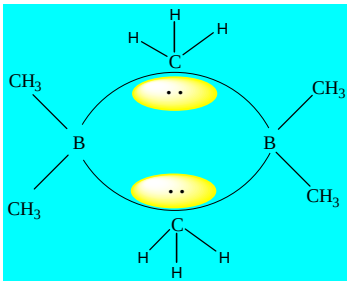

Scheme 58 : representation of $B_2(CH_3)_6$

Chapter 3

Coordination Complexes

Introduction

A **complex** is a polyatomic structure consisting of one or more cations (most often metallic) surrounded by several ligands which are molecules or ions that delocalize part of their electron density on the cation, thus forming chemical bonds with it. The subdivisions of chemistry describing the formation, structure and reactivity of these complexes are organometallic chemistry (if the complex contains metal-carbon bonds) and coordination chemistry (if not).

I- Reminder

1°) History: Werner complexes

The foundations of coordination chemistry were developed by **Alfred Werner** Swiss chemist between 1875 and about 1915 under the constant criticism and suggestions of **S.M. Jorgensen** Danish chemist. [6]. Werner studied a series of complexes $Co^{III}Cl_3,nNH_3$ by highlighting different chemical properties:

$$CoCl_3,6NH_3(1)+Ag^+(excès)\rightarrow 3AgCl(solide)$$

$$CoCl_3,5NH_3(2)+Ag^+(excès)\rightarrow 2AgCl(solide)$$

$$CoCl_3,4NH_3(3)+Ag^+(excès)\rightarrow 1AgCl(solide)$$

Werner concluded that cobalt is always surrounded by six ligands in such compounds. He introduced the following notation for compounds (1), (2) and (3):

$$[Co(NH_3)_6]Cl_3 \quad (1)$$

$[Co(NH_3)_5]Cl_2$ (2)

$[Co(NH_3)_4]Cl_2$ (3)

The species outside the brackets are not part of the complex. They help maintain the electroneutrality of the solid; they are counteranions. Depending on the complexes, zero, one or two chloride ions are bound to the cobalt.

2°) Definition

A complex is obtained by carrying out a **Lewis acid-base** reaction between:

- a metal (Lewis acid),
- a ligand (Lewis base).

Example : the formation of the complex $[Co(NH_3)_6]^{3+}$ is an acid-base reaction according to Lewis.

$$Co^{3+} + 6NH_3 \rightarrow [Co(NH_3)_6]^{3+}$$

Lewis Acid (Central Atom or Ion) + Lewis Base (Ligands) → Complex

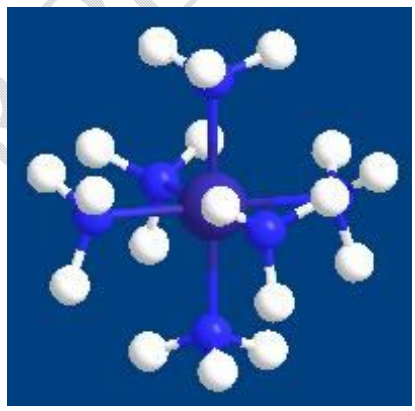

Figure 30 : representation of complex $[Co(NH_3)_6]^{3+}$

II- Classification of ligands

The general formula of a complex is **$[ML_n]$** where:

M is the central atom (ion). It is the coordinating center: **M** centers are mainly ions of metals (rarely those of metals of groups I_A and II_A).

L represents the atoms, ions or molecules linked to **M**; these are the ligands. These are chemical species that have electrons to give (atoms with free electron pairs, anions, molecules with π electrons).

n is the number of ligands attached to **M**; it is the coordination number (C.N. = 2 -12).

Ligands can be classified according to their charge, the type of donor atoms or the number of donor atoms.

1°) By the load

L anionic: F^-, Cl^-, Br^-, I^-, OH^-, CN^-…

L neutral: H_2O, NH_3, CO, NO…

2°) By the type of donor atoms

The atoms of a ligand that are directly bonded to M:

O = H_2**O**, **O**H^-, RCO**O**$^-$, **O**NO^-,…

N = **N**H_3, **N**O_2^-, **N**CS^-, C_6H_5**N** (py = pyridine), H_2**N**-CH_2-CH_2-**N**H_2 (en = ethylenediamine).

S = **S**CN^-, R_2**S…**

C = **C**O, **C**N^-…

X^- = F^-, Cl^-, Br^-, I^-,…

π donor = $H_2C = CH_2$, alkenes, alkynes, aromatic hydrocarbons,…

3°) By the number of donor atoms

L monodentates only engage in a connection with **M** : H_2O, NH_3, X^-, OH^-,…

L multidentates engage several bonds (of several atoms) with the same

M = **L chelator** from which the complex structures obtained are **chelates** (from greek: **khélé** = pliers, pincers).

L bidentate (C.N. = 2)

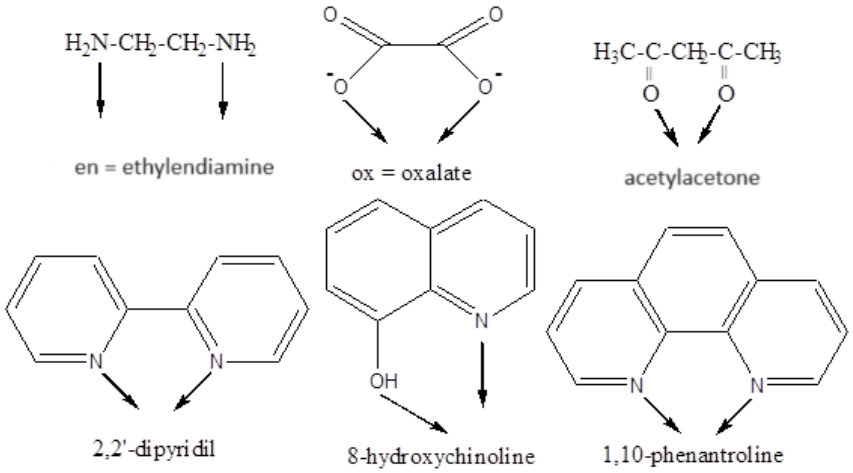

Scheme 59 : representation of some chelating ligands

L hexadentate (C.N. = 6)

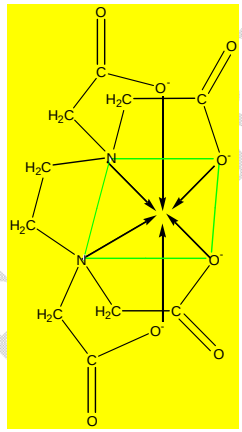

Scheme 60 : representation of the ethylenediaminetetraacetate ion: $EDTA^{4-}$

III- Classification of complexes

Complexes can be classified according to their charge, the number of coordinating centers or the type of complexes.

1°) By the load

Anionic complexes: $[ML_n]^{x-}$, example : $K_2^{2+}[Ni(CN)_4]^{2-}$, potassium tetracyanonickelate (II).

Cationic complexes: $[ML_n]^{x+}$, example : $[Co(H_2O)_4Cl_2]^{+}Cl^{-}$, tetra-aquadichlorocobalt(III) chloride.

Neutral complexes: $[ML_n]^{0}$, example : $[Pt(NH_3)_2Cl_2]$, diaminedichloroplatinum (II).

2°) By the number of coordinating centers

Mononuclear complexes have only one M.

Polynuclear complexes with several M bonds linked by bridges which can be monoatomic or polyatomic.

3°) By the type of complexes

"**Simple**" complexes

Chelate complexes

Organometallic complexes.

IV- Nomenclature of complexes

Ligands are named alphabetically. Then the name of the metal is written, followed by its oxidation number in parentheses, in Roman numerals, immediately after the name.

1°) Writing the chemical formulas of coordination complexes

The formulas are written: $(cations)_m[M^{ox}(X)_p(L)_q]^{n\pm}(anions)_r.S$; ox in roman numerals.

When the ligand is bridging we use the prefix μ. If the ligand is multicentric, the prefix used is σ.

2°) Coordination Chemistry Vocabulary

Coordination center = cation M^{z+} ($z > 0$) ;

Ligand = neutral molecule (L) or anion (X^{n-}, termination – O) ; S solvent ;

Coordinating atom = atom bonded to M ;

Organometallic complex corresponds to $z \leq 0$ + organic ligands;

Polynuclear complex = number of coordination centers > 1 ;

Coordination number = number of bonds between ligands and a coordination center.

3°) Mononuclear complexes

The usual name of the ligand is kept when it is neutral. The suffix "o" is added to the root of the ligand name if it is anionic.

Table 8 : Nomenclature of some neutral ligands

Molecules	Name of the molecule	Ligand
H_2O	Water	-OH_2 aqua
NH_3	Ammonia	-NH_3 ammine
CO	Carbon monoxide	-CO carbonyl
NO	Nitric oxide	-NO nitrosyl
C_5H_5N	Pyridine	-NC_5H_5 pyridine

Table 9 : Nomenclature of some anionic ligands

Anion	Name of the anion	Ligand	Name of the ligand
Cl^-	Chloride	-Cl	Chloro
O_2^-	Oxide	-O	Oxo
OH^-	Hydroxide	-**O**H	Hydroxo
CO_3^{2-}	Carbonate	-**O**CO**O**-	Carbonate
CN^-	Cyanide	-**C**N	Cyano
SO_4^{2-}	Sulfate	-**O**SO_3	Sulfate
$S_2O_3^{2-}$	Thiosulfate	-**S**SO_3	Thiosulfate
$C_2O_4^{2-}$	Oxalate	-**O**$(CO)_2$**O**-	Oxalate
SCN^-	Thiocyanate	-**S**CN	Thiocyanote
SCN^-	Thiocyanate	-**N**CS	Isothiocyanate
NO_2^-	Nitrite	-**O**NO	Nitrite
S^{2-}	Sulfide	-S	Thio
HS^-	Hydrogen sulfide	-SH	Thiolo
O_2^{2-}	Peroxide	-**O**-O	Peroxo

Whatever they are, their number is specified by a Greek prefix:

di (2), tri (3), tétra (4), penta (5), hexa (6), hepta (7), octa (8), nona (9), deca (10), undeca (11), dodeca (12),…

If the ligand is **polydentate**, the name of the ligand is included in parentheses and the prefix **bis** (for 2 ligands) or **tris** (for 3 ligands) is added to the whole: $[Co(H_2N\text{-}CH_2\text{-}CH_2\text{-}NH_2)_3]^{3+}$ tris(ethylenediamine)cobalt (III).

We write the number and nature of the ligands, the nature of the central ion (or atom) and in parentheses a Roman numeral which specifies the oxidation number of the metal.

When there are different ligands in the same structure, they are named in alphabetical order.

For **coordinating centers**, the degree of oxidation of the element concerned (metal center M) is always specified. In addition, when the latter is involved in:

- An **anionic** complex: the suffix "**ate**" is added to the root of its usual name and the whole (name of **M** and degree of oxidation) follows the name(s) of the ligand(s). Otherwise, the name of the metal is noted.

  Examples : $[Fe^{3+}(CN)_6]^{2-}$ = hexacyanoferrate ion (II) ;

  $[Cu^{2+}Cl_4]^{2-}$ = tetrachlorocopper ion (II).

- A **cationic** complex – see a neutral complex – its name is not modified but nevertheless follows that (those) of the ligand (s); $[Ni^{2+}(H_2O)_6]^{2+}$ = ion hexa-aquanickel (II) ; $[Cr^{3+}(Br)_3(NH_3)_3]^0$ = tribromotriamine chromium (III). In case of vowel splitting, either a separating hyphen is used or elision is practiced.

4°) Polynuclear complexes

The previous rules certainly remain valid but we add a prefix μ to the ligand(s) ensuring the bridging between the metal centers M.

$\{[Cr(NH_3)_5]_2(\mu - OH)\}Cl_5$ = μ pentachloride – hydroxo bis [penta (ammine) chromium (III)].

V- Geometry of some complexes

To determine the geometry of the complexes, the theory of hybridization is used. It will therefore be necessary to start by determining the state of hybridization of the central metal, for this:

- We look for as many empty orbitals as dative bonds around the central element;
- We sum the empty orbitals of the central element;
- The hybridization of the central metal depends on the nature of the ligands surrounding it. The **Fajans-Tsuchida** spectroscopic series classifies ligands according to the strength of their field:

CO > CN^- > NO_2^- > ethylene diamine > NH_3 > CH_3CN > $\underline{N}CS^-$ > H_2O > $C_2O_4^{2-}$ > OH^- > F^- > NO_3^- > Cl^- > $\underline{S}CN^-$ > S^{2-} > Br^- > I^-. (In red the strong field ligands, in blue the medium field ligands and in black the weak field ligands).

- If the ligands are **strong field** (low spin) the free electrons of the (n – 1)d orbital are coupled. In this case we add in the order *(n – 1)d, ns, np* the empty orbitals of the central element; we thus obtain the following hybridizations: dsp^2, dsp^3, d^2sp, d^2sp^2 or d^2sp^3. The same phenomenon is obtained if the central element belongs to the second and third series of transition elements. In this case, **diamagnetic** complexes are obtained if the number of electrons *nd* is even.

- If the ligands are **low-field** (high spin), the free electrons of the *(n – 1)d* orbital are not coupled. In this case, the empty orbitals of the central element are added in the order *ns*, *np*, *nd*; this gives the hybridizations: sp^3, sp^3d, sp^3d^2. In this case, **paramagnetic** complexes are obtained.

The geometries of the complexes according to the type of hybridization of the central element are grouped in Table 10.

Table 10 : geometries versus hybridization type

Complexes	Number of connections	Hybridization	Geometry
AL_4	4	sp^3	Tetrahedron
AL_4	4	dsp^2	Square plan
AL_4	4	d^2sp	Square plan
AL_5	5	sp^3d	Trigonal bipyramid
AL_5	5	dsp^3	Square-based pyramid
AL_5	5	d^2sp^2	Square-based pyramid
AL_5	5	d^3sp	Square-based pyramid
AL_6	6	sp^3d^2	Octahedron
AL_6	6	d^2sp^3	Octahedron
AL_6	6	dsp^3d	Octahedron

Example 1 : Geometry of $NiCl_4^{2-}$:

Ni^{2+} : (Z = 28) [Ar] $3d^8$. Cl^- ions being weak field ligands, we sum the 4s orbital and the 3 ***4p*** orbitals; Ni^{2+} is $\boldsymbol{sp^3}$ hybridized; the geometry of the complex is a **tetrahedron**.

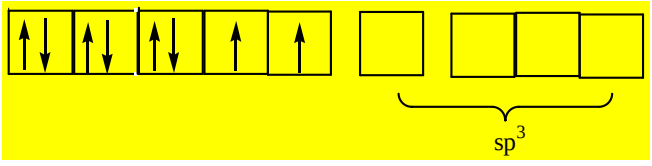

Figure 31 : electronic structure of Ni^{2+}

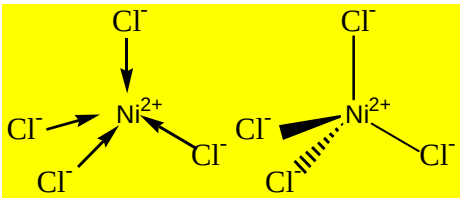

Scheme 61 : representation of $NiCl_4^{2-}$

Example 2 : Geometry of $Ni(CN)_4^-$

CN^- ions being strong field ligands all the electrons of the ***3d*** orbital are coupled. We sum in the central metal the empty ***3d*** orbital; the ***4s*** orbital and two ***4p*** orbitals: Ni^{2+} is $\boldsymbol{dsp^2}$ hybridized; the geometry of the complex is a square plane.

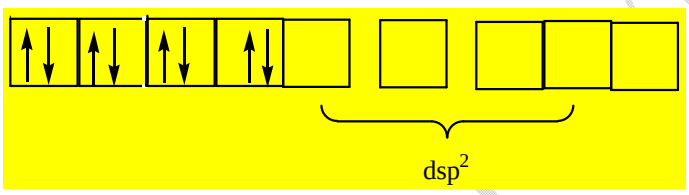

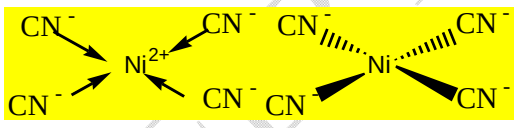

Scheme 62 : representation of $Ni(CN)_4^-$

Example 3 : Geometry of $[Os(NH_3)_5]^{2+}$

Os^{2+} (Z = 76) : $1s^2 2s^2 2p^6 3s^2 3p^6 4s^2 3d^{10} 4p^6 5s^2 4d^{10} 5p^6 4f^{14} 5d^6$. The geometry of the complex is a **square-based pyramid**.

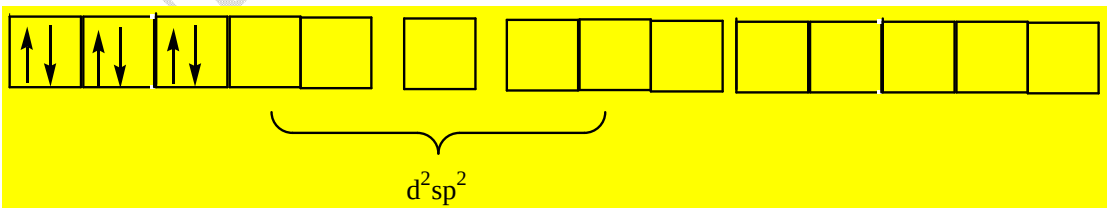

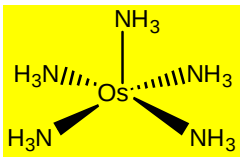

Scheme 63 : representation of $[Os(NH_3)_5]^{2+}$

Application exercise: Let us name the following complexes after having determined and represented their geometry.

$[PdCl_2(PPh_3)_2]$

Oxidation degrees of metal: $x + 2(-1) + 2(0) = 0 \Rightarrow x = +2$

$_{46}Pd^{2+}$: $[Kr]4d^8$

Palladium is a transition metal of the second series. Therefore, the complex is strong field; the ***4d*** electrons are paired. The ligands contribute four doublets around the central metal, the hybridization is dsp^2.

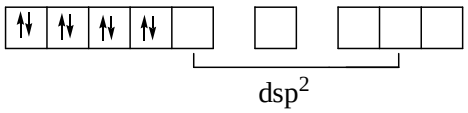

Hybridization = dsp^2

Geometry = square plan

Name = Dichlorobis(triphenylphosphine)palladium(II)

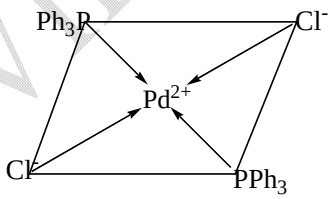

Scheme 64 : representation of $[PdCl_2(PPh_3)_2]$

VI- Complexes of infinite type

1°) Simple bridges

They are of the form:

Scheme 65 : representation of the structure of $(AX)_n$

The molecular structure of the complex $\{MnL(CH_3CO_2)\}_n$ is an example of an infinite structure, with **L** being N,N'-(2-hydroxypropan-1,3-diyl)-bis-(salicylaldimine). The asymmetric unit represents a manganese atom, a ligand molecule, and an acetate group. Each manganese atom is coordinated to two oxygen atoms of two acetate groups, two oxygen atoms, and two nitrogen atoms of the dideprotonated ligand molecule [7].

The Mn(III) ion adopts a geometry in which the equatorial plane is formed by the Schiff base atoms that are bonded to the metal. Two iminic nitrogen atoms (N1 and its symmetrical) and two phenolic oxygen atoms (O3 and its symmetrical) form the equatorial plane. The coordination around the Mn(III) undergoes a Jahn-Teller effect as expected for a distorted octahedron in a complex of a d^4 ion.

The shortest distances are found in the equatorial plane (Mn1-O3 = 1.8788 Å and Mn1-N1 = 2.0516 Å). The oxygen atoms O1 and O2 from the acetate groups occupy the axial positions (Mn1-O1 = 2.1610 Å and Mn1-O2 = 2.232 Å with the angle O1-Mn1-O2 = 158.61°). These facts show the compression due to the **Jahn-Teller effect** because of the difference in filling of the $\mathbf{e_g}$ orbitals and the $\mathbf{t_{2g}}$ orbitals; there is a lifting of degeneracy of these orbitals resulting from the geometric point of view by a differentiation of the metal-ligand lengths in the plane and in trans thus giving a deformed octahedron.

Each acetate group acts as a bridging bidentate. Each of the two oxygen atoms is monodentate and is bonded to a different Mn(III) ion. The structure reveals that we have a $\{MnL(CH_3CO_2)\}_n$ polymer in which the $\{MnL(CH_3CO_2)\}$ units are bonded via axial coordination of the acetate groups. The oxygen atom of the alcohol function is uncoordinated.

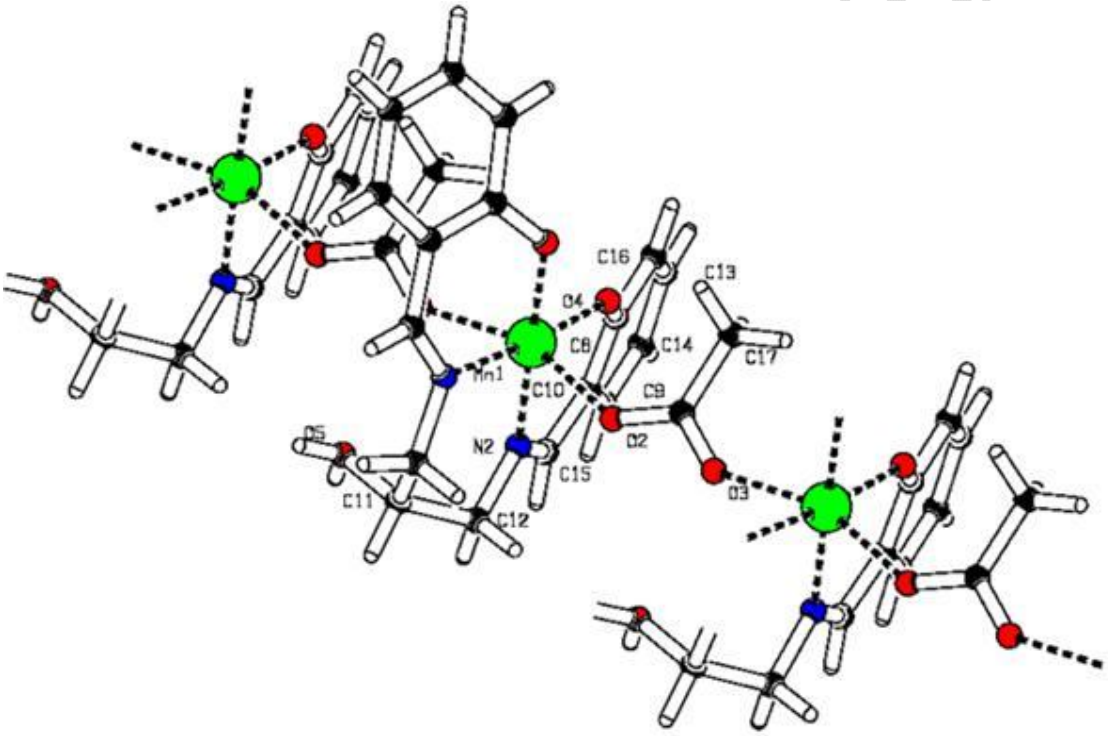

Figure 32 : representation of $\{MnL(O_2CCH_3)\}_n$

In the following example the motifs are linked by a single acid-base bond as in the case of $[CuCl_3]_x^{2-}$; Cu^+ et 3 Cl^-.

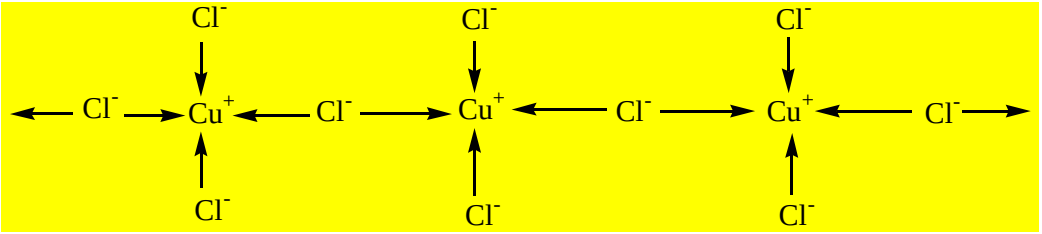

Scheme 66 : representation of $[CuCl_3]_x^{2-}$

In this case the coordination number of the central element increases by one and the structure is called **infinite chain** when the bridges develop in one direction. If several bridges develop in **two** or **three** directions, we obtain **infinite layered** structures or **three-dimensional structures with infinite layers**.

2°) Determination of an infinite type structure

Let AX_n be the molecular formula of a complex. Experimental study allows us to say whether the molecule is discrete or infinite. In the case where it is infinite; it can be determined if we know the environment of the central element and the empirical formula AX_n. We start by considering the hybridization state of the central element in the monomeric molecule. The hybridization state in the infinite type structure will be a higher hybridization state.

This state of hybridization directly gives the coordination of the central element in the infinite structure. We then define a sum whose value **n** is equal to the number of elements linked to the central element in the monomeric structure and whose number of terms **m** is equal to the coordination. These terms are generally units or fractions whose denominator is generally 2 or 4, exceptionally 3. When we have a unit, this means the ligand is linked to a single central element; when we have ½, it is linked to 2 central elements…

The numerator of the fraction is always equal to 1. So **n** is the sum of **m** fractions in $\frac{1}{x}$ with x = 1, 2, 3 or 4. If **n** = **m** the structure is discreet. **m** is at most equal to 6. **A** can be an atom or a group of atoms and in this case the acid site will be the central element. **X** can be an atom or a group of atoms.

If we take for example AX_3 ; n = 3. Let's suppose m = 4 ; $n = \frac{1}{x}+\frac{1}{x}+\frac{1}{x}+\frac{1}{x}$ from where $n = \frac{1}{2}+\frac{1}{2}+1+1 = 3$

x is the number of central atoms that share a ligand.

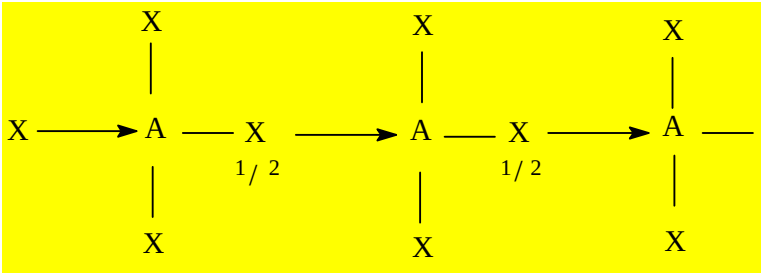

Scheme 67 : representation of AX_3

If m = 5 we have : $n = \frac{1}{x}+\frac{1}{x}+\frac{1}{x}+\frac{1}{x}+\frac{1}{x} = 3$ either: $n = \frac{1}{2}+\frac{1}{2}+\frac{1}{2}+\frac{1}{2}+1 = 3$

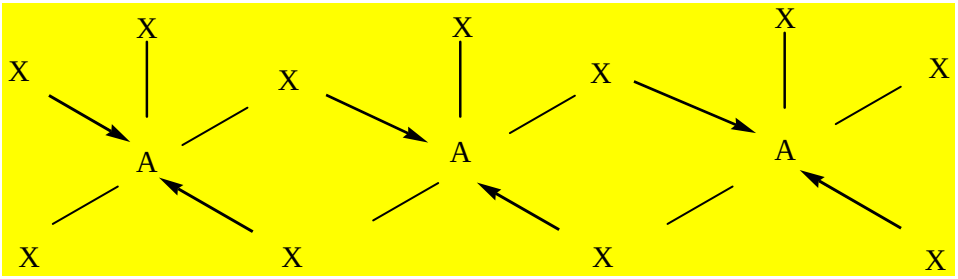

Scheme 68 : other representation of AX_3

Example

The crystal structure of the product $\{Cd(H_5L)_4(NO_3)_2\}_n$ reveals a one-dimensional polymeric complex maintained by the ligand L = N-1-[1-(1H-pyrrol-2-yl)ethylidene] carbonohydrazone which is a bidentate bridging ligand in the structure. Each ligand is a donor through its oxygen atom and through its nitrogen atom. In the complex, each cadmium Cd(II) ion is coordinated to four ligands and two nitrate ions. Two of these ligands are linked to the cadmium through their oxygen atoms and the other two are coordinated to the central ion through their nitrogen atoms; two monodentate nitrates complete the structure. The cadmium(II) ion is thus hexacoordinated [8].

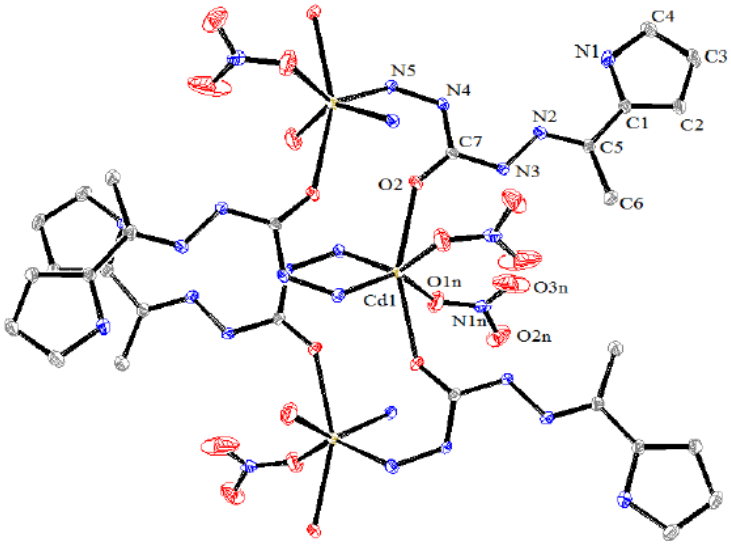

Figure 33 : representation of $\{Cd(H_5L)_4(NO_3)_2\}_n$

The crystal structure of the cadmium(II) complex shows a polymer chain where each metal ion is hexacoordinated. The environment of the central Cd(II) metal is best described as a distorted trigonal antiprism which is not common for coordination number six. Hydrogen-

like interactions between neighboring chains of the complex provide cohesion to the infinite structure.

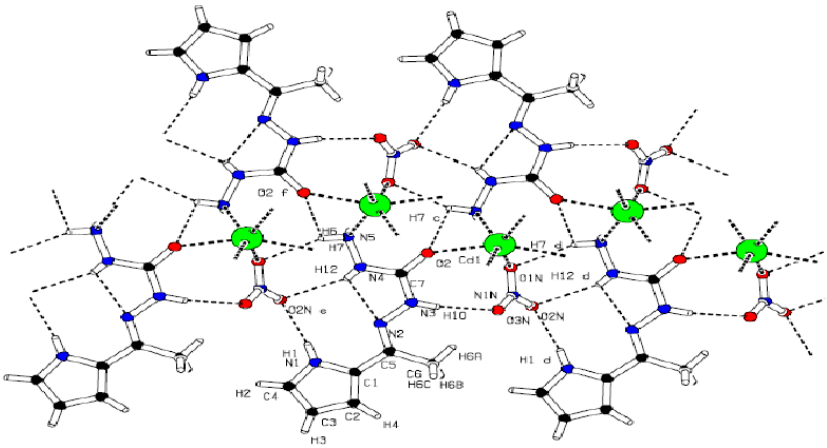

Figure 34 : three-dimensional structure of $\{Cd(H_5L)_4(NO_3)_2\}_n$

VII- The different geometries of coordination complexes

Coordination is the number of metal-ligand bonds around a given metal. Coordination can range from 1 to 12 (but extreme values are rare). Complexes mostly have coordination numbers ranging from 2 to 9. The most common coordinations are 4 and 6. The spatial arrangement of the ligands depends on the coordination number (C.N.) of the complex.

Ligands are of different types; among the most common we find molecules like water H_2O or ammonia NH_3 or anions like chlorides Cl^-, cyanides CN^-, hydroxides OH^--… As a first approximation, the capacity of a ligand to bind to a metal is correlated with its nucleophilicity.

For most structures, the metal ion is placed at the center of a sphere where the different ligands are placed (the ion-ligand distance is then considered identical). Ligand-metal orbital overlaps and electrostatic repulsions between ligands tend to form regular geometric structures. Metal complexes respect VSEPR theory except when fine electronic factors (which can be linked to distortions), which is the case for example for Cu(II) and Ni(III) complexes which are often in octahedral geometry with a tetragonal distortion (2 bonds in one axis, longer or shorter than the other 4) or square planar (tetragonal distortion pushed to infinity), which are not canonical geometries predicted by VSEPR theory.

Steric hindrance due to the coordination of hindered ligands can also modify the geometry of complexes.

Below is a list of the most common structures according to the coordination number (CN) (also called coordination):

- CN = 2 : linear
- CN = 3 : triangular
- CN = 4 : tetrahedral or square plan
- CN = 5 : bipyramidal with triangular base or pyramidal with square base
- CN = 6 : octahedral
- CN = 7 : bipyramidal with pentagonal base
- CN = 8 : square antiprismatic
- CN = 9 : tri-capped trigonal prism
- CN = 10 : bicapped square antiprism
- CN = 11 : all-faced capped trigonal prism
- CN = 12 icosahedron or dodecahedron

In many cases, the actual geometry deviates from the theoretical structure. For example, the complex may contain different ligands (the lengths of the ion-ligand bonds are no longer identical, and in this case we are in the presence of an irregular or deformed polyhedron). The size of the ligands can modify the structure of the complex by too great a steric pressure. Also in the case of complexes with polydentate ligands, the structure of the entities carrying the electronic pairs ensuring coordination to the metal may be incompatible with the geometric requirements of coordination; this results in distorted complexes.

The structure of a complex will depend on its coordination number, equal to the number of σ bonds between the ligands and the central atom). The coordination number of a ligand is between 2 and 9, but complexes include a large number of ligands (greater than 6). The most frequent coordination numbers are 4 and 6. The number of metal-ligand bonds depends on the size, configuration and charge of the metal ion. Most ions can accept several coordination numbers, thus adopting different geometries.

The chemistry of complexes is dominated by the interactions between the d (or f) atomic orbitals of the central ion and the s and p orbitals of the ligands. The s, p and d orbitals of the metal can accommodate a total of 18 electrons (for f-block elements, this maximum increases to 32 electrons). The maximum coordination number therefore depends on the electronic configuration of the metal (more specifically on the number of vacant orbitals that can generate a ligand-metal σ bond). However, unlike the octet rule in organic chemistry, the **EAN** rule of 18 electrons is not absolute and many stable complexes do not respect it.

The coordination number of a complex also depends on the size of the ligands and the metal cation. Small ligands around a large cation result in little steric hindrance, which leads to large coordination numbers.

Example : $[Mo(CN)_8]^{4-}$

Small cations surrounded by large ligands will have low coordination numbers.

Example : $Pt[P(CMe_3)_3]_2$

For the transition metals of the ***3d*** series, which include metals of biological interest (and which are the most abundant on Earth) such as copper, zinc, manganese, iron, etc.; the coordination number is usually between 4 and 6. Due to their large size, the lanthanides, actinides and transition metals of the ***4d*** and ***5d*** series may have large coordination numbers (> 6).

1°) Coordination number 2

Few coordination complexes 2 are known; they are generally ions with oxidation number +I of group I_B or complexes of mercury (II). This is the case of $[Cu(NH_3)_2]^+$, $[Ag(NH_3)_2]^+$, $CuCl_2^-$, $Hg(CN)_2$. However, these complexes can receive other ligands and give complexes with a higher coordination number.

Example : $[Ag(NH_3)_2]^+ + 2NH_3 \rightarrow Ag(NH_3)_4^+$

The stability of 2-coordinate complexes is generally low.

2°) Coordination number 3

Coordination number 3 is very rare with d elements, the geometry is generally a chain or a network. Many complexes that were believed a priori to have a coordination number of 3 actually have a higher coordination number; this is the case of the complex $[CuCl_3]^{2-}$ which has an infinite chain structure with a tetrahedral environment around the copper, therefore of coordination 4.

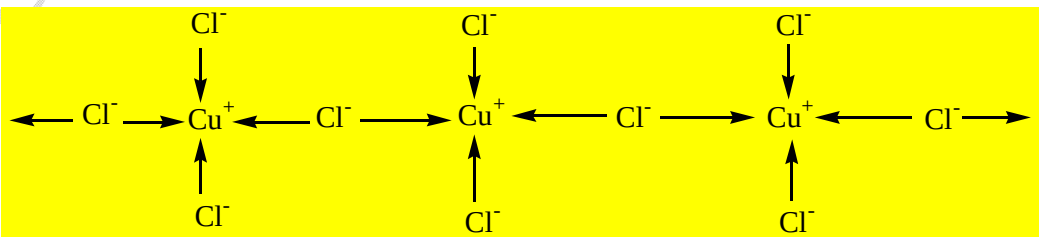

Scheme 69 : representation of $[CuCl_3]^{2-}$

$[Cu(CN)_2]^-$ has an infinite chain structure with a 3-coordinated copper. In $[HgI_3]^-$ we have a discrete structure and a 3-coordination.

3°) Coordination number 4

There are two types of 4-coordinate complexes: square planes and tetrahedra. Tetrahedral complexes are favored by paramagnetic complexes.

Tetrahedral geometries are those predicted by the V.S.E.P.R. theory (in the same way that V.S.E.P.R. predicts the tetrahedral shape of methane in organic chemistry). They are favored by:

- Large ligands Cl^-, Br^-, I^-, metals that have a rare gas type configuration such as $Be^{2+}(1s^2)$ or Zn^{2+} : $_{18}[Ar]3d^{10}$, cation is small.

- Metals whose complex is paramagnetic such as Co^{2+} : $_{18}[Ar]3d^7$.

As with asymmetric carbons, tetrahedral complexes can exhibit optical activity if all four substituents are different.

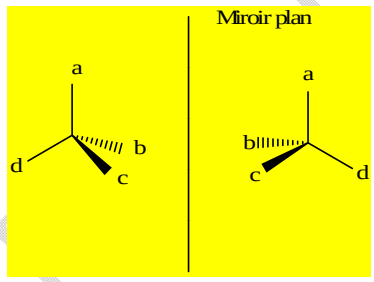

Scheme 70 : Two optical isomers of tetrahedral geometry

Example : This is the case of the zinc (II) complex with the ligand (E)-N'-(2-hydroxybenzylidene)isonicotinohydrazide of formula $ZnCl(SCN)(H_2L_B)_2$. The complex crystallizes in an orthorhombic system with space group Ama2, The lattice parameters are: a = 26.0306 (2) Á, b = 16.0094 (1) Á, c = 6.840 Á. The asymmetric unit contains two neutral molecules of the ligand H_2L_B linked to the Zn^{2+} ion by their pyridine nitrogen atom, a thiocyanate ion SCN^- linked by its nitrogen atom, a chloride ion Cl^- coordinated to the Zn^{2+} and a free water molecule.

The Zn(II) ion is therefore tetracoordinated (figure 35) and the environment around the Zn(II) metal center is a **deformed tetrahedron**. This deformation is proven by the difference in interatomic distances around the Zn^{2+}, but also by the fact that the bond angles deviate by 109.28°. Indeed, the lengths of the Zn-N bonds are 1.979 (4) Á and 2.052 (3) Á while those of the Zn-Cl bonds are 2.1919 (12) Á. The bond angles around Zn^{2+} n in the basal plane vary in the

interval (103-125°). The N3-Zn-N4 angle is 103.11(10)°, the N4-Zn-Cl1 angle is 125.21(12)° while the N3-Zn-N3i angles are between 103.12(10)° and 110.52(14)°.

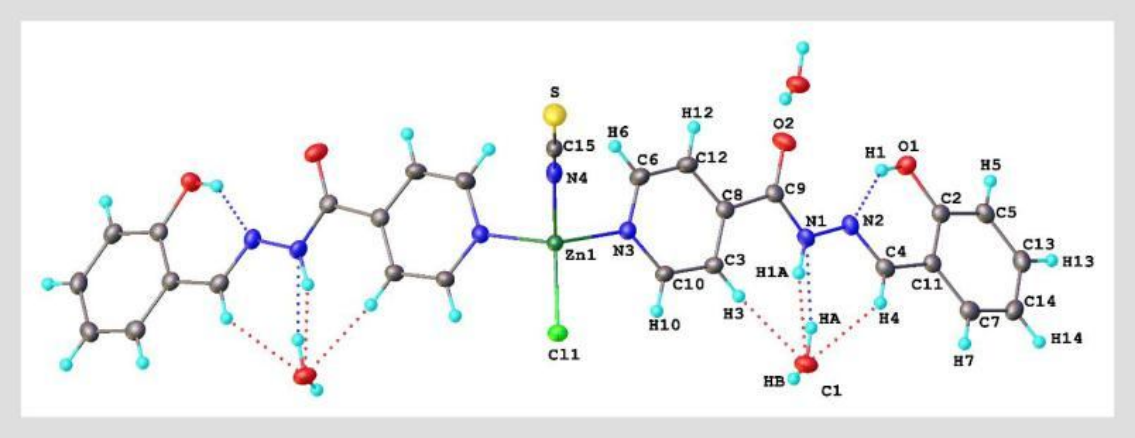

Figure 35 : Asymmetrical unit of the complex $[ZnCl(SCN)(H_2L_B)_2]\cdot 2H_2O$

The **square planar geometry** is generally associated with a d^8 electronic configuration: Ni^{2+}, Pd^{2+}, Pt^{2+}, Au^{3+}, Rh^{+}. Square planar complexes that are surrounded by two types of ligands (formula MA_2B_2) can exhibit cis-trans isomerism.

Trans Isomer Cis Isomer

Scheme 71 : The two isomers of MA_2B_2

These two isomers have different chemical properties.

Thus cis-platinum or cis-diammine dichloro-platinum (CDDP) [cis-$Pt(NH_3)_2Cl_2$] exhibits anticancer activity that the trans isomer does not. It is thought that in the case of the cis isomer, platinum binds to DNA, with the chloride ligands first replaced by water molecules and then by a DNA base such as guanine.

Consider the example of the copper(II) complex with the ligand N,N'-(2-hydroxypropan-1,3-diyl)-bis-(salicylaldimine). In this compound the Cu(II) metal center is tetracoordinated with a square planar environment. The atoms O1, O2, N1 and N2 form the basal plane for Cu(II). The metal center has a **distorted square planar** environment.

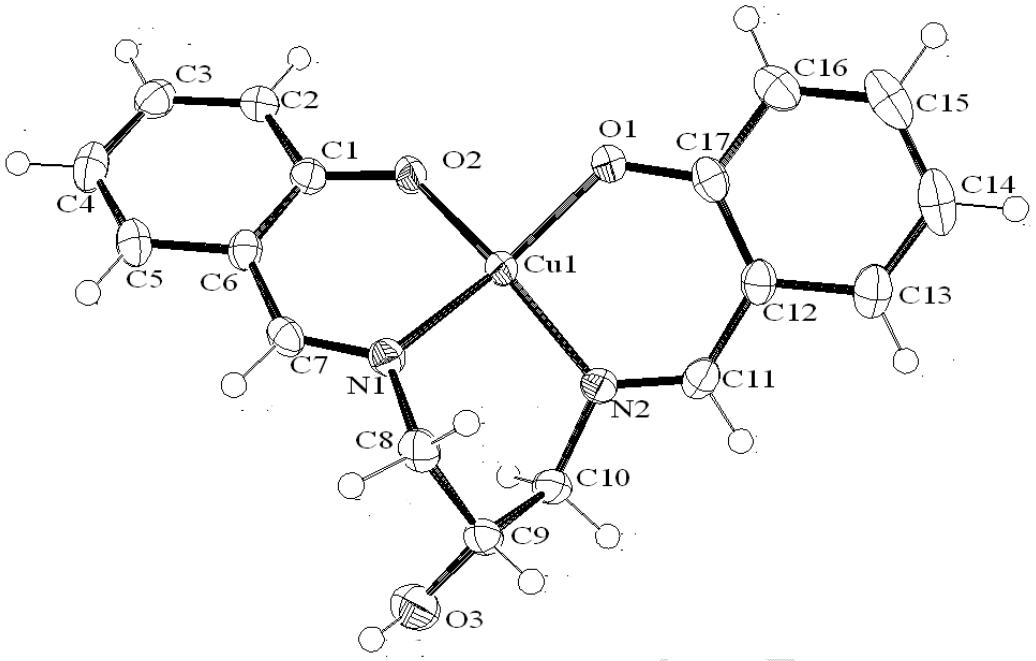

Figure 36 : complex with N, N'-(2-hydroxypropan-1,3-diyl)-bis-(salicylaldimine) and Cu(II)

The copper(II) complex with 2-{[2-(2-Aminoethylamino)ethylimino]methyl}phenol exhibits a square planar geometry around the central Cu^{2+} element as does the Cu(II) complex (2-{[2-(2-Aminoethylamino)ethylimino]methyl}phenolato-$\kappa^4 O,N',N'',N''$)copper(II) perchlorate [9]. The asymmetric unit of the complex $\{Cu(H_2L)\}\cdot ClO_4$ consists of two Cu(II) ions coordinated with Schiff base ligands and two perchlorate anions. The Schiff bases are linked to Cu(II) ions via three nitrogen atoms and one oxygen atom. Each ligand exhibits a square planar geometry around the copper(II). Intermolecular hydrogen bonds involving the NH groups and the oxygen atoms are observed.

The Cu-O distances are 1.891 and 1.895° while the Cu-N distances are between 1.930 and 2.011 Å. These values are lower than those observed for the copper complex obtained with the ligand of 4-chloro-6-hydroxymethyl-2-[(3-aminopropylimino)methyl]phenol (Jiang et al, 2009). The sum of the angles around the Cu1 ion is 359.59° and around the Cu^{2+} ion is 360.3°. These facts indicate that there are very small distortions of the square planar geometry around the Cu(II) ion. In both molecules the Cu(II) ions are located approximately in the same

plane (dihedral angles N2-N1-Cu1-C8 = 178.4°, N2-N1-Cu1-C8 = 178.4°, N5-Cu2-N4-C18 = 178.9° and O2-Cu2-N4-C19 = 177.4°).

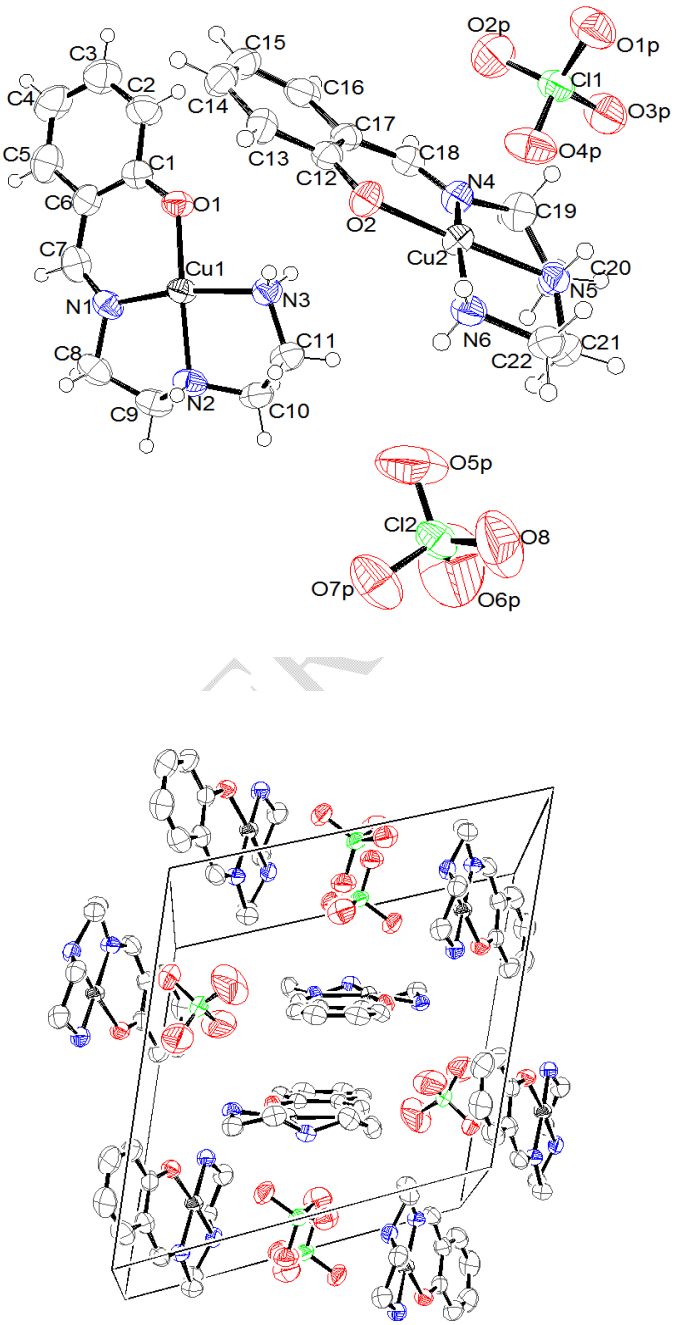

Figure 37 : structure and crystal lattice of the (2-{[2-(2-Aminoethylamino)ethylimino]methyl}phenolato-κ^{4}O,N',N'',N'')copper(II)perchlorate

4°) Coordination number 5

There are basically two geometries:

Scheme 72 : representation of the trigonal bipyramid and the square-based pyramid

4-1 Trigonal bipyramid

Three ligands form an equilateral triangle (**equatorial ligands**). The metal is located at the center of this triangle. The last two ligands (**axial ligands**) are located perpendicular to the previous plane. This is the case for the classic meolecules PCl_5, PF_5 (see figure 29).

4-2 Square-based pyramid

Example 1 : In the crystal of the mononuclear complex $Zn_2(H_3L)_2Cl_2]\cdot(CH_3OH)_2$, each Zn(II) metal center is pentacoordinated by a nitrogen atom, a sulfur atom, two phenolic oxygen atoms of two ligands, and a chloride ion. For the two-ligand molecule, the phenolic oxygen atom serves as a bridge between the two Zn(II) ions. For the two metal centers, the coordination polyhedron is best described as a square-based pyramid. The molecules are linked together by multiple hydrogen-bonding interactions resulting in a three-dimensional network [10]. The asymmetric unit contains two zinc atoms, two molecules of deprotonated ligand, two chloride atoms, and two molecules of the solvent methanol in a network. Each of the ligands acts in a tridentate manner through an iminolic nitrogen atom, a sulfur atom, and a phenolic oxygen atom that serves as a bridge between two zinc(II) centers.

Chelation results in the formation of a five-membered ring ZnSCNN and a six-membered ring NCCCOZn. Each of the Zn(II) centers resides in a square-based pyramidal environment distorted according to the Addison parameter $\tau = 0.0962$; $\tau = (\alpha - \beta)/60$ where α and β are the largest angles subtended by the Zn(II) ion. The basal plane is occupied by three atoms (N, O, S) of the same ligand molecule and a phenolic oxygen atom of the second ligand molecule. The apical position is occupied by a chloride ion. The sum of the angles in the basal plane of 339.62° deviates strongly from the ideal value of 360° and the angles formed by the apical chloride atom with the atoms in the basal plane are greater than 90° (Cl1—Zn1—O1 = 101.37°; Cl1—Zn1—$N3^i$ = 106.24°; Cl1—Zn1—$S1^i$ = 110.53°; Cl1—Zn1— $O1^i$ = 109.85°) indicating a severe distortion of the geometry around the zinc(II) center. The Zn1-O1- $Zn1^i$ and O1-Zn1- $O1^i$ angles are 102.72° and 77.18°, respectively. The Zn-Cl distance of 2.3066 Å is greater than the value reported for a square-based pyramidal complex of zinc. The values of

bond distances for Zn1-O1 and Zn1- $O1^{i}$ are slightly different with 2.033 and 2.038 Å, respectively. The Zn1-S1 interatomic distance of 2.380 Å is longer than the average value of 2.2529 Å found for a complex of semicarbazide derivatives. The values of C2-N3 and C1-S1 distances of 1.280 Å and 1.705 Å are indicative of a double bond upon coordination to the Zn2 ion while the C1-N2 bond distance (1.342 Å) has a single bond character. These facts clearly show that no thioiminolization occurs during the reaction.

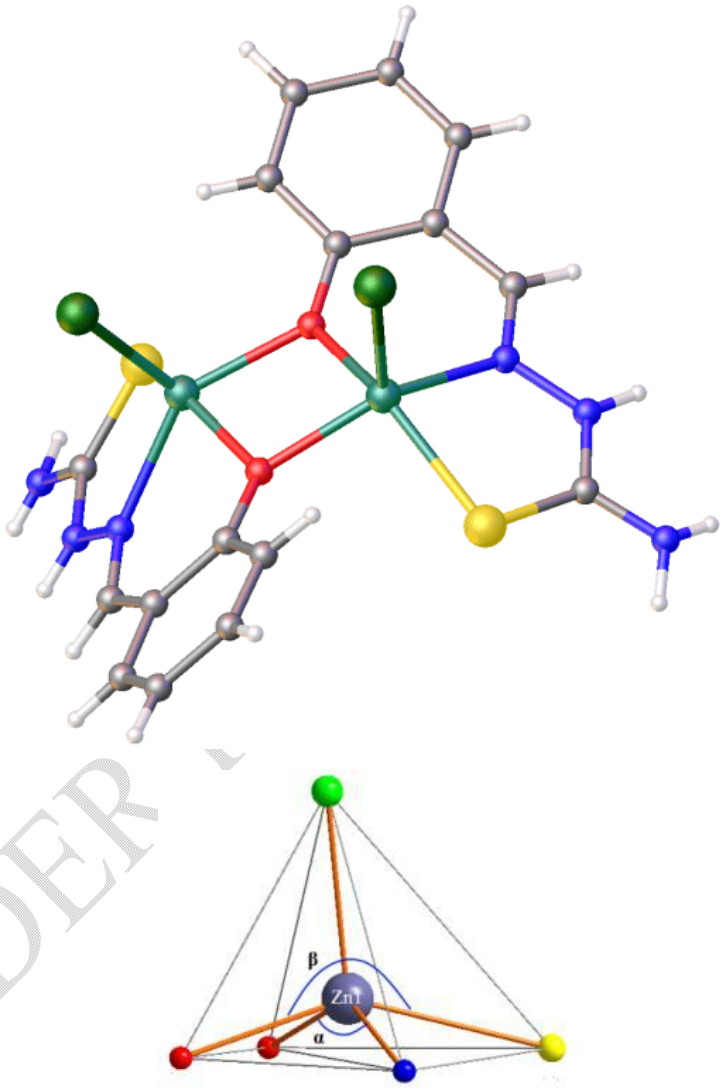

Figure 38 : crystal structure of the complex of zinc (II) with the ligand 1-(2-hydroxybenzylidène) thiosemicarbazide solvent-free and the coordination polyhedron of the zinc (II)

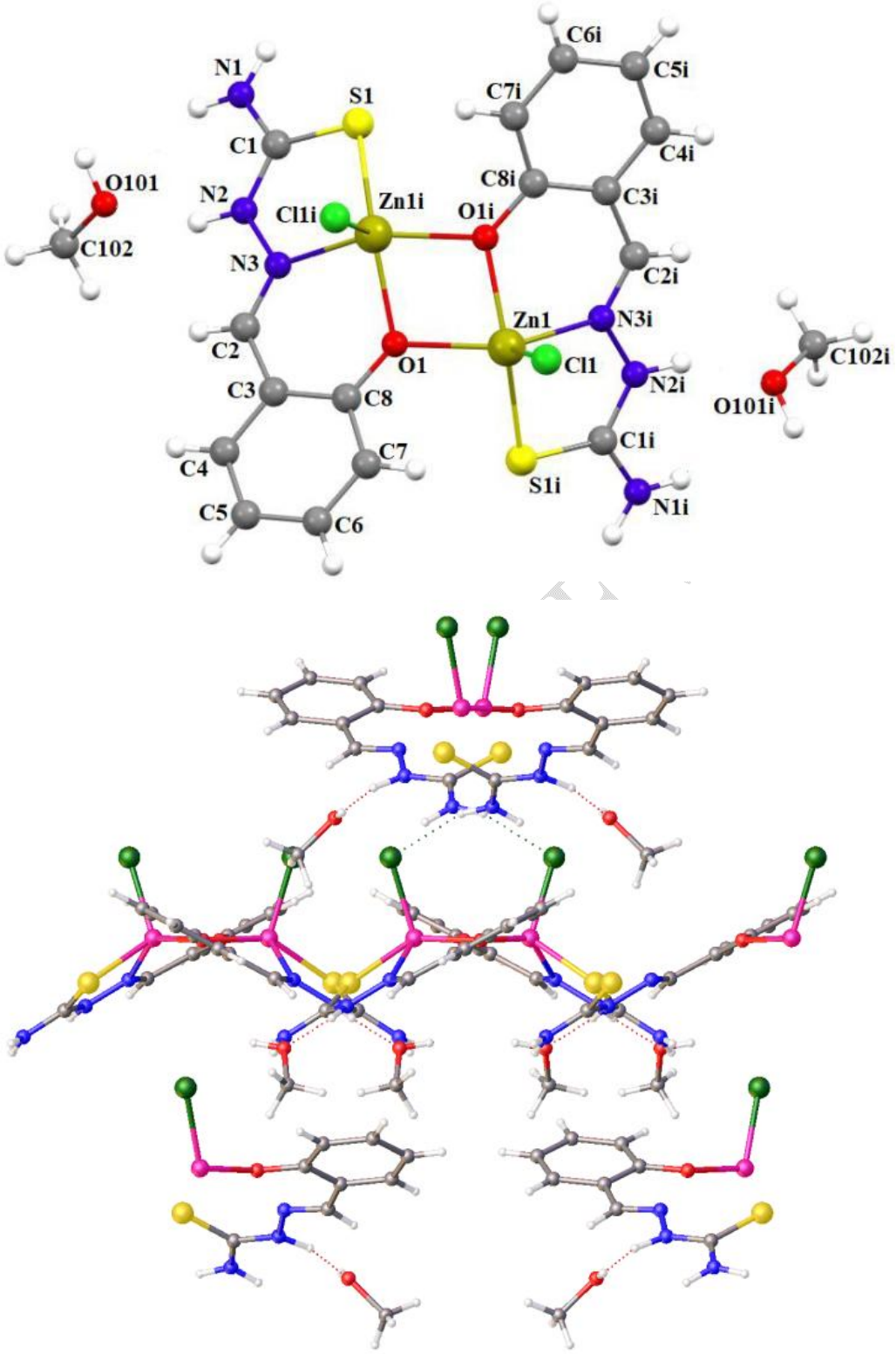

Figure 39 : structure cristalline du complexe du zinc (II) avec le ligand 1-(2-hydroxybenzylidène) thiosemicarbazide with the solvent and a representation of the complex of zinc (II) showing intermolecular and intramolecular hydrogen bonds as dotted lines

Example 2 : The complex $[ZnCl_2(C_{18}H_{14}N_4O)]_2$ of zinc (II) with dichloro{N'-[phenyl(pyridin-2-yl-κN)-methylidene]isonicotinohydrazide-κ^2N',O} crystallizes with two molecules in the asymmetric unit, which differ in the tautomeric forms (neutral and zwitterionic) of the coordination of the organic ligand. In both molecules, the Zinc (II) ion has a slightly distorted square-based pyramidal geometry (Addison parameter or trigonal angular structural parameter $\tau = (\beta-\alpha)/60 = 0.098$) by two nitrogen atoms, one oxygen atom of the Schiff base of the ligand and two monodentate chloride anions. The crystal lattice is stabilized by the hydrogen bonds N-H...N and N-H...Cl [11]. The ligand molecules coordinate respectively to one of the zinc(II) ions in a tridentate manner in its hydrazide form and to the other zinc(II) center in its tautomeric form where the uncoordinated pyridine ring nitrogen atom is protonated by the proton from the nitrogen of the hydrazide moiety. In both cases, the coordination creates two five-membered chelate metal rings. The two molecules of the asymmetric unit interact by N-H···N hydrogen bonding between the two uncoordinated pyridine rings. The bond between the Zn(II) center and the pyridine nitrogen atom are slightly (2.200 and 2.131 Å) different from the other two Zn-N bonds (2.078 and 2.136 Å). These distances are comparable to those found in the complex $[Zn(H_2BzpClPh)Cl_2]$ ($H_2BzpClPh$ est 2-benzoylpyridinepara-chloro-phénylhydrazone) (Despaigne et al, 2009). The C1-O1 bond distance of 1.252 Å is consistent with that of a higher single bond while the C19-O2 bond distance of 1.217 Å is consistent with that of a double bond. The Zn2-O2 bond distance is 2.248 Å while the Zn1-O1 length is 2.127 Å. The decrease in length is consistent with the presence of a negative charge at the O1 oxygen atom, which increases the strength of the Zn1—O1 bond. The largest angles around the Zn(II) centers (<β>: N3—Zn1—O1 = 148.50° and <β> N7—Zn2—O2 = 114.79°) are slightly larger than the second ones (<α>: N2—Zn1—Cl2 = 128.30° and <α>: N6—Zn2—Cl3 = 133.10°). The value of the distortion [$\tau = (\beta-\alpha)/60$] of the coordination polyhedron, $<\tau> = 0.337$ for Zn1 and $<\tau> = 0.191$ for Zn2 can be compared to the ideal value of 1 for a trigonal bipyramid and 0 for a square-based pyramid

(Addison et al., 1984), the environment of the metal center can be determined. Each zinc(II) center has a square-based pyramidal geometry with appreciable distortions as shown by the Addison parameter <τ>. The basal plane for the Zn(II) center is respectively constructed by the coordination of two nitrogen atoms, one oxygen atom of the ligand, and one chloride ion acting as the monodentate anion of zinc.

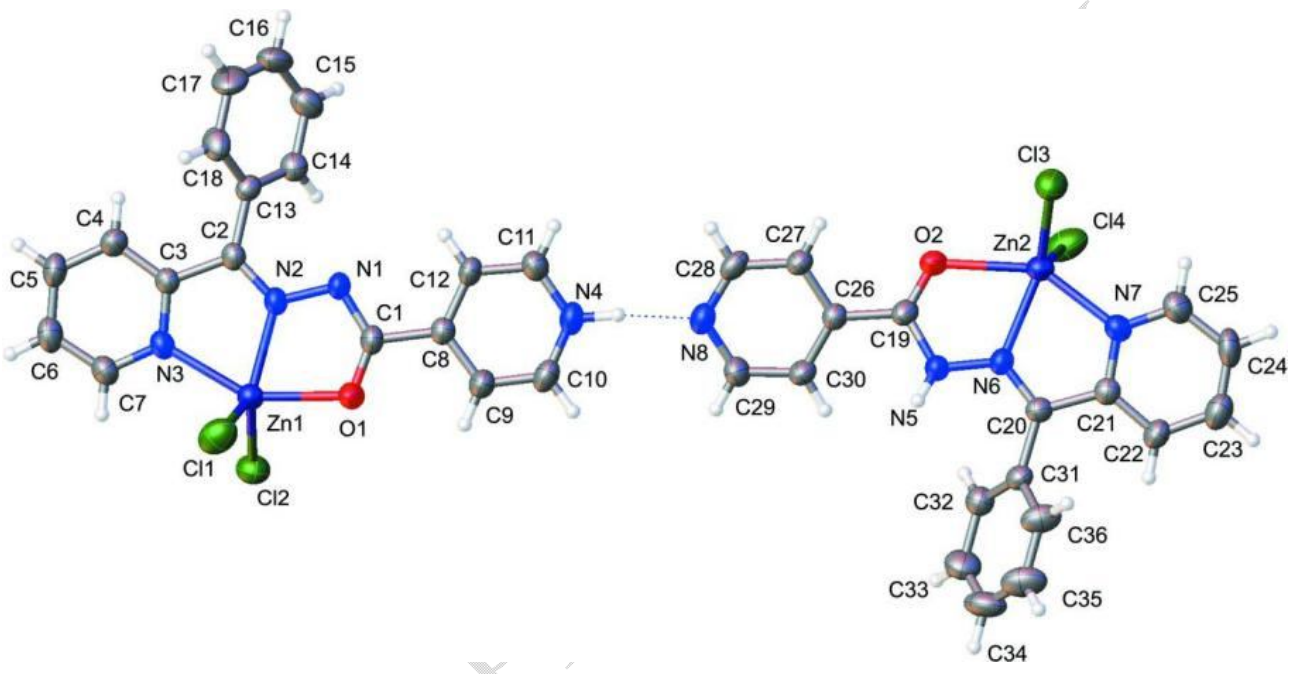

Figure 40 : crystal structure of the complex $[ZnCl_2(C_{18}H_{14}N_4O)]_2$

Example 3 : For the manganese(II) complex with the ligand 2-{[2-(2-hydroxybenzylideneamino)ethylimino]methyl}phenol, the Mn(III) ion adopts a geometry in which the equatorial plane is formed by the Schiff base atoms that are bonded to the metal. Two iminic nitrogen atoms (N1 and its symmetrical N2) and two phenolic oxygen atoms form the equatorial plane. A water molecule is in the apical position, giving a pentacoordinated Mn^{3+}. Also noted is the presence of an uncoordinated perchlorate anion and a free water molecule. Four atoms of the ligand form a square (**equatorial atoms**). The metal is located in the center of this square. The last atom (**axial atom**) is located perpendicular to the previous plane.

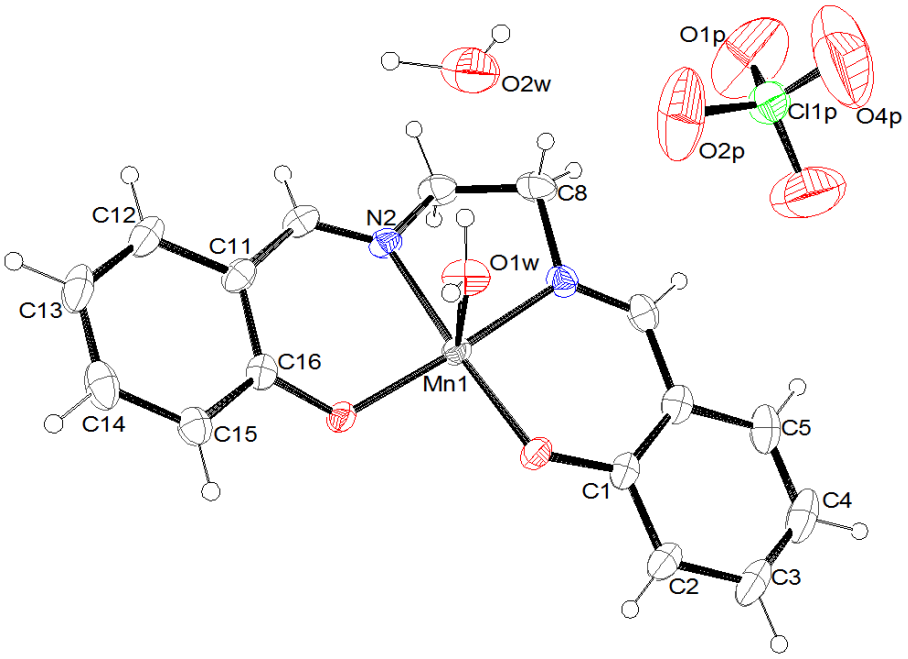

Figure 41 : Crystal structure of the manganese(II) complex with the ligand 2-{[2-(2-hydroxybenzylideneamino)ethylimino]methyl}phenol

We intentionally omit the hydrogen atoms for clarity.

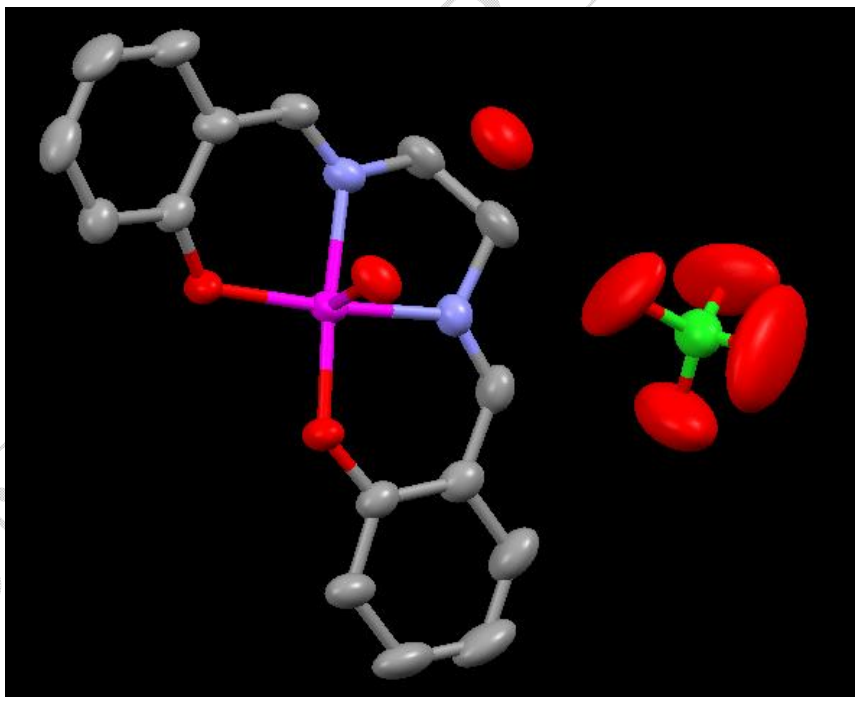

Figure 42 : Crystal structure of the manganese(II) complex with the ligand 2-{[2-(2-hydroxybenzylideneamino)ethylimino]methyl}phenol without hydrogen atoms

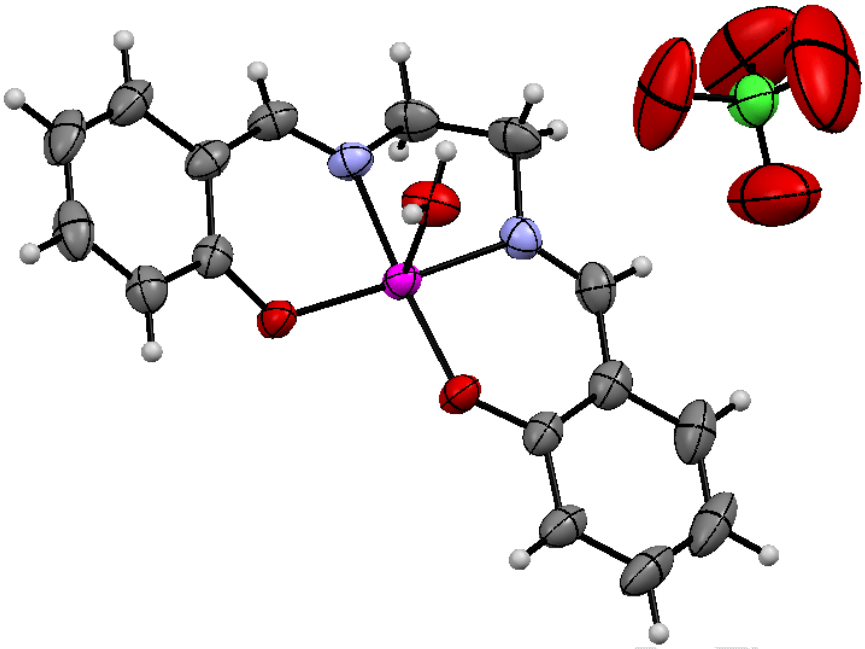

Figure 43 : Crystal structure of the manganese(II) complex with the ligand 2-{[2-(2-hydroxybenzylideneamino)ethylimino]methyl}phenol without the free water molecule

Here we omit the uncoordinated water molecule. The crystal lattice is shown in the following figure:

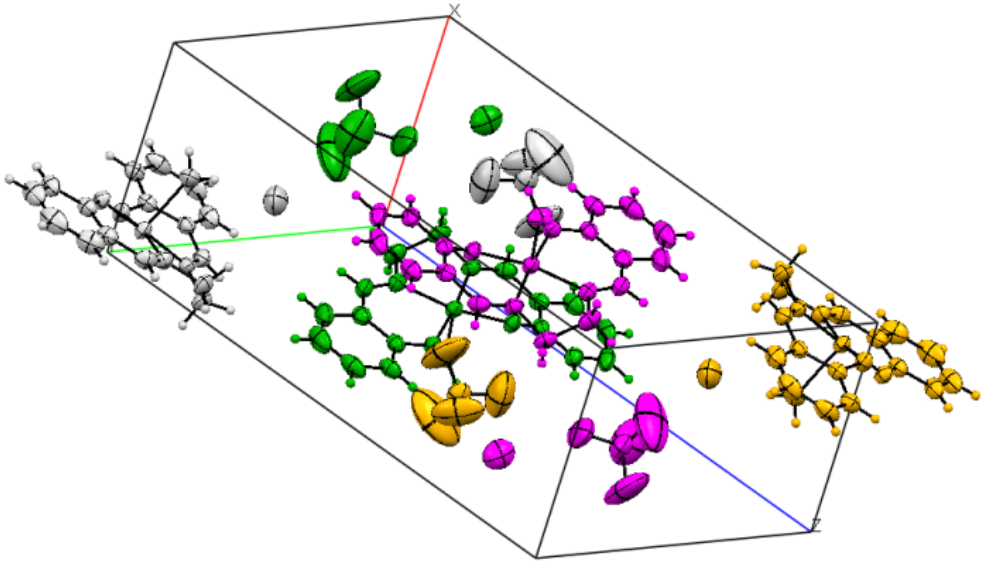

Figure 44 : crystal lattice of the manganese (II) complex with the ligand 2-{[2-(2-hydroxybenzylideneamino)ethylimino]methyl}phenol

Example 4 : Also the example of the di-l-chlorido-μ:4κ^2*Cl*:*Cl*-2:3κ^2*Cl*:*Cl*-dichlorido-2κ*Cl*,4κ*Cl*-bis-[μ_3-ethoxy(pyridin-2-yl)méthanolato-1:2:3κ^3*O*:-N,O:O;1:3:4κ^3*O*:*O*:*N*,*O*] bis[μ_2-éthoxy(pyridin-2-yl)méthanolato-1:2κ^3N,O:O;3:4κ^3*N*,*O*:*O*] tetracopper (II). The environment around each copper(II) ion is pyramidal with a deformed square base [12].

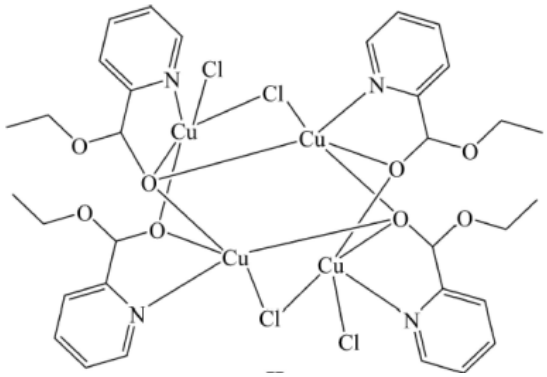

Scheme 73 : Structure of the complex $[Cu_4(C_8H_{10}NO_2)_4Cl_4]_n$

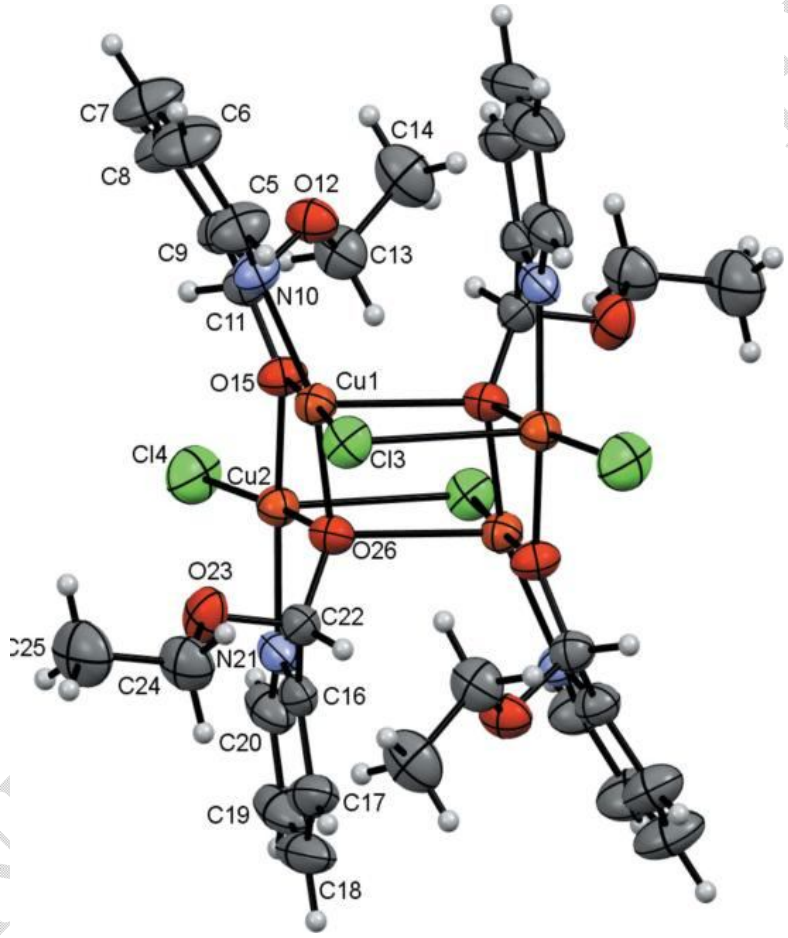

Figure 45 : ORTEP diagram of the tetranuclear copper (II) complex

The tetranuclear complex has four Cu(II) metal centers, two of which are mutually interconnected via two enolate oxygen atoms, while the other two Cu(II) cations are linked by a chloride anion and an enolate oxygen atom. In the structure, the two open cube units with seven vertices each share one side composed of two Cu(II) ions bridged by two enolate oxygen atoms. Each of the five-coordinated Cu(II) cations has a square-based pyramidal environment NO_3Cl. Each of the other two five-coordinated Cu(II) cations has a distorted

square-based pyramidal environment NO_2Cl_2. In the crystal, a series of intramolecular hydrogen bonds C—H…O and C—H…Cl are observed in each tetranuclear monomer unit, which is connected to four tetranuclear monomer units by intermolecular hydrogen bonds C—H…O, thus forming a two-dimensional structure.

Le complexe tétranucléaire à cube ouvert se situe autour d'un centre d'inversion cristallographique, chaque ligand mono déprotoné se coordonnant avec un ion Cu(II) à travers un atome d'azote pyridinique et un atome d'oxygène alcoolate, formant des anneaux chélatés à cinq chaînons. La molécule forme également des liaisons hydrogène intramoléculaires entre un ion chlorure terminal et un atome d'hydrogène aromatique (C20-H20···Cl4) et aussi entre un pont chlorure et un hydrogène aromatique (C9-H9···Cl3 et C13-H13B···$Cl3^i$). Des contacts C—H···O sont également trouvés. Il y a deux environnements Cu(II) : Cu1NO3Cl et Cu2NO2Cl2. Deux molécules du ligand agissent comme des ponts entre deux ions Cu(II) voisins à travers leurs atomes d'oxygène d'alcoolate tandis que les deux autres molécules de ligand sont pontants. La structure se compose de deux noyaux Cu3O3Cl. Le premier noyau comprend des atomes Cu1, $Cu1^i$, Cu2, en mode de coordination pontant η^3-O O26, $O26^i$, un atome O15 en mode de coordination pontant η^2-O et un ion $Cl3^i$ à 2 ponts [code de symétrie : (i) x + 3/2, y - 1/2, -z + 3/2)]. Le deuxième noyau comprend des atomes Cu1, $Cu1^i$, $Cu2^i$, des atomes à 3 ponts O26, $O26^i$, un atome $O15^i$ à 2 ponts et un ion Cl3 à 2 ponts.

The open-cube tetranuclear complex is located around a crystallographic inversion center, with each mono-deprotonated ligand coordinating with a Cu(II) ion through a pyridine nitrogen atom and an alkoxide oxygen atom, forming five-membered chelate rings. The molecule also forms intramolecular hydrogen bonds between a terminal chloride ion and an aromatic hydrogen atom (C20-H20…Cl4) and also between a chloride bridge and an aromatic hydrogen (C9-H9…Cl3 and C13-H13B… $Cl3^i$). C—H…O contacts are also found. There are two Cu(II) environments: Cu1NO3Cl and Cu2NO2Cl2. Two ligand molecules act as bridges between two neighboring Cu(II) ions through their alkoxide oxygen atoms while the other two ligand molecules are bridging. The structure consists of two Cu3O3Cl nuclei. The first nucleus comprises Cu1, $Cu1^i$, Cu2 atoms, in η^3-O bridging coordination mode O26, $O26^i$, an O15 atom in η^2-O bridging coordination mode and a 2-bridged $Cl3^i$ ion [symmetry code: (i) x + 3/2, y - 1/2, -z + 3/2)]. The second nucleus comprises Cu1, $Cu1^i$, $Cu2^i$ atoms, 3-bridged atoms O26, , $O26^i$, a 2-bridged $O15^i$ atom and a 2-bridged Cl3 ion.

The range of Cu—O—Cu angles is [99.76 (6)–102.98° (6)] and the Cu1—Cl3—$Cu2^i$ angle is 84.39°(2). These differ considerably from the 90° angles of an ideal cube. The two Cu3O3Cl cubes are joined by a perfectly rectangular side defined by the Cu1, O26 and Cu^i, $O26^i$ atoms. The values of the two different edge lengths of the rectangular sides are 2.4280 (14) and

1.9684 (13) Á. The other faces of the two open cubes are irregular with different lengths, namely Cu1—O26^{i} = 2.4280 (14) Á, Cu2—O26 = 1.9707 (14) Á, Cu1—Cl3 = 2.2181 (6) Á and Cu2—Cl3 = 2.8134 (6) Á. The Cu1 ion (Cu1^{i}) and the atoms of each of the two CuO3NCl units are connected in η^2-O bridging coordination mode and η^3-O bridging coordination mode of a deprotonated hydroxyl group and a chloride ion to three other Cu(II) cations. In the CuO2NCl2 unit, Cu2 ions (Cu2^{i}) are bound by η^2-O bridging coordination mode and η^3-O bridging coordination mode from a deprotonated hydroxyl group and a chloride ion to two other Cu(II) cations with Cu1—Cu2 and Cu1-Cu2^{i} distances of approximately 3.012 and 3.408 Á, respectively. These are in good agreement with literature values (Qin et al., 2014). The distances of oxygen atoms in the bridge positions to the cupric ions are asymmetric with Cu1—O26i, Cu1—O26, and Cu2—O26 lengths of 2.4280 (14), 1.9684 (13), 1.9707 (14) Á, respectively, while the Cu1—O15 and Cu2—O15 lengths are 1.9170 (13) and 1.9324 (13) Á, respectively. These lengths are consistent with those of related structures (Lazarou et al., 2018; Tabassum et al., 2017). The environment of both Cu(II) cations is pyramidal with a distorted square base. The largest angles around Cu1 and Cu2 are O15—Cu1—Cl3 [176.95°(5)], O26— Cu1—N10 [156.02°(7)], O26—Cu2—Cl4 [170.05°(5)] and O15—Cu2—N21 [157.61°(7)].

The Addison parameters τ are 0.348 for Cu1 and 0.207 for Cu2 (Addison et al., 1984), indicating considerable distortion; $\tau = (\alpha - \beta)/60$ where α and β are the largest angles subtended by the Cu ion. The basal plane around each of the Cu1 and Cu2 cations is formed by a chloride anion, a pyridine nitrogen atom, and two enolate oxygen atoms while the apical positions are occupied by an enolate oxygen atom for Cu1 and a chloride anion for Cu2. The Cu1—Cl3 and Cu2—Cl3 copper–halogen bond lengths of 2.2181 (6) and 2.8134 (6) Á, respectively, are in good agreement with those of a chloride ion in the bridging position (Choubey et al., 2015). The Cu2—Cl4 bond length of 2.1987 (7) Á indicates an unidentified terminal chloride ion (Kalinowska-Lis et al., 2011). The four cupric ions occupy the vertices of a parallelogram with the angles Cu1—Cu2—Cu1^{i} and Cu2—Cu1—Cu2^{i} of approximately 63.59 and 116.41°. The sum of the angles in the parallelogram is 360° and the lengths of the two diagonals, Cu1—Cu1^{i} and Cu2—Cu2^{i}, are 3.399 and 5.461 Á, respectively, and are comparable to values found in a similar complex reported in the literature (Monfared et al., 2009). All O—Cu angles in the open cube are between 99.76 (6) and 102.96° (6) and the Cu1—Cl3—Cu2^{i} angle is 84.39° (2). They are different from those in an ideal cube. These bridge angles are also smaller than those reported for similar complexes (Banerjee et al., 2013; Swank et al., 1979), but they are almost equal to those in the complex $[Cu_2(qsalBr)_2Cl_2](DMF)$ where qsalBr=8-aminoquinoline with 5-bromo-salicylaldehyde (Liu

et al., 2009). This is a small Cu1—Cu2 [3.4082(4)Á] difference from those found in another dichloro-bridged copper(II) complex (Banerjee et al., 2013).

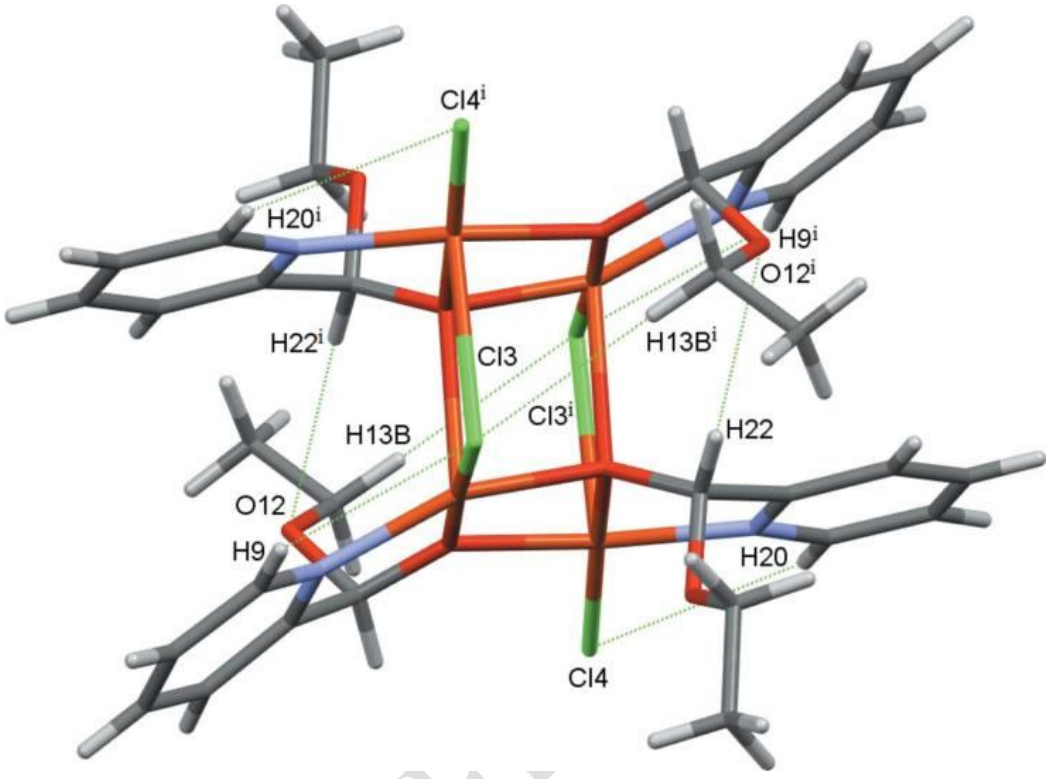

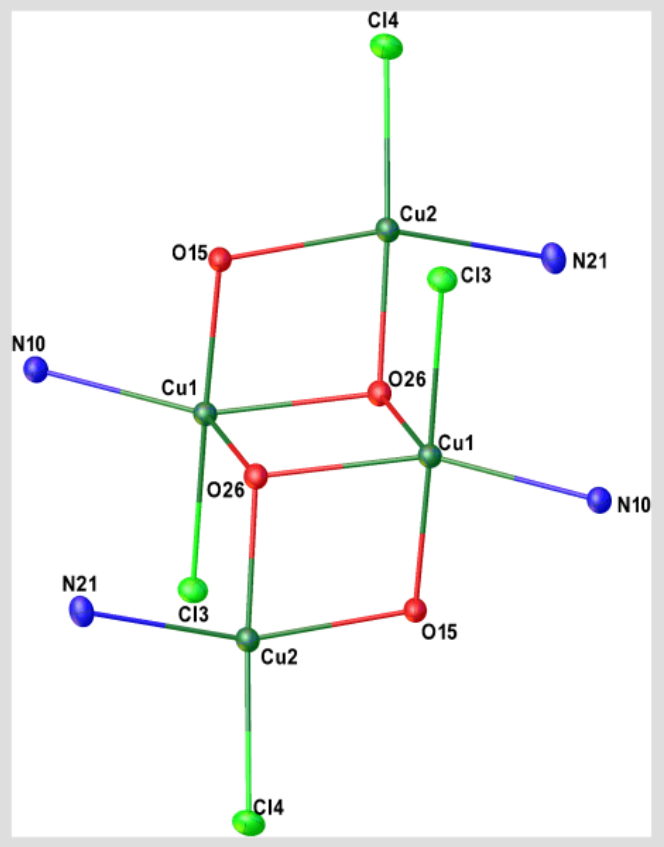

Figure 46 : Crystal structure of the tetranuclear copper(II) complex

5°) Coordination number 6

The most common geometry is that of the octahedron. There are three kinds of deformation of octahedral complexes:

- Tetragonal deformation: elongation or compression along an axis of rotation of order 4 of the octahedron
- Trigonal deformation: elongation or compression along one of the four third-order rotation axes of the octahedron which pass through the center of the faces ;
- Rhombohedral deformation: elongation or compression.

In the octahedron, the ligands are located at the center of the faces of a cube, with the metal at the center of this cube. The octahedral geometry can exhibit isomerism in the case where there is more than one ligand. The $\mathbf{MA_4B_2}$ octahedral compounds exhibit two isomers:

- The *cis* isomer in which the two **B** ligands are neighbors (angle **B – M – B** = 90°),

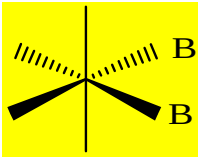

Scheme 74 : representation of the cis isomer

- The *trans* isomer in which the two **B** ligands are opposite (**B – M – B** = 180°).

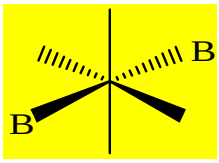

Scheme 75 : representation of the trans isomer

The octahedral MA_3B_3 compounds have two isomers:

- The **facial** isomer (fac) in which the three ligands A (or B) are on the same face of the octahedron.

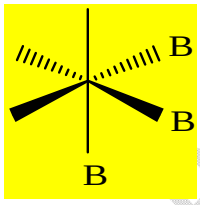

Scheme 76 : representation of the facial isomer

- The **meridional** isomer (mer) in which the three ligands A (or B) and M are coplanar.

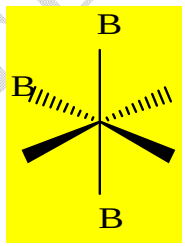

Scheme 77 : representation of the meridional isomer

Example 1 : Bis-{N-[1-(pyridin-2-yl-κN)ethylidene]nicotinehydrazide-κ^2N',O} reacts with cobalt(II) and copper(II) perchlorates, the resulting complexes have octahedral environments around cobalt(II) and copper(II) [13]. Complexes of Co(II), $[Co(C_{26}H_{24}N_8O_2)]\cdot(ClO_4)_2\cdot(H_2O)_2$ (1), and Cu(II), $[Cu(C_{26}H_{23}N_8O_2)]\cdot(ClO_4)$ (2), have been synthesized. Compound 1 crystallizes in the triclinic space group P-1. Compound 2 crystallizes in the monoclinic space group P21/c. In the structure of the mononuclear complex 1, the Co(II) cation is coordinated by two ligand molecules. The basal plane around the Co(II) cation is occupied by two pyridine nitrogen atoms and two carbonyl oxygen atoms. Two iminic nitrogen atoms occupy the apical positions of the distorted square-based pyramidal

geometry. Mononuclear 2 consists of a ligand-coordinated Cu(II) and a monodeprotonated ligand molecule. The metal center is in a distorted octahedral environment. The basal plane around the Cu(II) is occupied by two pyridine nitrogen atoms and two carbonyl oxygen atoms, with the apical position occupied by the two iminic nitrogen atoms.

In the crystal structure of the coordination compound $[Co(C_{26}H_{24}N_8O_2)]\cdot(H_2O)_2\cdot(ClO_4)_2$ (1), the Co(II) center is hexacoordinated by two pyridine nitrogen atoms, two iminic nitrogen atoms, and two carbonyl oxygen atoms of the ligand. The coordination environment can be described as a severely distorted octahedron. The basal plane around the Co(II) cation is occupied by the pyridine nitrogen atoms N4 and N8 with Co–N distances of 1.920 and 1.915 Å and the carbonyl oxygen atoms O1 and O2 with Co–O distances of 1.887 and 1.905 Å. The bond lengths are slightly shorter than the values reported for related complexes. The apical positions are occupied by the iminic nitrogen atoms N3 and N7 with Co–N distances of 1.853 and 1.856 Å. These values are shorter than those reported in the literature. Upon coordination, each of the two ligand molecules, which acts as a tridentate ligand, formed two five-membered rings with the Co(II) center: N-C-C-N-Co and O-C-N-N-Co. For each ligand, the two-membered rings share a nitrogen atom N3 and N7, respectively. The angles imposed by the five-membered rings are strongly deviated from the ideal angles of 90° for a regular octahedron (82.56–101.36°). These angles are smaller than those reported in the literature. In the basal plane, the transoid angles O2–Co1–N8 and O1–Co1–N4 are 165.37° and 165.34° respectively while the cissoid angles range from 87.59 to 93.98°.

The sum of the angles subtended by the Co(II) donor atoms in the equatorial plane (O1-O2-N4-N8) is 363.65°; indicating approximately coplanarity for these atoms as shown by the effective value of 0.0422 Å. The angle value of 175.12° is defined by the atoms in the apical position: N3–Co1–N7. A geometric analysis was performed on the π-π stacking in the cobalt complex. Considering the crystal structure of the cobalt complex, there are two types of π-π stacking interactions between the 2-substituted pyridyl rings (N4-C9-C13 and N8-C22-C26) and those between the 3-substituted pyridyl rings (N1-C1-C5 and N5-C14-C18) with Cg···Cg distances of 3.881 and 3.824 Å, respectively.

In complex 2, Cu(II) is in an octahedral environment. A neutral ligand molecule coordinates the Cu(II) center through its pyridine nitrogen atom, its iminic nitrogen atom, and its carbonyl oxygen atom. In addition, a monodeprotonated ligand molecule coordinates the Cu(II) center through its pyridine nitrogen atom, its iminic nitrogen atom, and its iminolate oxygen atom. In each case, two five-membered rings N-C-C-N-Cu and O-C-N-N-Cu are formed. The environment around the metal ion is highly distorted octahedral as shown by the transoid angles (149.64° and 165.60°), the cissoid angles (90.06–97.37°) and the apical O1–Cu1–N1

angle of 149.64°. Two iminol nitrogen atoms, one iminol oxygen atom and one pyridine nitrogen atom occupy the basal plane, while one pyridine nitrogen atom and one carbonyl oxygen atom occupy the apical positions. The Cu–N distances range from 2.050 to 2.277 Å and are consistent with the values reported in the literature.

The Cu1–O1 and Cu1–O2 distances are 2.099 and 2.130 Å, respectively, showing the difference in negative charge of these two oxygen atoms. In fact, the iminolate oxygen atom O1 is more negatively charged than the carbonyl oxygen atom O2 and the O2 bond to Cu1 is stronger, resulting in a shorter distance as observed for similar complexes. In addition, the C–O bonds in the two ligand molecules are slightly different. The C21-O2 bond (1.271 Å) is longer than the C8-O1 bond (1.264 Å) which has a double bond character. The sum of the angles subtended by the donor atoms to Cu(II) in the equatorial plane (N2 O2 N6 N5) is 359.95°; indicating an approximate coplanarity for these atoms, as shown by the rms value of 0.0780 Å.

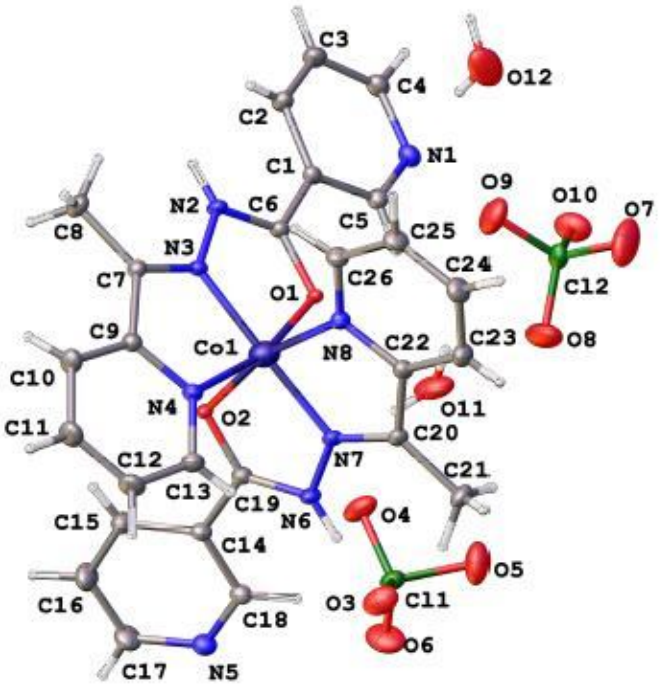

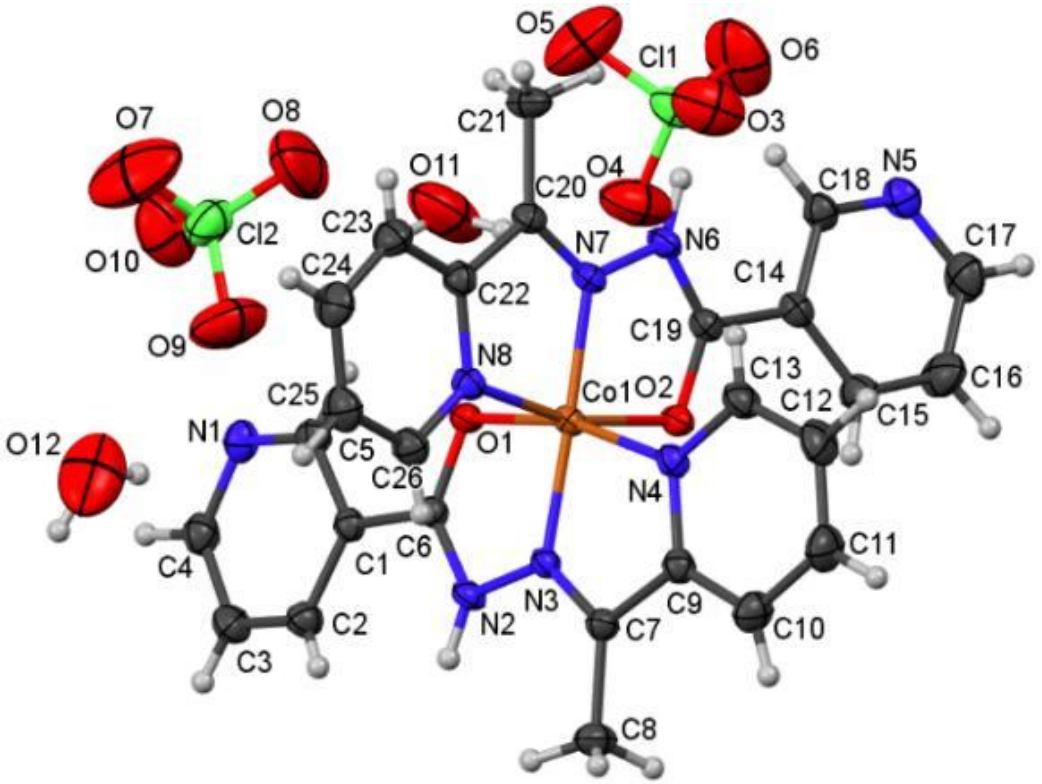

Figure 47 : Crystal structures of cobalt(II) perchlorate complex 1 with bis-{N-[1-(pyridin-2-yl-κN)ethylidene]nicotinehydrazide -κ²N',O}

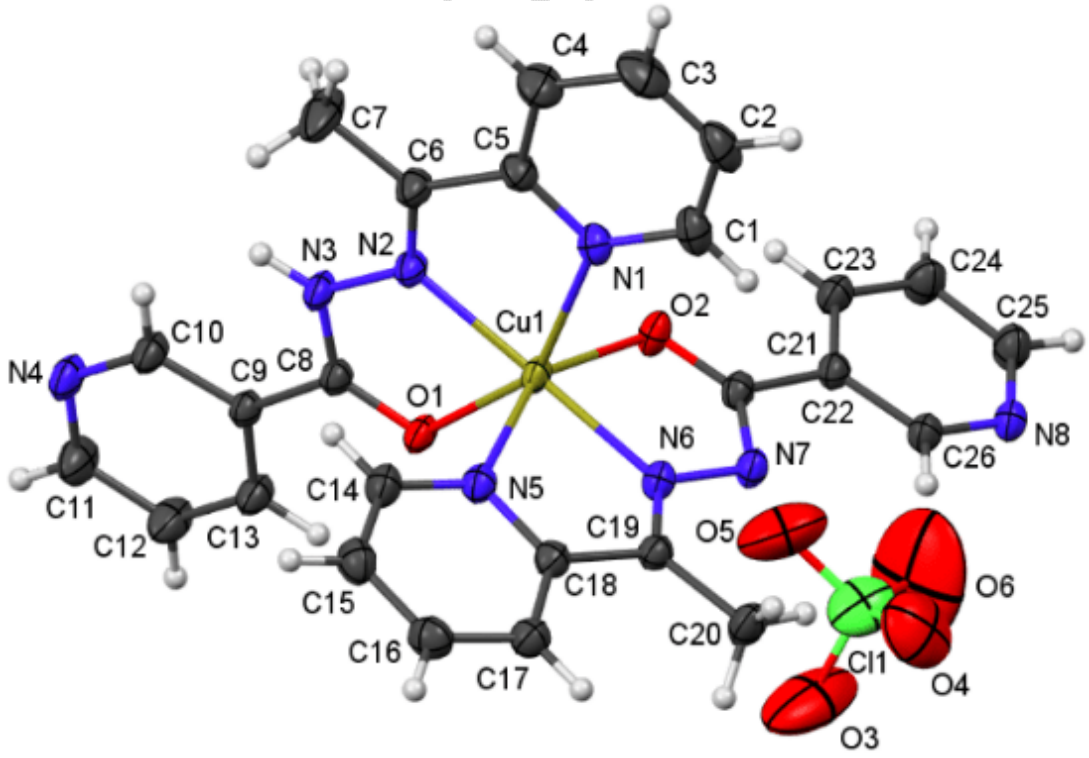

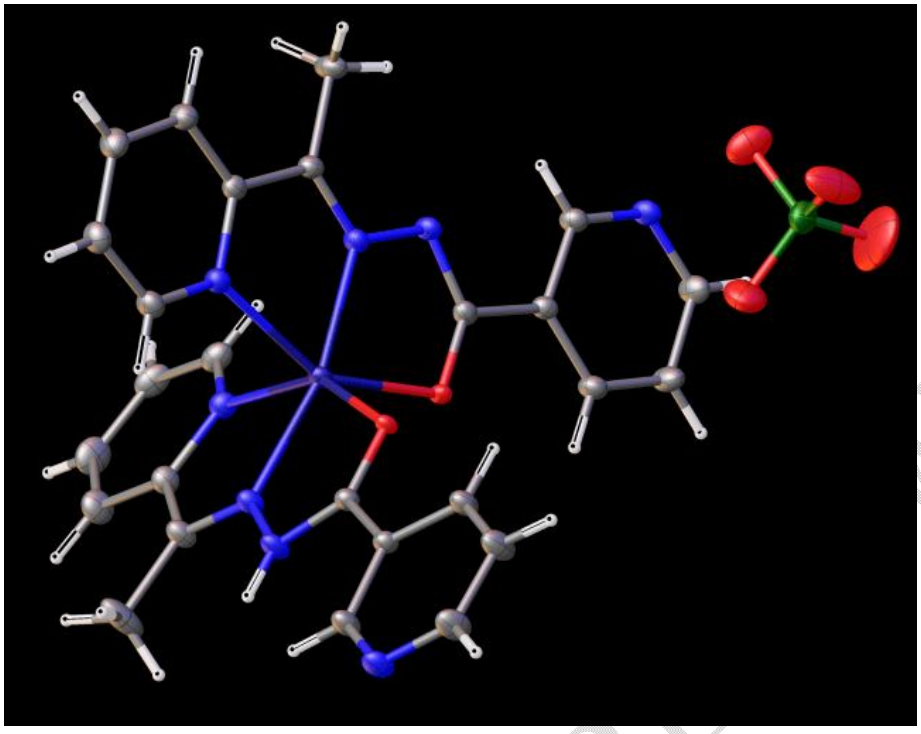

Figure 48 : Crystal structures of copper(II) perchlorate complex 2 with bis-{N-[1-(pyridin-2-yl-κN)ethylidene]nicotinehydrazide -κ²N',O}

Example 2 : A nickel(II) complex with N-benzoylpyridine-2-carbohydrazide is synthesized. The geometric environment around the nickel(II) ion is an octahedron. Nickel(II) is hexacoordinated by two ligand molecules that bind to the metal center via two nitrogen atoms and one oxygen atom per ligand molecule. The Ni(II) atom has a distorted octahedral environment [14]. A 90° deviation of the bond angles implies chelation (O2–Ni–O4 = 93.3°; O4–Ni–N2 = 91.0°; N2–Ni–N5 = 92.6°; N5–Ni–O2 = 94.4°) presumably due to the formation of a five-membered ring. The bond distances are: d(N1—Ni) = 1.964 Å, d(N2—Ni) = 2.102, d(N4—Ni) = 1.970 Å, d(N5—Ni) = 2.094 Å, d(O2—Ni) = 2.178 Å, d(O4—Ni) = 2.139. The bond lengths d(N1—Ni) and d(N4—Ni) indicate a strong bond between Ni(II) and these atoms. The bond lengths d(C1—O1) = 1.245; d(C7—O2) = 1.261 Å; d(C20—O4) = 1.250 Å and d(C14—O3) = 1.254 Å show the existence of a double bond.

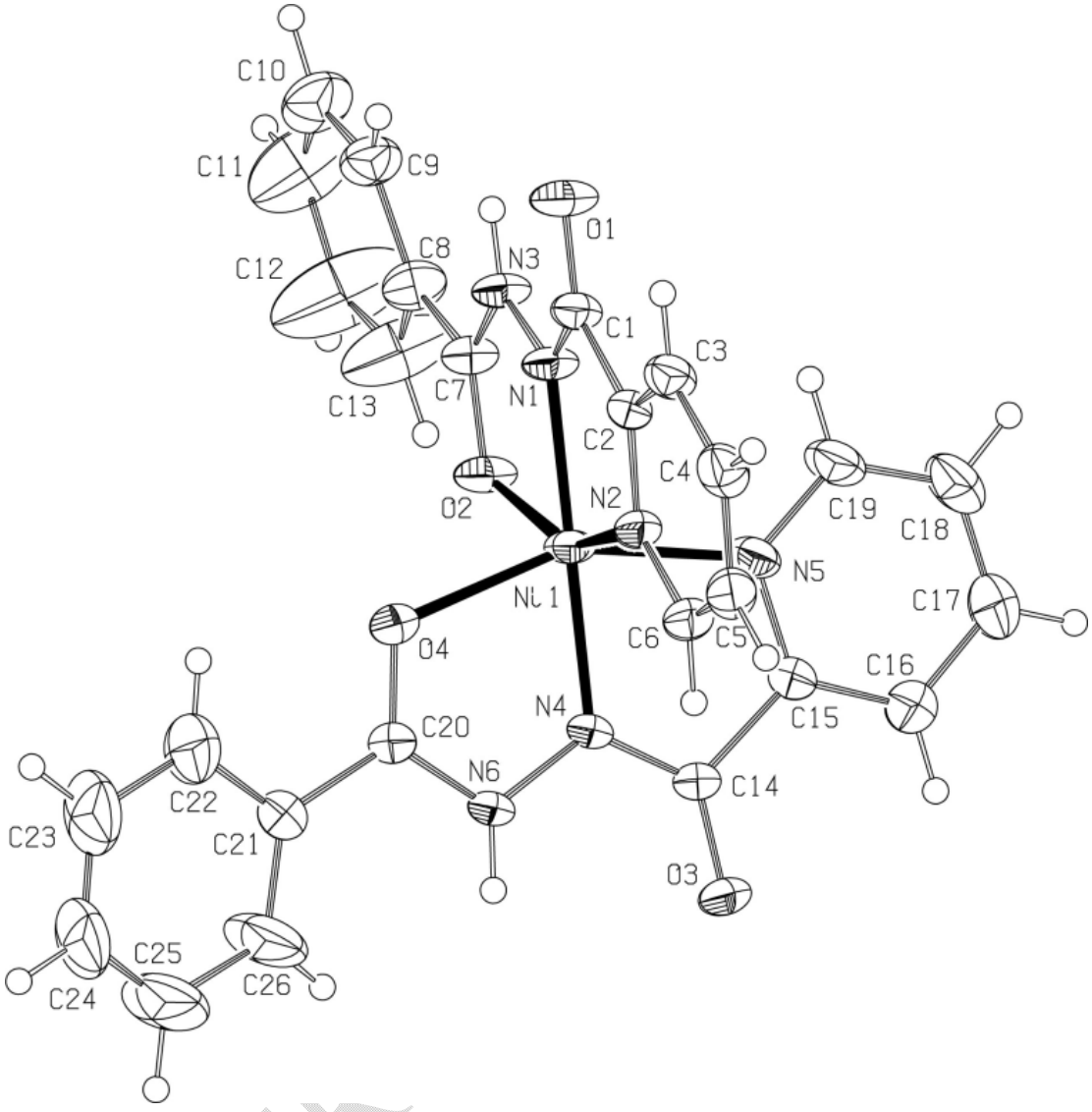

Figure 49 : Crystal structure of the nickel(II) complex with the N-benzoyl pyridine-2-carbohydrazide

Example 3 : The trinuclear complex of nickel(II) with 2-({2-[2-(2-hydroxybenzylamino)ethylthio]ethylamino}methyl)phenol gives a central nickel(II) ion with a distorted octahedral environment. Its ORTEP diagram is shown in the following figure:

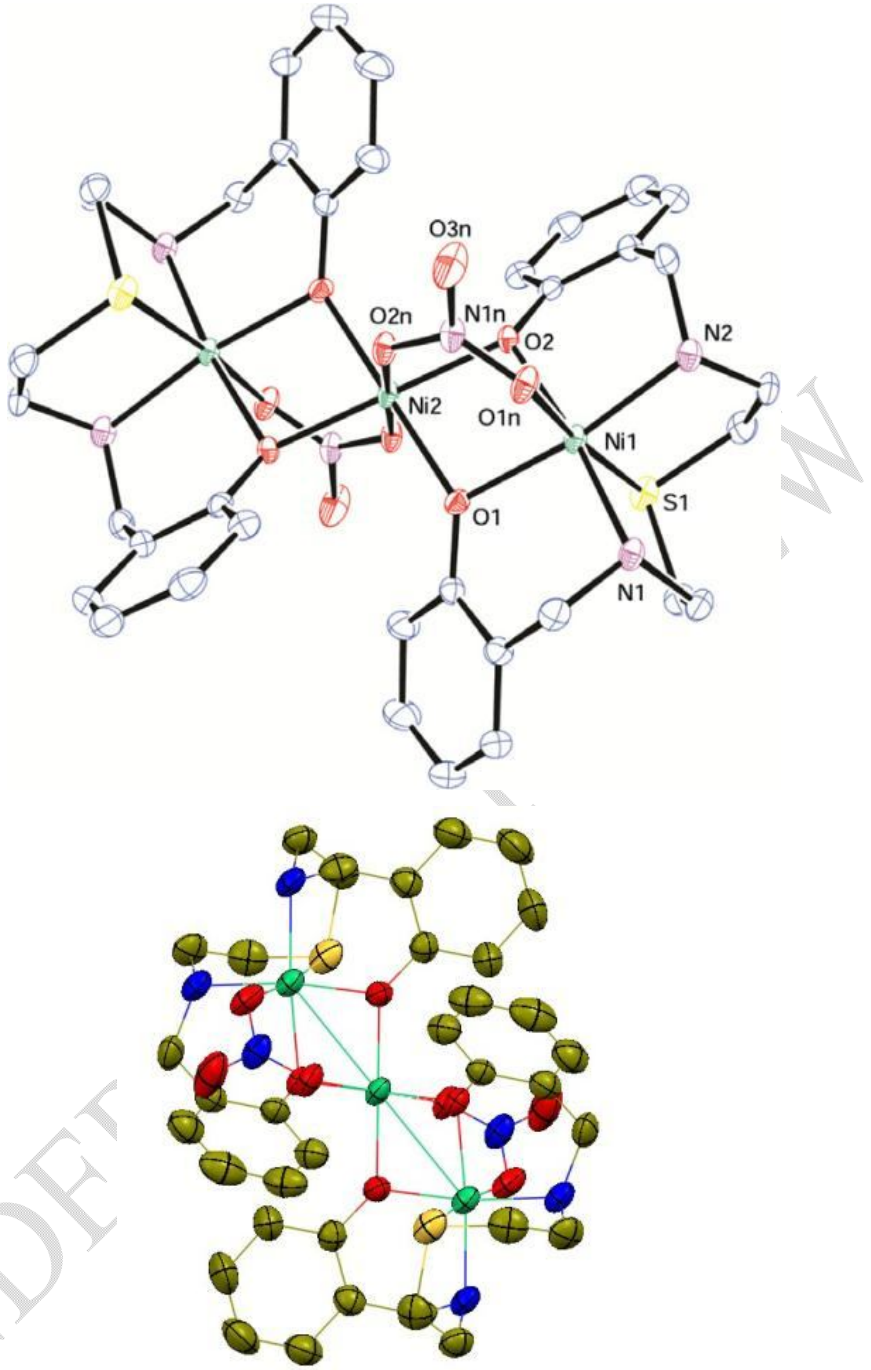

Figure 50 : Crystal structure of the trinuclear nickel(II) complex with the 2-({2-[2-(2-hydroxybenzylamino) ethylthio]ethylamino}methyl)phenol

It is coordinated to the oxygen atoms of the bridging phenolate groups of two ligand molecules that constitute the equatorial plane with Ni2 located in this plane [15]. The axial positions are occupied by two oxygen atoms from the bridging bidentate nitrate groups. The three nickel(II) ions have an octahedral environment. Its PLUTON diagram is shown in the following figure:

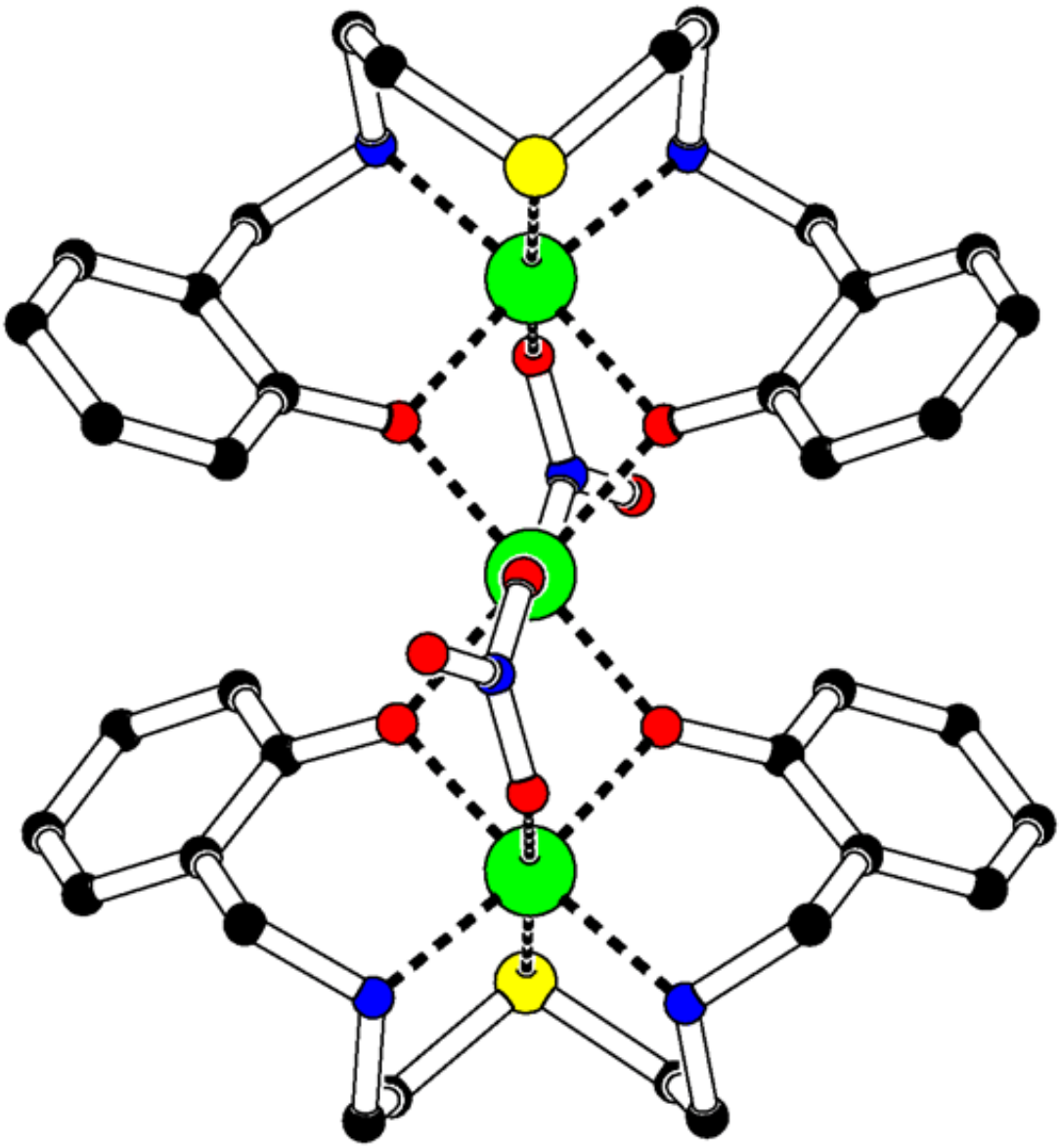

Figure 51 : PLUTON diagram of the trinuclear nickel (II) complex with the 2-({2-[2-(2-hydroxybenzylamino) ethylthio]ethylamino}methyl)phenol

Example 4 : The Schiff base behaves as a tridentate ligand in the copper(II) complex with N,N'-(2-hydroxypropan-1,3-diyl)-bis-(salicylaldimine). In the case of the complex the nitrate groups form a bidentate bridge. The terminal copper(II) ion has a square-based pyramidal environment while the central copper(II) ion has a distorted octahedron environment [7].

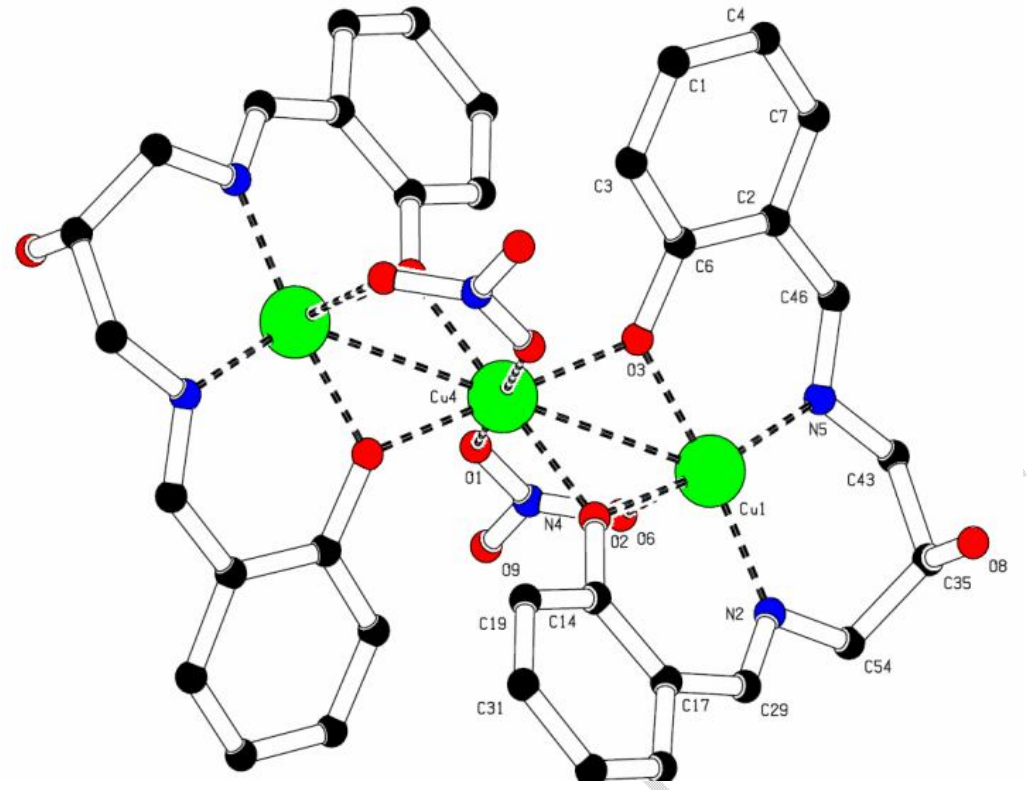

Figure 52 : Crystal structure of the copper(II) complex with the N, N'-(2-hydroxypropan-1,3-diyl)-bis-(salicylaldimine)

Example 5 : The nickel(II) complex with 2-({2-[2-(2-hydroxybenzylideneamino)ethylthio]ethylimino}methyl)phenol is binuclear, with the two centers linked by two bridging phenolate groups [7]. The geometry around the metal ion can be described as a slightly distorted octahedron, with one site consisting of the five donor atoms of the N2SO3 ligand: two imine nitrogen atoms, one sulfur atom, and the two oxygen atoms of the phenolate groups. The sixth position is occupied by the oxygen of the phenolate which serves as a bridge between the two ligands. The equatorial plane of the octahedron is formed by N2-S1-O1-O2 and the distance between this plane and the Ni(II) ion is 0.0243 Å. The axial positions are occupied by a nitrogen atom of the imine function and an oxygen atom of the bridging phenolate, respectively. The shortest distance (2.024 Å) is the bond between the nickel(II) ion and the phenolate oxygen, Ni1-O1 and the longest distance (2.5717 Å) is the bond between the nickel(II) ion and the sulfur atom, Ni1-S1.

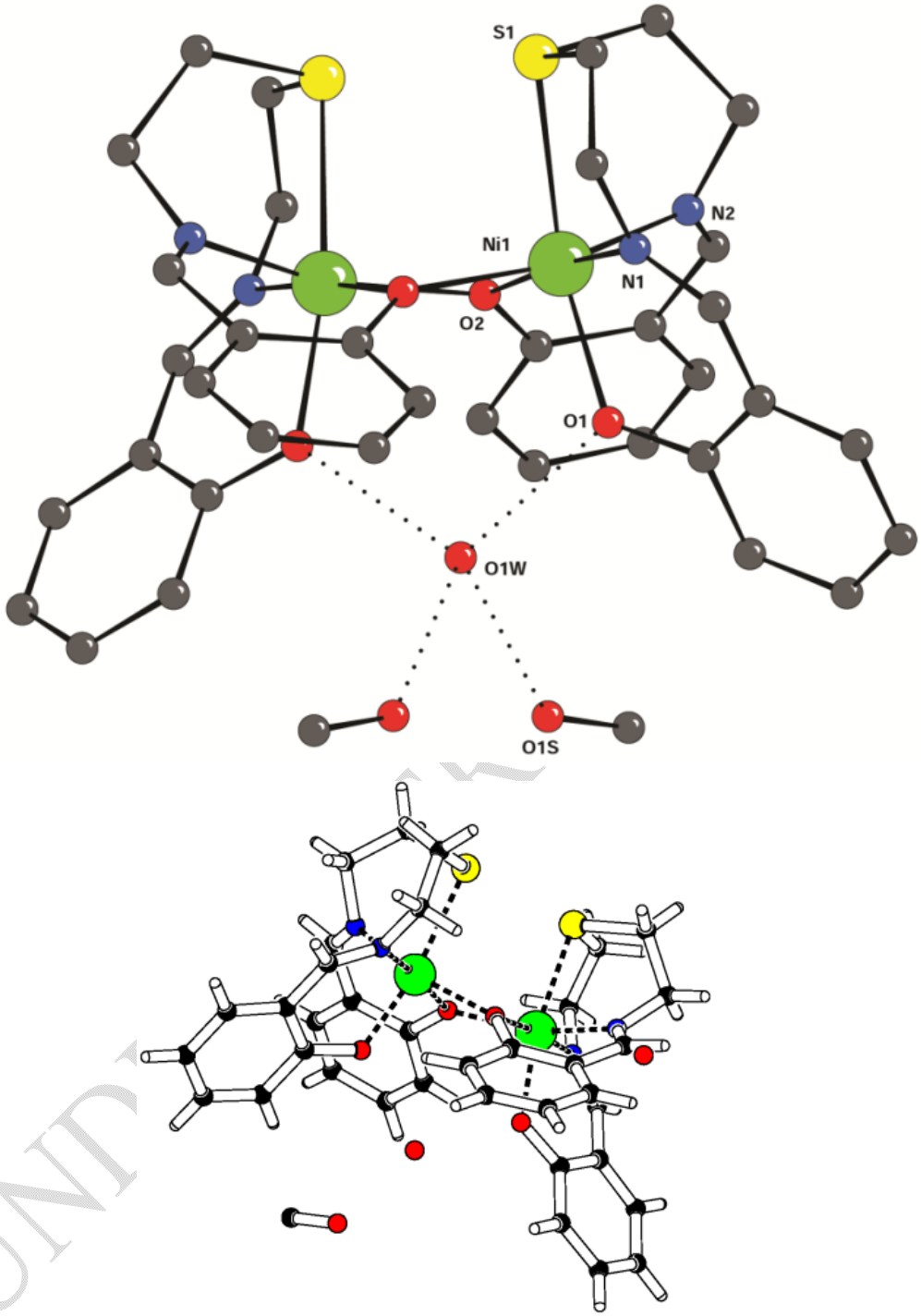

Figure 53 : Crystal structures of the nickel (II) complex with the 2-({2-[2-(2-hydroxybenzylideneamino) ethylthio]ethylimino}methyl)phenol

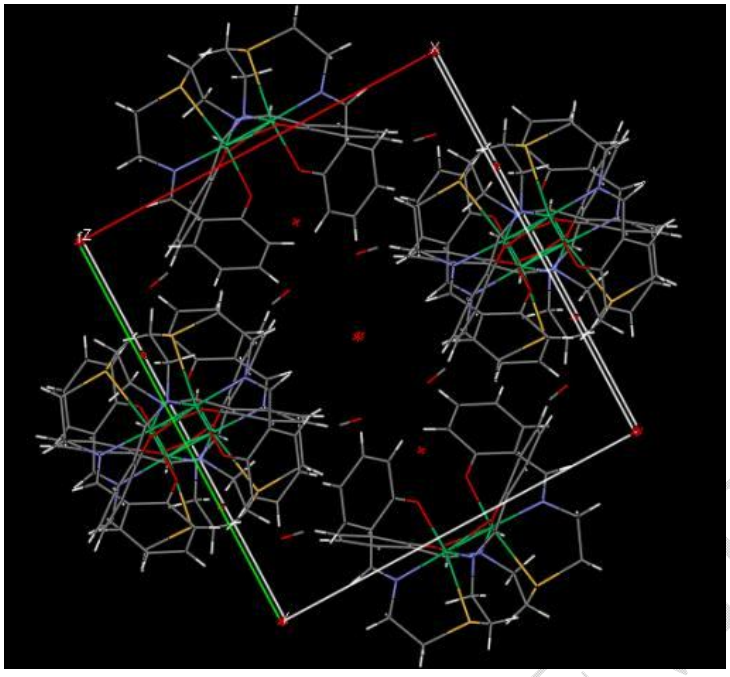

Figure 55 : crystal lattice of the nickel (II) complex with the 2-({2-[2-(2-hydroxybenzylideneamino) ethylthio]ethylimino}methyl)phenol

Example 6 : A novel nitrite-bridged dinuclear Mn(III) compound $\{[Mn(L)(H_2O)](NO_2)[Mn(L)(H_2O)]\}\cdot(ClO_4)$ has been synthesized. The two ligand molecules encapsulate a Mn(III) ion in a tetradentate manner through two phenolate oxygen atoms and two azomethine nitrogen atoms. The two methoxy oxygen atoms of each ligand molecule remain uncoordinated. In the structure, each manganese(III) ion is located inside the six N2O4 donor atoms. The environment around each Mn(III) cation is best described as a distorted octahedral geometry, in which the plane is occupied by the atoms of the ligand molecule and the axial positions are occupied by an oxygen atom of a coordinated water molecule and an oxygen atom of the nitrite. The two Mn(III) ions are bridged by a 1,3-nitrito group. Numerous intermolecular hydrogen bonds established between water molecules as donors and phenox or methoxy oxygen atoms as acceptors connect the dinuclear units in a three-dimensional network [16].

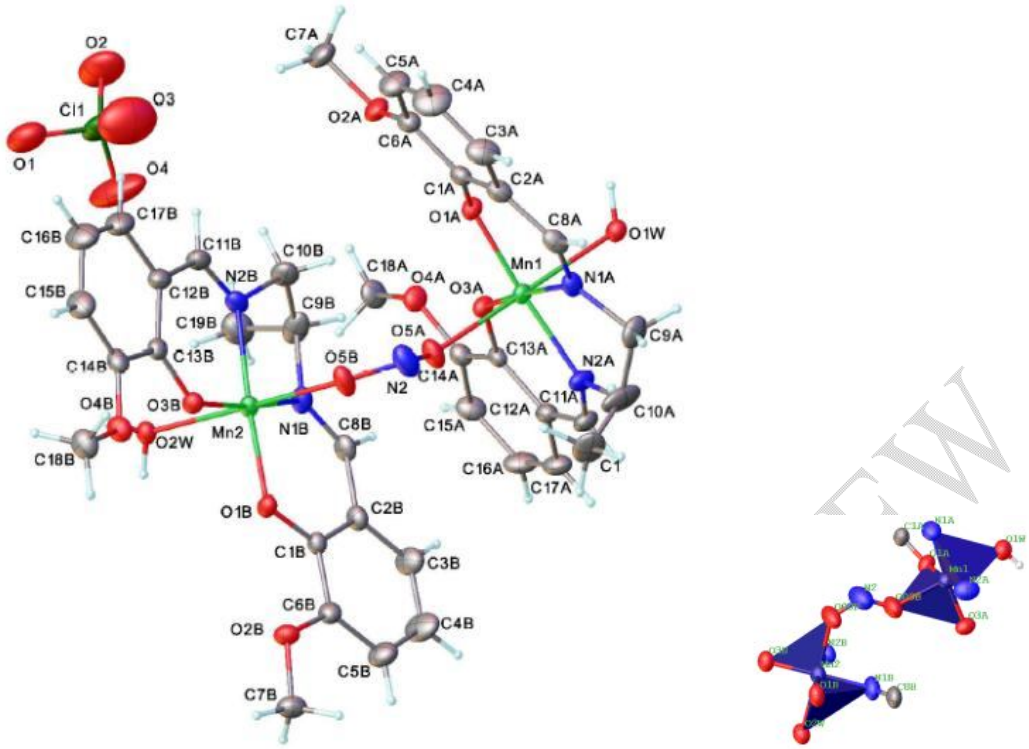

Figure 56 : crystal structure of the complex {[Mn(L)(H_2O)](NO_2)[Mn(L)(H_2O)]}·(ClO_4)

Example 7 : A new mononuclear Cobalt(III) compound with the ligand 2,2'-{propane-1,2-diyl-bis[nitrilo(E)methylidene]}bis(6-methoxyphenol) has been synthesized.

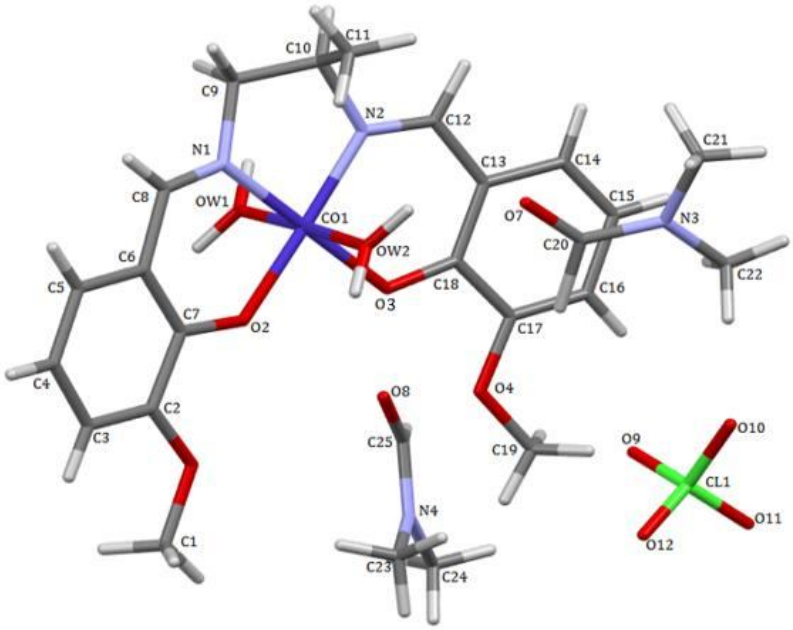

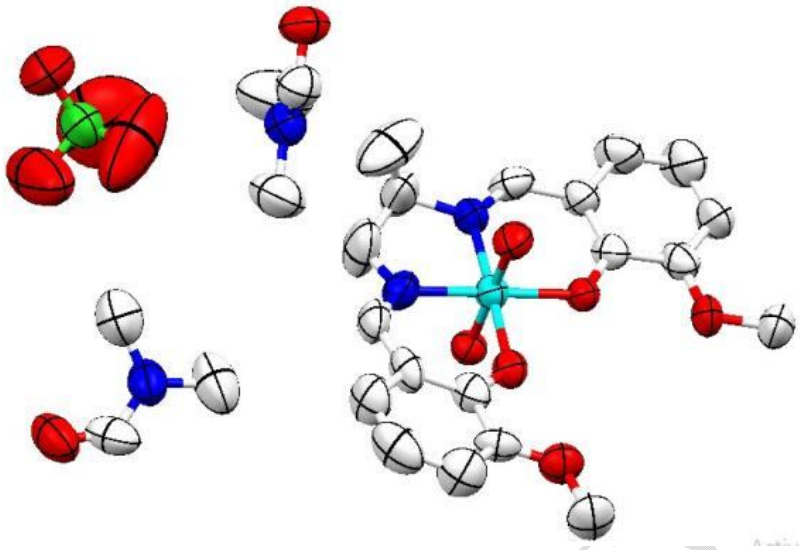

Figure 57 : crystal structure of the complex $C_{11}H_{10}Cl_{0.92}CoNO$

The cobalt(III) ion has a slightly distorted octahedral coordination geometry. Indeed, Co(III) is coordinated by two imine nitrogen atoms, N1 and N2, two phenox oxygen atoms, O2 and O3 from a deprotonated Schiff base ligand, and two oxygen atoms Ow1 and Ow2 from water. There are also two neighboring DMF molecules and a free perchlorate anion. A 90° gap in bond angles involving chelation is observed: N2—Co1—N1=84.4°; N2—Co1—O3=95.1° O2—Co1—N1=93.9°; O2—Co1—O3=86.6°). The bond distances of interest are: d(Co1-N1)=1.883 Å, d(Co1- N2)=1.870 Å, d(Co1- O2)=1.876 Å, d(Co1- O3)=1.909 Å, d(Co1-Ow1)=1.925 Å, d(Co1- Ow2)=1.905 Å. Otherwise the angles (N2-Co1-O2=178.3°; N1-Co1-O3=178.8°; Ow1-Co1-Ow2=177.4°) are different from 180° and the angles (N2-Co1-Ow2=92.0°; O2-Co1-Ow2=88.2°; O2-Co1-Ow1=89.2°; N1-Co1-Ow2=90.8°; N1-Co1-Ow1=89.1°; O3-Co1-Ow2=90.3°; O3-Co1-Ow1=89.9°) are different from 90°.

6°) Coordination number 7

The fact that octahedral complexes are stable means that the introduction of a seventh ligand creates steric discomfort and therefore instability, but it is possible to arrive at heptacoordinated complexes which can appear in the form of a pentagonal bipyramidal complex or a single-capped octahedron.

Example : The structure of the aquachlorido(nitrato-κ^2O,O')-[1-(pyridin-2-ylmethylidene-κN)-2-(pyridin-2-yl-κN)hydrazine-κN']manganese(II) complex is illustrated in the following figure in which the Mn(II) cation is heptacoordinated [17]. The asymmetric unit comprises a discrete molecule in which the Mn(II) cation is heptacoordinated. The coordination

polyhedron of the Mn(II) center is best described as a distorted pentagonal bipyramid with a MnN3O3Cl chromophore. The basal plane is occupied by two nitrogen atoms of the pyridine rings, one nitrogen atom of the imine function, and two oxygen atoms of the chelating bidentate nitrate group. The ligand nitrogen atoms bonded to the metal have angles of 69.85° (N1—Mn1—N2) and 69.62° (N2—Mn1—N4), which are slightly different from the ideal angle for a regular pentagon (72°). The sum of the equatorial angles around Mn(II) is 359.72°. The angle formed by the atoms in the axial position around Mn(II) [Cl1—Mn1—O1W = 179.07°] is very close to the ideal value of 180°. The Mn-O/N bond lengths are longer than those observed in the manganese heptadentate complex [Mn(L)$(NO_3)_2$] [L is 2,6-bis(1-butyl-1H-benzo[d]imidazol-2-yl)pyridine; Kose, McKee et al., 2014]. The apical Mn1—Cl1 bond [2.4999 Å] is the longest and is comparable to those found for the complex [Mn(L)$(Cl)_2$] MeOH, [Mn1—Cl1=2.4849, Mn1—Cl2=2.5465 Å] {L is 2,6-bis[(2-hydroxyphenylimino)methyl]pyridine; Kose et al., 2015}. The second axial bond is the shortest distance in the structure [Mn1—O1W = 2.2239 Å]. The two pyridine rings are connected by a disordered C-CH=N-NH-C chain in which the bond lengths are slightly different from those observed in similar complexes. Two intramolecular hydrogen bonds, C1—H1···O2 and C11—H11···O3, are also observed in the structure.

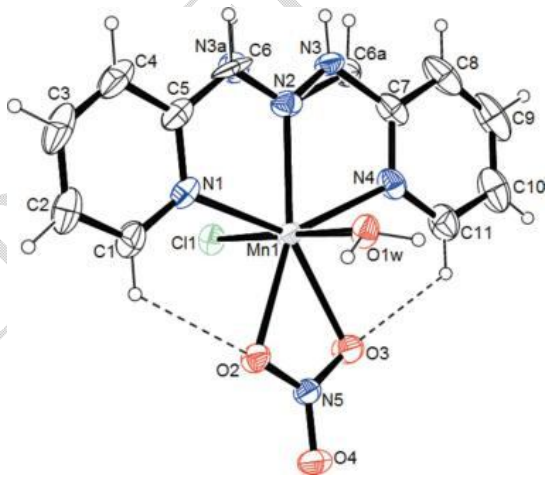

Figure 58: crystal structure of the complex aquachlorido(nitrato-k^{2}O,O')-[1-(pyridin-2-ylmethylidene-kN)-2-(pyridin-2-ylkN)hydrazine-kN']manganese (II)

7°) Coordination number 8

Example : A Schiff base (H_2L), derived from o-vanillin and nicotinic hydrazide, and its complexes with the lanthanide Ytterbium have been synthesized. The compounds found {[$(OS(CH_3)_2)(\eta^2$-$OOCH_3)$Yb](μ-L)$_2$[Yb(η^2-$OOCH_3$)$(OS(CH_3)_2)$]} are isostructural. This entity acts in its dideprotonated form by an azomethine nitrogen atom, a phenox oxygen atom,

and an iminolate oxygen atom [18]. The two Yb(III) ions are bridged by two phenox oxygen atoms, forming a dinuclear complex. The complex crystallizes in the monoclinic space group C2/c. The ytterbium atoms are octa-coordinated, and their coordination polyhedra are best described by a square antiprismatic geometry. The aromatic rings of the ligand molecule are twisted with a dihedral angle of 29.23° between their mean planes. The electronic spectra of the complexes, recorded in DMF, show absorption bands in the ranges [242-335 nm] and [385-405 nm] nm attributed to the π→π* and n→π* transitions within the ligand. The new band observed, in each spectrum, at about 477 nm is attributed to the transfer band of the ligand to the Yb^{3+} ions.

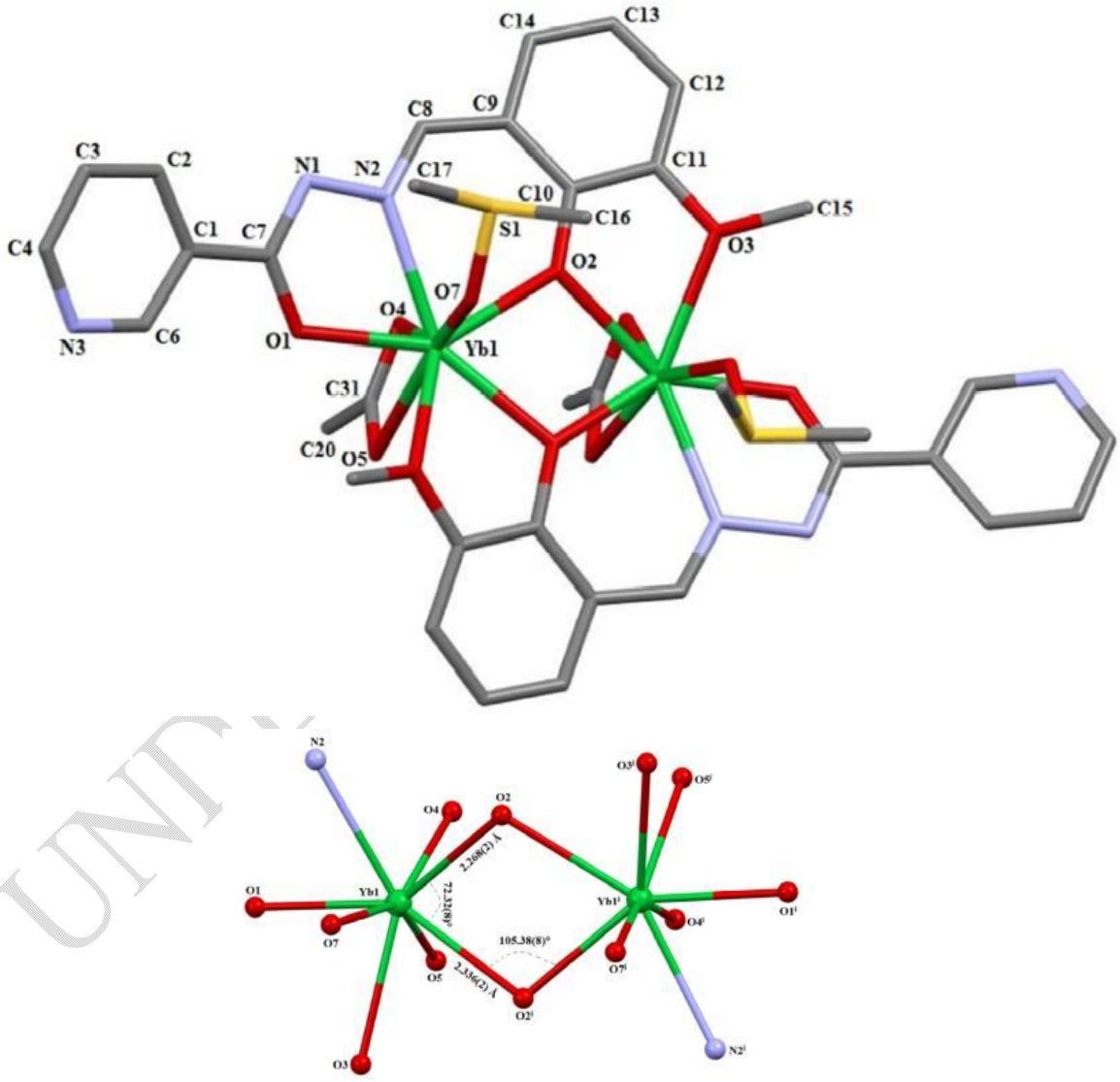

Figure 59 : Crystal structure of the complex with Ytterbium III

8°) Coordination number 9

Example 1 : Given a praseodymium acetate complex, the acyclic nature of the ligand is confirmed by X-ray diffraction. The studied dinuclear complex of structure {[Pr(L)(η^2–

$OOCCH_3)(H_2O)](\eta^1{:}\eta^2{:}\mu\text{–}OOCCH_3)_2[Pr(L)(\eta^2\text{–}OOCCH_3)(H_2O)]\}$ is that of a noncoordinated praseodymium. The environment around the metal is a three-capped trigonal prism [19]. The complex crystallizes in the monoclinic system with the space group $P2_1/n$. The asymmetric unit contains two Pr^{3+}ions, two monodeprotonated organic ligands, four acetate ions and two water molecules. The crystal structure consists of two analogous entities of $[Pr(L)(\eta^2\text{–}OOCCH_3)(H_2O)]$ bridged by two acetate groups acting in $\eta^1 : \eta^2 : \mu\text{–}OOCCH_3$ coordination mode. Each Pr^{3+}ion is coordinated by a ligand molecule via an azomethine nitrogen atom, a pyridine nitrogen atom, and a carbonyl oxygen atom resulting from two chelating rings PrOCCN and PrNCCN. The Pr^{3+} ion is coordinated by an acetate group in bidentate-chelating mode and a water molecule. The Pr^{3+} ion has coordination 9. The Pr–O distances are between 2.4200 and 2.6712 Å and are typical of a bidentate-acetate-chelating group. The two metal centers are finally connected by a pair of bridging-chelating acetato ligands that act in $\eta^1 : \eta^2 : \mu^2$-$OOCCH_3$ coordination mode. Two different bond values are noted: two typical bond values of 2.455 and 2.6712 Å (Pr1–O5 and Pr1– $O5^i$) and 2.555(2) Å (Pr1–O6i). These values are comparable to the values reported in the literature. The largest Pr–O distance (Pr1–O5i = 2.6712 Å) is observed in the chelating-bridging coordination mode $\eta^1 : \eta^2 : \mu^2$-$OOCCH_3$, while the shortest Pr–O bond length (Pr1–O3 = 2.484 Å) is observed in the chelating coordination mode η^2–$OOCCH_3$. The Pr–N distances are 2.594 and 2.612 Å. The longest Pr-N distance is due to the nitrogen atom belonging to the pyridine ring, as observed for similar complexes. The C–O bond in the coordinated acetate groups has an intermediate character between a C–O single bond and a C=O double bond. Indeed, the bond length values observed in the two acetate groups coordinated for C–O (1.249 Å–1.273 Å) are shorter than that of a single C–O bond (1.430 Å) and longer than that of a double bond (1.220 Å). The N2–C8 bond length value of 1.290 Å is consistent with the double bond character.

The Pr···Pr distance bridged by two acetate anions is 4.2777 Å. All bond lengths are normal and fall within similar ranges to those reported for dinuclear lanthanide complexes with the same hydrazone ligand. Chelation of the hydrazino ligand to the Pr^{3+} cation yields two to five membered chains (PrNCNN and PrNCCN) with occlusion angles of 61.46° (N2–Pr1–N3). The ligand angles, which involve the Pr(III) ion, are slightly larger than the angle subtended by the oxygen atoms of the bidentate-chelating acetate groups: O2–Pr1–O3 = 51.71° and $O5^i$–Pr1– $O6^i$ = 49.43°. These angle values are comparable to the values reported for the complex $[Pr(C_9H_4N_2O_4)(C_2H_3O_2)(H_2O)]_2$. The bond angle value of 68.23° of the bridged oxygen atoms of the $\eta^1 : \eta^2 : \mu^2$–acétate coordination modes [O5–Pr– $O5^i$] is comparable to that observed in the homologous complex of $[Tb_2(CH_3COO)_6(H_2O)_4]\cdot 4H_2O$. The Pr1–O5– $Pr1^i$ angle value (111.77°) is in the expected range for the $\eta^1 : \eta^2 : \mu^2$–acétate coordination modes. The dihedral

angle formed by the planes of the two terminal pyridine rings is 15.61°. The three sets of donors namely atoms [(O1, N3, O5)], [(O2, O6, N2)] and [(O3, O5^{i}, O8)] form three planes with the sums of the angles at Pr1 of 358.19°; 359.21° and 349.03° respectively. Two of the nine-vertex coordination polyhedra are known. The coordination sphere around the nine-coordinated praseodymium atom is best described by a distorted three-capped trigonal prism in which N2, O2 and O5 are the caps as shown in Figure 61.

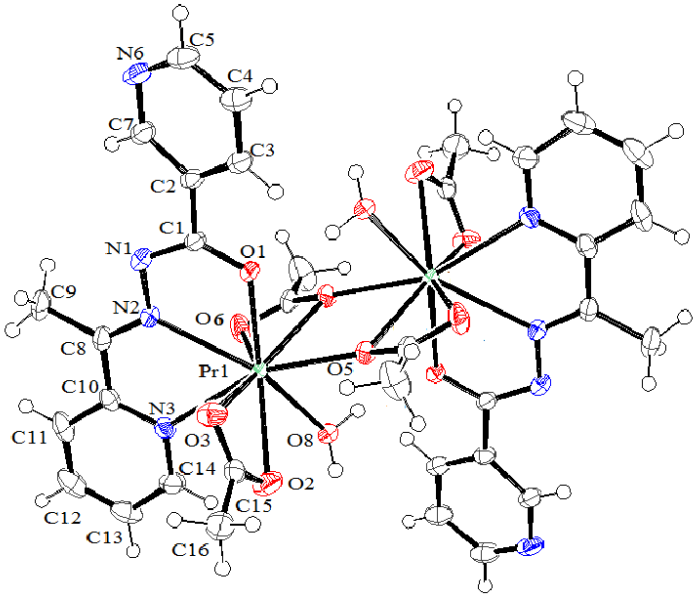

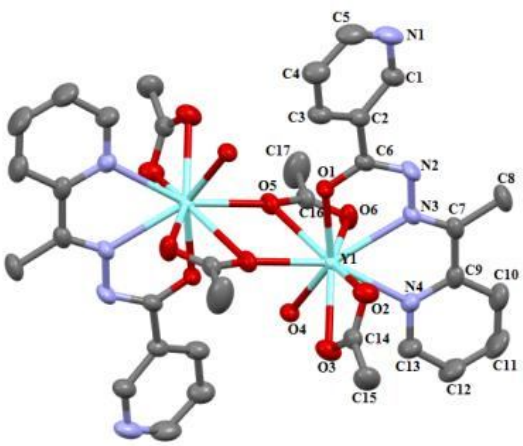

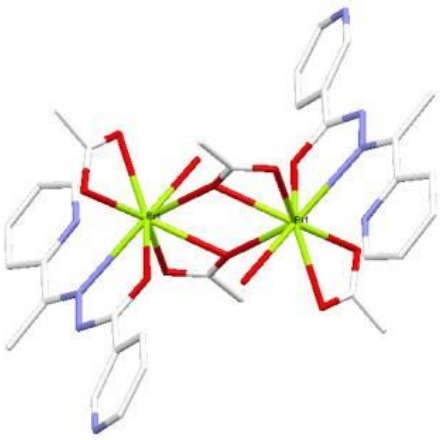

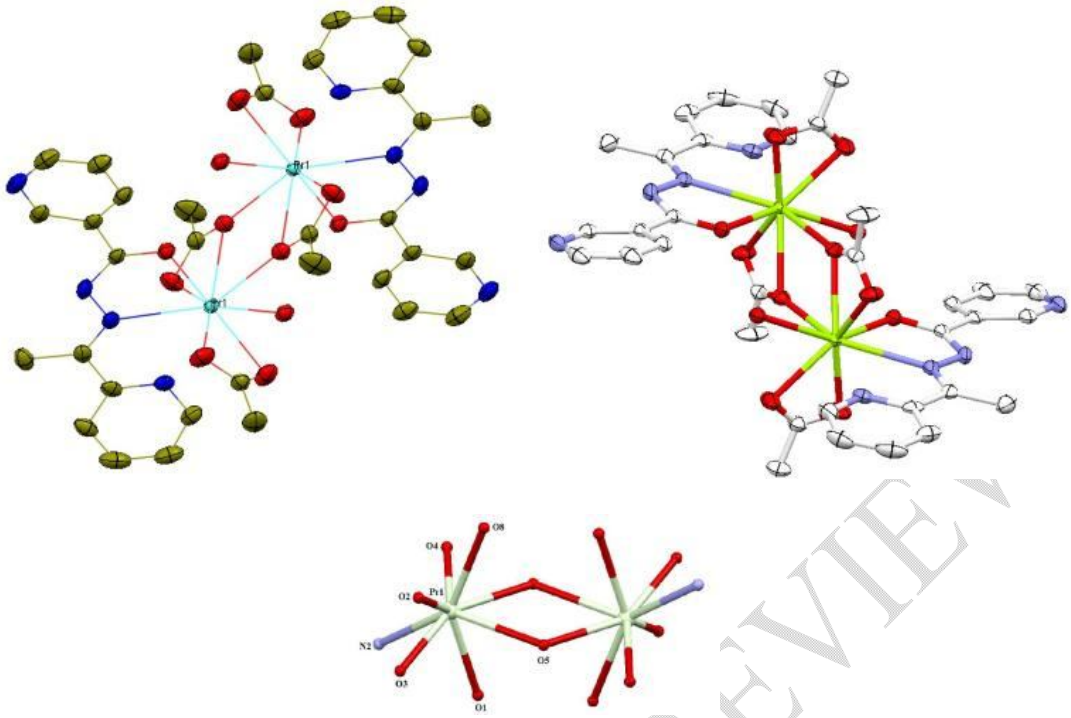

Figure 60 : Crystal structures of complexes of praseodymium(III) acetate and yttrium(III) with N'–(1– (pyridin–2–yl)ethylidene nicotinohydrazide

Example 2 : Let us also give the example of the complex of Samarium (III) nitrate with 1-(pyridin-2-yl)-2-(pyridin-2-ylmethylene)hydrazine. The complex studied is that of a noncoordinated Samarium. The study by X-ray diffraction reveals isotopic binuclear structures where each metal ion is coordinated to nine (9) atoms in the same mode with two nitrogen atoms of the pyridine rings, one iminic nitrogen atom, four oxygen atoms of the acetate groups and two oxygen atoms of the water molecule, which gives a distorted trigonal prism geometry. The two metal centers have a tri-capped trigonal prism geometry, the Schiff base playing the role of tridentate ligand [20].

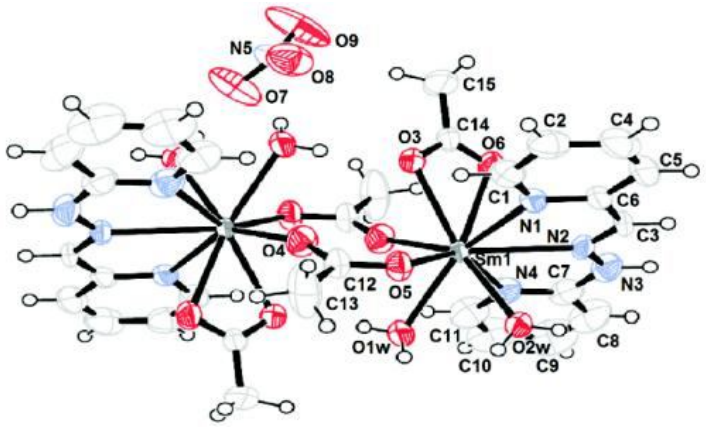

Figure 61 : Crystal structure of the complex of Samarium(III) nitrate with 1□(pyridin□2□yl)□2□(pyridine□2□ylmethylene)hydrazine

Example 3 : Let us also give the example of the complex of Yttrium (III), Erbium (III) and Terbium (III) nitrate with 1-(pyridin-2-yl)-2-(pyridin-2-ylmethylene)hydrazine. The complexes studied are those of a noncoordinated environment around the lanthanide. The Schiff base acts as a tridentate ligand with three nitrogen atom donors, thus forming two five-membered chelating rings. For example, the environment of the Tb^{3+} ion can be described as a slightly distorted tri-capped trigonal prism with distorted base faces N1, N2, O2 and O3, $O5_{water}$, $O6_{water}$. The crystal structure is stabilized by hydrogen bonds giving a three-dimensional network. Carboxylate groups can adopt various coordination modes due to the coordination sites due to electron pairs per oxygen atom of the carboxylate group, which can cause the generation of new structures. This ability allows the acetate group to coordinate with one, two, or three metal centers. The complexes are linked in centrosymmetric dimers by O-H...O hydrogen bond pairs between one of the two water molecule coordinators ($O5_{water}$) and the acetate oxygen atom O1. The second bound water molecule ($O6_{water}$) acts as a hydrogen atom donor, forming hydrogen bonds with the free water molecule and the nitrate anion. The acetate oxygen atoms act as acceptors in the hydrogen bonds with the HN groups of the adjacent complex [21].

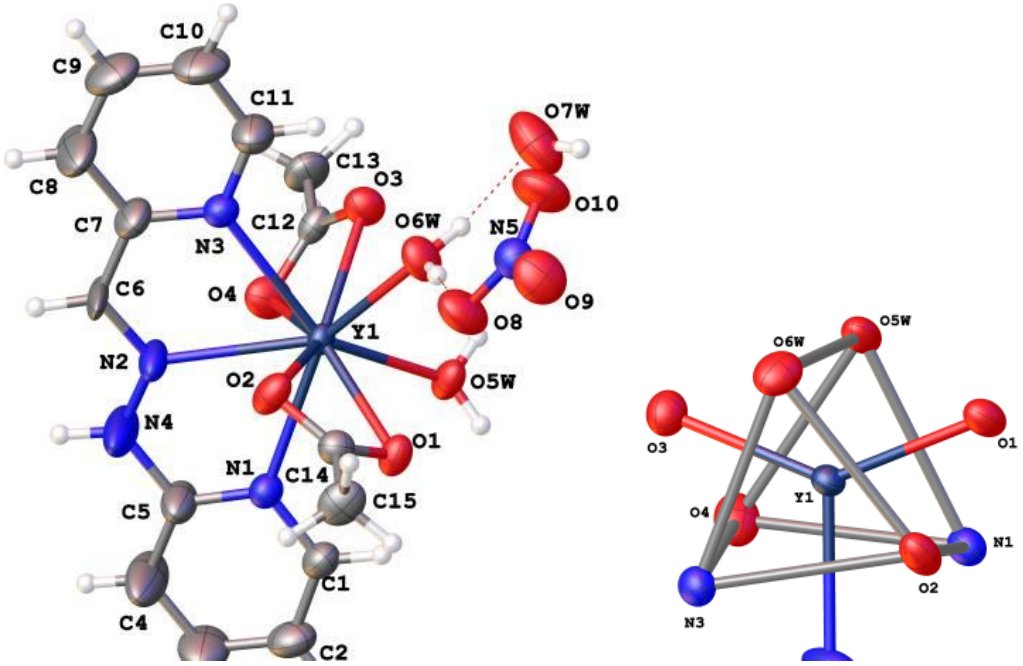

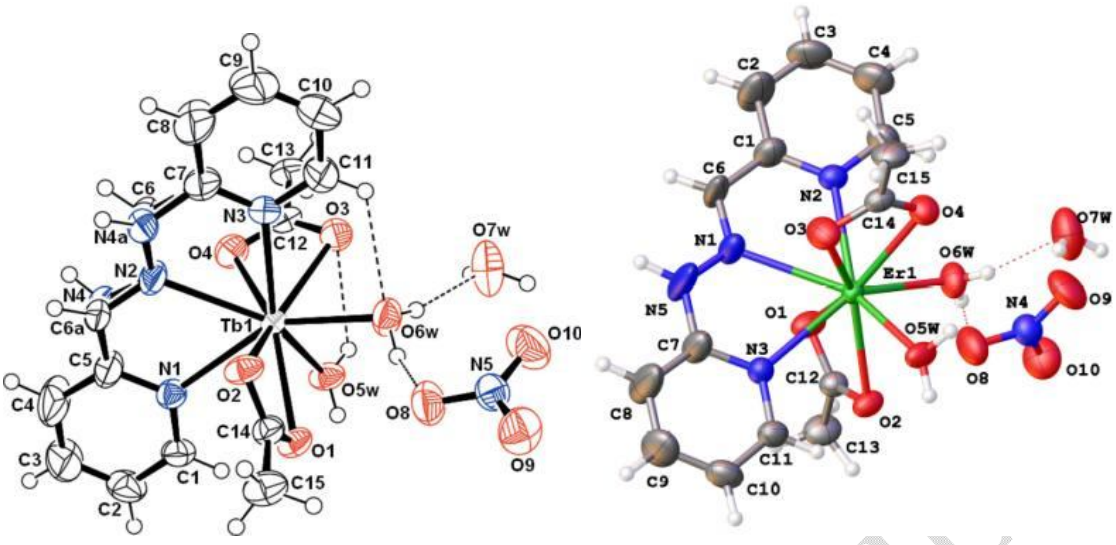

Figure 62 : Crystal structures of the complexes of Yttrium(III), Erbium(III) and Terbium(III) nitrate with 1□(pyridin□2□yl)□2□(pyridine□2□ylmethylene)hydrazine

9°) Coordination number 10, 11 and 12

These coordination numbers are rare. They occur with f elements and sometimes with d elements. For CN = 12 the complex of Neodymium (III) with N'-(1-(pyridin-2-yl)ethylidene)nicotinohydrazide of formula $[Nd(HL)_2(NO_3)_2(H_2O)_2]\cdot(NO_3)$ is duodecacoordinated and its coordination polyhedron can be described as an icosahedron or dodecahedron [19]. The Nd(III) center has coordination **12**. One of the nitrates has been omitted for clarity in Figure 64. The complex crystallizes in the monoclinic system with space group C2/c. The structure of the complex is consistent with the formula $[Nd(HL)_2(NO_3)_2(H_2O)_2]\cdot(NO_3)$. The asymmetric unit contains one Nd^{3+} ion, two neutral organic ligands, three nitrate ions and two water molecules. These species are associated as a cation $[Nd(HL)_2(NO_3)_2(H_2O)_2]^+$ while a nitrate anion NO_3^- remains free. Crystallographic study shows that the cation is formed with 1:2 [Nd:HL] and 1:2 [$Nd:NO_3^-$]. In the complex, each ligand acts in a tridentate manner through an azomethine nitrogen atom, a pyridine nitrogen atom and a carbonyl oxygen atom resulting from the two-membered chelating rings NdOCCN and NdNCCN. The Nd(III) centre is of twelve coordination and the geometry around the lanthanide ion can be described as an icosahedron. The $Nd–O_{hydrazino}$ distances and $Nd–O_{water}$ distances are 2.4772 Å and 2.4665 Å, respectively. The distances, when O comes from the bidentate nitrate groups, are between 2.581 and 2.637 Å and the Nd–O distances are longer. These observations are in agreement with those reported in the literature. The $Nd–N_{(pyridine)}$ and $Nd–N_{(imine)}$ distances are 2.644 Å and 2.685 Å respectively, the longest distance belonging to the imino of the nitrogen atom. In the chain –C6–N2–N3H–C8(O1), C6–N2 and C8–O1 bond lengths values of 1.278 and 1.243 Å are consistent with the double bond

character while the C8-N3 distance of 1.332 Å and the N2-N3 distance of 1.383 Å are indicative of a single bond.

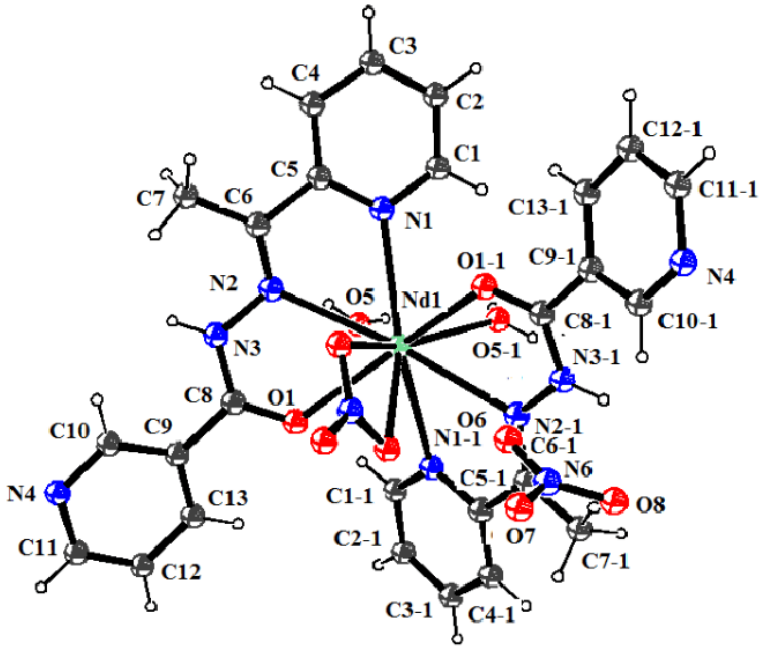

Figure 63 : ORTEP diagram of the crystal structure of the Neodymium(III) nitrate complex with the N'–(1–(pyridin–2–yl)ethylidene)nicotinohydrazide by omitting one of the nitrates

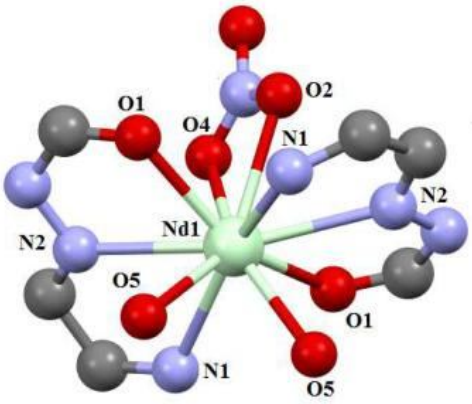

Figure 64 : Neodymium (III) environment with the N'–(1– (pyridin–2–yl)ethylidene)nicotinohydrazide by omitting one of the nitrates

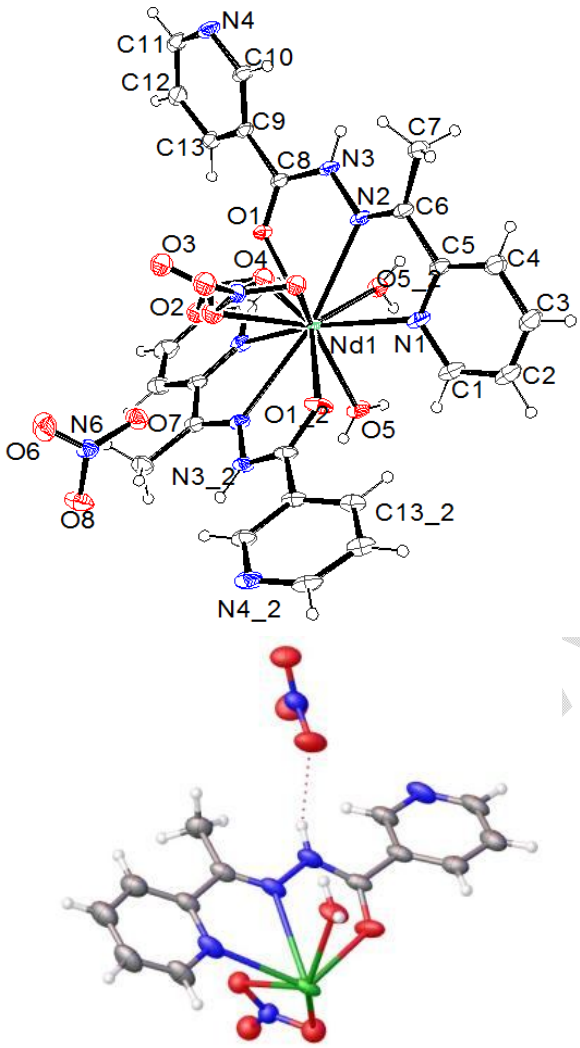

Figure 65 : Crystal structure of the complex of Neodymium(III) nitrate with N'–(1– (pyridin–2–yl)ethylidene)nicotinohydrazide

An example of **10**-fold coordination is obtained with the cerium coordination polymer where each tridentate Schiff base molecule acts in the monodeprotonated form by a phenolate oxygen atom, a nitrogen atom and a carbonyl oxygen atom, resulting in a six-membered chelating ring CeNCCCO and a five-membered chelating ring CeNNCO [22]. The occlusion angles defined by the two chelating rings are 69.1° and 61.6°, respectively. These angles are comparable to the values reported for six-membered and five-membered rings. The bond angles of the ligands, which involve the Ce(III) ion, are slightly larger than the angle subtended by the oxygen atoms of the chelating bidentate nitrate groups: O3–Ce1–O5 = 47.61° and O7–Ce–O9 = 50.2°. The value of the Ce1–O5–Ce1 angle [161.7°] is in the expected range for $\eta^1{:}\eta^2{:}\mu^2$–nitrate coordination modes. The Ce(III) center is ten-coordinate and the geometry around the lanthanide ion can be described by a distorted bicapped square

antiprism. The Ce–$O_{phenolate}$ distance, a distance value of 2.31 Å, is shorter than the Ce–O_{ketone} distance [2.511 Å] and the Ce–O_{water} distance [2.507 Å]. In fact, the negatively charged phenolate oxygen atom binds more strongly to Ce^{3+} than the neutral oxygen atom.

The longest distance between Ce^{3+} and the chelating ligand atoms is due to the nitrogen atom of azomethine with a value of 2631 Å. The Ce–ONO2 distances range from 2663 to 2689 Å and are the longest Ce–O distances. The largest Ce–O distance (Ce–O7 = 2689 Å) is observed in the chelating-bridging coordination mode $\eta^1:\eta^2:\mu$, while the shortest Ce–O bond length (Ce1–O7 = 2563 Å) is observed in the chelating coordination mode η^2–NO_3. These observations are consistent with those reported in the literature. The metal centers are finally bridged by a pair of chelating-bridging nitrato ligands that act in the coordination mode $\eta^1:\eta^2:\mu$. In the organic moiety -C7-N1-N2-C8-O2, C7-N1 and C8-O2, the bond length values of 1298 Å and 1241 Å are consistent with double bond character while the C12-N3 distance of 1331 Å and the N1-N2 distance of 1399 Å indicate single bond character. The C-O bond in the coordinated nitrate groups has an intermediate character between the C-O single bond and the C=O double bond. All bond lengths are normal and fall within similar ranges as those reported for compounds derived from the same hydrazone ligand. The units cluster along and perpendicular to the 2_1-axes generating a non-centrosymmetric lattice. Numerous intermolecular hydrogen bonds consolidate the structure into a three-dimensional lattice.

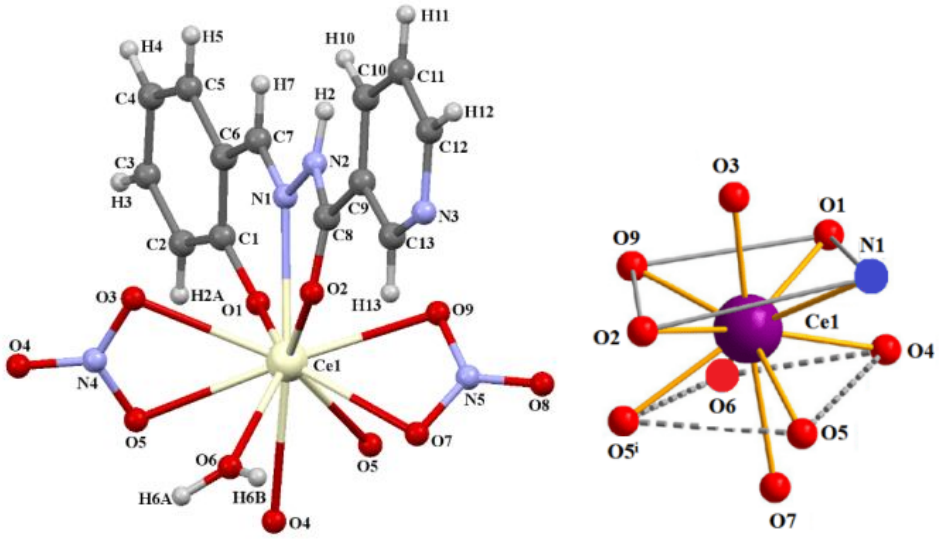

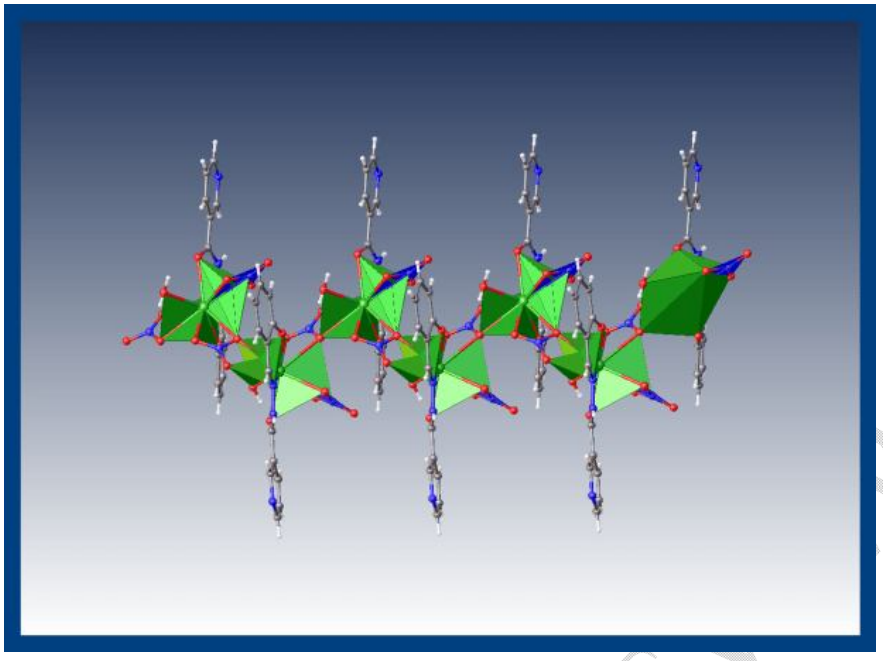

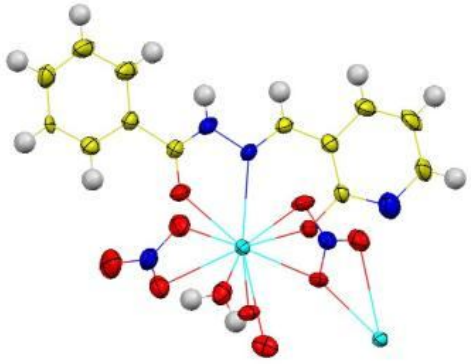

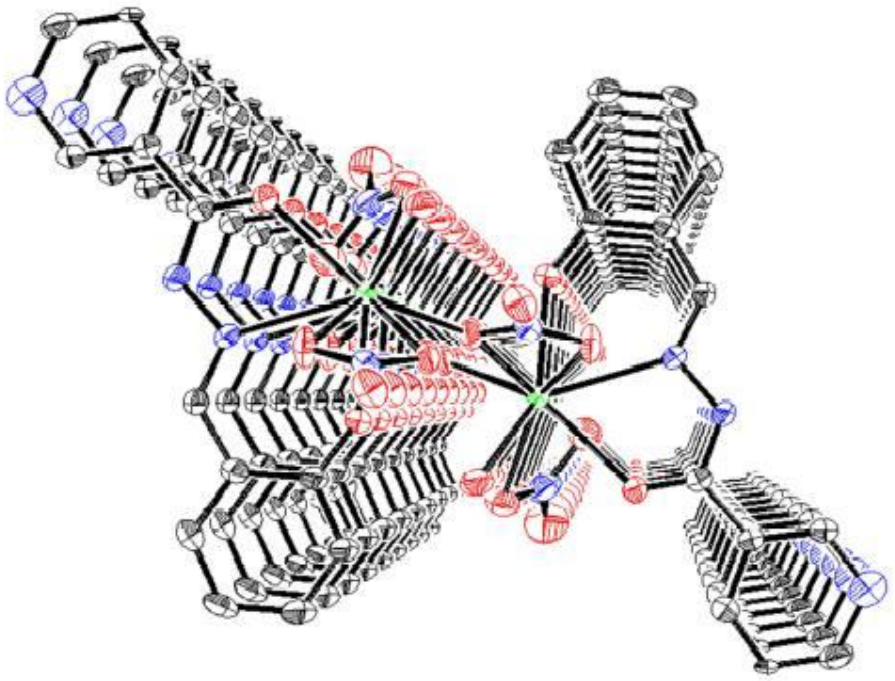

Figure 66 : Coordination polymer $Ce(NO_3)_2(HL).H_2O$ showing the distorted two-headed square antiprism coordination geometry of the central Ce(III)

An example of a neutral heterodinuclear compound [Cu(II)La(III)] was obtained by the "brick-by-brick" method and it crystallizes in the monoclinic system with a space group of P2/n. The asymmetric unit of the structure of $[Cu_2(\mu\text{-}L_2)La(NO_3)]$ contains two molecules of the dideprotonated ligand L^{2-}, two Cu(II) ions, one La(III) ion, and two bidentate nitrate anions. In the structure of the dinuclear complex, the Cu(II) ion and the La(III) ion are bridged by two phenolate oxygen atoms. The Cu(II) ion has a square planar geometry with the basal plane formed by two iminic nitrogen atoms and two phenolic oxygen atoms. The cissoid angles around the Cu(II) ion, which are in the range [84.3°-85.5°], deviate significantly from their ideal values of 90°. The diagonal basal angles O3ACu1AN1A=173.6° and O2ACu1AN2A=177.0°, respectively, deviate slightly from the ideal values of 180°. The copper(II) ion lies almost in the plane defined by the N2O2 site. The values of the bond distances are 1.904 Å for [Cu1AN2A] and 1.915 Å for [Cu1AN1A], and the Cu-O distances 1.883 Å and 1.905 Å, are different. The Cu-O distances are 1.883 Å and 1.905 Å while the Cu-N distances are 1.904 Å and 1.915 Å. This fact indicates that there are distortions of the square planar geometry around the Cu(II) ion.

The La(III) ion, which occupies the largest open site of the Schiff base ligand, is bonded to two phenolate oxygen atoms, two methoxy oxygen atoms of the ligand, and two oxygen atoms of a bidentate nitrate group of each ligand. The La-O-phenoxo bond distances are of the order of 2.534 Å - 2.568 Å. The distances between the La(III) cation and the two oxygen atoms of the

bidentate nitrate [La1AO5A = 2.625 Å; La1AO6A = 2.704 Å] show that the geometry is distorted. The La(III) cation is located in the planar cavity defined by the two phenolate oxygen atoms and the two methoxy oxygen atoms. The Cu-La distance is 3.543 Å. The positive charge of the Cu(II) and La(III) ions is balanced by the deprotonated L^{2-} ligand and the nitrate anion. The La(III) ion is octacoordinated. In this complex, the copper(II) ion is housed in the internal compartment [N2O2] formed from two nitrogen atoms of the azomethine functions and two oxygen atoms of two phenolate groups of the ligand. Lanthanum is housed in the external cavity [N2O2] formed from four oxygen atoms from two phenolate and methoxy groups. The Cu(II) ion has a deformed square planar geometry, it is surrounded by [N2O2] atoms. The lanthanum(III) ion is hexacoordinated, the two phenolate oxygen atoms act as a bridge with the Cu(II). The coordination sphere of the lanthanum(III) ion is completed by the two oxygen atoms of the methoxy group and the oxygen atoms of the chelating bidentate nitrate ion.

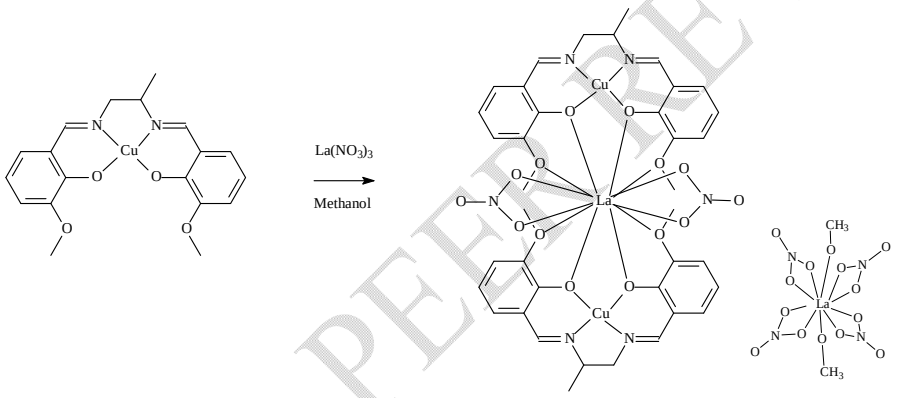

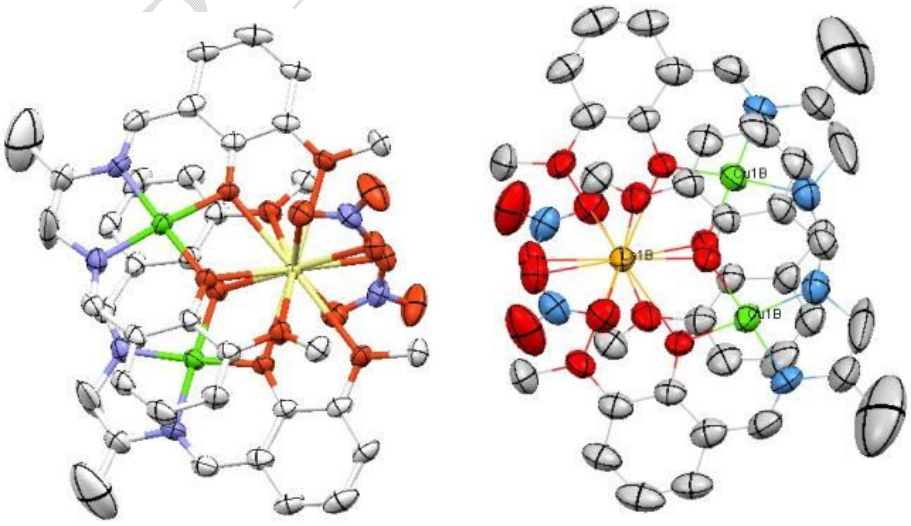

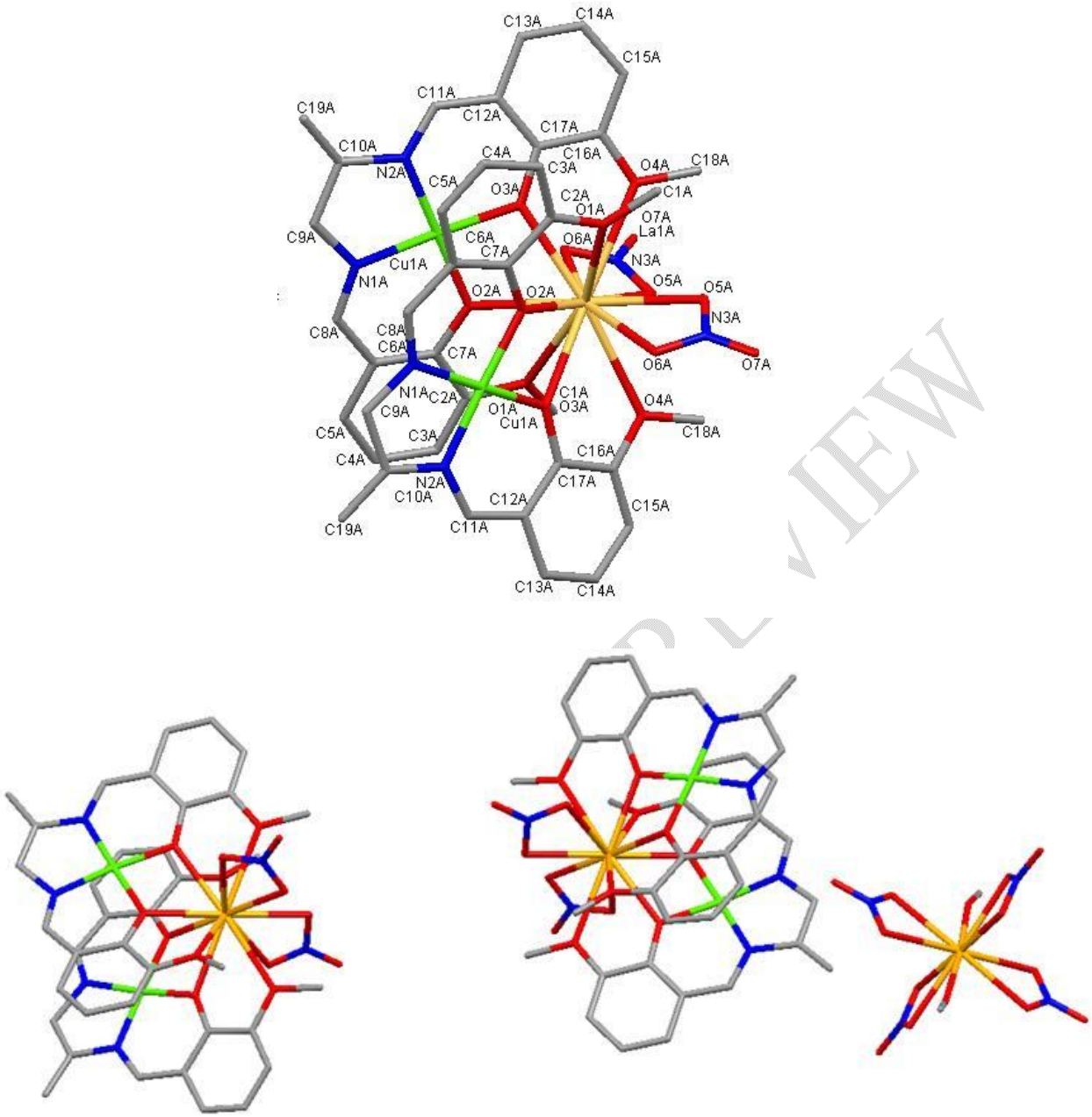

Figure 67 : Representations of complex $[Cu(Lc)La(NO_3)]_2{\cdot}La(NO_3)_4$

VIII- Isomerism in complexes

1°) Geometric isomerisms

Geometric isomerism occurs in octahedral and square-planar complexes but not in tetrahedral complexes. When, in such complexes, ligands are in adjacent positions, the descriptor *cis* is used, and when they are in opposite positions, the descriptor *trans* is used. When three identical ligands or the three coordinating functions of a tridentate ligand occupy a face of an octahedron, it is called a **facial** isomer (*fac*); if they occupy an edge of the octahedron, it is called a **meridional** isomer (*mer*).

2°) Chain or bond isomerism

They are found in complexes with ligands that have two potentially bonding atoms and that can bond through one of the donor atoms in a given situation and through the other in another complex. Ambidentate ligands such as SCN^- can give bonding isomers depending on whether they are bonded through nitrogen or sulfur. Sulfur can undergo back-bonding, which is not the case for nitrogen. In some complexes, the presence of large substituents can impose the sulfur atom as the donor atom given the possibility of back-bonding. In reality, when the sulfocyanide is an N donor, a linear skeleton is formed with the central metal; when it is an S donor, the skeleton is bent and can introduce problems.

3°) Optical isomerism

Optical isomerism occurs when the mirror image of a molecule is not superimposable with the original molecule; they are found in complexes where there is no plane of symmetry. Such chemical species are called chiral. Pure samples of optical isomers rotate the plane of polarization of polarized light. The following compounds are examples of optical isomer pairs in coordination chemistry. Optical isomerism is found in complexes with CN = 6 with at least one bidentate ligand.

Octahedral complexes can exhibit optical isomerism in the case where the ligands have more than one coordination site. This is for example the case of the ligand ethylenediamine (***en*** : $NH_2CH_2CH_2NH_2$). A classic example is the complex $[Co(ox)_3]^{3-}$ (ox = $^-OOC–COO^-$). The complexes Δ and Λ are images of each other by reflection in a mirror plane.

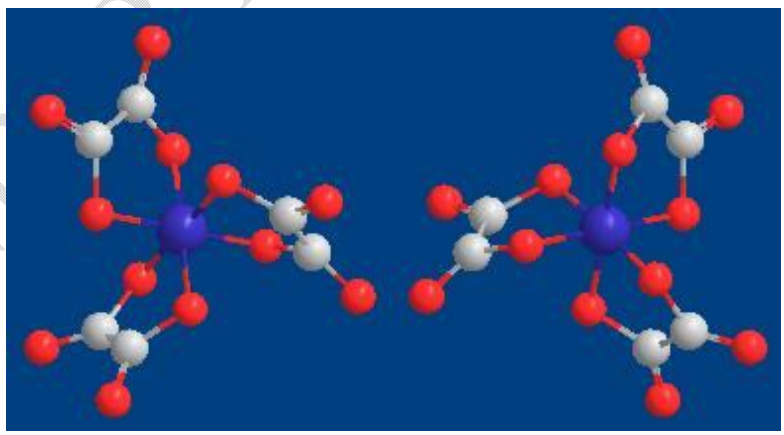

Figure 68 : representations of Λ-$[Fe(ox)_3]^{3-}$ and Δ-$[Fe(ox)_3]^{3-}$

4°) Conformational isomer

This isomerism occurs only for certain metal complexes with electronic configuration d^3. It results from a change in the geometry of the complex.

IX- Chelate effect

Entities carrying several donor atoms that can act as ligands are polydentate or chelating ligands (their denticity is greater than **1**). The binding of polydentate ligands is entropically favored compared to that of monodentate ligands. If ligands that are at least bidentate can form 5- or 6-membered rings with the central cation (these rings are, as in organic chemistry, thermodynamically favored), the stability of the complex is improved. This is the chelate effect. The etymology of this word reveals its meaning: in fact, it derives from the Greek khêlê: “clamp, pincer”. The additional stabilization due to the chelate effect originates from the fact that the binding to the central cation of the first function that can serve as a ligand places the other free doublets of the molecule close to the cation, which is entropically favorable. Consider the following reaction, where a Ni^{2+} ion complexed by six NH_3 ligands sees these substituted by 3 bidentate ligands ethylenediamine (***en***) : $[Ni(NH_3)_6]^{2+} + 3\boldsymbol{en} \rightarrow [Ni(en)_3]^{2+} + 6NH_3$

The complexes are stabilized by chelate effect. Ethylenediaminetetraacetate is an example of a chelating polydentate ligand.

Chapter 4

CRYSTAL FIELD THEORY

Introduction

This theory was developed around the 1930s by the Americans **BETHE** and **VANVLECK**. Ligands are considered to be point charges interacting with the central element; the interactions are purely electrostatic. This resource presents a more intuitive way to explain the formation of the chemical bond in coordination complexes according to the crystal field model. In this model, the interactions that exist between the orbitals of the metal ion and the coordinating ligands are taken into account. It explains how the ligands perturb, in different ways, the various ***d*** orbitals of the metal, according to the type and spatial arrangement of the coordinating ligands.

I- Magnetic properties

A compound is paramagnetic if it has electrons with unpaired spins, i.e. single electrons; it is attracted by a magnetic field.

A compound is diamagnetic if all the electrons are paired; it is repelled by a magnetic field.

The magnetic moment M, which is an induced moment, is the resultant of the spin moment M_S and the orbital moment M_L. For a transition element engaged in a complex, the orbital moment is most often zero. M therefore only depends on the spin moment. The magnetic moment is expressed by the effective Bohr magneton number given by:

$n_{eff} = \sqrt{n(n+2)}$; **n** is the number of single electrons or $n_{eff} = 2\sqrt{S(S+1)}$ where S corresponds to the spin of the atom (S = 1/2 n) ; n_{eff} S expressed in Bohr magneton; magnetic moment associated with one mole of electrons:

$$1\mu_B = \frac{eh}{4\pi m_{e^-}} = 9.274.10^{-24}(S.I.)$$

Table 11 : Magnetic moment of some transition elements

n	1	2	3	4	5
S	1/2	1	3/2	2	5/2
n_{eff}	1.73	2.83	3.87	4.90	5.92
Exemples	$CuSO_4.5H_2O$	K_3CrF_6	$Cr(NH_3)_6I_3$	K_3MnF_6	$MnSO_4.4H_2O$

II- Crystal field model for an octahedral complex

If we consider a M^{n+} metal in the gaseous state freed from any interaction, the five ***d*** orbitals have the same energy. They are said to be degenerate (same energy level).

If this metal is in interaction with 6 ligands that we will assume to be point charges. There is certainly attraction between the cation and the ligands but at a given moment of the approach there are repulsions between the electrons of the ligand and the electrons of the metal. The crystal field model, based on electrostatic interaction, is based on the destabilization of the central metal ion by the approach of the ligands.

In the crystal field approach, ligands are considered as negatively charged centers that interact with the electrons of the ***d*** orbital lobes of the metal; the repulsion between these identically charged entities leads to a repulsive interaction.

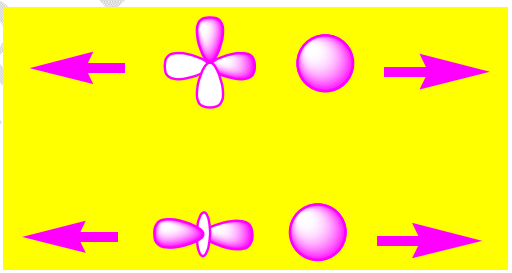

Scheme 78 : "d/ligand orbital" repulsion

When a transition element surrounds itself with ligands, their electrostatic interaction destabilizes the metallic species. As the ligands approach, the central ion is destabilized, its energy increases. The consequence of the destabilization of the central ion is the **lifting of degeneracy** and the splitting of the 5 atomic orbitals into two series of atomic orbitals: 2 OA $\boldsymbol{e_g}$ et 3 OA $\boldsymbol{t_{2g}}$.

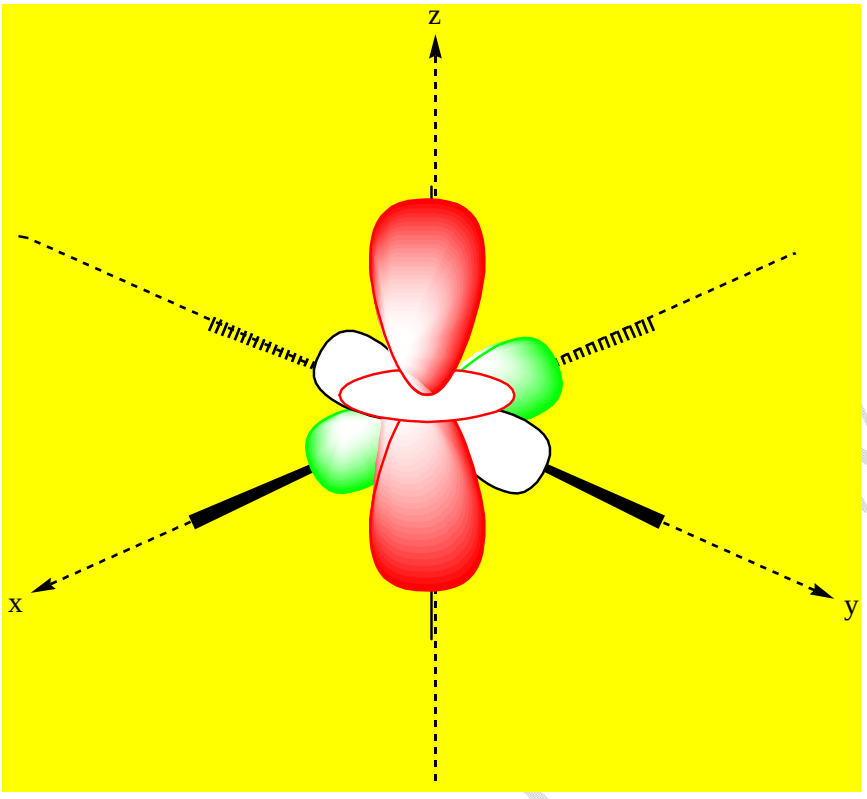

Scheme 79 : representation of square orbitals d

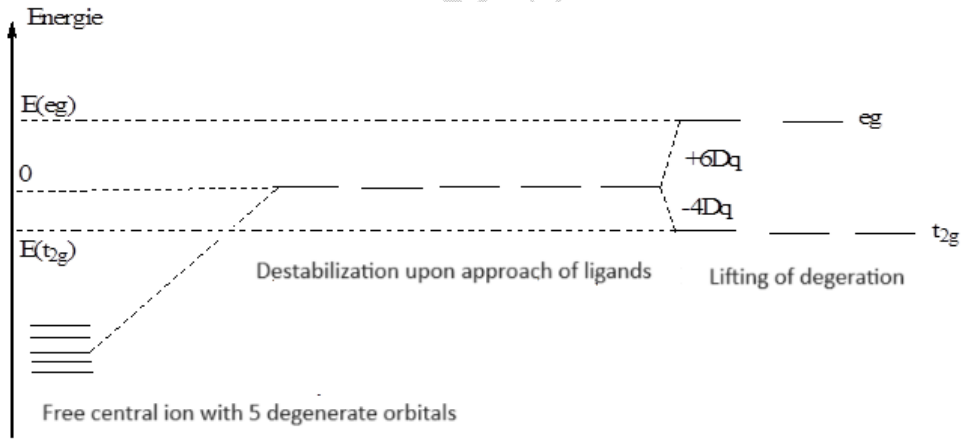

Figure 69 : orbital bursting e_g et t_{2g}

In the case of an octahedral environment of the metal ion, the $d_{x^2-y^2}$ and d_{z^2} lobes of the orbitals are centered along the Ox, Oy, Oz axes pointing **towards** the ligands.

On the other hand, the lobes d_{xy}, d_{yz} and d_{zx} centered along the bisectors of the angles xOy, yOz, zOx point **between** the ligands.

For a d^1 the ligands being considered (for the single electron) as negatively charged centers, the population of the ***d*** orbitals will be governed by the minimization of the electrostatic repulsions. The lobes of the mixed orbitals dxy, dyz and dzx being further away from the ligands than those of the square orbitals $d_{x^2-y^2}$ and d_{z^2}, it follows that if the electron occupies one of the three orbitals (d_{xy}, dy_z and d_{zx}) the electrostatic repulsions will be minimized.

The electron, by placing itself in one of these three orbitals (which are perfectly identical from a symmetry point of view), will minimize its energy. This amounts to considering that the three orbitals dxy, dyz and dzx are of lower energy than the orbitals $d_{x^2-y^2}$ and d_{z^2}.

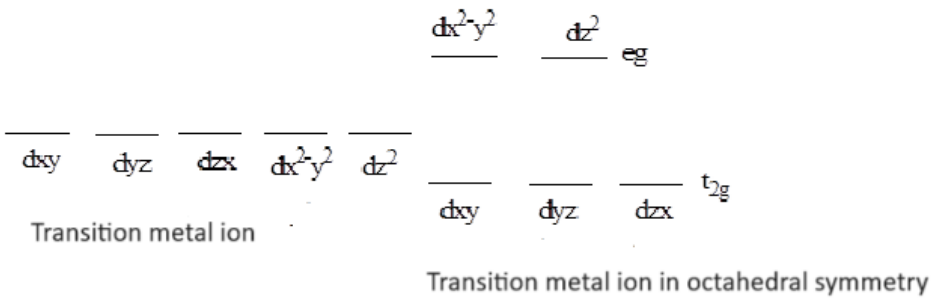

Figure 70 : Energy diagram

The extent of destabilization of the five ***d*** orbitals and the lifting of degeneracy depends on the shape and symmetry of the complex. It is evaluated by the energy difference between two groups of orbitals ($d_{x^2-y^2}$ and d_{z^2}) and (d_{xy}, d_{yz} and d_{zx}). It is called **crystal field energy**.

La présence des six ligands en symétrie octaédrique provoque ainsi un écart énergétique (ou champ octaédrique) ou énergie de dédoublement des orbitales Δ_0 = 10 Dq entre les orbitales e_g *et* t_{2g}. Dq étant une unité faisant intervenir la nature du ligand et du métal ; la notification 10 Dq provient du fait que cette énergie est mesurée par spectroscopie optique. The presence of the six ligands in octahedral symmetry thus causes an energy gap (or octahedral field) or orbital splitting energy $\Delta 0$ = 10 Dq between the e_g and t_{2g}.orbitals. Dq being a unit involving the nature of the ligand and the metal; the notification 10 Dq comes from the fact that this energy is measured by optical spectroscopy.Δ_0 = 10 Dq represents the splitting of the octahedral crystal field which; in terms of energy expresses the separation of the t_{2g} and e_g levels.

$\Delta_0 = Nhc/\lambda$ (in kJ/mol) ; λ being the wavelength of the absorption band

$\Delta_0 = 1/\lambda$ (in cm^{-1}) ; 1 cm^{-1} corresponds to $11.96266.10^{-3}$ kJ/mol

In the spherical type distribution the orbitals are degenerate when going from the spherical distribution to the octahedral distribution the mixed orbitals stabilize while the square orbitals destabilize.

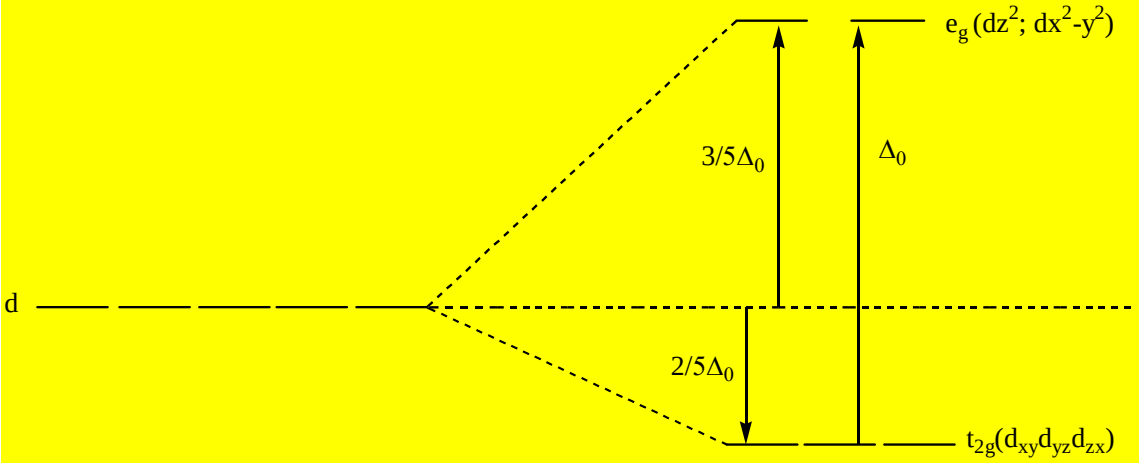

Figure 71 : orbital splitting e_g and t_{2g}

In this geometry, it is the OA d_{z^2} and $d_{x^2-y^2}$ (e_g) pointing in the direction of approach of the ligands that are more destabilized than the OA d_{xy}, d_{yz}, d_{xz} (t_{2g}) pointing along the bisectors of the bond angles. The energy gap Δ_0 between the OM t_{2g} and the OM e_g is a characteristic of the "strength" of the field created by the ligands. For the free metal ion of d^n configuration the electronic structure of thefundamental is governed by Hund's rule which states that this state is the one with the highest spin multiplicity. For ligands inducing a high Δ_0 we will speak of weak field ligands which give "high spin" type complexes (the electrons do not tend to couple and the spin remains high) and for a more reduced Δ_0 of strong field ligands which give "low spin" type complexes (the electrons tend to couple and the spin is generally weak).

1°) Weak-field and strong-field electronic configurations

In the case of an octahedral complex, such as $[Fe(H_2O)_6]^{2+}$ or $[Fe(CN)_6]^{4-}$, the crystal field model shows that the destabilization of the central ion, upon approaching the ligands, is accompanied by the lifting of the degeneracy of the five OA ***d*** of the iron (II) ion into two levels, and followed by a new distribution of electrons on new OAs: the OA e_g and t_{2g}.

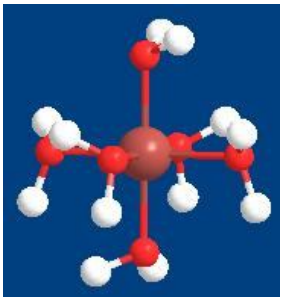

Figure 72 : $[Fe(H_2O)_6]^{2+}$ 3/5 Δ_0 = + 6Dq et - 2/5 Δ_0 = - 4Dq

The value of the energy gap Δ_0 depends on the nature of the ligand: we therefore distinguish between ligands with weak fields (high spin) and with strong fields (low spin). For $[Fe(H_2O)_6]^{2+}$, Δ_0 (H_2O) = 124.41 kJ/mol (λ = 961.5 nm) and for $[Fe(CN)_6]^{4-}$, Δ_0 (CN^-) = 404.34 kJ/mol (λ = 295.8 nm).

Depending on whether the ligand is "strong" or "weak", a strong-field or weak-field complex will be formed.

Depending on the value of the energy Δ_0 between the two energy levels E (e_g) and E (t_{2g}), the electrons will have the possibility of positioning themselves either by pairing on the t_{2g} orbital, or by remaining unpaired on the e_g orbitals.

It is by comparing Δ_0 to the electron pairing energy (P) that we will distinguish between strong-field and weak-field complexes. For Fe^{2+}, P = 229.68 kJ/mol.

The electronic structure of the ion Fe^{2+} is : $1s^2\,2s^2\,2p^6\,3s^2\,3p^6\,3d^6$.

Therefore, for $[Fe(H_2O)_6]^{2+}$, as Δ_0 < P, it will be "less expensive" in energy to place the 6 electrons of the iron (II) ion on the e_g level than to pair them because the cost to go and populate the e_g orbitals is compensated by a higher exchange interaction – which is related to Hund's rule. This is the high spin or weak field situation.

The configuration of the iron(II) ion in $[Fe(H_2O)_6]^{2+}$ is therefore: t $t_{2g}^4 e_g^2$, and the complex is **paramagnetic** due to the presence of 4 unpaired electronic spins (S = 4.1/2 = 2).

For $[[Fe(CN)_6]^{4-}$, as Δ_0 > P, it will be "less expensive" in energy to pair the 6 electrons of the iron (II) ion than to place them on the e_g level because the energy cost to pair electrons in a t_{2g} orbital is lower than that required to populate an e_g orbital. This is the low spin or strong field situation.

The configuration of the iron(II) ion in $[Fe(CN)_6]^{4-}$ is therefore: $t_{2g}^{6}e_g^{0}$, and the complex is **diamagnetic** due to the absence of unpaired electronic spins (S = 0).

Depending on the value of the crystal field energy (10 Dq), a metal ion in octahedral symmetry can adopt two different electronic configurations, both of which respect the following considerations:

- Either the electrons can populate all the e_g and t_{2g} orbitals. In this case **Hund**'s rule is respected but the electrons "pay a cost" to go and lodge themselves in the e_g orbitals higher in energy by 10 Dq than the t_{2g} orbitals;
- Either the value of 10 Dq is very high and only t_{2g} orbitals can be populated. In this case, the “cost” to be paid is related to the fact that the electrons must pair in the same orbital. An electron must enter an orbital with a spin antiparallel to that of the electron already present.

Thus, two distributions of electrons in the *d* orbitals can be considered (an example is given for a d^5 ion in the figure below). They correspond to two different electronic configurations:

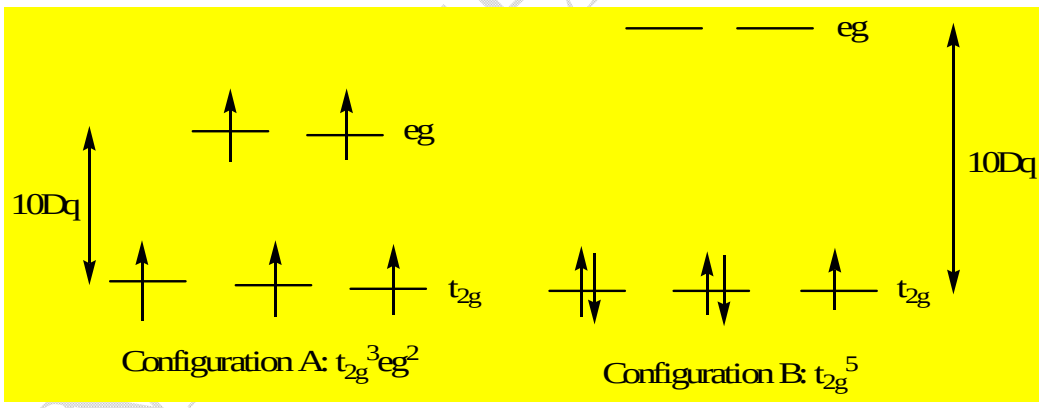

Figure 73 : Representation of two electronic configurations of a d^5 ion depending on whether the value of 10 Dq is low (case A) or high (case B)

Thus, two electronic configurations are possible and called **weak field** configuration (A) or **strong field** configuration (B).

2°) Comparison “Electron Pairing Energy / Crystal Field Energy”

The difference between strong-field and weak-field configurations is the number of unpaired electrons. Let's go back to the previous examples:

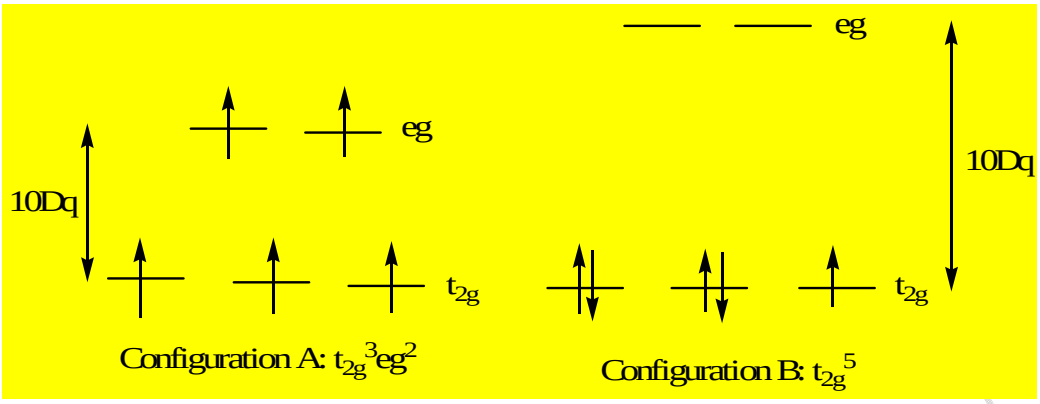

Figure 74 : Representation of two electronic configurations of an ion d^5

For A, all electrons are unpaired while for B, only 1 electron is unpaired. Therefore, two important characteristics appear:

- the value of the total spin quantum number S ($S = \sum s$ with $s = \pm\frac{1}{2}$) can characterize an electronic configuration,
- The electron pairing energy can constitute a reference energy to the extent that the passage from A to B (corresponding to an increase of 10 Dq) is accompanied by an increase in the number of paired electrons A → S = 5/2, B → S = 1/2.

The reference energy is therefore the electron pairing energy, denoted P.

Thus, if 10 Dq < P it will be easier to populate the higher energy orbitals (e_g in an octahedral environment) than to pair electrons in those of lower energy (example: t_{2g}).

The most stable configuration will be A, and will be called the low-field or high-spin configuration.

On the other hand, if 10 Dq > P, it is the pairing that will be favored.

The most stable configuration will then be B, and will be called the strong field or low spin configuration.

3°) Crystal Field Stabilization Energy (CFSE)

Each electronic configuration can be associated with a crystal field stabilization energy (CFSE). It corresponds to the gain or loss of energy of the ion in octahedral symmetry compared to spherical symmetry.

As a general rule, a metal complex will always adopt the lowest energy configuration. Consider a complex in octahedral symmetry, it adopts the following energy scheme:

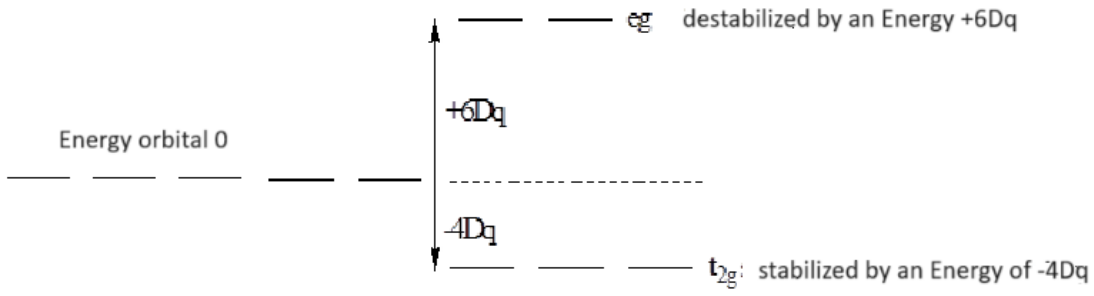

Figure 75 : Energy diagram

In a spherical complex, the energy of the d orbitals is taken as zero energy. In a complex with octahedral symmetry, the set of t2g orbitals is lower in energy by 4 Dq; as for the set of eg orbitals, it is higher by 6 Dq.

In such a complex, if the electrons are forced to pair in the same orbital, the stabilization energy of the crystal field will be altered by the pairing energy **P** of the electrons.

For the configuration $t_{2g}^{x} e_{g}^{y}$ having **p** pairs of paired electrons, the stabilization energy of the crystal field CFSE is calculated according to:

$$ESCC = x(-4Dq) + y(+6Dq) + pP = x(-2/5\ \Delta_0) + y(3/5\Delta_0) + pP$$

p is the number of electron pairs likely to be formed in the distribution.

It corresponds to the gain or loss of energy of the ion in octahedral symmetry compared to spherical symmetry.

III- Crystal field model for the tetrahedral complex

Now consider the case of a tetrahedral ligand environment. A tetrahedron can always be inscribed in a cube.

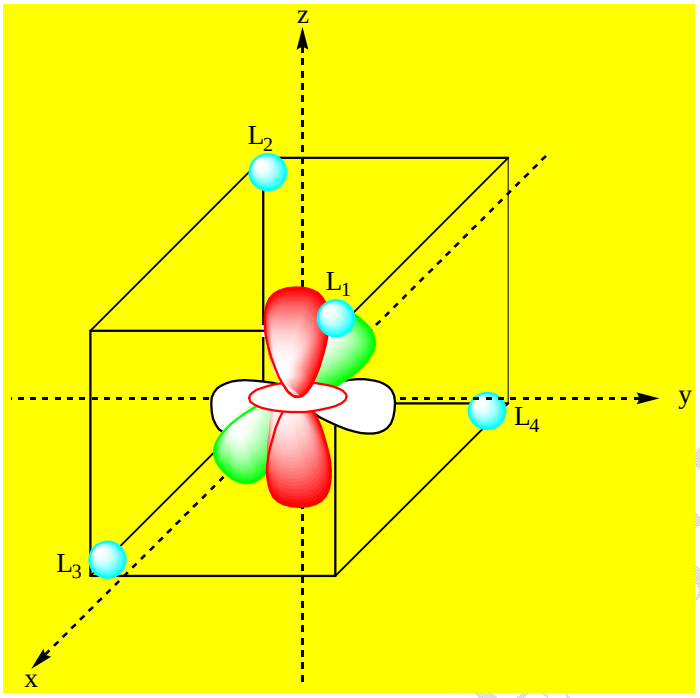

Scheme 80 : representation of square d orbitals in a tetrahedral distribution

- *How to position the lobes of the two types of d orbitals?*

The lobes of the $d_{x^2-y^2}$ and d_{z^2} orbitals point towards the midpoint of the faces of the cube. In contrast, the lobes of the d_{xy}, d_{yz} and d_{zx} orbitals point towards the midpoint of the edges.

- *Case of a $d^1(Ti^{3+})$:*

The electron will go to the region of space (lobes of the orbitals) where the electrostatic repulsion energy will be minimized.

The lobes furthest from the ligands are those corresponding to the square orbitals $d_{x^2-y^2}$ and d_{z^2} (pointing towards the center of the faces) while those of the mixed orbitals d_{xy}, d_{yz} and d_{zx} point towards the middle of the edges.

The energy diagram of the *d* orbitals in tetrahedral symmetry is given in the following figure. There is no longer a g index because the complex is no longer centrosymmetric.

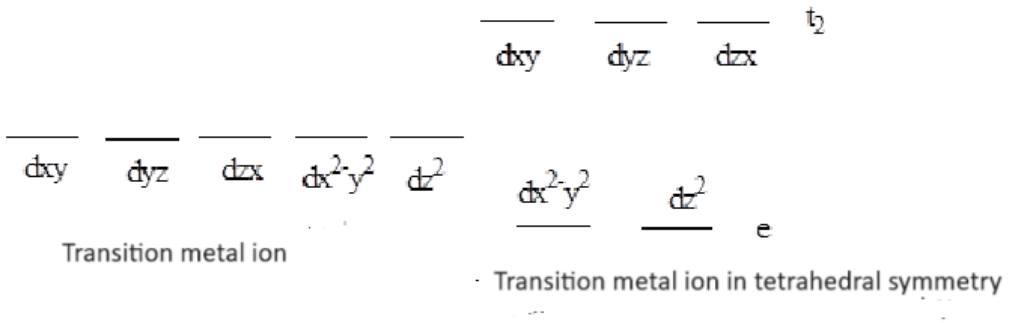

Figure 76 : Energy diagram of d orbitals for a transition ion in a tetrahedral environment

In the case of the tetrahedral environment, none of the lobes of the *d* orbitals point in the direction of the ligands. It follows that the electron/ligand electrostatic repulsion forces will be weaker than in the case of an octahedral environment (where the lobes of the $d_{x^2-y^2}$ and d_{z^2} orbitals are directed directly towards the ligands). It follows that the energy splitting between the two groups of orbitals will be weaker for the tetrahedral environment. For example, for the same transition ion and identical ligands: $\Delta_t = 4/9\ \Delta_0$.

IV- Distortions: Case of a tetragonally deformed octahedral complex and a square plane

A number of distortions of the geometry of the regular octahedron frequently occur, either because the ligands do not all occupy an equivalent situation, or are not all identical. These deformations are elongations or compressions in the direction of these axes. When the trans ligands are pulled, because of the increase in the ML distance the repulsions existing between the electrons of L and those of M in the regular octahedron become weaker in the case of the tetragonally deformed octahedron. Given this decrease in these repulsions, the d_{z^2} orbital which was very destabilized because of these strong repulsions will stabilize in the case of the tetragonally deformed octahedron (weaker repulsions). This movement of the ligands in the trans position will also affect the energy of the mixed orbitals having a z component.

However, this movement will affect d_{z^2} much more than it will affect the energy of the mixed orbitals because the pressure of the L electrons on the d_{z^2} electrons of M because of their position on the M – L path is much stronger than that of the ligand electrons on the electrons of the mixed orbitals in z. We will have a stabilization of d_{z^2} and of the mixed in z relative to their level in the regular octahedron.

If we assume that the global perturbation of the 6 ligands on the metal is the same in the complex of the regular octahedron and in the tetragonally deformed complex, the stabilization of the orbitals with a z component will have to be compensated by the destabilization of the orbitals with a xy component. If we continue the tetragonal deformation to infinity then the trans ligands detach from the metal and we obtain a square planar complex which results in an even greater stabilization of the orbitals with a z component and a destabilization of the orbitals with a xy component.

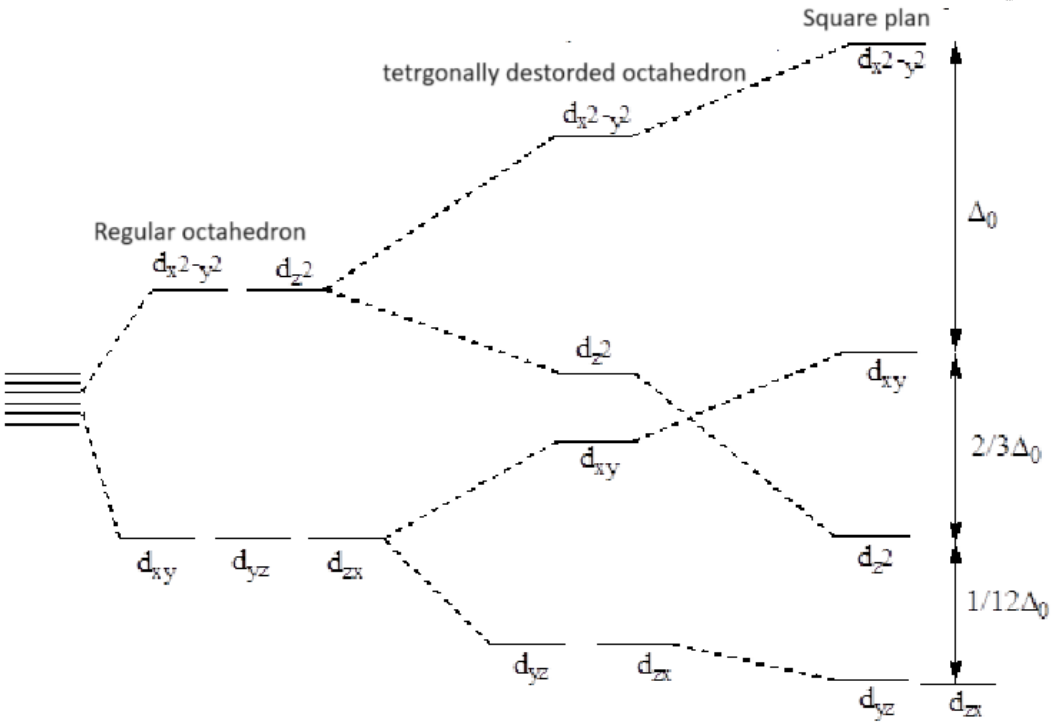

Figure 77 : energy diagram of a tetragonally distorted octahedral complex and a square plane

V- Jahn-Teller effect

The Jahn-Teller effect, also known as the "Jahn-Teller distortion," describes the distortion of the geometry of nonlinear molecules in certain situations. Historically, this effect was proposed in a theorem published in 1937 by **Hermann Arthur Jahn** and **Edward Teller**, in which they demonstrated that any nonlinear molecule with a degeneratefundamental will undergo a geometric distortion that removes this degeneracy, which will have the effect of decreasing the total energy of the molecule. This effect is observed in octahedral complexes of some hexacoordinate transition metals. In particular, copper(II), chromium(II), and manganese(III). Placed in an octahedral ligand field, the five degenerate d orbitals of a transition metal are subdivided into two groups of orbitals, T_{2g} (d_{xy}

d_{xz} and d_{yz}) and E_g ($d_{x^2-y^2}$ and d_{z^2}). The T_{2g} orbitals are therefore triply degenerate while the E_g orbitals are doubly degenerate. Since the Cu^{2+} ion has a d9 configuration, the E_g level contains three electrons, one of which is unpaired. Since both orbitals of the E_g level are degenerate, the single electron can be placed indifferently in one or the other of the $d_{x^2-y^2}$ or d_{z^2} orbitals, leading to the existence of a degenerate fundamental level, which gives rise to the Jahn-Teller effect. This type of complex will undergo a distortion along one of the quaternary symmetry axes (which is designated as the z'z axis), which has the effect of lifting the orbital degeneracy and decreasing the total energy of the complex. This distortion is generally manifested by an elongation of the metal-ligand distances along the z'z axis, but can occasionally cause a shortening of this bond (the Jahn-Teller theorem does not predict the direction of the distortion, but the existence of unstable geometries). When this type of distortion occurs, it has the effect of decreasing the electrostatic repulsion between the electron pair of the ligand, which is a Lewis base, and the electrons of the central metal having a component along the z'z axis, thus decreasing the energy of the complex. It is responsible for the distortion of the hexa-aquacopper(II) complex, $Cu(H_2O)_6]^{2+}$, which is predicted to have an octahedral geometry. The two axial Cu-O bonds are about 240 pm, while the four equatorial Cu-O bonds are about 190 pm. Even when all ligands are equivalent, experience has shown that distortions to the octahedral geometry can still be observed. They are attributed to this effect. The Jahn-Teller theorem states that "when a metal of an octahedral complex is such that there is a difference in the filling of the e_g orbitals and the t_{2g} orbitals, there is a lifting of the degeneracy of these t_{2g} or e_g orbitals, resulting from the geometric point of view in a differentiation of the metal-ligand lengths in the plane and in trans, thus giving a tetragonally deformed octahedron". The distortion is very important in the case of a d^9 and a d^4 high spin or d^7 low spin. It is infinite in the case of a d^8 "low spin". The maximum Jahn-Teller effect in a d^8 low spin explains the departure of the trans ligands and the formation of the square plane. A distortion of the molecule geometry lowering the symmetry will give a more stable state, partially or completely lifting the degeneracy. It is clear that the d^1 configuration is a good candidate for the Jahn-Teller distortion. Indeed, thefundamental is triply degenerate (the electron can be on one of the three OMs t_{2g} d_{xy}, d_{yz} or d_{xz}), and the excited state doubly $(t_{2g})^0(e_g)^1$ (the electron is either on d_{z^2} or on $d_{x^2-y^2}$). In both cases a distortion is likely. However, the Jahn-Teller theorem does not indicate the type of distortion or its amplitude. It only specifies that a lower symmetry will give rise to a more stable state. In octahedral complexes, the Jahn-Teller effect is mainly observed when an odd number of electrons occupy the E_g level. This condition is verified when the metal has a d^9, or d^4 high spin (weak field), or d^7 low spin (strong field) configuration for which thefundamental of the theoretical

octahedral complex is degenerate (E_g^3 or E_g^1). A Jahn-Teller effect should also be observed when the T_{2g} orbitals are not complete. But the E_g orbitals, unlike the T_{2g} orbitals, point towards the ligands, which makes the distortion much stronger in the first case than in the other.

VI- Experimental measurement: transition metals and colors

Transition metal complexes are often colored. Their color is a consequence of the energy separation of the e_g and t_{2g} orbitals. The color of the complexes is explained by a *d-d* transition during which an electron passes from the t_{2g} level to the eg level for an octahedral geometry. Let us take the simplest case of a transition ion with a single d electron ($\boldsymbol{d^1}$) in an octahedral environment. The following figure gives the energy diagram of the d orbitals (in octahedral symmetry).

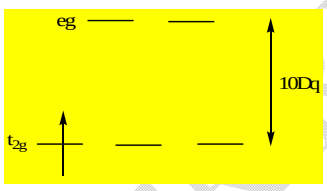

Figure 78 : Energy diagram of d orbitals

This diagram is summarized in two energy levels (that of the t_{2g} orbital group and that of the eg orbital group). If this complex receives a photon of energy **hν** such that **hν = 10 Dq**, then the electron can pass from t_{2g} to e_g. There is absorption of the corresponding radiation. If this radiation is located in the visible spectrum, then the complex is colored. The position of the absorbed radiation allows the experimental determination of 10 Dq (energy of the crystal field or energy difference between the e_g and t_{2g} orbital groups).

VII- Main factors governing the value of 10 Dq

Quatre facteurs principaux gouvernent la valeur de l'énergie du champ cristallin : Four main factors govern the value of crystal field energy:

- The nature of the central element;
- Its degree of oxidation of the central metal;
- Geometry;

- The nature of the ligand.

1°) The nature of the central element

Δ_o decreases when going up a column and decreases on a line. The d^4 and d^5 metals are therefore generally low spin. The role of this factor on the value of 10 Dq can be linked to the increase in the extension of the d orbitals when going from the 1st series (***3d***) to the 2nd (***4d***) and 3rd (***5d***) of the central element. This extension of the *d* orbitals leads to bringing closer the areas of space that can be occupied by the electron of the ligands and therefore to increasing the electrostatic repulsion "electron-ligands". It follows that if we go from an element of the 1st series to the 3rd series of transition metals (*3d* → *4d* → *5d*), the energy of the crystal field (10 Dq) increases.

Example : For $[Co(H_2O)_6]^{3+}$ ($3d^6$), 10 Dq = 247.62 kJ/mol (λ = 483 nm) whereas for $[Rh(H_2O)_6]^{3+}$ ($4d^6$), 10 Dq = 322.99 kJ/mol (λ = 370.4 nm).

4d orbitals are more diffuse (bulky) than ***3d*** orbitals. Therefore, the crystal field energy of rhodium is larger than that of cobalt.

2°) The oxidation state n+ of the central element

The more positively charged the metal, the closer the ligands will be. Δ_o will therefore be larger because the e_g orbitals will be even more destabilized. Increasing the formal oxidation state of a transition element amounts to decreasing the number of ***s*** and ***d*** electrons. It follows that, the number of protons remaining constant, the electrostatic attraction "nucleus-electrons" becomes stronger and the average distance "electron-nucleus" is shorter. The size of the transition ion decreases. As the distance "transition ion-ligand" decreases, the electrostatic repulsion forces increase. Consequently, the energy of the crystal field increases. Therefore, the field is all the greater as the charge of the metal is higher.

If n+ increases then 10 Dq increases. For $[Cr(H_2O)_6]^{2+}$ Δ_o = 11 000 cm^{-1} whereas for $[Cr(H_2O)_6]^{3+}$ Δ_o = 20 500 cm^{-1}.

3°) Geometry

The ligand field is weaker in tetrahedral geometry than in octahedral geometry. High-spin behavior is therefore generally observed in tetrahedral geometry. The symmetry of the ligand environment plays an important role in the value of the crystal field energy. All other

factors being equal, the crystal field energy of a transition element in octahedral symmetry is greater than that of the same element in tetrahedral symmetry.10 $Dq_{(tetra)}$ = 4/9 10 $Dq_{(octa)}$.

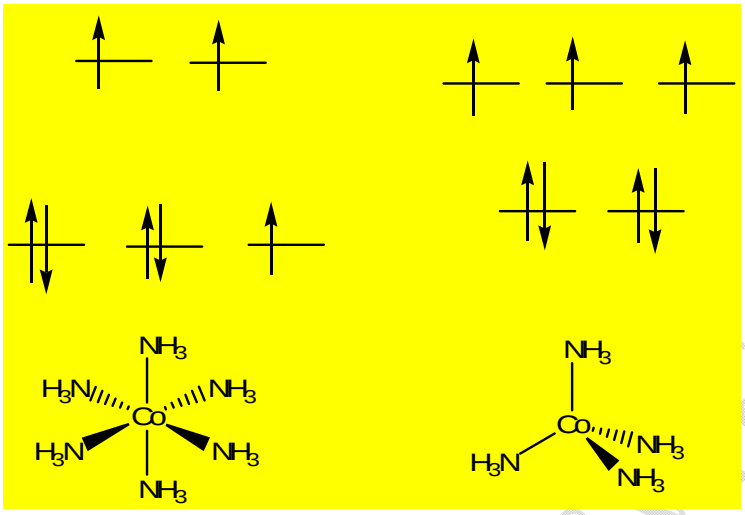

Scheme 81 : $[Co(NH_3)_6]^{2+}$ $3d^7$ 10 Dq = 122,02 kJ/mol (980,4 nm) et $[Co(NH_3)_4]^{2+}$ $3d^7$ 10 Dq = 70,58 kJ/mol (1695 nm)

4°) The nature of the ligand

The last factor that influences the energy of the crystal field is the nature of the ligands. The influence of this factor on the value of 10 Dq has been evaluated by spectroscopic measurements. Experience leads, for complexes differing only by the nature of their ligand, to classify the latter according to their ability to increase the energy gap 10 Dq. The value of 10 Dq decreases according to the **Fajans-Tsuchida** spectrochemical series which classifies ligands according to the strength of their field. This series is called the spectrochemical series because it is related to the color of the complexes.

Example : Let's take the two complexes: $\left[Ni(H_2O)_6\right]^{2+}$ is green, it absorbs red (λ = 700 nm), $\left[Ni(NH_3)_6\right]^{2+}$ is blue, it absorbs the orange color (λ = 600 nm). The more the compound absorbs light at higher energies (and therefore at lower wavelengths), the more the energy of the crystal field increases. We deduce from this that: 10 $Dq(NH_3)$ > 10 $Dq(H_2O)$.

VIII- Electronic configuration changes

When the difference between 10 Dq and P is small (of the order of the thermal energy kT), it is possible for the low spin and high spin states to coexist, in equilibrium with each

other. We thus have three possible situations. From the example of the Co^{3+} ion (d^6 configuration).

- When 10 Dq < P, the ion is in the "weak field" configuration "high spin".
- When 10 Dq > P, the ion is in "strong field" configuration "low spin".
- When 10 Dq – P ≈ kT, both spin states can be present and their proportion depends on the temperature (intermediate situation).

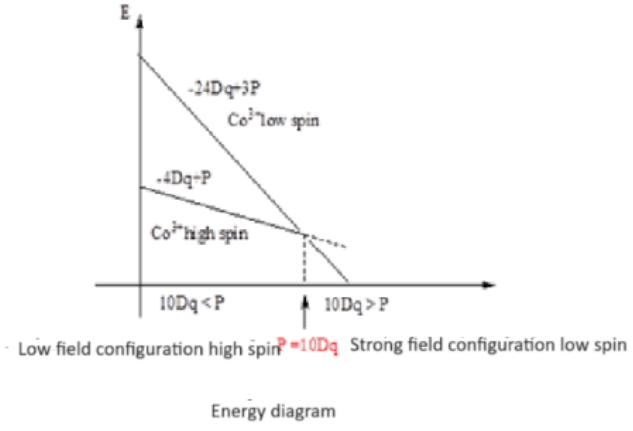

Figure 81 : energy diagram of a d^6

Application exercise

Write the electronic configurations of the d orbitals relative to the following octahedral complex ions:

1°) a complex of Nb(III),

2°) a complex of Mo(II) if 10 Dq is greater than the electron pairing energy,

3°) a Mn(II) complex if 10 Dq is less than the electron pairing energy,

4°) an Au(I) complex,

5°) an Ir(III) complex with 10 Dq greater than the electron pairing energy.

Correction

Element	Ion	Octahedral ion
Nb (Z=41) : [Kr] $4d^4 5s^1$	Nb(III) : [Kr] $4d^2 5s^0$	$t_{2g}^2 e_g^0$

Mo (Z=42) : [Kr] $4d^5 5s^1$	Mo(II) : [Kr] $4d^4 5s^0$	10 Dq > *P* strong field $t_{2g}^4 e_g^0$
Mn (Z=25) : [Ar] $3d^5 4s^2$	Mn(II) : [Ar] $3d^5 4s^0$	10 Dq < *P* weak field $t_{2g}^3 e_g^2$
Au (Z=79) : [Xe] $4f^{14} 5d^{10} 6s^1$	Au(I) : [Xe] $4f^{14} 5d^{10} 6s^0$	$t_{2g}^6 e_g^4$
Ir (Z=77) : [Xe] $4f^{14} 5d^7 6s^2$	Ir(III) : [Kr] $4f^{14} 5d^5 6s^0$	$t_{2g}^6 e_g^0$

Chapter 5

SpectroScopy and magnetiSm of complexes

I- T Russell-Saunders terms

If we consider a polyelectronic atom, the orbital magnetic moment of the atom will be obtained by summing the contributions of the different electrons. Similarly, the total spin magnetic moment will be obtained by considering the sum of the contributions of each of the electrons. Each electron has an individual orbital angular magnetic moment and an individual spin moment. These moments can couple in two ways.

- **1st case:** The individual orbital magnetic moments couple strongly together to give a resultant denoted $\vec{L}$. The spin magnetic moments of the individual electrons couple strongly together to give a resultant denoted $\vec{S}$. The two resultants $\vec{L}$ and $\vec{S}$ couple weakly to give a total magnetic moment denoted $\vec{J}$. This will be called the **Russell–Saunders** coupling.

- **2nd case:** The individual orbital and spin moments $\vec{l}$ and $\vec{s}$ couple very strongly to give a total angular momentum then these different total individual moments $\vec{j}$ couple weakly to give a total angular momentum $\vec{J}$. This is called a **spin-orbit** coupling. It has been shown experimentally that the interaction $\vec{l}$ and $\vec{s}$ is all the weaker as the atoms are light. Thus for light elements we will mainly use the first case. When the elements are heavy, that is to say beyond chromium, it is necessary to involve the spin-orbit coupling.

To define an orbital, we must have the value of ***l*** of the subshell to which it belongs and the value of the magnetic quantum number **m**; but in each subshell, the value of ***l*** is always equal to the maximum of **m**.

We can determine the possible values of the quantum numbers *L* and *S* knowing that for each value of *L*, the quantum number M_L can take the 2L+1 values +L, L-1, …, -L+1, -L and that for each value of *S*, the quantum number M_S can take the 2S+1 values +S, S-1, …, -S+1, -*S*. In the case of atoms, we know that the energy of the subshells is linked to the value of ***l*** (secondary quantum number). Recall that for a given ***n***, ***l*** can take the integer values from 0 to *n*-1. For a given ***l***, the magnetic quantum number ***m*** takes the values from –***l*** to +***l***.

Once we have determined the set of values of M_L and M_S, we will simply need to combine each of the values of M_L with a value of M_S. We thus define the set of possible combinations called microstates: all the possible ways of placing the electrons of a metal in the orbitals. From these, we will define the values of $\vec{L}$ and $\vec{S}$ which allow us to obtain the Russell-Saunders terms.

Each term is represented by the notation $^{2S+1}\Gamma$ where $2S+1$ is the spin multiplicity and Γ is put for S, P, D, F, G, … depending on whether L is worth 0, 1, 2, 3, 4, … For example.

- Li : $1s^2 2s^1$; $M_L = 0$ d'où $L = 0$ we have an S-type orbital.

  $M_S = ½$ from where ^2S.

- Be: $1s^2 2s^2$; $M_L = 0$ et $M_S = 0$ from where ^1S.
- C : $1s^2 2s^2 2p^2$; Statistics allow us to evaluate the number of possibilities of placing ***p*** objects in ***n*** boxes, according to:

$$C_n^p = \frac{n!}{p!(n-p)!}$$

It is the number of microstates where ***n*** is the maximum number of electrons in the subshell and ***p*** is the number of electrons in the subshell.Sous-couche p : 2 électrons ; the number of microstates is $\frac{6!}{2!4!} = 15$

+1	0	-1

↑	↑	

$M_L = 1 + 0 = 1$; $M_S = ½ + ½ = 1$

$M_L = 1 - 1 = 0$; $M_S = ½ + ½ = 1$

$M_L = 0 - 1 = 1$; $M_S = ½ + ½ = 1$

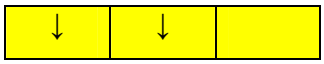

$M_L = 1 + 0 = 1$; $M_S = - ½ - ½ = - 1$

$M_L = 1 - 1 = 0$; $M_S = - ½ - ½ = - 1$

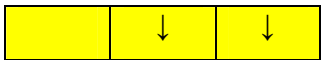

$M_L = 0 - 1 = -1$; $M_S = - ½ - ½ = - 1$

$M_L = 1 + 0 = 1$; $M_S = - ½ + ½ = 0$

$M_L = 1 - 1 = 0$; $M_S = - ½ + ½ = 0$

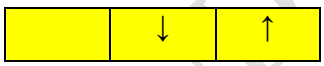

$M_L = 0 - 1 = - 1$; $M_S = - ½ + ½ = 0$

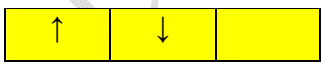

$M_L = 1 + 0 = 1$; $M_S = ½ - ½ = 0$

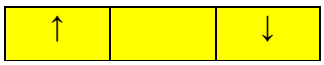

$M_L = 1 - 1 = 0$; $M_S = ½ - ½ = 0$

M_L = 0 - 1 = -1 ; M_S = ½ - ½ = 0

M_L = 1 + (1) = 2 ; M_S = ½ - ½ = 0

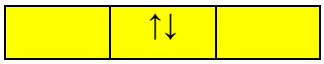

M_L = 0 + 0 = 0 ; M_S = ½ - ½ = 0

M_L= -1 - 1 = -2 ; M_S = ½ - ½ = 0

Table 12 : the **15** microstates of carbon

M_L	**M_S = 1**	**M_S = 0**	**M_S = -1**
2	-	$(1^+,1^-)$	-
1	$(1^+,0^+)$	$(1^+,0^-),(1^-,0^+)$	$(1^-,0^-)$
0	$(1^+,-1^+)$	$(1^+,-1^-),(1^-,-1^+),(0^+,0^-)$	$(1^-,-1^-)$
-1	$(0^+,-1^+)$	$(0^+,-1^-),(0^-,-1^+)$	$(0^-,-1^-)$
-2	-	$(-1^+,-1^-)$	-

In summary we have:

M_L				M_S
+2	↑↓			0
0		↑↓		0
-2			↑↓	0
+1	↑	↑		+1

0	↑		↑	+1
-1		↑	↑	+1
+1	↓	↓		-1
0	↓		↓	-1
-1		↓	↓	-1
+1	↓	↑		0
0	↓		↑	0
-1		↓	↑	0
+1	↑	↓		0
0	↑		↓	0
-1		↑	↓	0

Let us take the microstate (1^+,1^-) which corresponds to M_L = 2 hence the term is **D** and M_S = 0 hence $^{\mathbf{1}}\mathbf{D}$.

M_L = 1 hence the term is **P** ; M_S = 1 from where $^{\mathbf{3}}\mathbf{P}$.

M_L = 0 hence the term is **S** et M_S = 0 from where $^{\mathbf{1}}\mathbf{S}$.

Finally the carbon terms are: $^1S^1D^3P$.

Which corresponds to the fundamental term ^3P.

When an atom has multiple terms; the Russell-Saunders term of thefundamental is the one that corresponds to the multiplicity $2M_S + 1$ of the spins, **maximum**. Thefundamental term is therefore ^3P. The S and D terms have the same spin multiplicity, i.e. 1. **Hund**'s rule states that when 2 Russell-Saunders terms have the same spin multiplicity, the l**owest energy term** is the one that corresponds to the largest value of *L*, i.e. ^1D and finally ^1S. The Russell-Saunders terms of carbon are: $^3P^1D^1S$.

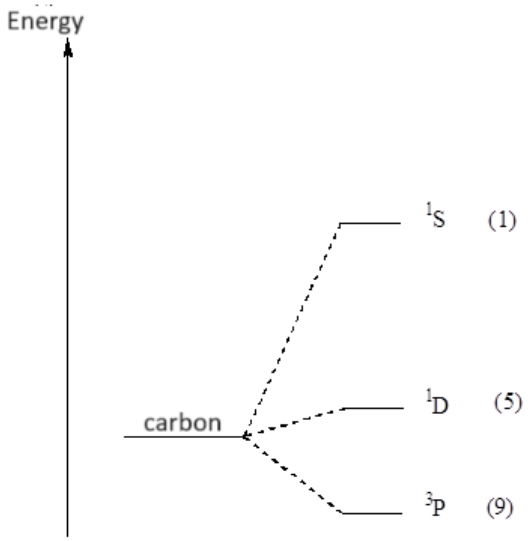

Figure 80 : energy diagram of a $^3P^1D^1S$

- For a d^2 we have:

+2	+1	0	- 1	- 2
↑↓				

$M_L^{max} = 4$

+2	+1	0	- 1	- 2
↑	↑			

$M_S^{max} = ½ + ½ = 1$ when electrons are decoupled.

The 45 classified microstates of M_L and M_S are gathered in the following table:

Table 13 : Microstates of an ion d^2

M_L	$M_S = 1$	$M_S = 0$	$M_S = -1$
4		$(2^+,2^-)$	

3	$(2^+,1^+)$	$(2^+,1^-),(2^-,1^+)$	$(2^-,1^-)$
2	$(2^+,0^+)$	$(2^+,0^-),(2^-,0^+),(1^+,1^-)$	$(2^-,0^-)$
1	$(2^+,-1^+),(1^+,0^+)$	$(2^+,-1^-),(2^-,-1^+),(1^+,0^-),(1^-,0^+)$	$(2^-,-1^-),(1^-,0^-)$
0	$(2^+,-2^+),(1^+,-1^+)$	$(2^+,-2^-),(2^-,-2^+),(1^+,-1^-),(1^-,-1^+),(0^+,0^-)$	$(2^-,-2^-),(1^-,-1^-)$
-1	$(1^+,-2^+),(0^+,-1^+)$	$(1^+,-2^-),(1^-,-2^+),(0^+,-1^-),(0^-,-1^+)$	$(1^-,-2^-),(0^-,-1^-)$
-2	$(0^+,-2^+)$	$(0^+,-2^-),(0^-,-2^+),(-1^+,-1^-)$	$(0^-,-2^-)$
-3	$(-1^+,-2^+)$	$(-1^+,-2^-),(-1^-,-2^+)$	$(-1^-,-2^-)$
-4		$(-2^+,-2^-)$	

Table 14 : The Russell-Saunders terms of the s and p orbitals

Configuration	Degeneration	Terms
s^1		$^{\mathbf{2}}\mathbf{S}$
s^2		$^{\mathbf{1}}\mathbf{S}$
p^1 et p^5	6	$^{\mathbf{2}}\mathbf{P}$
p^2 et p^4	15	^{1}S, ^{1}D, $^{\mathbf{3}}\mathbf{P}$
p^3	20	^{2}P, ^{2}D, $^{\mathbf{4}}\mathbf{S}$

Table 14 : Russell-Saunders terms of d orbitals (Fundamental terms in bold)

Configuration	Degeneration	Terms
d^0 et d^{10}		^{1}S
d^1 et d^9	10	^{2}D
d^2 et d^8	45	$^{\mathbf{3}}\mathbf{F}$, ^{1}G, ^{1}D, ^{3}P, ^{1}S
d^3 et d^7	120	$^{\mathbf{4}}\mathbf{F}$, ^{4}P, ^{2}G, ^{2}H, ^{2}P, ^{2}D, ^{2}F, ^{2}D
d^4 et d^6	210	$^{\mathbf{5}}\mathbf{D}$, ^{3}H, ^{3}G, ^{3}F, ^{3}D, ^{3}P, ^{3}P, ^{1}I, ^{1}G, ^{1}G, ^{1}F, ^{1}D, ^{1}D, ^{1}S, ^{1}S
d^5	252	$^{\mathbf{6}}\mathbf{S}$, ^{4}G, ^{4}F, ^{4}D, ^{4}P, ^{2}I, ^{2}H, ^{2}G, ^{2}G, ^{2}F, ^{2}F, ^{2}D, ^{2}D, ^{2}D, ^{2}P, ^{2}S

A spin-orbit coupling occurs if *L* and *S* associate. The interaction parameter *J* is defined by the relation: $J = L + S$. This coupling not only partially removes the degeneracy of each term but can also couple terms that do not have the same orbital symmetries or spin multiplicities by mixing states with the same *J*.

II- Application of coupling to electronic spectra

The Russell–Saunders terms in an octahedral field split into several components. The transitions that can occur can only occur between terms of the **same spin multiplicity** because the number of single electrons must remain the same. This is why compounds such as $[Mn(H_2O)_6]^{2+}$ that contain a metal in d5 should in principle be colorless, just like zinc complexes. The color of a complex is determined by the wavelengths not absorbed by this complex. In the case of $[Mn(H_2O)_6]^{2+}$ there is the **lifting** of the ban, i.e. the jump is not allowed and if it can be done it will be with great difficulty. Everything happens as if the electron leaves thefundamental and falls back to this state without reaching the destination state. This forbidden jump is allowed by the vibrations of the molecule; for this reason the bands of these forbidden jumps are extremely weak.

- The terms break out in O_h symmetry as follows:

$S \rightarrow A_{1g}$

$P \rightarrow T_{1g}$

$D \rightarrow E_g + T_{2g}$

$F \rightarrow A_{2g} + T_{1g} + T_{2g}$

$G \rightarrow A_{1g} + E_g + T_{1g} + T_{2g}$

$H \rightarrow E_g + 2T_{1g} + T_{2g}$

$I \rightarrow A_{1g} + A_{2g} + E_g + T_{1g} + 2T_{2g}$

Components may be once degenerate (A species), doubly degenerate (E species), or triply degenerate (T species); subscripts 1 and 2 to distinguish similar degeneracy states.

Example : $[Ti(H_2O)_6]^{3+}$ has a band; Ti^{3+} (d^1) has Russell-Saunders terms ^2D. The components dart the multiplicity of the term; $^2D \rightarrow {}^2E_g + {}^2T_{2g}$.

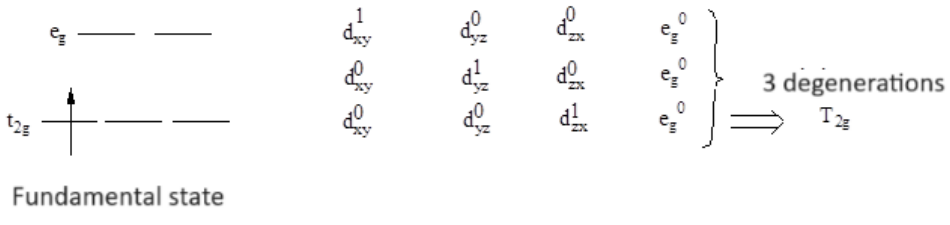

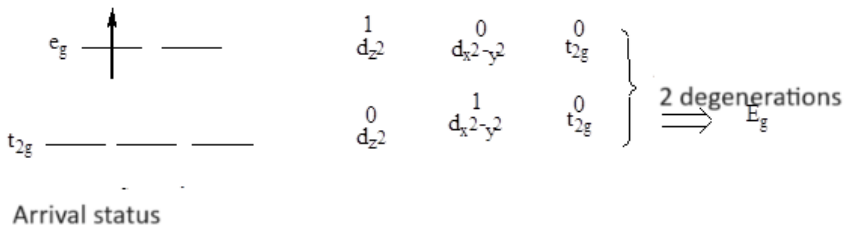

Figure 81 : transition $^2D \rightarrow {}^2E_g + {}^2T_{2g}$

Transition : $T_{2g} \rightarrow E_g$

We see that there are 3 ways to write thefundamental and that one of the Russell-Saunders components of thefundamental has a degeneracy of order 3. We can write the arrival state in 2 different ways. One of the components of the Russell-Saunders terms of the arrival state has a degeneracy of order 2. It is therefore the number of times that it is possible to write thefundamental in the arrival state which will allow on the basis of the degeneracy which of the components is the fundamental component of the Russell-Saunders fundamental term. The other component(s) are the arrival components. There is only one fundamental component and several arrival components. Instead of saying that the band of the spectrum of $[Ti(H_2O)_6]^{3+}$ is due to a transition from the t2g orbitals to the eg orbitals, we will say that this transition is from a T_{2g} state to an E_g state [5].

III- Orgel diagram

Orgel diagrams represent the energy of the different levels as a function of the strength of the field. It can be seen that the lifting of the degeneracy is all the greater as the field is strong.

A single Orgel diagram represents four electronic situations: a d^2 complex has the same irreducible representations in tetrahedral and octahedral geometry. Moreover, thanks to the electron-hole analogy, a d^8 ion has the same spectral terms as a d^2 ion but with an inverse degeneracy lift. To illustrate this analogy, a d^1 ion and a d^9 ion have a ^2D fundamental term. By adding the ligand field, there is a degeneracy lift in ^2T2_g and ^2E_g. For the d^1 ion, the fundamental has $^2T_{2g}$ symmetry; it corresponds to the microstate (t_{2g}); while the excited state has ^2E_g symmetry; it corresponds to the microstate (e_g). We therefore have $E(^2T_{2g}) < E(^2E_g)$. Conversely, for a d^9 ion, the microstate associated with ^2E_g is $(t_{2g})^6(e_g)^3$ and the microstate associated with $^2T_{2g}$ is $(t_{2g})^5(e_g)^4$. We deduce $E(^2E_g) < E(^2T_{2g})$. The energy order is reversed [5].

For a $d^9 \rightarrow {}^2D$

If we consider Cu^{2+} which is $\boldsymbol{d^9}$ we have an inverse diagram compared to that of Ti^{3+} which is $\boldsymbol{d^1}$. Such a diagram representing the energy as a function of the components is called an **Orgel** diagram. For the diagram of a tetrahedral $\boldsymbol{d^1}$ and $\boldsymbol{d^9}$ ${}^2D \rightarrow {}^2E + {}^2T_2$.

For a d^1 ; ${}^2E \rightarrow {}^2T_2$ and a d^9 ; ${}^2T_2 \rightarrow {}^2E$.

Eventually : $d^1Oh \equiv d^9Td$ et $d^1Td \equiv d^9Oh$

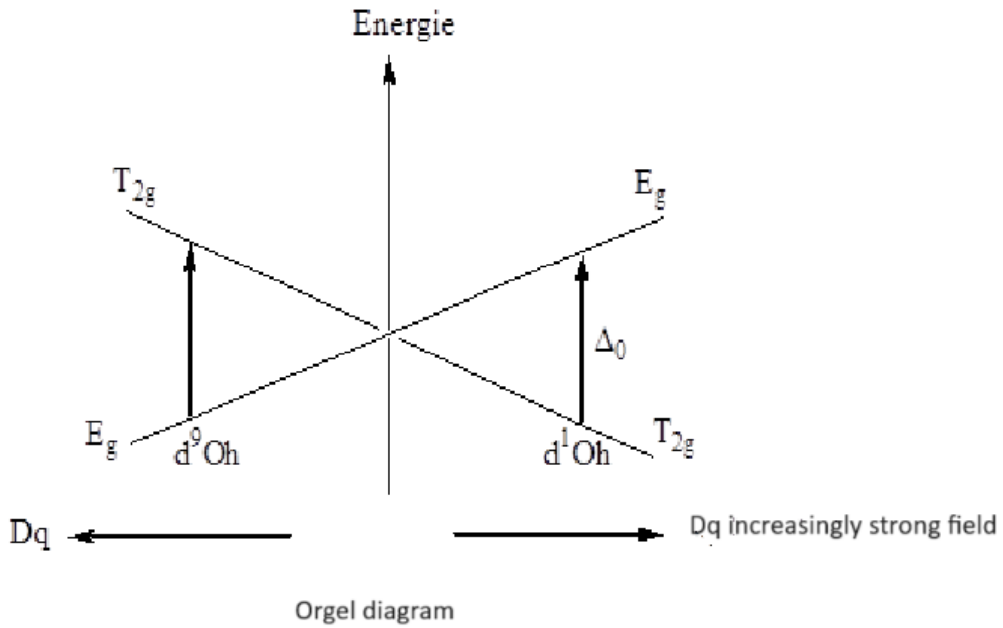

Figure 82 : Orgel diagram of a d^1 and a d^9

If we associate increasingly strong field ligands with a given metal, we see an increasingly greater difference between T_{2g} and E_g.

When 2 metals have complementary numbers of electrons on their subshell ***d***, the Orgel diagram of one in tetrahedral configuration is the equivalent of the Orgel diagram of the other in octahedral configuration; whereas the Orgel diagram of one in tetrahedral or octahedral configuration is the inverse of the Orgel diagram of the other in tetrahedral or octahedral configuration. Orgel diagrams are used to account for the spectra of "high spin" type complexes. For "low spin" type complexes, **Tanabé-Sugano** diagrams are used.

IV- Tanabe-Sugano diagram

In reality, we find both the strong field situation and the weak field situation. Tanabe-Tsugano diagrams therefore go further than Orgel diagrams because they allow us to follow the energy evolution of the levels regardless of the strength of the ligand field. They also allow us to easily go back quantitatively to the parameters Δ_o and B; something impossible with crystal field theory. On Tanabe-Tsugano diagrams, unlike Orgel diagrams, it is the fundamental that serves as a reference. The two axes are dimensionless because they are related to the value of B. For some diagrams, there is a break in the slope and a vertical bar (complex d^4 to d^7) which mark the transition from the strong field situation to the weak field.

Take the example of $[Co(NH_3)_6]^{3+}$ which is a diamagnetic complex. The Russell-Saunders terms of Co^{3+} are : ^5D ^3H ^3F ^3G ^1I ^1G ^1S.

If we consider the Tanabé-Sugano diagram of a d^6 we see that it contains the Orgel diagram of a "high spin" d^6. This is the first part of this diagram. We see in fact that the Russell-Saunders term in thefundamental in the case of a "high spin" is ^5D which splits into $^5T_{2g}$ and ^5E_g. This allows us to account for the single band of the spectra of a "high spin" complex of a d^6. When the complex is "low spin" in the case of a d^6 the Russell-Saunders term in thefundamental is no longer ^5D but ^1I. If we consider the filling of the t_{2g} orbitals in an O_h environment we see that there is only one way to write this arrangement, that is to say:

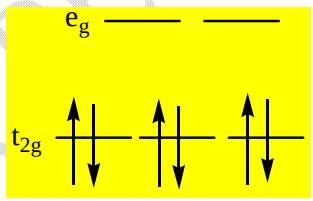

Figure 83 : representation of the d orbitals of a d^6

This is why the fundamental component is A_{1g}. And all the transitions will start from this fundamental component towards the other components deriving from the Russell-Saunders terms of multiplicity **1**.

In reality the spectrum of $[Co(NH_3)_6]^{3+}$ has 2 bands. If we consider a first simple transition we obtain the configurations:

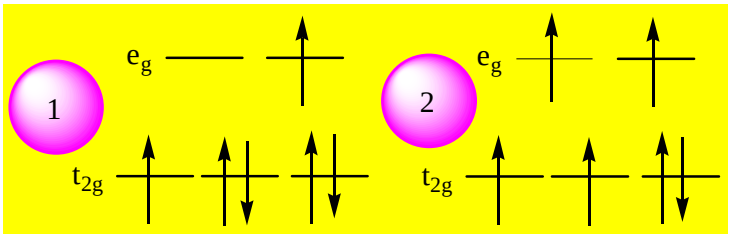

Figure 84 : transitions of d^6

Configuration 1 is triply degenerate and is called T_{1g}. If we consider a double electronic jump, we obtain 2 which is triply degenerate and which we will call T_{2g}. The 2 absorptions present on the spectrum of $[Co(NH_3)_6]^{3+}$ correspond well to the transitions:

$A_{1g} \rightarrow T_{1g}$ et $A_{1g} \rightarrow T_{2g}$

Other transitions, although theoretically possible, cannot be detected by the UV spectrophotometer.

V- Spin-orbit couplings

- To find the energy levels resulting from the action of the spin-orbit coupling on a given term, it is therefore necessary to calculate all the possible values of the quantum number M_J associated with and deduce the possible values of J knowing that for each value of J, M_J takes the 2J+1 values J, J-1, . . ., -J + 1,-J. The level obtained is noted by adding the index J to the term from which it comes. For example, for the fundamental term ^3F of the d^2 configuration, we have:

$S = 1$, from where $M_S = \pm 1, 0$
$L = 3$, from where $M_L = \pm 3, \pm 2, \pm 1, 0$

We deduce that the possible values of J are:

$J = 4$ which corresponds $M_J = \pm 4, \pm 3, \pm 2, \pm 1, 0$
$J = 3$ which corresponds $M_J = \pm 3, \pm 2, \pm 1, 0$
$J = 2$ which corresponds $M_J = \pm 2, \pm 1, 0$

- The levels from ^3F to which we will give the name of state will be noted $^3F_4$, $^3F_3$ and $^3F_2$. The 2J +1 degeneracy of each of these states can only be completely lifted by the action of an external perturbation, for example a magnetic field. An empirical rule proposed

again by **Hund** makes it possible to predict thefundamental. If the shell is less than half-filled (configuration d^1 to d^4), thefundamental is given by the smallest value of *J*; if the shell is more than half-filled, it is the largest value of *J* which corresponds to thefundamental. Thisfundamental, in the case of the d^2 ion, is therefore $^3F_2$.

Spin-orbit coupling not only partially lifts the degeneracy of each term but can also couple terms that do not have the same orbital symmetries or spin multiplicities by mixing states with the same *J*. This second-order effect is all the more important as the spin-orbit coupling is stronger and the terms are less spaced, i.e. the electronic repulsion is weak. This coupling of different terms is thus almost negligible for transition ions of the first series; it plays a certain role with those of the second series and even more so with those of the third.

VI- Optical properties of coordination compounds (*d-d* transitions and qualitative interpretation of spectra)

The color of the complexes results from intraconfigurational transitions between ***d*** orbitals. Indeed, the energy difference between t_{2g} and eg orbitals equal to Δ varies between 149.53 kJ/mol and 299.06 kJ/mol, i.e. an energy range corresponding to the visible spectrum of electromagnetic radiation (800 nm > λ > 400 nm). An electronic transition corresponds to the passage of an electron from the fundamental level to an excited level. When it takes place, matter absorbs a photon whose energy rigorously corresponds to the energy difference between the fundamental term and an excited term. It also follows selection rules: one linked to the orbital moment and the other linked to the spin moment. An authorized transition takes place if the orbitals involved during this process are such that $\Delta l = \pm 1$ and $\Delta S = 0$.

d - d transitions are forbidden according to the first rule because $\Delta l = 0$, but they are observed thanks to relaxation mechanisms essentially linked to electron-nucleus couplings (role of vibrations). On the other hand, a ***d - d*** transition with spin change is forbidden according to both rules. Here too, it can be observed thanks to much less efficient relaxation mechanisms linked to the couplings between spin moments and orbital moments of the electrons. Consequently, these transitions are much less intense than the spin-permitted ***d - d*** transitions.

The electronic spectrum (measure of the variation of the absorbance of a solution as a function of λ) can be formed by one or more electronic transitions. If a complex presents **only**

one transition, then the color of this complex corresponds to the **complementary** color of the color **absorbed** during the transition (example red and green; blue and yellow).

1°) Single-band spectra: interpretation of the color of complexes

This situation occurs in complexes of Ti^{3+} ions of $\boldsymbol{d^1}$ configuration. An aqueous solution of $[Ti(H_2O)_6]^{3+}$ is red. The absorption spectrum is formed by a single band with λ_{max} = 510 nm. The absorbed color is green, the complex appears in the complementary color, namely red. The observed band is interpreted as the transition of the electron from the t_{2g} orbital to the eg orbital. The energy of this transition has the value of Δ = 234.55 kJ/mol, corresponding to a wavelength of 510 nm.

A similar case is that of the hexa-aqua ion of copper (II): $[Cu(H_2O)_6]^{2+}$of configuration $\boldsymbol{d^9}$. In this case, the compound is blue-green, and its spectrum consists of a single band located at 840 nm. It absorbs red, and therefore appears of the complementary color. The spectrum is analyzed in a similar way. We can see this transition as the passage of the electron from a t_{2g} orbital to an e_g orbital. The transition always has the energy Δ. In this case, Δ is 143.55 kJ/mol (λ = 833.3 nm).

From the analysis of these two spectra, experimental proof is given that the crystal field Δ increases with the charge of the transition ion. In general, $\Delta_M^{3+} > \Delta_M^{2+}$.

2°) Two-band spectrum: role of "electron-electron" repulsion

Consider the visible spectrum of the complex $[Cr(H_2O)_6]^{3+}$ whose lowest energy configuration is t_{2g}^3 ($\boldsymbol{d^3}$). This is formed by two bands of similar intensity at 208.15 kJ/mol (λ = 575 nm) and 294.28 kJ/mol (λ = 406.5 nm), whose origin is to be sought in $t_{2g} \rightarrow e_g$ transitions. One way to achieve this transition is to promote the electron from the d_{xy} orbital to the d_z^2 orbital. In this case, the electron density is relocated during the transition from an xy plane to a z direction already rich in electrons (the d_{zx} and d_{yz} orbitals are occupied). However, there is another way to achieve this transition by moving the electron from the dzx orbital to the d_z^2 orbital. In this case, the electron density will simply be relocated along a z axis already rich in electrons before the transition. It is easy to see that for the first case the electronic repulsion will increase greatly during the transition, and much less in the second case. Consequently, the two transitions considered appear at different energies.

The other possibilities of transitions $t_{2g} \rightarrow e_g$ will be similar to either case, so that the complex has two bands in its absorption spectrum.

In the first case, the electron density shifts strongly towards the ligands on the z axis. While in the second case, the shift is much weaker.

It is the **lowest energy** transition that will allow us to determine Δ. We therefore determine Δ = 208.15 kJ/mol (λ = 575 nm).

VII- Quantitative interpretation of spectra

To understand the origin of the second transition for the $[Cr(H_2O)_6]^{3+}$ complex, it is necessary to study in more detail the electronic structure of the transition ions and take into account the **electron-electron repulsion (ER)**. Until now, this has been introduced in the case where it is maximum, that is to say when two electrons occupy the same orbital, in the form of an energy quantity P. When P is much larger than Δ_0, the electronic structure of the ion considered is profoundly modified: the strong-field complex prefers to associate all its electrons in t_{2g} orbitals for the sake of energy gain. When two electrons occupy two different orbitals oriented in space in a common direction, the electron-electron repulsion is weaker but it exists. It will have the effect of creating several levels of different energies from a degenerate state resulting from a configuration.

A given configuration $(t_{2g})^a(e_g)^b$ gives rise, due to the "electron-electron" repulsion, to several different energy levels, represented by a spectroscopic term. The transitions between spectroscopic terms have energies covering the visible range. The optical spectra of coordination compounds are therefore not interpreted as an electronic jump $t_{2g} \rightarrow e_g$, but as a transition between spectroscopic terms ($T_{2g} \rightarrow E_g$).

In the same way that we compared P and Δ_0, we will compare the **electron-electron repulsion** treated as a whole (which will subsequently be noted **ER**) and the crystal field. We begin by examining two limiting cases:

The weak field situation $\mathbf{\Delta_0 << ER}$ and the strong field situation $\mathbf{\Delta_0 >> ER}$.

1°) Electronic structure of weak field complexes

The crystal field is weak, the effects of the **ER** dominate: $\mathbf{\Delta_0 << ER}$. We first consider the effect of the **ER** on the energy levels of the free ion. The five ***d*** orbitals (or if we take into

account the spin the ten spin-orbitals) are all of the same energy. For the d^3 configuration, we must place three electrons (or three objects) among ten spin-orbitals (or ten boxes). Statistics allows us to evaluate the number of possibilities of placing ***p*** objects in ***n*** boxes, according to:

$$C_n^p = \frac{n!}{p!(n-p)!}$$

With ***n***, number of spin-orbitals and ***p***, the number of electrons. For d^3, ***n*** = 10, ***p*** = 3, or $C_n^p = 120$. There are 120 possibilities to arrange 3 electrons on 10 spin-orbitals.

The d^3 configuration alone groups together 120 states of equivalent energy equal to three times the energy of a ***d*** orbital, or $3.E_d$. The **ER** will remove this degeneracy by creating eight different energy levels called spectroscopic terms. The energy of each term is obtained using a sophisticated calculation involving bielectronic integrals quantifying the **ER**.

Now consider the effect of the crystal field on the spectroscopic terms of the free ion. This only acts on the orbital part (the spin multiplicity will not be modified) by continuing to lift the orbital degeneracy of the terms. For example, in the same way that the five ***d*** orbitals are split under the effect of an octahedral field into three t_{2g} orbitals and two e_g orbitals, the D symmetry terms will be split into T_{2g} and E_g terms. The F symmetry terms will be transformed into terms: $A_{2g} + T_{1g} + T_{2g}$.

2°) Electronic structure of strong-field complexes

, le champ cristallin est fort, et ses effets sur les niveaux d'énergie dominent.

L'effet du champ cristallin sur une configuration d^n est traité dans un premier temps. Ainsi les orbitales ***d*** deviennent en champ octaédrique les orbitales t_{2g} d'énergie et les orbitales e_g d'énergie. A partir de la configuration d^3, on obtient les configurations d'énergie et de dégénérescence différente :

Δ_0 >> ER, the crystal field is strong, and its effects on the energy levels dominate.

The effect of the crystal field on a d^n configuration is treated first. Thus the d orbitals become in octahedral field the t2g orbitals of energy -2/5 Δ_0 and the eg orbitals of energy -3/5 Δ_0. From the d^3 configuration, we obtain the configurations of different energy and degeneracy:

- $(t_{2g})^3$ of energy equal to $3(-2/5\ \Delta_0) = -\ 6/5\ \Delta_0$,
- $(t_{2g})^2(e_g)^1$ of energy equal to $2(-2/5)\Delta_0 + 3/5\Delta_0 = -\ 1/5\ \Delta_0$,
- $(t_{2g})^1(e_g)^2$ of energy equal to $-2/5\Delta_0 + 2(3/5\Delta_0) = 4/5\ \Delta_0$,
- $(e_g)^3$ of energy equal to $3(3/5\Delta_0) = 9/5\ \Delta_0$.

The **ER** has the effect of partially lifting this degeneracy to create the series of spectroscopic terms already identified in the first situation. This situation gives access to the energy of the terms.

3°) "Weak field-strong field" correlation. Tanabé-Sugano diagrams

Reality being very often intermediate between a weak field and a strong field, we establish a term-by-term correlation from the weak field approach to the strong field approach (next figure).

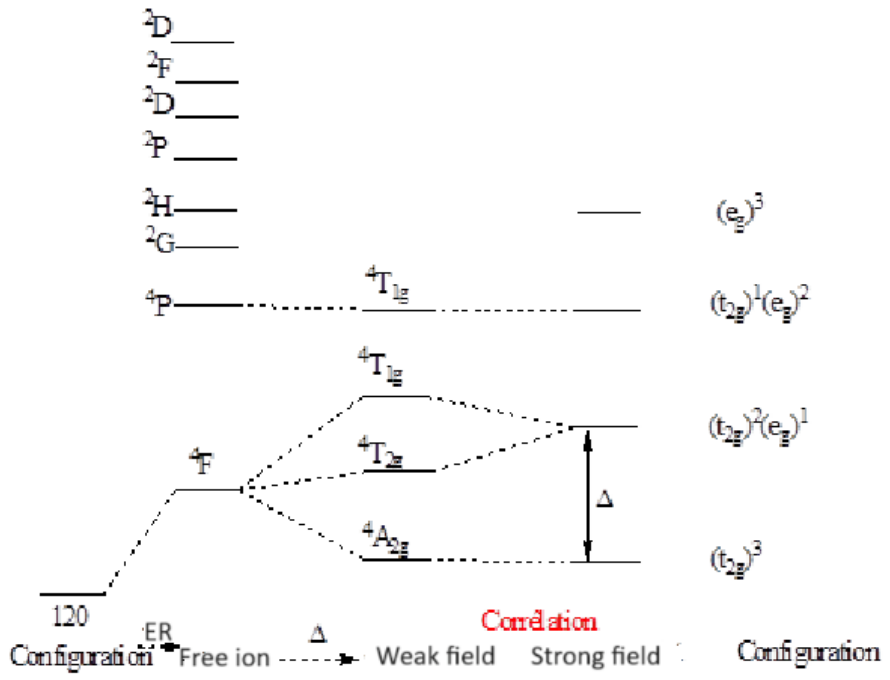

Figure 85 : Spectroscopic terms of the complexed ion d^3 weak field and strong field

This correlation results in the construction of a **Tanabé-Sugano** diagram (figure below), where the energy of the terms is plotted according to E/B = f (Δ/B), B (term relating to electronic repulsion) being the **Racah** parameter. The fundamental term is thus merged with the abscissa axis.

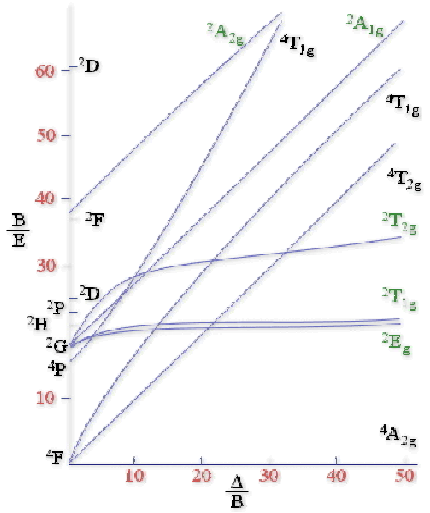

Figure 86 : Tanabé-Sugano diagram for the d^3 configuration

4°) Interpretation

Interpreting a spectrum means that we are able to identify the excited terms reached during each of the transitions by considering the **Tanabé-Sugano** diagram describing the configuration studied.

If we measure the UV-visible spectrum of the octahedral complex $[V(H_2O)_6]^{3+}$, we obtain the following spectrum:

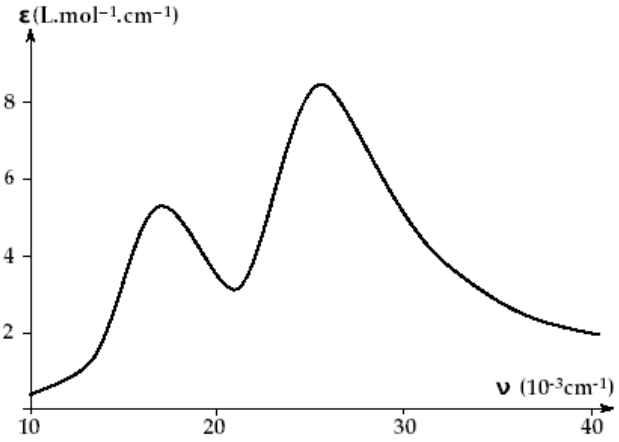

Figure 87 : UV-Visible spectrum of $[V(H_2O)_6]^{3+}$

We see two absorption bands at 17500 cm^{-1} and 26000 cm^{-1}. The molar absorption coefficients are close to 10, these are indeed *d-d* transitions forbidden by symmetry and allowed by spin. We have a vanadium ion at degree III. Looking at the corresponding Tanabe-

Tsugano diagram, we see that the fundamental term is $^3T_{1g}(F)$. There are three possible transitions that keep the spin unchanged:

$^3T_{1g}(F) \rightarrow {}^3T_{2g}$, $^3T_{1g}(F) \rightarrow {}^3T_{1g}(P)$, $^3T_{1g}(F) \rightarrow {}^3A_{2g}(F)$.

A **qualitative** interpretation of the spectrum of $[Cr(H_2O)_6]^{3+}$ is as follows:

- The fundamental term is $^4A_{2g}$, a term from the **lowest energy** configuration $(t_{2g})^3$.
- The lowest energy excited configuration is $(t_{2g})^2(e_g)^1$. The **ER** will create two spectroscopic terms of the same spin multiplicity as the fundamental term $^4T_{2g}$ and $^4T_{1g}$. We obtain two transitions in the visible domain:
  - 1st transition : $^4A_{2g} \rightarrow {}^4T_{2g}$;
  - 2nd transition : $^4A_{2g} \rightarrow {}^4T_{1g}$.

A priori, a third transition should be observed, corresponding to the transition between thefundamental $^4A_{2g}$ and the highest energy excited term $^4T_{1g}$. In fact, this transition is too high in energy to be observed in the visible range.

We neglect the transition to the excited terms ^2E_g, $^2T_{1g}$. Indeed, the transition from the fundamental term $^4A_{2g}$ to these two terms of the same energy is a transition that modifies the spin of the system. This type of transition is forbidden according to the selection rules, therefore a priori unobservable. However, if we examine the spectrum carefully, there is a shoulder in the foot of the band corresponding to the transition $^4A_{2g} \rightarrow {}^4T_{2g}$; located below 191.4 kJ/mol ($\lambda = 625$ nm).

This shoulder corresponds to the weak $^4A_{2g} \rightarrow {}^4E_g$, $^2T_{1g}$ transition masked by the allowed spin transition. Once the qualitative analysis has been carried out, the **quantitative** interpretation of the spectrum allows Δ and B to be determined. To do this, a graphical resolution is carried out.

To determine the two unknowns Δ and B, we perform a graphical resolution. We note on the diagram that the slope of the first excited term $^4T_{2g}$ is equal to **one**. Consequently, we have for this term E2/B = 1. Δ/B, or E2 = Δ. The first transition directly gives the value of Δ, or Δ = 208.15 kJ/mol. To estimate B, we calculate the ratio (E2/B)/(E1/B) = E2/E1, or 294.28/208.15 = 1.41. This trick allows us to eliminate the unknown B on one of the axes. We then graphically look for the corresponding ratio E2/E1 = 1.41 on the y-axis, and when it is

found, we simply read the value of Δ/B on the x-axis, or 25. We therefore find for B = 8.37. 10^{-3} kJ/mol.

Let us give some examples of spectra of complexes of five elements of the first transition series.

- **Nickel (II) spectra**

In the electronic spectrum of a nickel(II) complex, a ligand → metal charge transfer band is predicted in the region (393-423) nm. The absorption bands observed in the region (304-347) nm are assigned to the n → π* transitions within the ligand. The metal-ligand charge transfer bands observed at 424 and 450 nm can be assigned to N → Ni and S → charge transfer, respectively. Similarly, three bands are predicted at around 380, 590 and 1030 nm. The band at 380 nm is assigned to the metal-ligand charge transfer while the other two are assigned to the *d-d* transitions: $^3A_{2g}$ (F) → $^3T_{1g}$ (P) and $^3A_{2g}$ (F) → $^3T_{2g}$ (F), respectively. This spectral fact is characteristic of an octahedral environment around nickel(II) [23].

A broad band of d → d transitions can be pointed at around 680 nm on the spectrum of Ni(II) complex and be attributed to the sum of two bands due to the transitions of an octahedral Ni(II) complex [24].

The high-intensity charge transfer band of the S → Ni of the three transitions at 513, 570 and 692 nm correspond to $^1A_{1g} \rightarrow {}^1A_{2g}$, $^1A_{1g} \rightarrow {}^1B_{1g}$ and $^1A_{1g} \rightarrow {}^1E_g$ for a square-planar Ni(II) complex. The absence of an absorption band above 1000 nm, due to the large crystal field splitting, also indicates a square-planar environment around nickel(II) [25].

In the electronic spectrum of a Ni(II) complex, an absorption band centered at 990 nm can be attributed to the $d \rightarrow d$ transitions. This transition assumes a trigonal bipyramidal environment around nickel(II) [26].

- **Copper (II) spectra**

The band pointed at 675 nm of a Cu(II) complex corresponds to a square-based pyramid around this metal ion. For a copper(II) complex, two bands at 631 and 787 nm are attributed to the *d-d* transition. This spectral fact is characteristic of a pentagonal environment around the copper(II) ion [27].

The electronic spectra of copper(II) complexes recorded in DMF showing absorptions in the (267-272) nm and (355-380) nm regions can be assigned to the π → π* transitions of the aromatic rings and n → π* transitions of the imine function of the ligand, respectively. The Ligand → Metal charge transfer band can be spotted in the spectra between 422 and 456 nm. In the region of d-d transitions, we predict three absorption bands centered at 730 nm,

920 nm and 1080 nm. They are assigned to the $^2B_1 \rightarrow {}^2E$, $^2B_1 \rightarrow {}^2B_2$ and $^2B_1 \rightarrow {}^2A_2$transitions, respectively. These transitions suggest a copper complex with an octahedral environment [28].

Le spectre d'un complexe de cuivre (II) peut présenter une large bande de transition $d \rightarrow d$ centré à 653 nm. Celle-ci suggère un environnement octaédrique autour du cuivre [29].

The spectrum of a copper(II) complex may exhibit a broad $d \rightarrow d$ transition band centered at 653 nm. This suggests an octahedral environment around the copper [29].

The UV-Visible spectrum of a copper complex may show a weak, broad absorption band in the d-d transition region at around 750 and 906 nm. These absorption bands suggest a square-planar environment around the Cu^{2+} metal ion. The UV-Visible spectrum of a copper complex may also reveal a single broad absorption in the d-d transition region. It is centered at around 845 nm and suggests a square-planar environment around the Cu^{2+} metal ion. The absorption at 520 nm corresponding to the $^2B_{1g} \rightarrow {}^2A_{1g}$ transition indicates a square-planar environment of Cu(II). Similarly, the absorption at 540 nm in the form of a shoulder attributed to the transition $^2B_{1g} \rightarrow {}^2A_{1g}$ gives a square plane around the Cu(II) ion [30].

- **Cobalt (II) spectra**

A UV-Vis spectrum of a Co(II) complex can show an absorption band at 420 nm, assigned to the ligand → metal charge transfer. A band identified at 422 nm can be assigned to that of the Ligand → Metal charge transfer.

A spectrum of the cobalt(II) complex can reveal two bands at around 475 and 1030 nm. These would be respectively assigned to the $^4A_2 \rightarrow {}^4T_1$ (P) and $^4A_2 \rightarrow {}^4T_1$ transitions, thus suggesting a tetrahedral environment around the cobalt(II) [31, 32].

In the spectrum of a cobalt(II) complex, the bands present at 610 and 675 nm are due to the $^2E_g \rightarrow {}^2T_{2g}$ and $^2E_g \rightarrow {}^2T_{1g}$ (P) transitions of an octahedral Co(II). In the spectrum of a cobalt complex, three $d \rightarrow d$ transition bands are predicted at 595, 610 and 670 nm. They are respectively assigned to the $^4T_{1g}$ (F) → $^4T_{1g}$ (P), $^4T_{1g}$ (F) → $^4A_{2g}$ (F) and $^4T_{1g}$ (F) → $^4T_{2g}$ (F) transitions observed for a Co(II) ion with an octahedral environment [33, 34]. The absorption at around 415 nm transition $^2A_g \rightarrow {}^2B_{3g}$ of Co(II) indicates a square plane of a cobalt(II) [35].

- **Manganese (II) spectrum**

In the case of a manganese(II) complex which is a d^5 ($t_{2g}^3 e_g^2$) the electronic transitions necessarily lead to a rotation change from S = 5/2 to S = 3/2 i.e. from $t_{2g}^3 e_g^2 \rightarrow t_{2g}^2 e_g^3$. These *d-d* transitions are doubly forbidden by the selection rules. The UV-visible spectra of the complexes, recorded in a DMF solution, can show bands in the (290-350) nm and (375-403) nm regions which are due to the $\pi \rightarrow \pi^*$ and $n \rightarrow \pi^*$ transitions within the ligand, respectively.

The electronic spectrum of a manganese(II) complex can predict a band at 446 nm assigned to the ligand → metal charge transfer band.

On the spectrum of a Mn(II) complex, three bands can be predicted in the $d \rightarrow d$ transition zone at 508, 512 and 520 nm attributed to those of manganese(II) with octahedral geometry [36].

The spectrum of a Mn(II) complex can present two very weak bands in the visible at 420 and 570 nm. They are due to the $^6A_1 \rightarrow {}^4T_{2g}$ and $^6A_1 \rightarrow {}^4T_{1g}$ transitions indicating a square-based pyramidal geometry around the Mn(II) ion [37]. The spectrum of a Mn(II) complex can give a band at 686 nm. It is assigned to a $d \rightarrow d$ transition observed for a high-spin Mn(II) $\boldsymbol{d^5}$ complex of configuration (S = 5/2) [38, 39].

- **Iron (II) Spectrum**

In the spectrum of an Fe(II) complex, the bands pointed at 450 and 510 nm are assigned respectively to the transitions $^2E_g \rightarrow {}^2T_{2g}$ and $^2Eg \rightarrow {}^2T_{1g}$ (P) for an iron(II) complex with an octahedral environment [40].

VIII- Magnetic properties of coordination compounds

1°) Macroscopic and microscopic description of the magnetism of molecular compounds

Another way to understand the strength of the crystal field is to measure the magnetic properties of the complexes. Two types of magnetic behaviors are expected for the complexes: paramagnetism (the compound is attracted to the region of maximum magnetic field) and diamagnetism (the compound is repelled to the region of minimum magnetic field). This is induced magnetism, meaning that the presence of an external magnetic field is necessary to highlight these behaviors. There are two types of magnetic behaviors for two complexes of the Fe^{2+} ion ($\boldsymbol{d^6}$ configuration): the $[Fe(H_2O)_6]^{2+}$ complex and the $[Fe(CN)_6]^{4-}$ complex. In the first case, there are unpaired electrons, so the complex is strong spin-weak field. In the second case, the electrons are all paired, so the complex is "weak spin-strong field".

2°) Magnetic measurements and Curie's law

Every molecule is the result of an association of atoms, each of which is composed of a positively charged nucleus around which negatively charged electrons gravitate. There is a close relationship between the electronic structure and the magnetic properties of a molecule.

The study of magnetic properties makes it possible to determine the structure of metal ion complexes as well as the nature (anti- or ferromagnetic) of the interaction between two or more metal centers. Thus, there is a close relationship between the structure and the magnetic

properties of a molecule. Molecular magnetism is a technique that makes it possible to understand the geometry and electronic structure of metal ions from magnetic susceptibility.

To study the magnetic properties of a substance, it is subjected to the action of an intense magnetic field. The sample then acquires a magnetization. Indeed, in the presence of a magnetic field $\vec{H}$, the different electronic or nuclear magnetic moments will divide into different energy levels. For the hydrogen nucleus characterized by a spin of value 1/2, the magnetization can take two positions called parallel or antiparallel. The parallel state being of lower energy, it is more populated and it results in the medium, a macroscopic nuclear magnetization noted M (magnetic moment per unit volume). This magnetization is proportional to the intensity of the applied magnetic field $\vec{H}$. The coefficient of proportionality, noted χ, defines the magnetic susceptibility of the medium considered: $M = \chi H$. When χ is positive, we say that the body in which the magnetization appears is paramagnetic; this effect comes from the unpaired electrons of the substance. When it is negative, the body is said to be diamagnetic; the substance is slightly repelled by the magnetic field, this effect comes from the paired electrons. Molecular magnetism is therefore a technique which allows to determine the state of perturbation of a metal ion from the susceptibility.

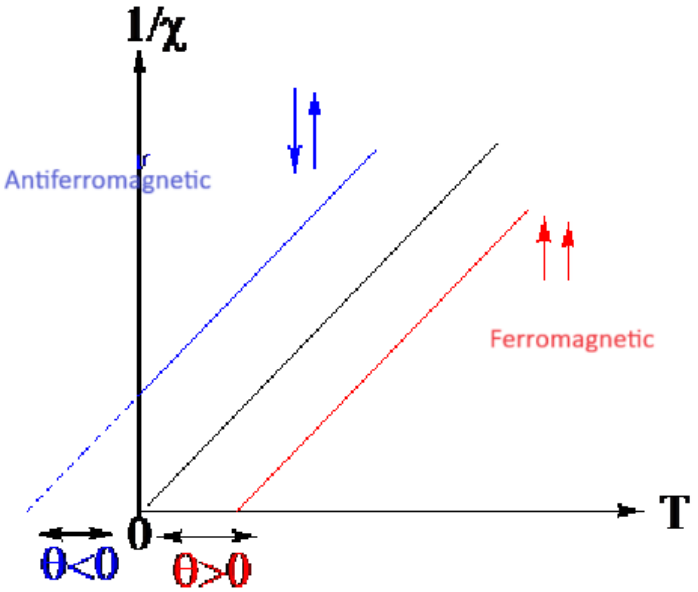

Figure 88 : representation of 1/χ as a function of absolute temperature

Diamagnetic susceptibility, present in all compounds, is negative and independent of temperature. It is linked to the circulation of paired electrons in their orbitals induced by the

external magnetic field. It is calculated from atomic contributions constituting the substance studied. Paramagnetic susceptibility exists only for compounds having unpaired electrons. It is positive and dependent on temperature. It is much more important than diamagnetic susceptibility. For complexes, it is useful to define a molar susceptibility noted χ_M. $\overline{\chi}_M = \overline{\chi}_D + \overline{\chi}_P$ The molar diamagnetic susceptibilities per atom or group of atoms are given in Table 15.

Table 15 : some examples of molar diamagnetic susceptibilities

Atoms	χ_i (10^6 cm^3/mol)	Atoms	χ_i (10^6 cm^3/mol)
H	– 2.85	O alcohol, ether	– 4.61
C	– 6.00	O aldehyde, ketone	+1.66
N open chain	– 5.55	O ester	– 3.36
N ring	– 4.61	F	–11.5
N monoacid	– 1.54	Cl	– 20.10
N diamide, imide	– 2.11	Br	– 30.6
Si	– 13	I	– 44.6
P	– 10	S	– 15
As	– 21	Se	– 23

The thermal dependence of the molar paramagnetic susceptibility is given by **Curie**'s law, according to the relation:

$$\chi_M = \frac{1}{8}\frac{g^2 s(s+1)}{T} \quad (cm^3 mol^{-1})$$

g is the **Zeeman** factor of the complex studied, and is close to the gyromagnetic factor of the electron g_e = 2.0023. The Curie constant C is the quantity equal to $C = \frac{1}{8} g^2 s(s+1)$; it depends on the spin studied and the g factor of the complex studied (next figure). Curie's law can be rewritten in the form of a product independent of the temperature $\chi_M T = C$.

Table 16 : product $\chi_M T$ as a function of spin

S	$\chi_M T = C$ ($cm^3 mol^{-1} K$)
1/2	0.375

1	1
3/2	1.875
2	3
5/2	4.375

For example, the complex $[Fe^{II}(H_2O)_6]^{2+}$ has a spin s = 2 and g = 2, so the product $\chi_M T$ is 3 $cm^3mol^{-1}K$. The diamagnetic complex $[Fe^{II}(CN)_6]^{4-}$ has a spin s = 0, so $\chi_M T$ is zero. The complex $[Cr^{III}(H_2O)_6]^{3+}$ has three single electrons in the t_{2g} orbitals, so s = 3/2, or $\chi_M T$ = 1.875 $cm^3mol^{-1}K$ with g = 2. Thus, the value of the product $\chi_M T$ allows us to know the number of single electrons in a compound.

For the binuclear complex of nickel(II) with 2-({2-[2-(2-hydroxybenzylamino)ethylthio]ethylamino}methyl)phenol, the value of the χT product at room temperature is 1.97 emu $K.mol^{-1}$, (Figure 89). This is somewhat lower than what is expected in the literature for two isolated Ni(II) ions (2.0 emu $K.mol^{-1}$, g = 2.00). After cooling, the χT product decreases steadily, with a more rapid descent below 100 K, reaching a value of 0.02 emu $K.mol^{-1}$ at 2 K. This behavior clearly indicates that antiferromagnetic interactions are active within the molecule, with a small percentage of paramagnetic impurities for residual paramagnetism at low temperatures. A satisfactory fit, illustrated in Figure 89, was obtained using the Van Vleck equation driven by the Hamiltonian $\hat{H} = -J\mathbf{S}_1\cdot\mathbf{S}_2 + g\mu_B\mathbf{B}\cdot\mathbf{S}$ and a small fraction of paramagnetic impurities, with best fit values g = 2.123 ± 0.004, J = - 66.4 ± 0.6 cm-1, % impurity = 1.5 ± 0.2. Some authors have reported the magnetic behavior of the nickel(II) phenolate bridge. They suggested that the phenolate group transmits an antiferromagnetic contribution.

They showed a linear relationship between the exchange interaction due to the value of the Ni-($O_{phenolate}$)2-Ni bridge angle. The dinuclear complexes $[Ni_2(L)(pyridine)_2]\cdot(ClO_4)_2$ (where L is 11,23-dimethyl-3,7,15,19-tetraazatricyclo[19.3.1.19,13]hexacosa-1(25),9,11,13(26),21,23-hexaene-25,26-diolate) and $[Ni_2(sym\text{-}hmp)_2](BPh_4)_2\cdot 3,5DMF\cdot 0,5$ (2-PrOH) (where [H(sym-hmp)] is 2,6-bis[(2-hydroxyethyl)methylaminomethyl]-4-methyl-phenol) show a relatively stronger antiferromagnetic interaction with the respective values J = - 67.1 cm^{-1} and J = - 69.7 cm^{-1}. Thus, as shown by the two bridges of the complex between nickel(II) ions, with Ni-($O_{phenolate}$), the sum of the angles is 100.64°, the amplitude of the antiferromagnetic interaction between the nickel centers is entirely within the expected range [15].

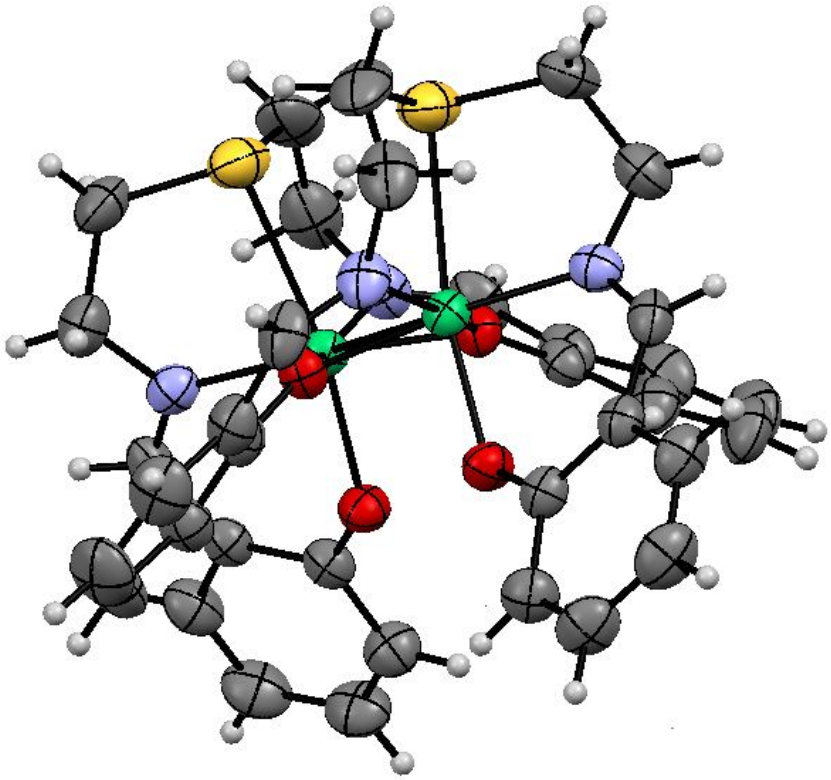

Figure 89 : representation of the binuclear complex of nickel (II) with 2-({2-[2-(2-hydroxybenzylamino) ethylthio]ethylamino}methyl)phenol

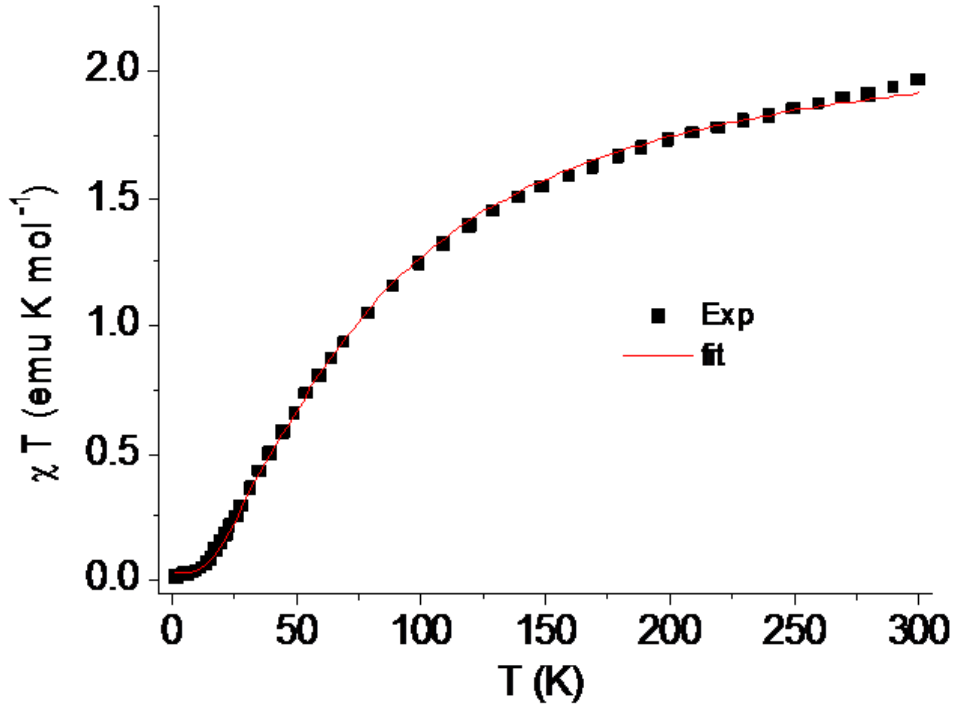

Figure 90 : χT as a function of the absolute temperature of the dinuclear complex

The χT product as a function of temperature for the trinuclear nickel(II) complex with the same ligand is shown in the following figure. The value of the χT product is 3.50 emu K.mol^{-1}at 300 K. It is somewhat higher than the spin-only value for three spins S = 1 with g = 2.00 (2.97 emu K.mol^{-1}) found in the literature and at 2 K the χT product is 0.90 emu K.mol^{-1}. Upon cooling from 300 K to 100 K, the χT product decreases steadily. Below 100 K, it decreases rapidly, suggesting an antiferromagnetic interaction between the different metal centers. Indeed, the interaction between the two terminal Ni(II)s is assumed to be negligible due to the large distance (3.0151 Å) between them. The magnetic analysis was then performed using the Hamiltonian $\hat{H} = J\,[\hat{\mathbf{S}}_1 \cdot \hat{\mathbf{S}}_2 + \hat{\mathbf{S}}_2 \cdot \hat{\mathbf{S}}_3]$, (where the two terminal nickel atoms are identified by $\hat{\mathbf{S}}_1$ and $\hat{\mathbf{S}}_3$ while the central nickel atom by $\hat{\mathbf{S}}_2$). Interestingly, in this approach thefundamental cannot be diamagnetic, so a meaningful model must include a correction for possible zero-field effects and/or intermolecular interactions:

$$\chi = \frac{\chi_M}{1 - \chi_M \theta}$$

The molar magnetic susceptibility χ_M is calculated based on the **Van Vleck** equation and θ is a phenomenological parameter that simulates the null effects of the field and/or intermolecular interactions.

The best correlation of the values obtained with the experimental data of the trinuclear complex are, g = 2.196 ± 0.005, J = -11.12 ± 0.3 cm-1, θ = - 0.86 ± 0.06 K.

In order to understand the coupling behavior, it is important to note that the Ni(II) centers are linked by two bridging β-Ophenolate atoms. The nature of the magnetic interaction is highly dependent on the M-O-M bond angle in the polynuclear Ni(II) complexes. The antiferromagnetic interaction is observed for Ni-O-Ni angles greater than 93.5° and a ferromagnetic coupling is observed for an angle value less than 93.5°. In this trinuclear complex, the bond angles of Ni1-O1-Ni2 and Ni1-O2-Ni2 are 97.4° and 99.9°, respectively. These values greater than 93.5° indicate an antiferromagnetic coupling. The antiferromagnetic parameters of the trinuclear complex are close to those of nickel(II) complexes linked by the bridging phenolate oxygen atoms observed in the literature.

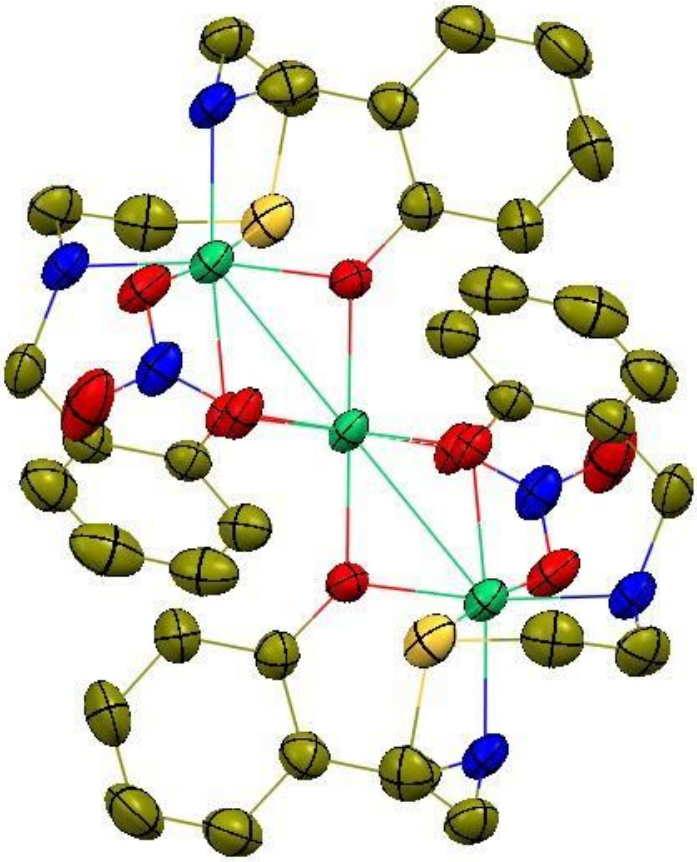

Figure 91 : representation of the trinuclear complex of nickel (II) with 2-({2-[2-(2-hydroxybenzylamino) ethylthio]ethylamino}methyl)phenol

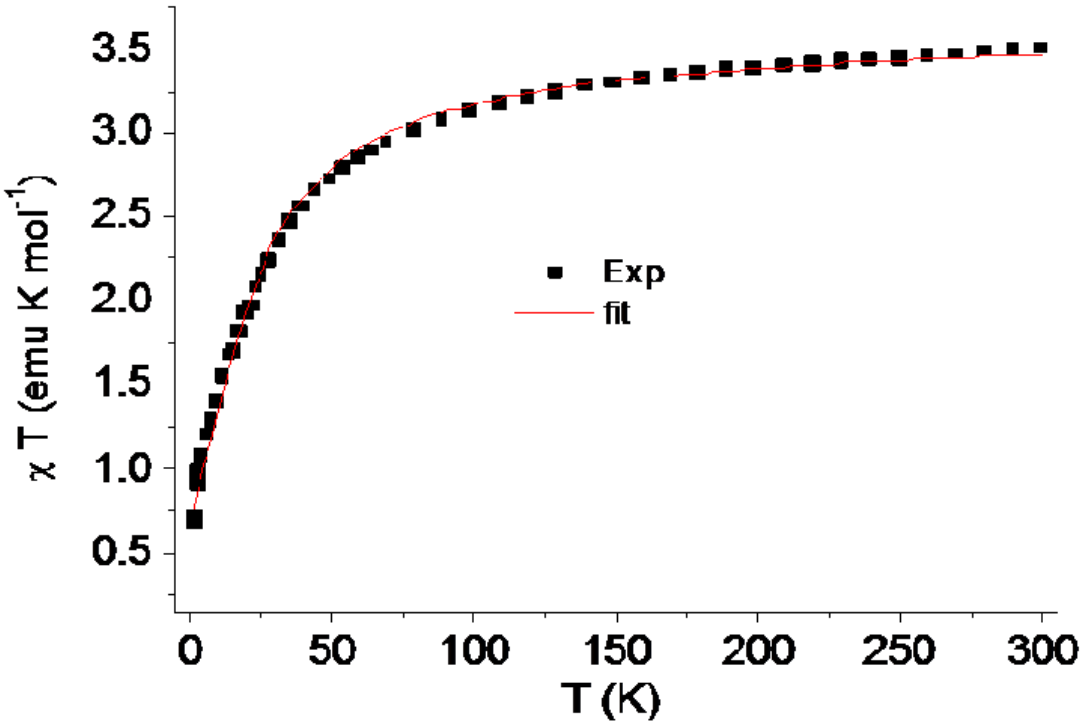

Figure 92 : χT as a function of the absolute temperature of the trinuclear complex

The ligand L, 2,6-diformyl-4-Chlorophenol-bis-(benzoylhydrazone) reacts with lanthanides and gives complexes $[Ln_2(H_2L)_3(NO_3)](NO_3)_2 \cdot (H_2O)_x$ represented below:

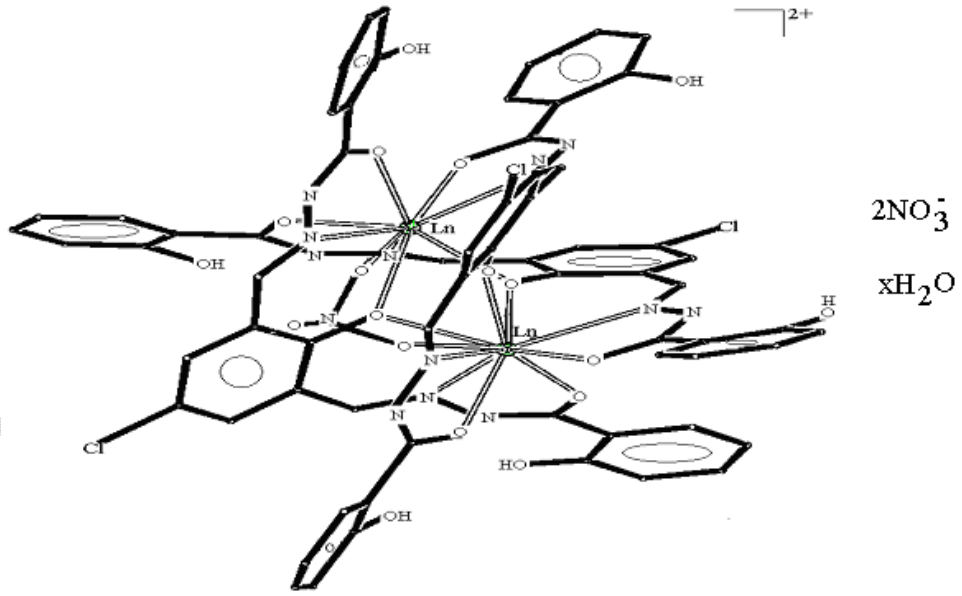

Figure 93 : Crystal structure of 2,6-diformyl-4-chlorophenol-bis-(benzoylhydrazone) complex with lanthanides

Magnetic measurements indicate that we have two types of complexes; complexes with a negative paramagnetic contribution are diamagnetic, such as the lanthanum complex

and yttrium [41]. Others, on the other hand, have a positive contribution and are paramagnetic. Thus the values of 3.3; 4.45; 2.16; 5.47 and 6.21 μ_B are the effective magnetic moments of the cerium, neodymium, samarium, praseodymium and ytterbium complexes respectively. For these complexes, the metals present have few single electrons. The complexes with a high number of single electrons are those of gadolinium, dysprosium and erbium. The respective values of the effective magnetic moments are 11.53; 15.86 and 16.7 μ_B. For all these complexes, it is noted that the values of the magnetic moments are in slight deviation from those found in the literature. This deviation may be due to the interaction between the two magnetic centers. The high magnetic moments indicate that the 4f electrons do not participate in the coordination.

Ligand L, 2,6-diformyl-4-Chlorophenol-bis-(2'-hydroxybenzoylhydrazone) reacts with lanthanum and magnetic measurements indicate that the complex is diamagnetic. This diamagnetic character is a fundamental property for $La^{3+}[Xe]5d^{0}6s^{0}$ ions. All electrons are paired.

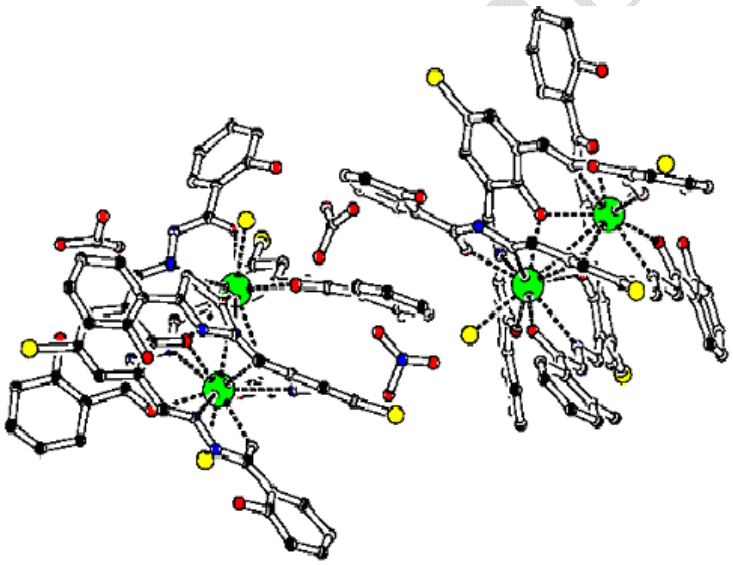

Figure 94 : Structure of the complex $[La_2(H_4L)_3(Cl)_2](NO_3).6H_2O$

The results of the magnetic moments show that the complexes contain two cations per unit. The values of the magnetic moments of Ce (2.56 μ_B), Pr (3.52 μ_B), and Sm (1.83 μ_B) are not very far from those of the free ions. On the other hand, the values of the effective moments of the complexes of Dy (10.50 μ_B), Nd (3.10 μ_B), Er (9.50 μ_B), and Gd (7.90 μ_B) deviate from the values of the free ions. This difference suggests the existence of interaction between the two ions. This coupling would be carried out via the nitrate and phenolate bridges which connect the two magnetic centers. However, the values of the magnetic moments show that the electrons of the ***4f*** orbitals are not engaged in the coordination bonds.

The yttrium and lanthanum complexes are diamagnetic. The synthesized complexes are dinuclear. To determine the nature and intensity of the magnetic interaction, the behavior of the quantities χT and $1/\chi$ of the gadolinium complex at variable temperature is studied.

The susceptibility χ of the complex increases with cooling. The curve $\chi T = f(T)$ is almost uniform throughout the temperature range. The behavior of the complex is paramagnetic. At a temperature of 300 K, the product χT is equal to 17.8 K.emu/mol. This value is slightly above that expected for the two Gd(III) ions with spin 7/2 and orbital moment L = 0 which is 2×8.15 = 16.3 K.emu/mol. With cooling, χT begins a slight rise around 100 K, indicating the presence of a weak ferromagnetic interaction between the two metal cations. This coupling is highlighted by the curve $1/\chi = f(T)$ shown in the following figure:

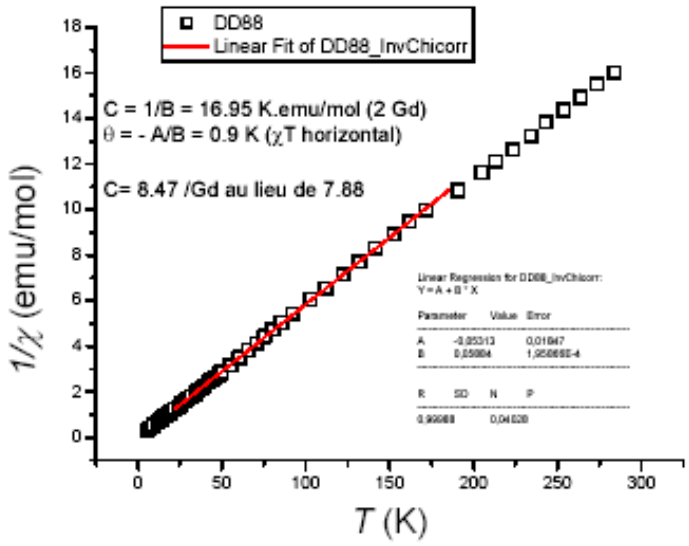

Figure 95 : Representation of $1/\chi = f(T)$

The parameterization of the inverse of the susceptibility using the Curie-Weiss law gives a value of the Weiss temperature T = 0.9 K [42]. This positive and low value of the Curie-Weiss temperature highlights the existence of a weak ferromagnetic coupling between the two Gd(III). This coupling is carried out via the phenolate bridge. The Curie constant is 16.95 K.emu/mol. The expected value for the 2 Gd(III) ions is 2×7.88 = 15.8 K.emu/mol. The total spin of gadolinium is S = 7/2, its total orbital moment is L = 0 with an isotropic g factor of 2. The order of magnitude of the experimentally found Curie constant is correct. Magnetic measurements at variable temperature make it possible to highlight the presence of a low-intensity ferromagnetic interaction between the two magnetic centers. This coupling is carried out via the phenolate bridge.

The interaction between the different ions, observed for some complexes, can constitute a model for the study of metalloenzymes. The same phenomenon is also present in

the active sites of metalloproteins so that biomagnetism becomes a major technique to understand the geometry and electronic structure of these sites.

The complex between N, N'-(2-hydroxypropan-1,3-diyl)-bis-(salicylaldimine) and copper (II) acetate is binuclear. Two molecules are found in the asymmetric unit. The compound. In this compound the Cu(II) ions are tetracoordinated with a square planar environment. The atoms O10, O2, N1 and O3 form the basal plane for Cu1 while the atoms O9, O1, N2 and O3 form the square plane for Cu2. The two metal centers have distorted environments and are linked by the alcoholic oxygen atom O3 of the ligand which forms a bridge between Cu1 and Cu2.

The value of μeff = 1.73 μ_B is equal to that of the free ion. For the binuclear complex the value of the effective moment (2.48 μ_B) shows that this complex is binuclear.

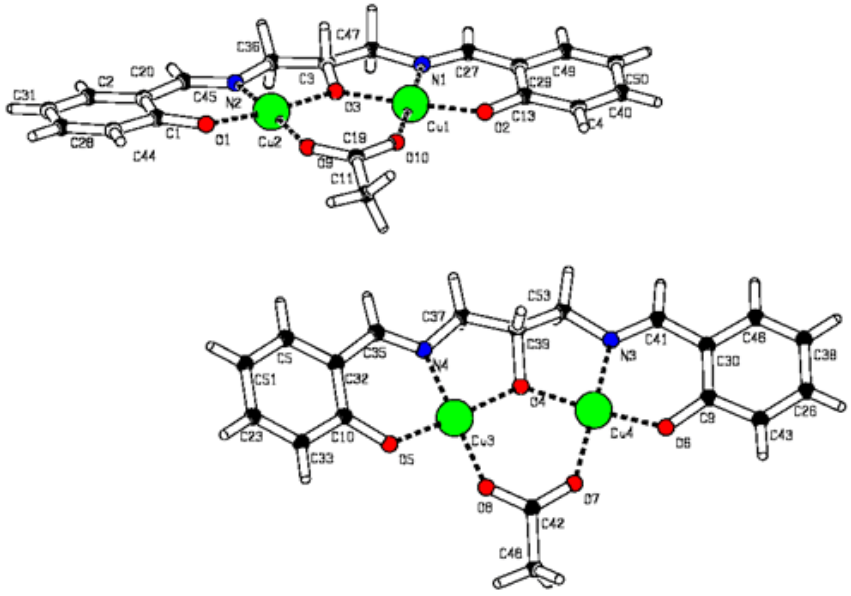

Figure 96 : Crystal structure of the binuclear complex between N,N'-(2-hydroxypropan-1,3-diyl)-bis-(salicylaldimine) and copper(II) acetate

The same ligand gives with copper(II) nitrate a centrosymmetric trinuclear structure with three aligned Cu atoms. The two terminal Cu atoms are pentacoordinated with two nitrogen atoms and three oxygen atoms. Two nitrogen atoms (N1 and N3) and two oxygen atoms (O4 and O5) belonging to the ligand form the base of the square pyramid which is deformed. The ligand N_2O_3 is tetradentate; the phenolic oxygen of the two ligand molecules are bridging and are bonded to Cu3 giving a CuO_4 motif while the oxygen atom of the alcohol group remains free.

The central copper atom Cu3 has a distorted octahedron as its environment. Four phenolic oxygen atoms (O4 and O5 and their respective symmetrical) form the base of the

square-based pyramid with two oxygen atoms (O10 and its symmetrical) from nitrate groups occupying the vertices of the octahedron. The Cu·····Cu distances are 2.974 Å and 2.948 Å. The average Cu3-O distances of 1.984 Å for the O-Ligand and 2.396 Å for the $O_{nitrate}$ are easily differentiated. The magnetic moment of the compound in the solid state gives 1.99 μ_B for the trinuclear complex [7].

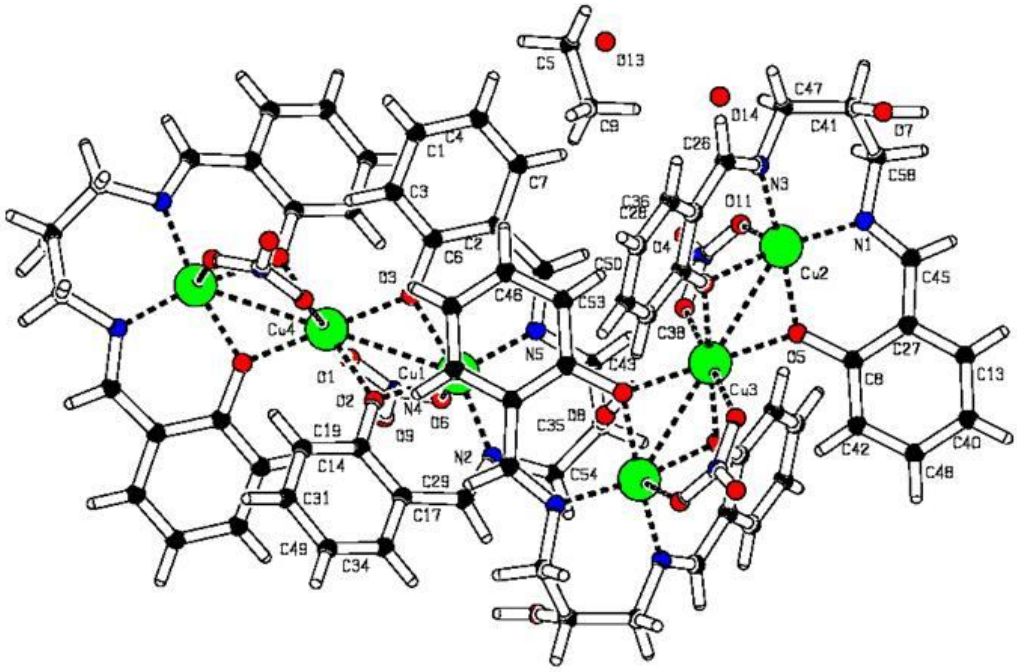

Figure 97 : Crystal structure of the trinuclear copper II complex

In some cases, the study of an active site can suggest original strategies to build new molecular materials. One of the major challenges in this field lies in the synthesis of a molecular system that exhibits permanent magnetization below a certain critical temperature. Therefore, compounds already synthesized exhibit spectacular magnetic bistability and could be incorporated into molecular components capable of storing information. At the crossroads of physics, biology and chemistry, with the prospect of the emergence of molecular components adapted to information processing, we are witnessing a renaissance in magnetism. Each of the two pentacoordinated Cu(II) cations has a pyramidal geometry with a deformed square base. The geometry of each of the other two Cu(II) is better described as a slightly square plane. It is a tetranuclear complex of copper(II) with the ligand 2-hydroxy-N,N'-bis[1-(2-hydroxyphenyl)ethylidene]propane-1,3-diamine.

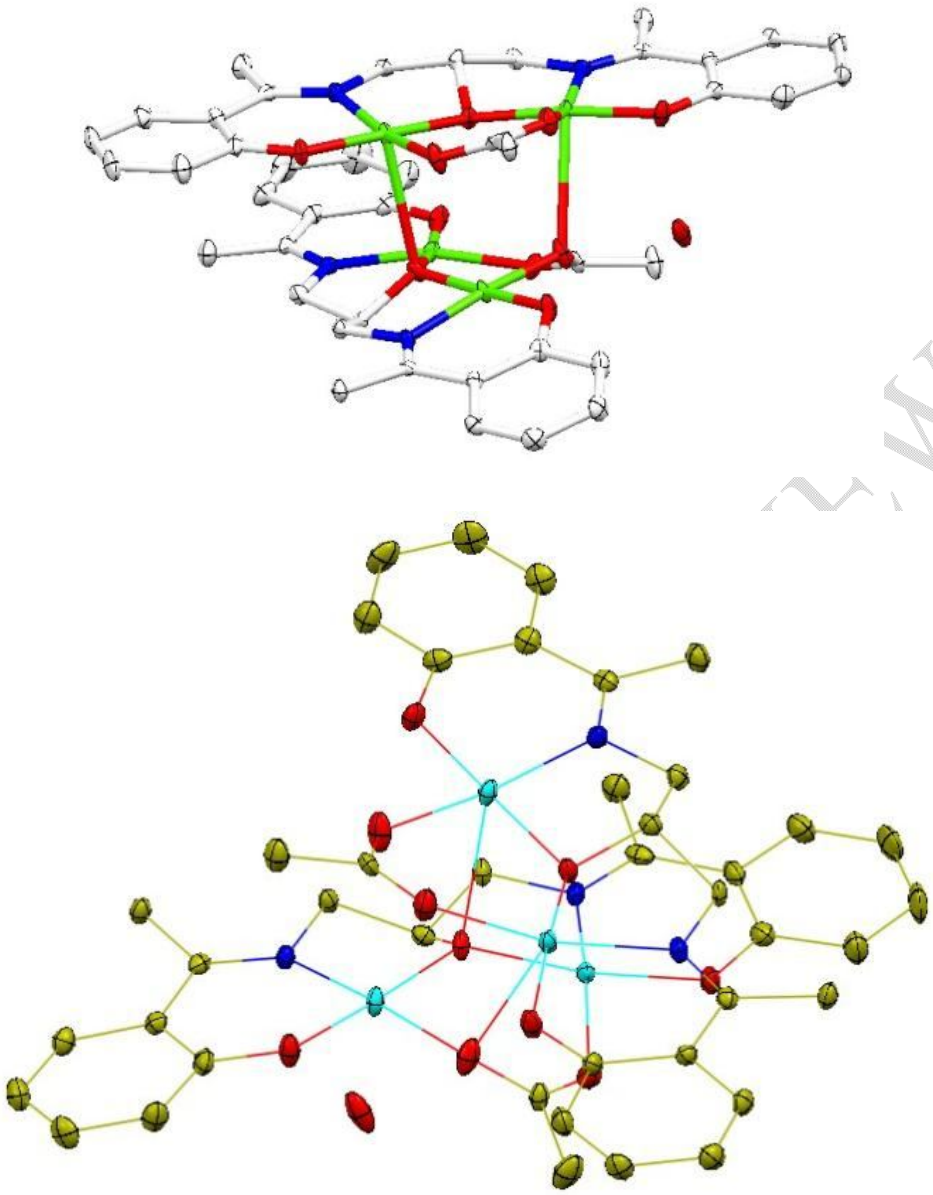

Figure 98 : Crystal structures of the tetranuclear copper II complex

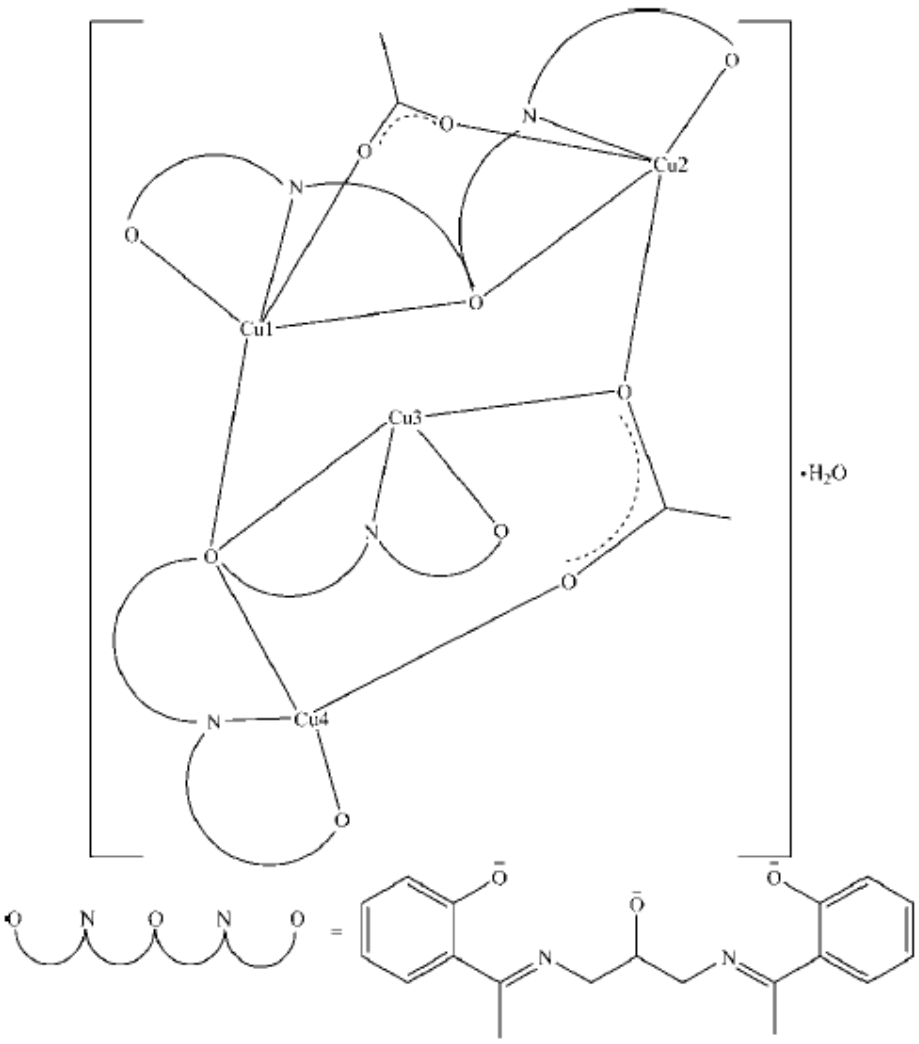

Scheme 82 : Crystal structure of the tetranuclear copper II complex

By removing the bonds between the oxygen of one of the copper (II) ligands of the other ligand we will have:

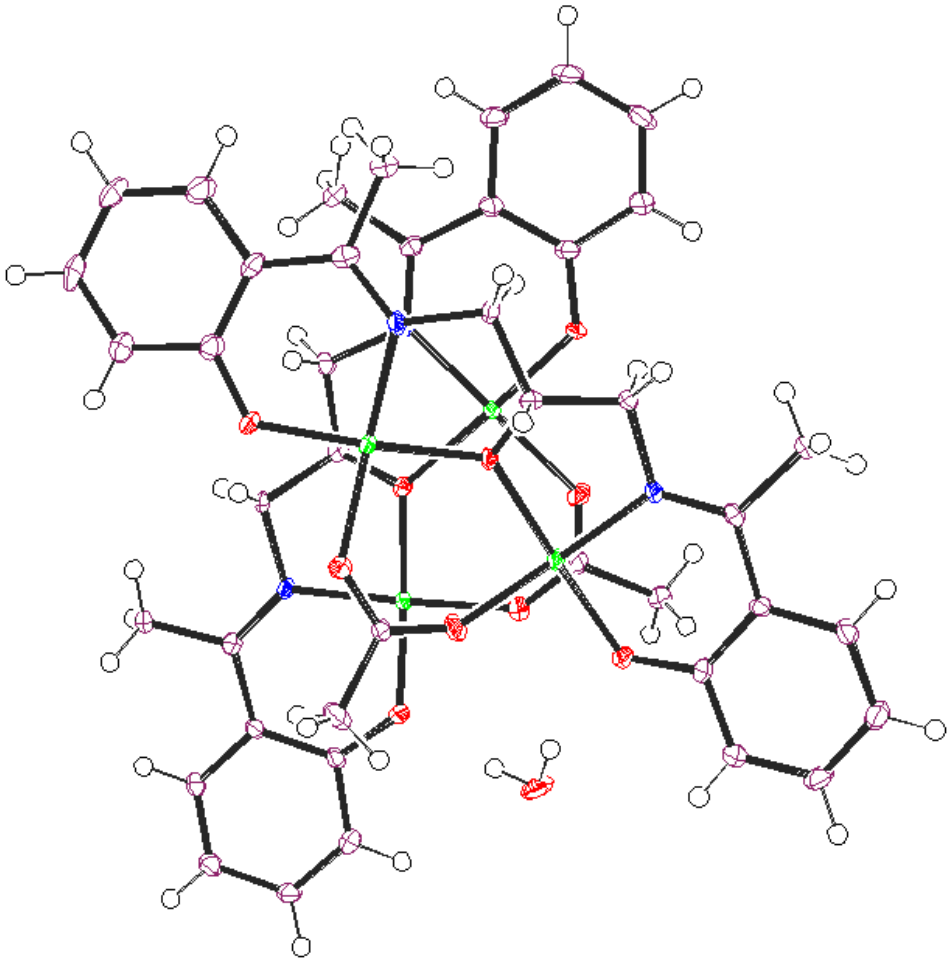

Figure 99 : Crystal structures of the tetranuclear copper II complex

The Schiff base (H_3L), derived from 2-acetyl pyrrole and carbon hydrazide, reacts with certain transition metal ions [Co(II), Ni(II), Cu(II), Zn(II), and Cd(II)] to give complexes of the formulas $[M(H_5L)_2(H_2O)_x]\cdot 2(NO_3)\cdot(CH_3CN)_z\cdot(H_2O)_{y-x}$ (M = Co, Ni, Cu, or Zn; $0 \leq x < y \leq 3$, z = 0 or 1) and $\{Cd(H_4L_A)(NO_3)\}_n$.. This acyclic Schiff base was prepared in a single step using the direct condensation of 2-acetyl pyrrole and carbon hydrazide in good yield. The synthesis and characterization of complexes using 1-(1-(1H-pyrrol-2-yl)ethylidene)carbon hydrazide as chelating ligand have been described.

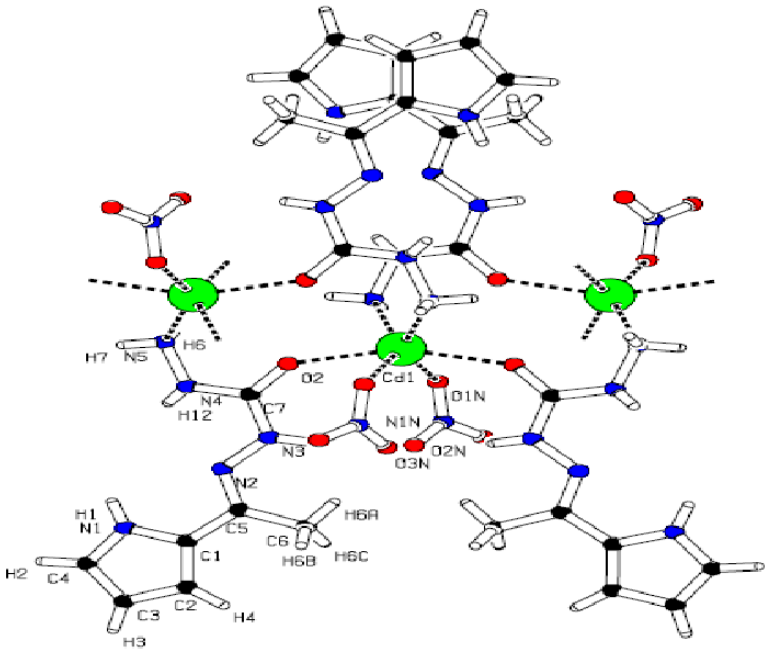

Figure 100 : representation of complex {Cd(H_4L_A)(NO_3)}$_n$

An intense band, observed in the UV Vis spectra of the Cu^{2+}, Ni^{2+} and Co^{2+} complexes near 250 nm, is attributed to the $\pi \rightarrow \pi^*$ transition corresponding to that of the aromatic rings. In this region, intense bands observed between 300 and 445 nm, are attributed to the $n \rightarrow \pi^*$ transition of the carbonyl group. For the copper (II) complex, two bands at 631 and 787 nm are pointed out and attributed to the *d-d* transition. This spectral fact is characteristic of a pentagonal environment around the copper (II) ion. The copper (II) complex shows a value of the magnetic moment μ_{eff} = 1.51 μ_B, lower than that of the spin of 1.73 μ_B expected for the mononuclear copper (II) complex. This low value is characteristic of a square-based pyramidal environment. In the electronic spectrum of the nickel(II) complex, three well-resolved bands at 378, 589 and 1030 nm are pointed out. The band at 378 nm is attributed to the metal-ligand charge transfer while the other two are respectively attributed to the *d-d* transitions: $^3A_{2g} \rightarrow {}^3T_{1g}$, $^3A_{2g} \rightarrow {}^3T_{2g}$ (F).

This spectral fact is characteristic of an octahedral environment around nickel(II). The nickel(II) complex shows a magnetic moment value μ_{eff} = 2.93 μ_B for a mononuclear octahedral nickel(II) complex. The UV-Vis spectrum of the cobalt(II) complex reveals two bands at 474 and 1029 nm. These are respectively attributed to the $^4A_2 \rightarrow {}^4T_1$(P) and $^4A_2 \rightarrow {}^4T_1$ transitions, thus suggesting a tetrahedral environment around cobalt(II). The complex reveals a magnetic moment value μ_{eff} = 4.1 μ_B comparable to those reported in the literature for tetrahedral cobalt(II) complexes.

The neutral tridentate Schiff base (E)-N^1-(2-(phenyl(pyridin-2-yl)methyleneamino)ethyl)ethane-1,2-diamine and L^2 is the neutral tetradentate Schiff base with the formula N-(phenyl(pyridin-2-ylmethylene)-2-(2-(2-(phenyl(pyridin-2-yl)methyleneamino)ethoxy)ethoxy)ethanamine are both derived from benzoylpyridine [43].

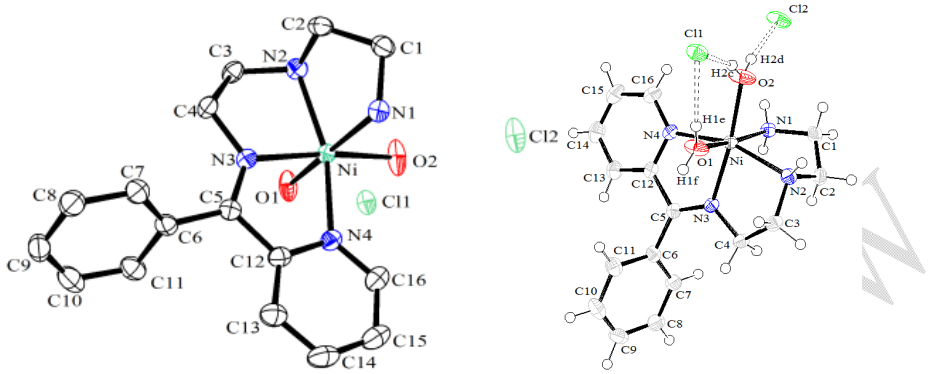

Figure 101 : Crystal structure of the complex with nickel II of E) -N^1-(2-(phenyl (pyridin-2-yl)methyleneamino) ethyl)ethane-1,2-diamine

The bands spotted in the electronic spectra of the Ni(II) complexes $[Ni(L^1)(H_2O)_2]\cdot(Cl)_2$ and $[Ni(L^2)(H_2O)_2]\cdot(NO_3)_2\cdot(H_2O)$ are consistent with an octahedral geometry around the Ni^{2+}. These transition bands assigned to: $^3A_{2g}(F) \rightarrow {}^3T_{2g}(F)$, $^3A_{2g}(F) \rightarrow {}^3T_{1g}(F)$ and $^3A_{2g}(F) \rightarrow {}^3T_{1g}(P)$ are respectively spotted at the ranges 11070-11090 cm^{-1}, 13200-13340 cm^{-1} and 16350-16505 cm^{-1} for the two nickel(II) complexes with L^1 and L^2 respectively. The magnetic moment values of 2.88 μ_B and 2.79 μ_B at room temperature for Ni(II) complexes with L^1 and L^2, respectively, indicate a high-spin mononuclear configuration with an octahedral configuration around the Ni(II). The electronic spectrum of the Cu(II) complexes $[Cu(L^1)(H_2O)_2]\cdot(Cl)_2\cdot(H_2O)$ and $[Cu(L^2)(H_2O)_2]\cdot(NO_3)_2\cdot(H_2O)$ reveals weak absorption bands at 16393 cm^{-1} and 16611 cm^{-1}, respectively, which are assigned to the $^2E_g \rightarrow {}^2T_{2g}$ transition indicating an octahedral environment around the copper(II) ions. The magnetic moment values of 1.77 μ_B and 1.70 μ_B for copper(II) complexes with L^1 and L^2, respectively, at room temperature indicate the presence of strong covalent bonds compared to copper(II) complexes with ionic or weak bonds (1.9-2.2 μ_B). These facts are characteristic of a mononuclear octahedral configuration around Cu(II). Additional bands are pointed out in both electronic spectra in the range 300-220 nm attributed to the transitions $n \rightarrow \pi^*$ et $\pi \rightarrow \pi^*$.

For the nickel(II) complex with the ligand 1,5-Bis[(2-Thiophenyl)Methylidene]Thiocarbonohydrazide the solid-state UV-Vis spectrum of the HL ligand shows two absorption bands at 294-296 and 328-334 nm due to the $\pi \rightarrow \pi^*$ transitions

of the aromatic rings and the n → π* transitions of the C=N groups. The UV-Vis spectrum was recorded in methanol in the region 260-800 nm for the nickel(II) complex. The metal-ligand charge transfer bands observed at 424 and 450 nm can be attributed to N → Ni and S → charge transfer, respectively. The high-intensity charge transfer band of the S → Ni of the three expected transitions correspond to $^1A_{1g} \rightarrow {}^1A_{2g}$, $^1A_{1g} \rightarrow {}^1B_{1g}$ and $^1A_{1g} \rightarrow {}^1E_g$ for the square-planar Ni(II) complex. Only a broad weak band in the 520-600 nm region is attributed to the *d-d* transition of square-planar nickel(II). These observations coupled with the analysis of the crystal structure by X-ray diffraction give a square-planar geometry for the nickel(II) complex.

Furthermore, the Schiff base (HL), derived from 2-benzoylpyridine and nicotinic hydrazide, and its complexes with some metal transition (Co, Ni, Cu, Zn) were synthesized. The electronic spectra of the complexes which are recorded in the DMF solution absorptions in the ranges 257-275 nm and 315-361 nm. These bands are attributed, respectively, to the π → π* transitions of the aromatic nuclei and n → π* transitions of the azomethine moiety of the organic ligand. The bands in the range 418-441 nm are attributed to the ligand-metal charge transfers. For the cobalt(II) complex, the bands at 465 and 499 nm are attributable, respectively, to the $^4T_{1g}(F) \rightarrow {}^4T_{2g}(P)$ and $^2E_g \rightarrow {}^2T_{1g}(P)$ transitions. In the UV region, a band appears at 383 nm due to the $^4T_{1g}(F) \rightarrow {}^4A_{2g}(F)$ transition. These bands are typical of an octahedral environment around the Co(II) cation. For this complex, the magnetic field moment value is 5.88 μ_B. In the spectrum of the Ni(II) complex, the bands are located at 444, 499, and 869 nm. They are assigned to the transitions $^1A_{1g} \rightarrow {}^1B_{1g}$, $^1A_{1g} \rightarrow {}^1E_g$ and $^3A_{2g}(F) \rightarrow {}^3T_{2g}$ in agreement with an octahedral geometry around nickel(II). This observation is confirmed by the magnetic moment value of 2.74 μ_B corresponding to an octahedral Ni(II) cation. The spectrum of the Cu(II) complex shows an absorption band at 678 nm which is assigned to the transition band $^2E_g \rightarrow {}^2T_{2g}$ indicating an octahedral geometry around Cu(II) cation. This observation is confirmed by magnetic moment value of 1.82 μ_B which indicates the presence of a Cu^{2+} ion in an octahedral environment. The spectrum of the Zn(II) complex shows strong absorption bands at 499 nm due to Ligand→Metal charge transfers [44].

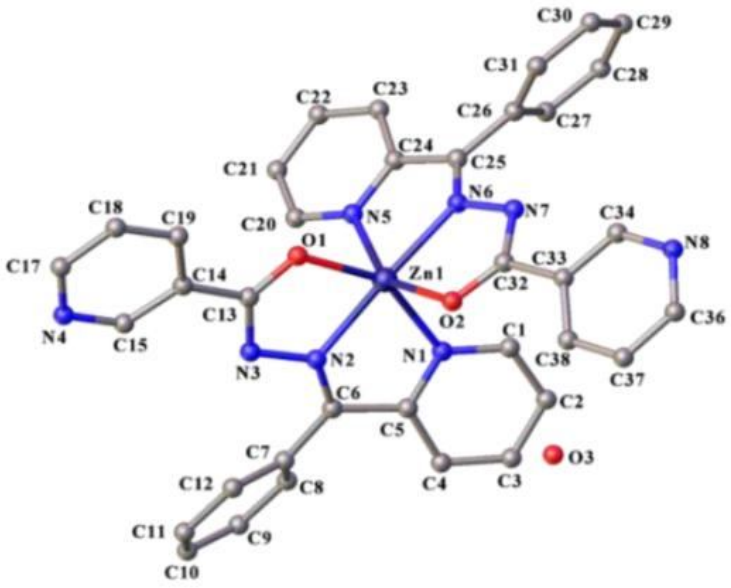

Figure 102 : Crystal structure of the complex of zinc II with N'-(phenyl(pyridin-2-yl)methylene)Nicotinohydrazide

For the complex $[Cu_2(\mu\text{-}L)_2La(NO_3)_2]_2{\cdot}La(NO_3)_4$, the value of the χT product at room temperature is 1.2 emu K mol^{-1}. Upon cooling from 300 K to 50 K, the χT product decreases steadily. After cooling, the χT product decreases steadily, with a more rapid decline below 50 K. Below 50 K, it decreases rapidly, suggesting an antiferromagnetic interaction between the different metal centers. This behavior clearly indicates that antiferromagnetic interactions are active within the complex, with a small percentage of paramagnetic impurities for residual paramagnetism at low temperatures. A satisfactory fit, illustrated in Figure 2, was obtained using the Van Vleck equation driven by the Hamiltonian $\hat{H} = -J\mathbf{S}_1\cdot\mathbf{S}_2 + g\mu_B\mathbf{B}\cdot\mathbf{S}$ and including a small fraction of paramagnetic impurities, with the best fit values g = 2.123 ± 0.004, J = -66.4 ± 0.6 cm-1, % impurity = 1.5 ± 0.2.

The magnetic analysis was then performed using the Hamiltonian $\hat{H} = J\,[\hat{\mathbf{S}}_1\cdot\hat{\mathbf{S}}_2 + \hat{\mathbf{S}}_2\cdot\hat{\mathbf{S}}_3]$, (where the two copper(II) ions are identified by $\hat{\mathbf{S}}_1$ and $\hat{\mathbf{S}}_3$ while the La(III) ion by $\hat{\mathbf{S}}_2$). Interestingly, in this approach thefundamental cannot be diamagnetic, so a meaningful model must include a correction for possible zero-field effects and/or intermolecular interactions:

$$\chi = \frac{\chi_M}{1-\chi_M\theta}$$

où χ_M la susceptibilité magnétique molaire, est calculée sur la base de l'équation Van Vleck et θ est un paramètre phénoménologique qui simule les effets nuls du champ et/ou des interactions intermoléculaires.

The magnetic behavior of the complex is governed by copper since lanthanum is diamagnetic.

where χ_M is the molar magnetic susceptibility, calculated based on the Van Vleck equation and θ is a phenomenological parameter that simulates the null effects of the field and/or intermolecular interactions.

The best correlation of the values obtained with the experimental data of the complex are, g = 2.196 ± 0.005, J = -11.12 ± 0.3 cm-1, θ = - 0.86 ± 0.06 K.

In order to understand the coupling behavior, it is important to note that the Cu(II) and La(III) centers are linked by two bridging μ-$O_{phenolate}$ atoms. The magnetic behavior of the complex is governed by copper since lanthanum is diamagnetic.

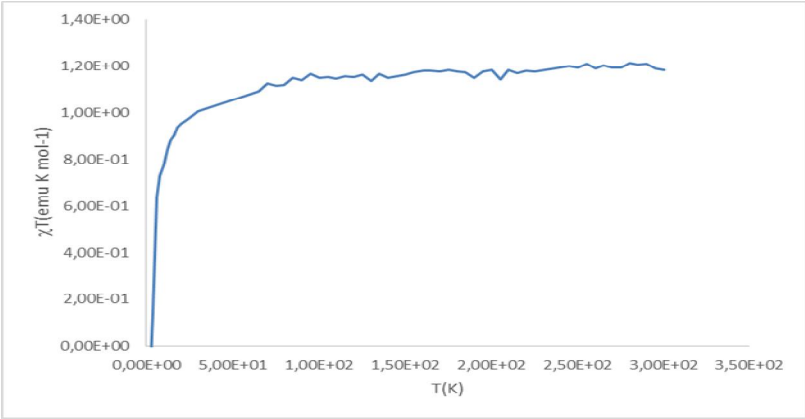

Figure 103 : $\chi T = f(T)$ of complex $[Cu_2(\mu\text{-}L)_2La(NO_3)_2]_2{\cdot}La(NO_3)_4$

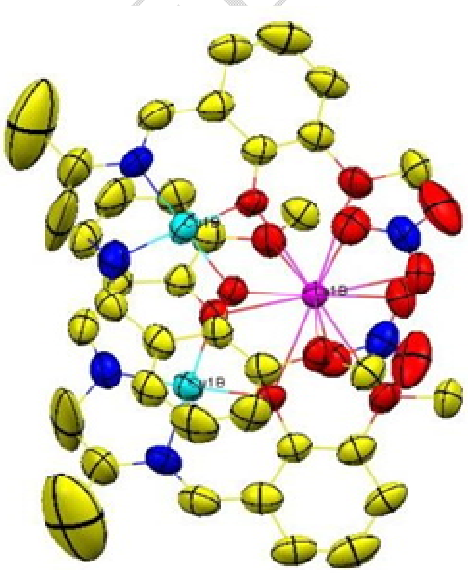

Figure 104 : Crystal of complex $[Cu(Lc)La(NO_3)]_2{\cdot}La(NO_3)_4$

Application exercise

A Ni^{2+} complex is found to have an experimental $\chi_M T$ product of 1.0 $cm^3mol^{-1}K$.

a. How many unpaired electrons are there in the Ni^{2+} ion?

b. Is the complex paramagnetic or diamagnetic?

c. Calculate the molar paramagnetic susceptibility χ_M that you would expect to measure at 298 K ? 100 K ?

Correction

a. We know that for a mononuclear complex the product $\boldsymbol{\chi_M T}$ is equal to a constant C independent of the temperature called the Curie constant. Its value is

C = ½ S(S + 1), S being the spin of the compound. For the nickel complex studied S = 1, which implies the presence of 2 single electrons.

b. By definition, a complex with a non-zero spin S is paramagnetic. A complex with a zero spin is diamagnetic. The complex studied is therefore diamagnetic.

c. At 298 K (respectively 100 K), the χ_M value of 0.0036 cm^3mol^{-1} (respectively 0.01000 cm^3mol^{-1}) is expected.

BIBLIOGRAPHICAL REFERENCES

[1] Structure de la matière, Chimie Inorganique, Théorie et application, Collection PRUNET. P. 49, 71, 73.

[2] A. COLLY ; Cours d'Atomistique et de Liaisons Chimiques, (Octobre 2001).

[3] Atomistique et structures, Précis de chimie, Cours Exercices résolus, Prépas PCSI-PC 1ère et 2e années. J. Mesplede, J.-L. QUEYREL.

[4] M. SIDIBE ; Fascicule personnel.

[5] L. DIOP ; Cours de chimie minérale.

[6] B. George Kauffman, California State University, A. Fresno. Stereochemical achievement of the first order : Alfred Werner's resolution of cobalt complexes, 85 years later. *Bull. Hist. Chem. 20* (1997).

[7] M. DIENG, I. THIAM, M. GAYE, A. S. SALL, A. H. BARRY. *Acta Chimica Slovenica* 53, 417-423 (2006).

[8] M. M. SOW, M. DIENG, F. B. TAMBOURA, O. DIOUF, M. GAYE. *IOSR Journal of Applied Chemistry (IOSR-JAC)* 2278-5736 (2016).

[9] M. DIENG, A. H. BARRY, M. GAYE, A. S. SALL, P. P.-LOURIDO and L. V.-MATARRANZ. *Acta Crystallographica* E67 (2011).

[10] O. SALL, M. DIENG, M. M. SOW, D. DIOUF, I. E. THIAM, P. RETAILLEAU, M. GAYE. IOSR *Journal of Applied Chemistry (IOSR-JAC)* 13, 27-37 (2020).

[11] A. SY, M. DIENG, I. E. THIAM, M. GAYE and P. RETAILLEAU. *Acta Crystallographica* E69, m 108 (2013).

[12] O. SALL, F. B. TAMBOURA, A. SY, A. H. BARRY, E. I. THIAM, M. GAYE and J. ELLENA. *Acta Crystallographica* E75 1069-1075 (2019).

[13] M. FAYE, M. M. SOW, P. A. GAYE, M. DIENG and M. GAYE. *European Journal of Chemistry* 159-164 (2021).

[14] M. DIENG, M. GAYE, A.S. SALL and R. WELTER. *Zeitschrift für Kristallographie* NCS 219 15-16 (2004).

[15] H. SAKIYAMA, K. TONE, M. YAMASAKI, M. MIKURIYA, *Inorg. Chim. Acta*, 365, 183 (2011).

[16] A. S. DIALLO, B. TRAORE, M. DIENG, I. E. THIAM, S. COLLES, J. ORTON and M. GAYE, *Earthline Journal of Chemical Sciences* 9,2, 267-282 (2023).

[17] M. SARR, M. DIOP, E. I. THIAM, A. H. BARRY, M. GAYE and P. RETAILLEAU. *Acta Crystallographica* E 74, 450 – 453 (2018).

[18] F. BARR, P. S. CAMARA, A. GUEYE, S. ZAZOULI, N GRUBER, F. B. TAMBOURA, M. DIENG, M. GAYE, *Science Journal of chemistry* 11(2) 56-63 (2023).

[19] M. FAYE, P. A. GAYE, M. M. SOW, M. DIENG, F. B. TAMBOURA, N. GRUBER and M. GAYE, *Earthline Journal of Chemical Sciences* 6,1, 99-117 (2021).

[20] M. N. GUEYE, M. DIENG, I. E. THIAM, D. LO, A. H. BARRY, M. GAYE and P. RETAILLEAU, *South African Chemical Institute* 70, 8-15 (2017).

[21] M. N. GUEYE, M. DIENG, D. LO, I. E. THIAM, A. H. BARRY, M. GAYE, A. S. SALL and P. RETAILLEAU. *European Journal of Chemistry* 137-14 (2017).

[22] M. FAYE, A. B. KAMA, M. N. GUEYE, M. DIENG, F. B. TAMBOURA, R. GAUTIER and M. GAYE. *Science Journal of Chemistry* 10, 161-169 (2022).

[23] R. PRINS, P. J. M. L. BIRKER, J. G. HAASNOOT, G. C. VERSCHOOR, J. REEDIJK, *Inorg. Chem.*, 24, 4128 (1985).

[24] C. TSERKEZIDOU, A. G. HATZIDIMITRIOU, G. PSOMAS, *Polyhedron* 117, 184–192 (2016).

[25] R. TAKJOO, R. CENTORE, *J. Mol.Struct.* 1031, 180–185 (2013).

[26] C. FERNANDES, G. PARRILHA, J. LESSA, L. SANTIAGO, M. KANASHIRO, F. S. BONIOLO, A. J. BORTOLUZZI, N. V. VUGMAN, M. H. HERBST, A. HORN Jr, *Inorg. Chim. Acta*. 359, 3167–3176 (2006).

[27] S. M. de M. ROMANOWSKI, F. TORMENA, V. A. dos SANTOs, M. de F. HERMANN and A. S. MANGRICH, J. Braz. *Chem. Soc.* 15(6), 897– 903 (2004).

[28] V. M. LEOVAC, M. D. JOKSOVIC, V. DIVJAKOVIC, L. S. JOVANOVIC, Z. SARANOVIC, A. Pevec, *J. Inorg. Biochem.* 53, 1094–1097 (2007).

[29] A. K. MAPARI, Int. J. Med. Chem. Anal., 4(1), 22–26 (2014).

[30] A. P. B. LEVER, *Inorg. Electron. Spectrosc., Elsevier,* Amsterdam, (1980).

[31] M. ALI, S. E. LIVINGSTON, D. J. PHILLIPS, *Inorg. Chim. Acta,* 5, 493 (1971).

[32] M. DUGGAN, N. RAY, B. HATHAWAY, G. THOMLINSON, *J. Chem. Soc. Dalton Trans.,* 1342 (1980).

[33] N. C. JANA, P. BRANDAO, A. SAHA, A. PANJA, *Polyhedron* 138, 31–36 (2017).

[34] M. M. I. M. HASNAN, N. ABDULLAH, S. M. SAID, M. F. M. SALLEH, S. A. M. HUSSIN, N. M. SHAH, *Electrochim. Acta* 261, 330–339 (2018).

[35] M. GABER, S. S. Al- SHIHRY, *Basic Appl. Sci.*, 5 (2), 181-195 (2004).

[36] S. F. A. KETLLE, *Physical Inorganic Chemistry*, Oxford University Press 213 (1996).

[37] R. N. EGEKENZE, Y. GULTNEH, R. BUTCHER, *Inorg. Chim. Acta* 478, 232–242 (2018).

[38] F.A. El–SAIED, A.N. Al–HAKIMI, M.A. WAHBA, M.M. E. SHAKDOFA, *Egypt. J. Chem.*, 60(1), 1– 24 (2017).

[39] B. K. SAHU, B. K. MAHAPATRA, *J. Indian Chem. Soc.*, 56, 822–825 (1979).

[40] T. A. YOUSEF, O. K. ALDUAIJ, S. F. AHMED, G.M.A. El–REASH, O. A. El–GAMMAL, *J. Mol. Struct.* 1119, 351–364 (2016).

[41] M. GAYE, F. B. TAMBOURA, A.S. SALL. *Bull. Chem. Soc. Ethiop*. 17(1), 27-34 (2003).

[42] M. DIOP, Thèse de Troisième cycle, Université Cheikh Anta Diop, Dakar (2004).

[43] D. LO, I. E. THIAM, M. DIENG, M. M. SOW, O. DIOUF, M. GAYE, *Journal of Applied Chemistry (IOSR-JAC)* 2278-5736 (2018).

[44] N. F. NDIAYE, F. DIOUF, A. GUEYE, F. B. TAMBOURA, M. DIENG, S. ZAZOULI, N. GRUBER and M. L. GAYE, *Chemical Science International Journal* 32,6, 41-52 (2023).